REFERENCES

Bagmai, A., Nateghi. M.R. and Massoumi., A. (1998) Electrochemical synthesis of highly electroactive polydiphenylamine/polybenzidine copolymer in aqueous solutions. Synthetic Materials, 97, 85-89.

Carpi, F., Chiarelli, P., Mazzoldi, A., and Rossi, D.D. (2003) Electromechanical characterisation of dielectric elastomer planar actuators: comparative evaluation of different electrode materials and different counterloads. Sensors and Actuators A, 107, 85–95.

Chandrasekhar, P. (1999). Fundamnetals and Applications of Conducting Polymers Handbook, USA: Kluwer Academic Publishers.

Cho, M.S., Seo, H.J.,Nam, J.D., Choi, H.R., Koo, J.C., Song, K.G., and Lee, Y. (2006) A solid state actuator based on the PEDOT/NBR system. Sensors and Actuators B. 119, 621–624.

Chotpattananont, D., Sirivat, A., and Jamieson, A.M. (2004) Electrorheological properties of perchloric acid-doped polythiphene suspensions. Colloid and Polymer Science. 282, 357-365.

Deependra, K., Shahid, A., and Seungyong, Y. (2004). Semiconducting and Metallic Polymers. Condensed matter physics II, 1-19.

Faez, R., Schuster R.H., and De Paoli M.A. (2002) A conductive elastomer based on EPDM and polyaniline II. Effect of the crosslinking method. European Polymer Journal. 38, 2459–2463.

Feher, J., Filipcsei, G., Szalma, J., and Zrinyi, J. (2001) Bending deformation of neutral polymer gels induced by electric fields. Colloids and Surfaces A: Physicochemical and Engineering Aspects. 183–185, 505–515.

Gazotti W.A., Jr, Faez, R., and De Paoli M-A. (1999) Thermal and mechanical behaviour of a conductive elastomeric blend based on a soluble polyaniline derivative. European Polymer Journal, 35, 35-40.

Gere, J.M. (1972) Mechanics of Materials, 3rd ed., London: Chapman & Hall; 515-516.

Hotta, A., Clarke, S. M. and Terentjev, E. M. (2002) Stress Relaxation in Transient Networks of Symmetric Triblock Styrene-Isoprene-Styrene Copolymer. Macromolecules, 35, 271-277.

Hua, F. and Ruckenstein, E. (2003) Water-soluble conducting poly (ethylene oxide)-Grafted polydiphenylamine synthesis through a "Graft Onto" process. Macromolecules, 36, 9971-9978.

Hua, F. and Ruckenstein, E. (2005) Hyperbranched Sulfonated Polydiphenylamine as a Novel Self-Doped Conducting Polymer and Its pH Response. Macromolecules, 38, 888-898.

Kim, J., Kang, Y., and Yun, S. (2007) Blocked force measurement of electro-active paper actuator by micro-balance. Sensors and Actuators A. 133, 401–406.

Kornbluh, R., Pelrine, R., Pei Q., Stanford, S., and Rosenthal, M. (2002) Dielectric elastomer artificial muscle for actuators, generators, and sensors, in Proceedings of The First World Congress on Biomimetics and Artificial Muscles (Biomimetics 2002), New Mexico, USA.

Krause, S. and Bohon, K. (2001) Electromechanical Response of Electrorheological Fluids and Poly(dimethylsiloxane) Networks. Macromolecules, 34, 7179-7189.

Kumar, D., and Sharma, R.C. (1998). Advances in conductive polymers. European Polymer Journal, 34, 1053-1060.

Kunanuruksapong, R. and Sirivat, A. (2007) Poly(*p*-phenylene) and acrylic elastomer blends for electroactive application. Materials Science and Engineering A .454–455, 453–460.

Lee, W.K., Kim, H.D., and Kim E.Y. (2006) Morphological reorientation by extensional flow deformation of a triblock copolymer styrene–isoprene–styrene. Current Applied Physics. 6, 718–722.

Ma, W. and Cross, L.E. (2004) An experimental investigation of electromechanical response in a dielectric acrylic elastomer. Applied Physics A, 78, 1201–1204.

Matsushita, Y., Tamura, M. and Noda, I. (1994) Tricontinuous Double-Diamond structure formed by Styrene-Isoprene-2-Vinylpyridine Triblock Copolymer. Macromolecules, 27, 3680-3682.

Moschou, E., Peteu, S., Bachas, L.G., Madou, M.J., and Daunert, S. (2004) Artificial muscle material with fast electroactuation under neutral pH conditions. Chemistry of Materials, 16, 2499-2502.

Nagata, Y., Masuda, J., Noro, A., Cho, D., Takano, A. and Matsushita, Y. (2005) Preparation and Characterization of a Styrene-Isoprene Undecablock Copolymer and Its Hierarchical Microdomain Structure in Bulk. Macromolecules, 38, 10220-10225.

Niamlang, S. and Sirivat, A. (2008) Electromechanical reponse of a crosslinked polydimethylsiloxane. Macromolecular Symposia, 264, 176-183.

Orlov, A.V., Ozkan, S.Zh. and Karpacheva, G.P. (2005) Oxidative polymerization of Diphenylamine: A mechanistic study. Polymer science ser. B. 48, 11-17.

Pelrine, R., Kornbluh, R., Joseph, J., Heydt, R., Pei, Q., and Chiba, S. (2000) High-field deformation of elastomeric dielectrics for actuators. Materials Science and Engineering C. 11, 89–100.

Pelrine, R.E., Kornbluh, R.D., and Joseph, J.P. (1998) Electrostriction of polymer dielectrics with compliant electrodes as a means of actuation. Sensors and Actuators A. 64, 77-85.

Puvanatvattana, T., Chotpattananont, D., Hiamtup, P., Niamlang, S., Kunanuruksapong, R., Sirivat, A., Jamieson, A.M. (2008) Electric field induced stress moduli of polythiophene/polyisoprene suspensions: Effects of particle conductivity and concentration. Materials Science and Engineering C. 28, 119–128.

Puvanatvattana, T., Chotpattananont, D., Hiamtup, P., Niamlang, S., Sirivat, A., Jamieson, A.M. (2006) Electric field induced stress moduli in polythiophene/polyisoprene elastomer blends. Reactive & Functional Polymers. 66, 1575–1588.

Rubinstein, M., and Colby, R. H. (2003) Polymer Physics; Oxford University Press: New York; 298-300.

Santana, H.D. and Dias F.C. (2003) Characterization and properties of polydiphenylamine electrochemically modified by iodide species. Materials Chemistry and Physics. 82, 882–886.

Sathiyanayanan, S., Muthukrishnan, S. and Venkatachari, G. (2006) Synthesis and anticorrosion properties of polydiphenylamine blended vinyl coatings. Synthetics Materials, 156, 1208-1212.

Sato, T., Watanabe, H., and Osaki, K. (1996) Rheological and Dielectric Behavior of a Styrene-Isoprene-Styrene Triblock Copolymer in *n*-Tetradecane. 1. Rubbery-Plastic-Viscous Transition. Macromolecules. 29, 6231-6239.

Schmidt, V., Domenech, S.C., Soldi, M.S., Pinheiro, E.A. and Soldi, V. (2004) Thermal stability of polyaniline/ethylene propylene diene rubber blends prepared by solvent casting. Polymer Degradation and Stability. 83, 519-527.

Shiga, T. (1997) Advances in Polymer Science, vol.134, Springer-Verlag, Berlin, Heidelberg. 20, 133-163.

Shiga, T., Okada, A., and Kurauchi, T. (1993) Electroviscoelastic effect of polymer blends consisting of silicone elastomer and semiconducting polymer particles. Macromolecules, 26, 6958-6963.

Suganandama, K., Santhosh, P., Sankarasubramanian, M.,Gopalan, A., Vasudevan, T. and Lee, K-P. (2005) Fe3+ ion sensing characteristics of polydiphenylamine-electrochemical and spectroelectrochemical analysis. Sensors and Actuators B. 105, 223–231.

Thanpitcha, T., Sirivat, A.,Jamieson , A.M. and Rujiravanit, R. (2005) Preparation and characterization of polyaniline/chitosan blend film. Carbohydrate Polymers. 64, 560-568.

Timoshenko, S.P. and Goodier, J.N. (1970) Theory of elasticity. 3rd ed. Auckland: McGraw-Hill; 41-46.

Tsai, Y.T., Wen, T.C. and Gopalan, A. (2003) Tuning the optical sensing of pH by poly(diphenylamine). Sensors and Actuators B, 96, 646-657.

Van Vught, F.A. (2000). Transparent and conductive polymer layers by gas plasma techniques. The Netherlands: L.M.H. Groenewoud.

Wang, Y.,Shen, J.S, and Long, C.F., (2001) The effect of casting temperature on morphology of poly(styrene-ethylene/butylene-styrene) triblock copolymer. Polymer, 42, 8443-8446.

Wen, T.C., Chen, J.B., and Gopalan, A. (2002) Soluble and methane sulfonic acid doped poly(diphenylamine)-synthesis and characterization. Materials letters, 57, 280-290.

Winter, H.H., Diane, D.B., Gronski, S.W., Okamoto, S. and Hashimoto, T. (1993) Ordering by Flow near the Disorder-Order Transition of a Triblock Copolymer Styrene-Isoprene-Styrene. Macromolecules, 26, 7236-7244.

Xue, H., Shen, Z., and Li, Y. (2001) Polyaniline-polyisoprene composite film based glucose biosensor with high permselectivity. Synthesis Materials, 124, 345-349.

Zhang, Q.M., Bharti, V., and Zhao, X. (1998) Giant electrostriction and relaxor ferroelectric behavior in electron irradiated poly(vinylidene fluoride-trifluoroethylene) copolymer. Science. 280, 2101–2104.

Zhao, Y., Chen, M., Liu, X., Xu, T., and Liu, W. (2005) Electrochemical synthesis of polydiphenylamine nanofibrils through AAO template. Materials Chemistry and Physics. 91, 518–523.

APPENDICES

Appendix A Identification of FT-IR Spectrum

Synthesized polydiphenylamine (PDPA) and dedoped Polydiphenylamine

Polydiphenylamine (PDPA) was synthesized via the oxidative polymerization of diphenylamine(DPA) to obtains doped-PDPA (D_PDPA) (Orlov *et al.*, 2005). The PDPA was dedoped by immersing in ammonium hydroxide solution to become neutral PDPA (De_PDPA). The polymers were first characterized for the functional groups by a FT-IR spectrometer (Thermo Nicolet, Nexus 670) in absorption mode with 32 scans and a resolution of ± 4 cm^{-1}, wavenumbers range of 4000-400 cm^{-1}, and using a deuterated triglycine sulfate as a detector. Optical grade KBr (Carlo Erba Reagent) was used as the background material. De_PDPA and D_PDPA were intimately mixed with dried KBr at a ratio of PDPA: KBr = 1:20.

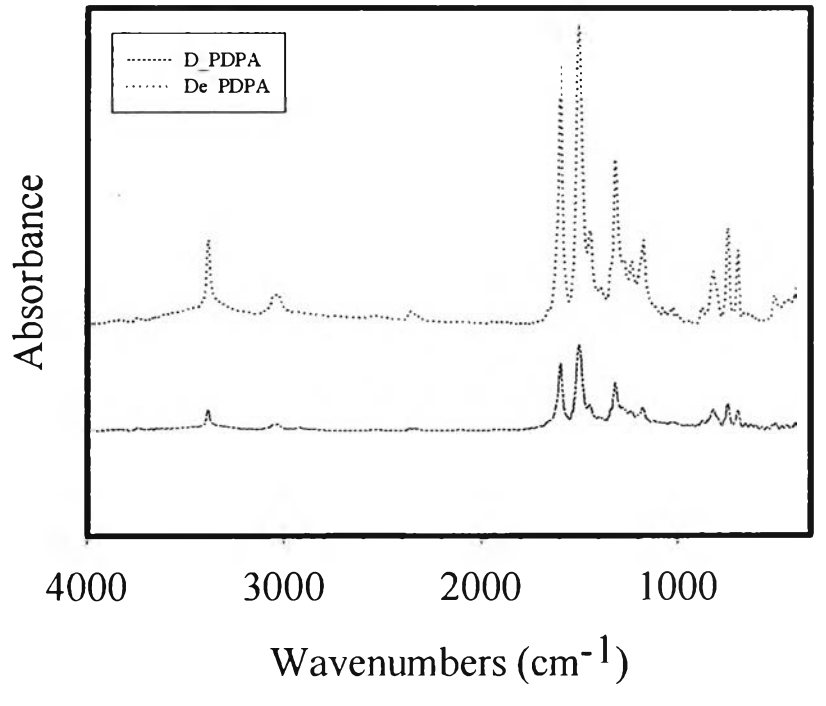

Figure A1 The FT-IR spectrum of doped-Polydiphenylamine (D_PDPA) and dedoped_polydiphenylamine (De_PDPA).

Table A1 The FT-IR absorption spectrum of D_PDPA and De_PDPA

Wavenumbers (cm^{-1})			Assignments	References
D_PDPA	**De_PDPA**	**References**		
3387	3387	3400	N-H (stretching)	Zhao *et al.,2005*
3034	3032	3100-3000	C-H Aromatic	Santana *et al.*,2003
1595, 1499	1595, 1501	1595, 1506	C=C (stretching)	Santana *et al.*,2003
1448	1447	1450	C=N (stretching)	Zhao *et al.,2005*
1317	1319	1317	C-N (stretching) Benzenoil	Santana *et al.*,2003
1173, 1237	1174, 1237	1260-1000	C-O Alcohol	Santana *et al.*,2003
824	822	812	1,4 disubstitute ring	Zhao *et al.,2005*
900-650	900-650	900-650	Substitution pattern on aromatic rings	Zhao *et al.,2005*

Variation of doping mole ratio ($N_{HCl}/N_{monomer}$) of PDPA

The dedope-PDPAr was doped with HCl at various doping mole ratio ($N_{HCl}/N_{monomer}$). The mole ratios chosen were 1:100, 1:10, 1:1, 10:1, 100:1, and 200:1. The dedoped-PDPA powder was stirred with HCl solutions for 24 hrs, filttered, and vacuum dried at 25°C for 24 hrs. To compare peaks intensity of FT-IR spectra of De_PDPA and D_PDPA of various doping mole ratios PDPA 10:1, 100:1, 200:1, and synthesized PDPA in 1 M HCl. 0.76 mg of each polymer was precisely mixed with 51.4 mg of dried-KBr, or 3:200 (g/g), the mixed samples were compressed into sample pellets. The FT-IR spectrum of each polymer is compared to each others as in the following (Figure A2).

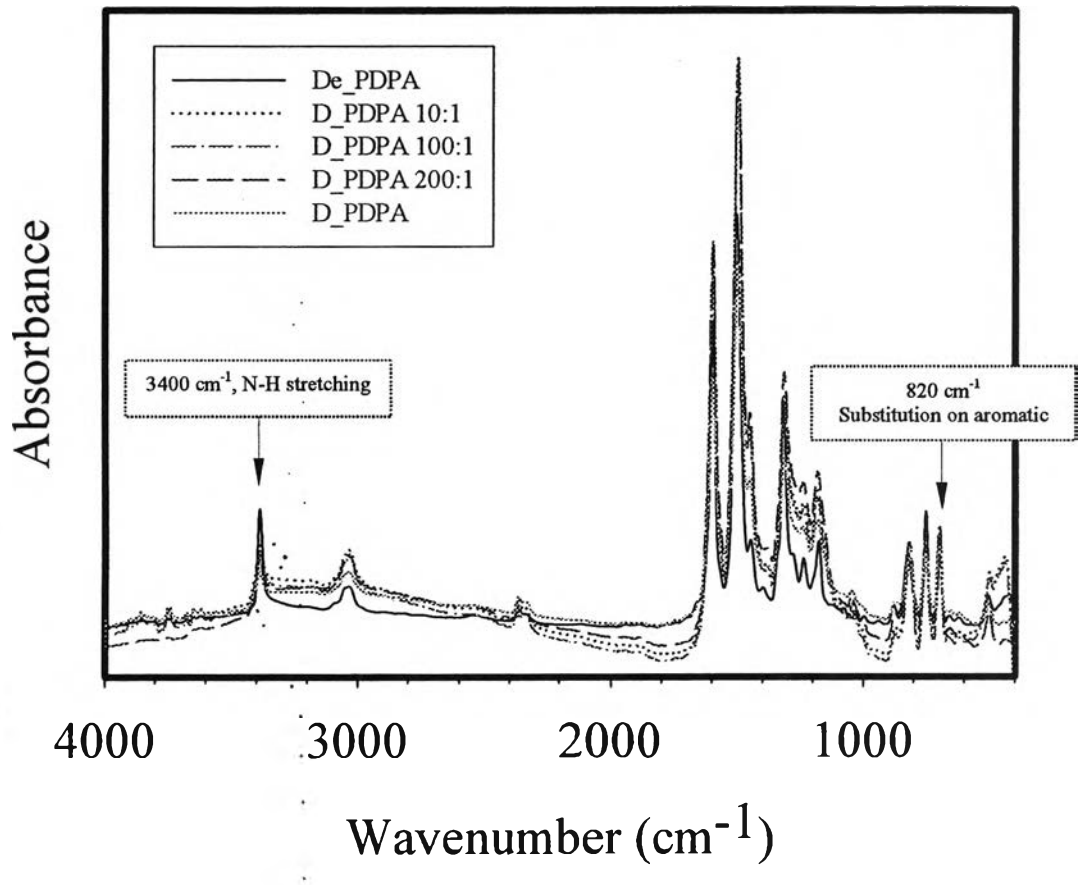

Figure A2 FT-IR spectra of dedoped-Polydiphenylamine (De_PDPA) and doped_Polydiphenylamine (D_PDPA) of various doping levels 10:1, 100:1, 200:1, and the synthesized PDPA in 1 M HCl.

The spectra show above the N-H stretching peaks at 3400 cm^{-1} (Zhao *et al., 2005*); the peak intensity significantly decreases as the doping mole ratio is increased (Figure A3). Moreover, in the range of 2000 cm^{-1} to 3800 cm^{-1}, the spectra of the doped PDPA become broad peaks while the spectrum of dedoped PDPA becomes shape and planar peak.

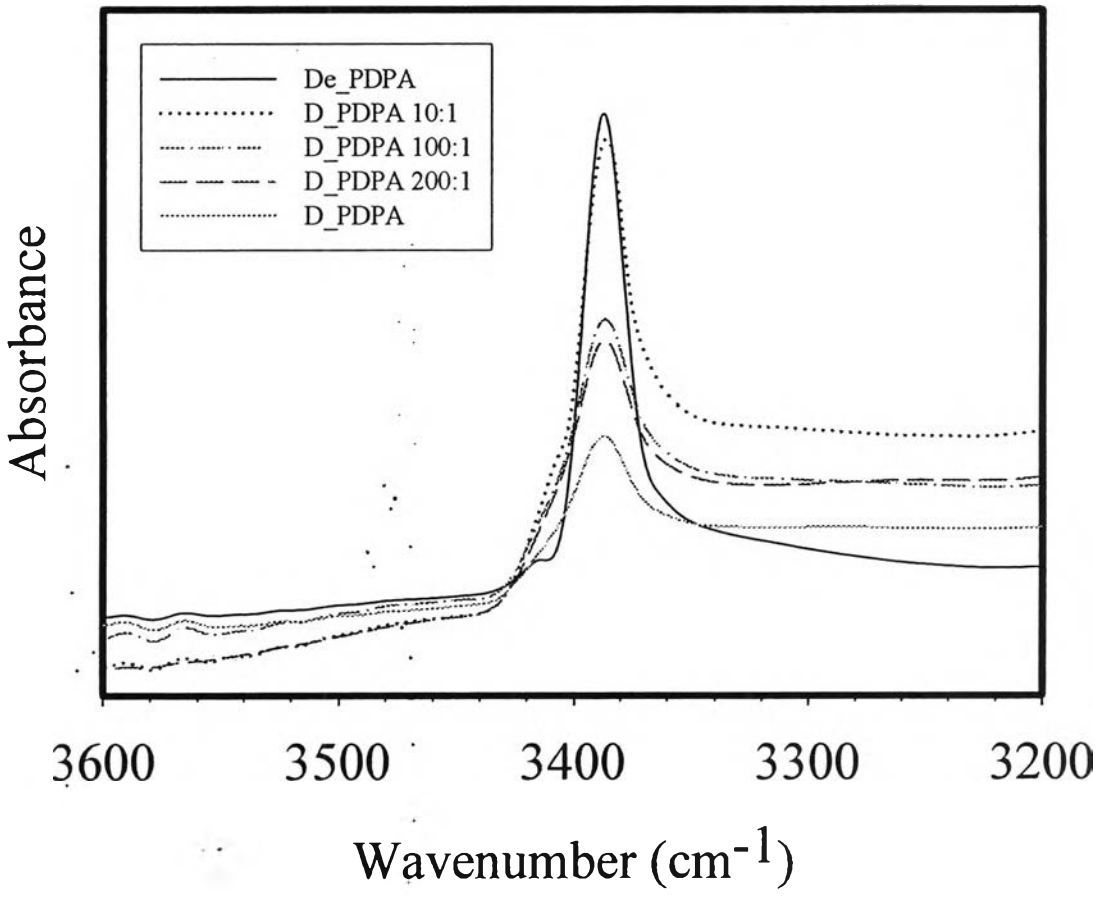

Figure A3 FT-IR spectra of dedoped-Polydiphenylamine (De_PDPA) and doped_Polydiphenylamine (D_PDPA) of various doping level 10:1, 100:1, 200:1, and the synthesized PDPA in 1 M HCl, at wavenumber between 3200-3600 cm^{-1}.

Appendix B Identification of Characteristic Peaks of Dedoped and Doped Poly(diphenylamine) from UV-Visible Spectroscopy

UV-Vis spectra were recorded with a UV-Vis absorption spectrometer (Perkin-Elmer, Lambda 10). Measurements were taken in the absorbance mode in the wavelength range of 200-900 nm. Doped-PDPAs were prepared by stirring the polymers powder with HCl solutions for 24 hours using various mole ratio of HCl to PDPA monomer (100:1 10:1 1:1 1:10 and 1:100). Dedoped-PDPA was dissolved in THF at the concentration of 0.05 g/L. Scan speed is 240 mm/min, and a slit width of 2.0 nm, using a deuterium lamp as the light source.

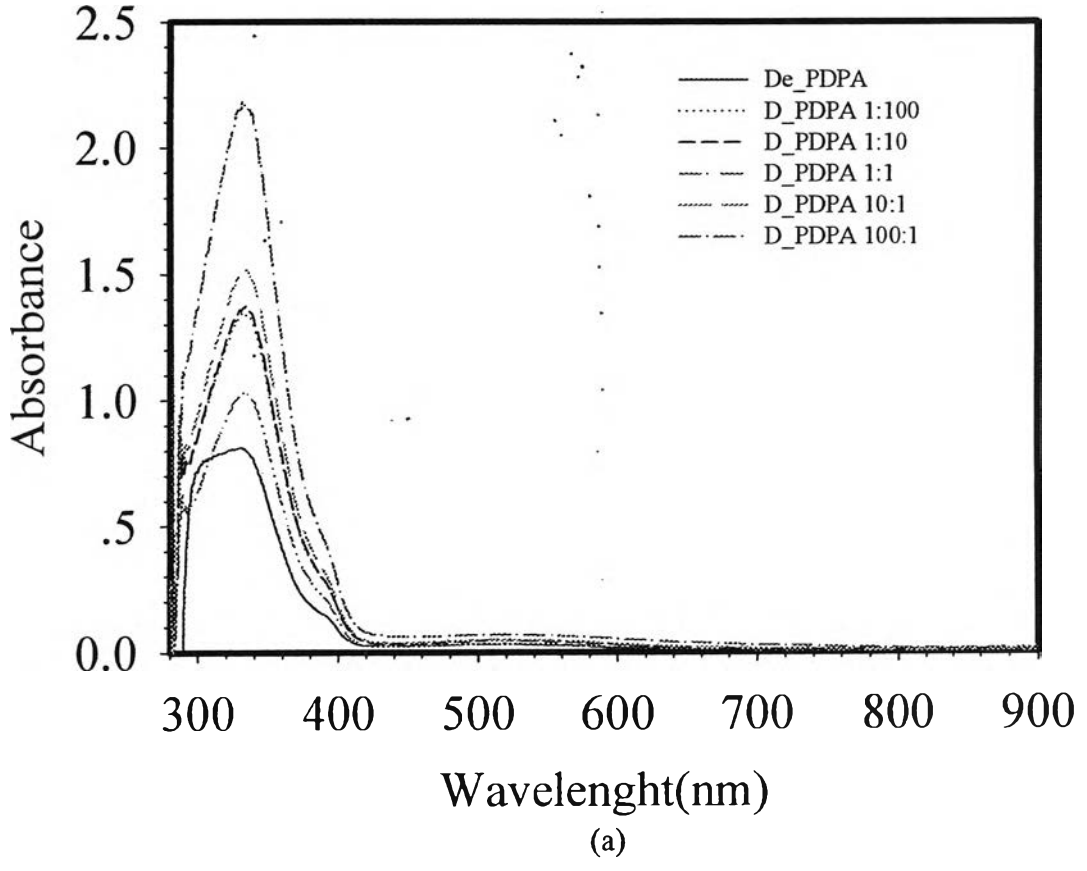

(a)

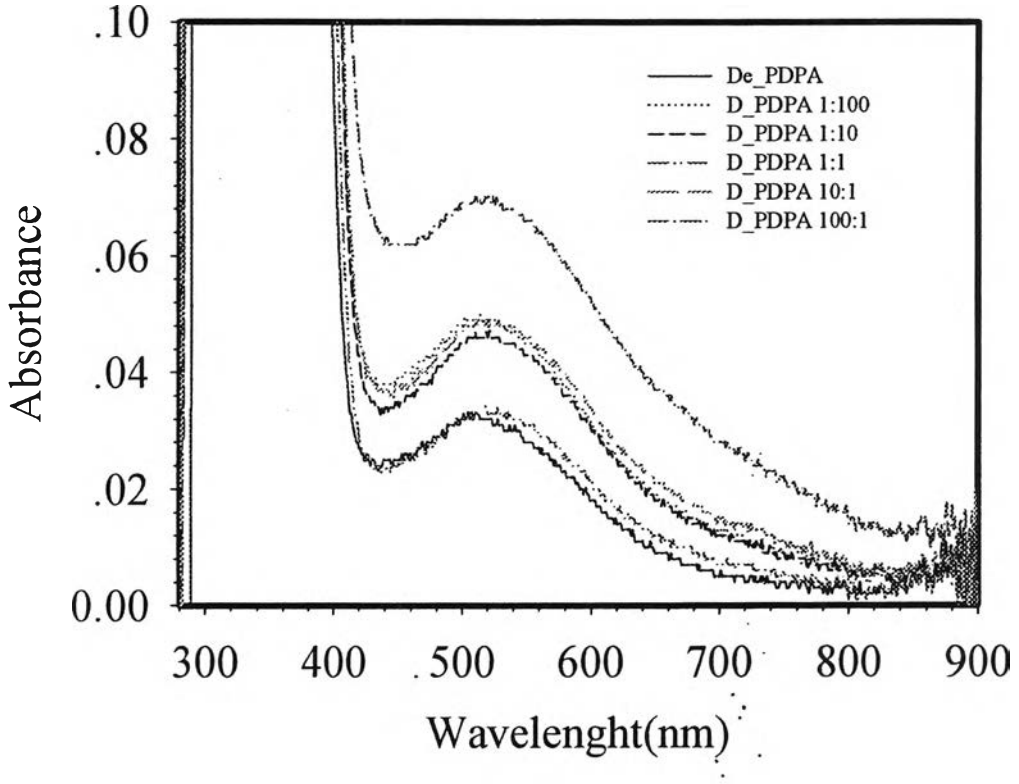

Figure B1 UV-Visible spectra of Dedoped-poly(diphenylamine)(De_PDPA) and HCl-doped poly(diphenylamine)(D_PDPA) at the mole ratio of acid to monomer of 100:1, 10:1, 1:1, 1:10 and 1:100 in THF : (a) the significant peak at wavelength about 320 nm for the Benzenoid ring; (b) the peaks at wavelength about 520nm indicating the neutralized amine.

Table B1 Absorbance spectra of Dedoped-poly(diphenylamine)(De_PDPA) and HCl-doped-poly(diphenylamine)(D_PDPA) at the mole ratio of acid to monomer 100:1, 10:1, 1:1, 1:10 and 1:100, in THF

	Wavelength (nm)			
De_PDPA	330	–	528	–
D_PDPA 100:1	332	–	524	–
D_PDPA 10:1	335	–	523	–
D_PDPA 1:1	335	–	519	–
D_PDPA 1:10	332	–	510	–
D_PDPA 1:100	331	–	514	–
	[320]	[460]	[520]	[630]
Assignment	¶-¶* transition of benzenoid ring	protonation of amine sites	neutralized	polaron
	Hua et al.,2003	Tsai et al.,2003	Hua et al.,2003	Hua et al.,2003

[ ] refer to results of the assignments cited from references.

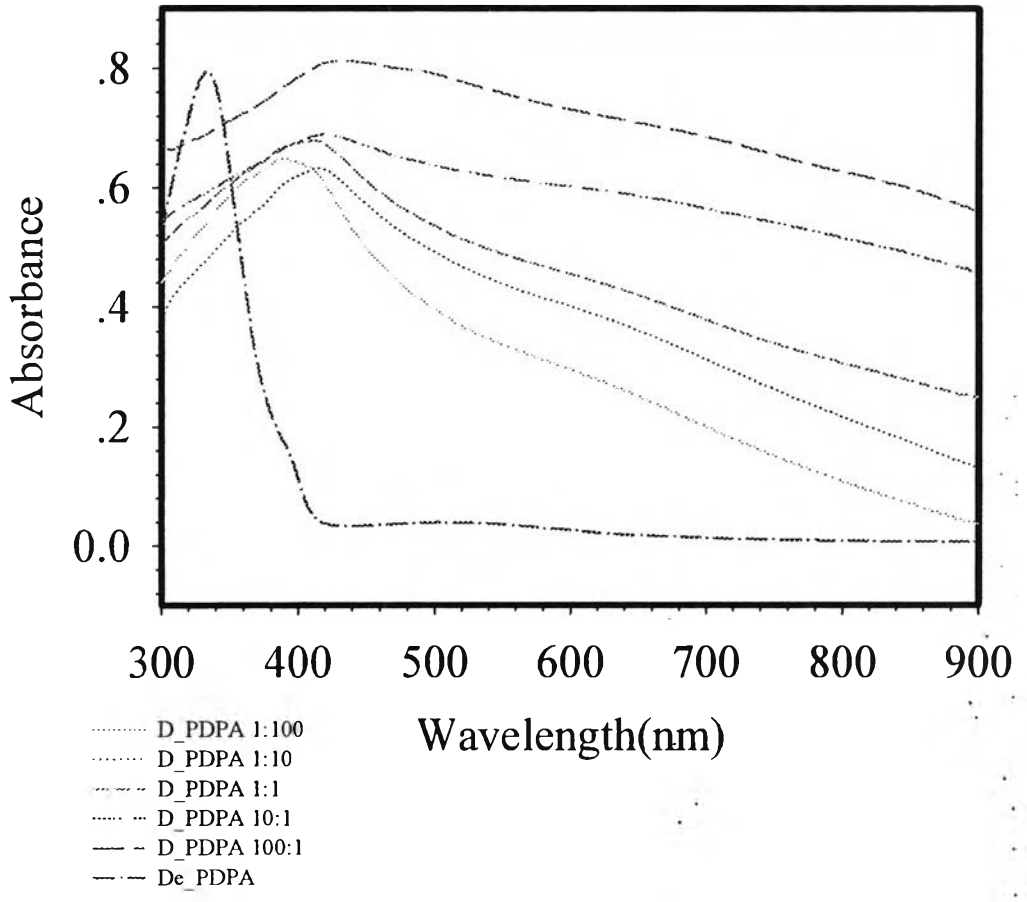

Figure B2 UV-Visible spectra of Dedoped-poly(diphenylamine)(De_PDPA) in THF and HCl-doped poly(diphenylamine)(D_PDPA) at the mole ratios of acid to monomer 100:1, 10:1, 1:1, 1:10 and 1:100, in HCl solutions at each concentrations : a) the significant peak at wavelength about 320 nm indicative of the Benzenoid ring; b) the peak at wavelength about 520nm indicative of neutralized amine.

Table B2 Absorbance spectra of Dedoped-poly(diphenylamine)(De_PDPA) in THF and HCl-doped poly(diphenylamine)(D_PDPA) at the mole ratios of acid to monomer of 100:1, 10:1, 1:1, 1:10 and 1:100 in HCl solution at each concentration

	Wavelength(nm)			
De_PDPA	330	–	528	–
D_PDPA 100:1	332	441	–	660(shoulder)
D_PDPA 10:1	335	420	–	650(shoulder)
D_PDPA 1:1	335	414	–	640(shoulder)
D_PDPA 1:10	332	416	–	640(shoulder)
D_PDPA 1:100	331	400	–	620(shoulder)
	[320]	[460]	[520]	[630]
Assignment	¶-¶* transition of benzenoid ring	protonation of amine sites	neutralized	polaron
	Hua et al.,2003	Tsai et al.,2003	Hua et al.,2003	Hua et al.,2003

[ ] refer to results of the assignments cited from references.

Appendix C The Thermogravimetry Analysis of dedoped-polydiphenylamine (De_PDPA)

The thermogravimetric analyzer (Perkin Elmer, TGA7) was used to determine the thermal behavior of polymers. The experiment was carried out by weighting a powder sample of 5-10 mg and placed it in a platinum pan, and then heated it under nitrogen flow with the heating rate 10 °C/min from 30-800°C. From Figure C1, the TGA thermogram of De_PDPA indicates degradation of De_PDPA main chain beyond the temperature of 440°C.

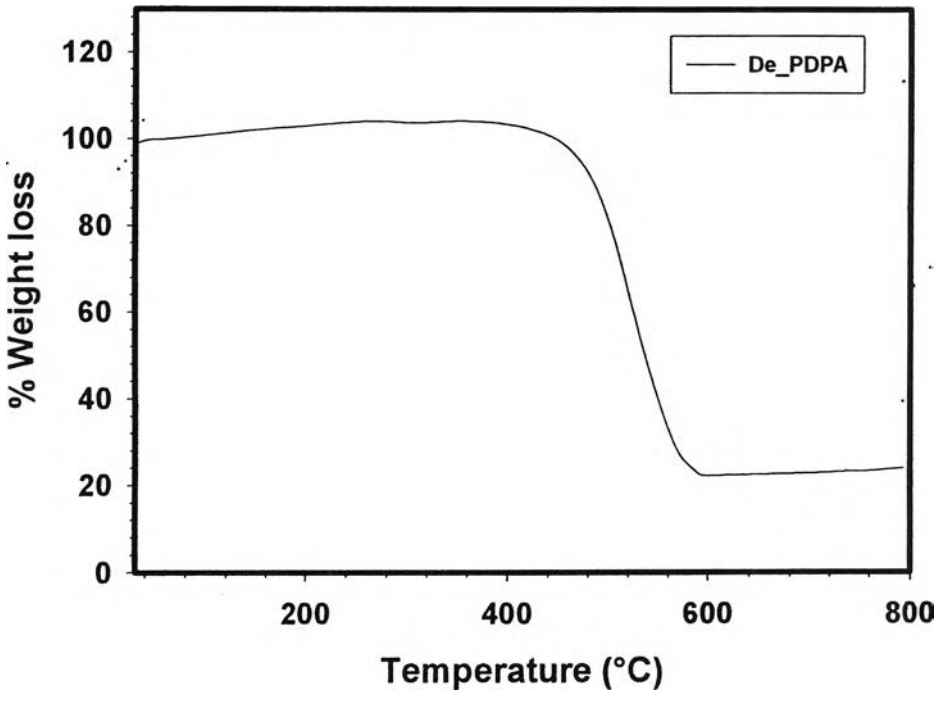

Figure C1 TGA thermogram of De_PDPA.

Appendix D Polarizing Optical Microscope

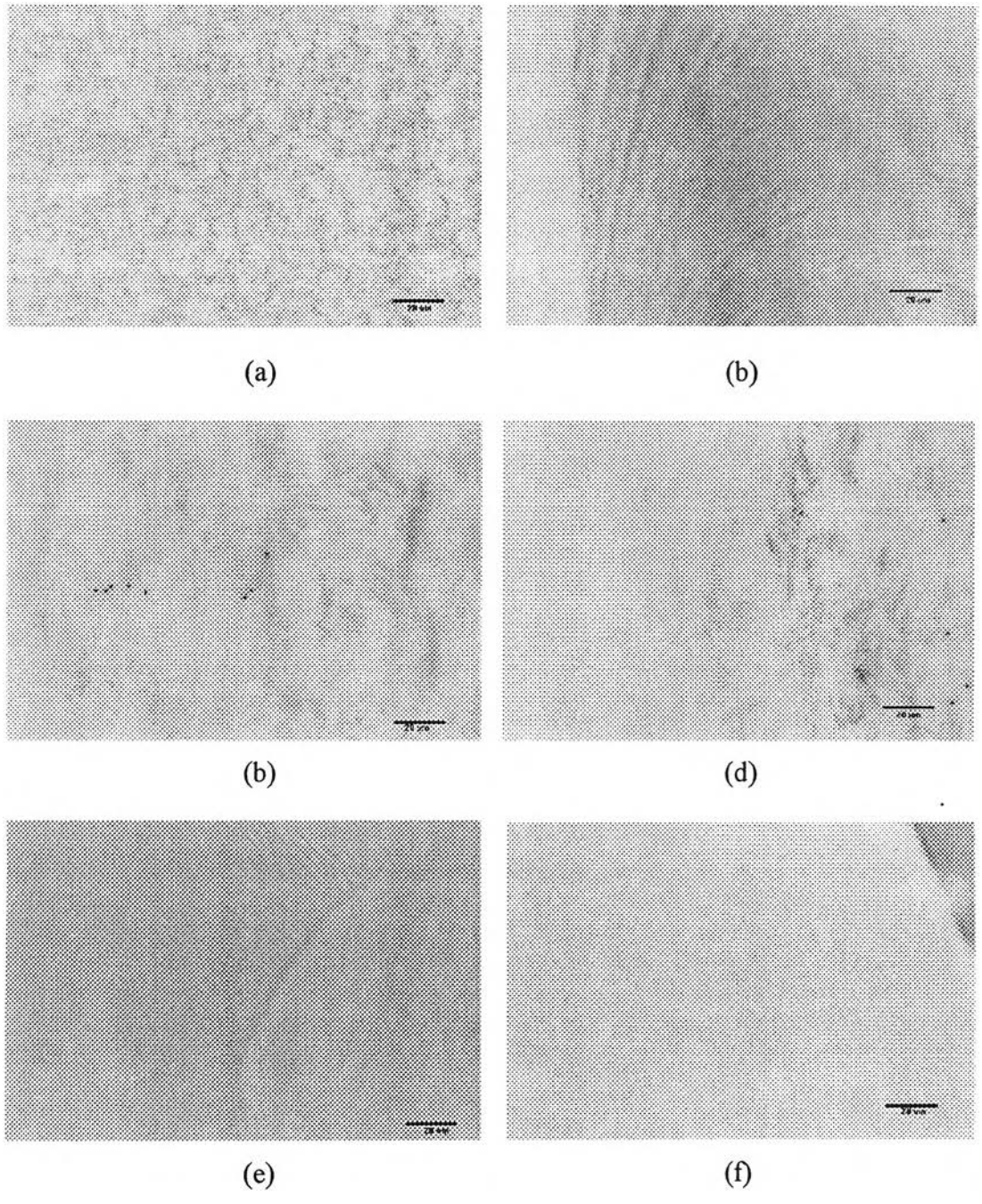

Figure D1 The morphology of SIS films prepared from 3% (w/v) SIS in toluene of: (a) D1114P (19 %wt PS, top view); (b) D1114P (19 %wt PS, side view); (c) D1164P (29 %wt PS, top view); (d) D1164P (29 %wt PS, side view); (e) D1162P (44 %wt PS, top view); (f) D1162P (44 %wt PS, side view), at 200 times magnification.

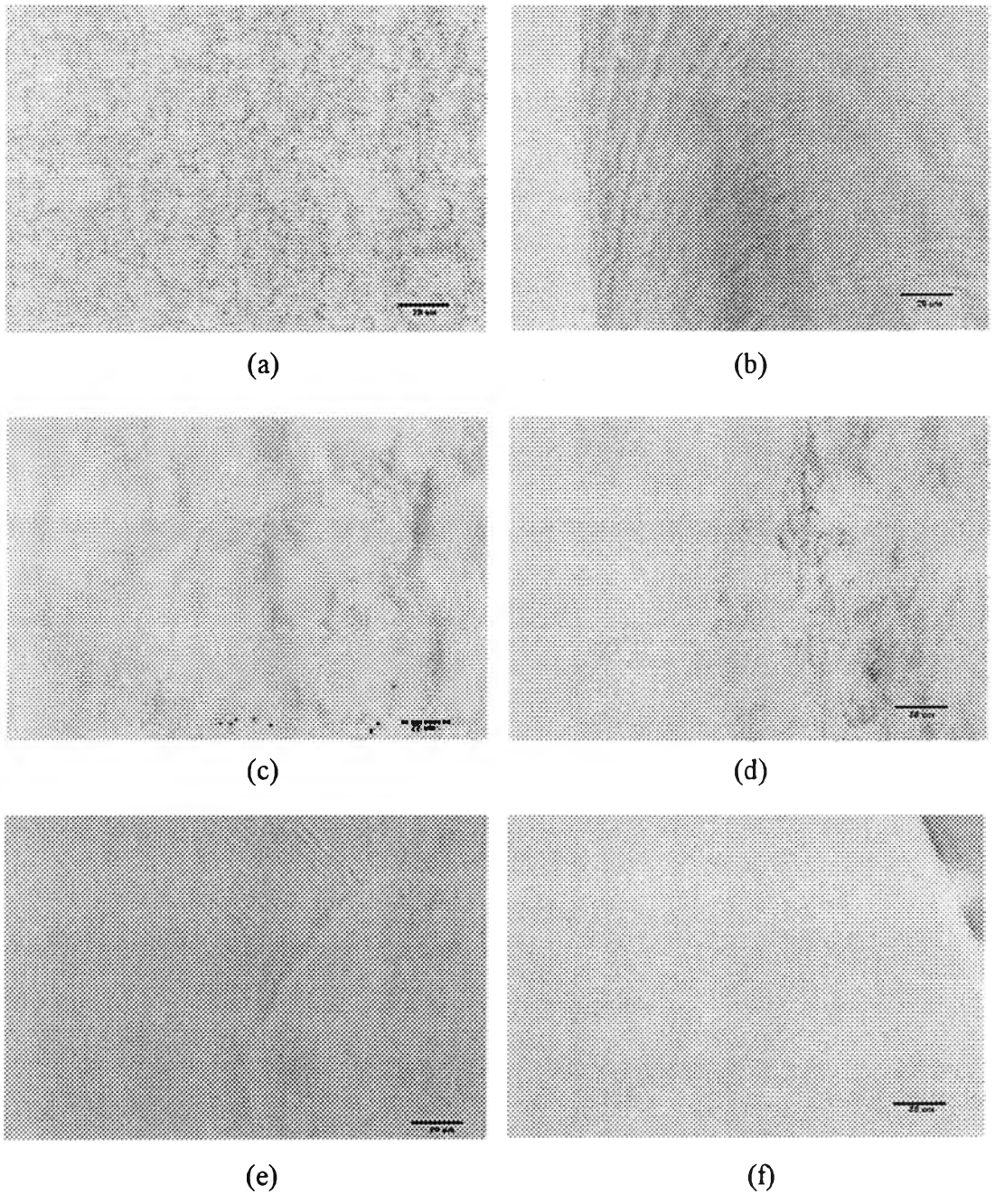

Figure D2 The morphology of SIS films prepared from 3% (w/v) SIS in toluene of: (a) D1114P (19 %wt PS, top view); (b) D1114P (19 %wt PS, side view); (c) D1164P (29 %wt PS, top view); (d) D1164P (29 %wt PS, side view); (e) D1162P (44 %wt PS, top view); (f) D1162P (44 %wt PS, side view), at 500 times magnification.

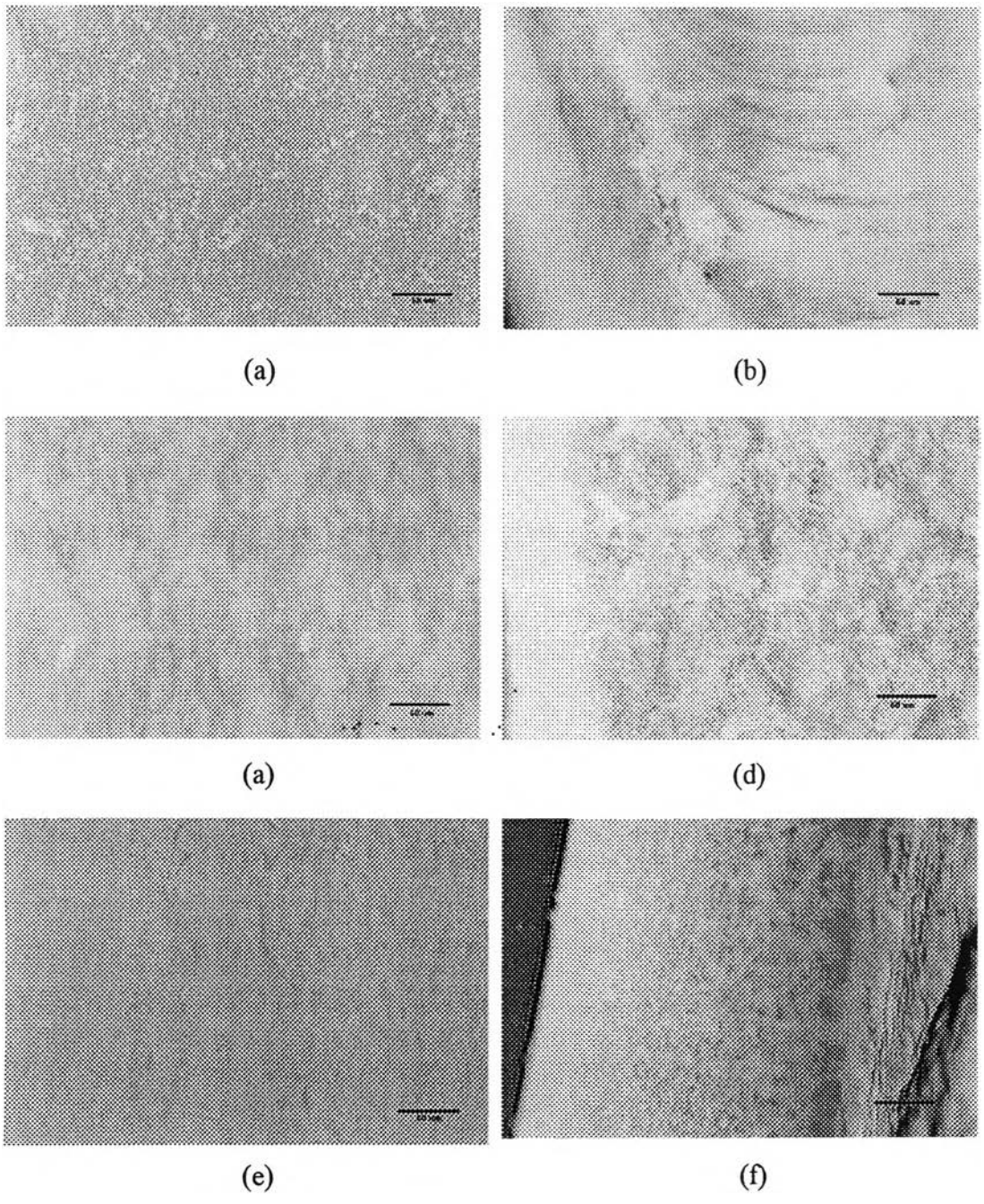

Figure D3 The morphology of SIS films prepared from 5% (w/v) SIS in toluene of: (a) D1114P (19 %wt PS, top view); (b) D1114P (19 %wt PS, side view); (c) D1164P (29 %wt PS, top view); (d) D1164P (29 %wt PS, side view); (e) D1162P (44 %wt PS, top view); (f) D1162P (44 %wt PS, side view), at 200 times magnification.

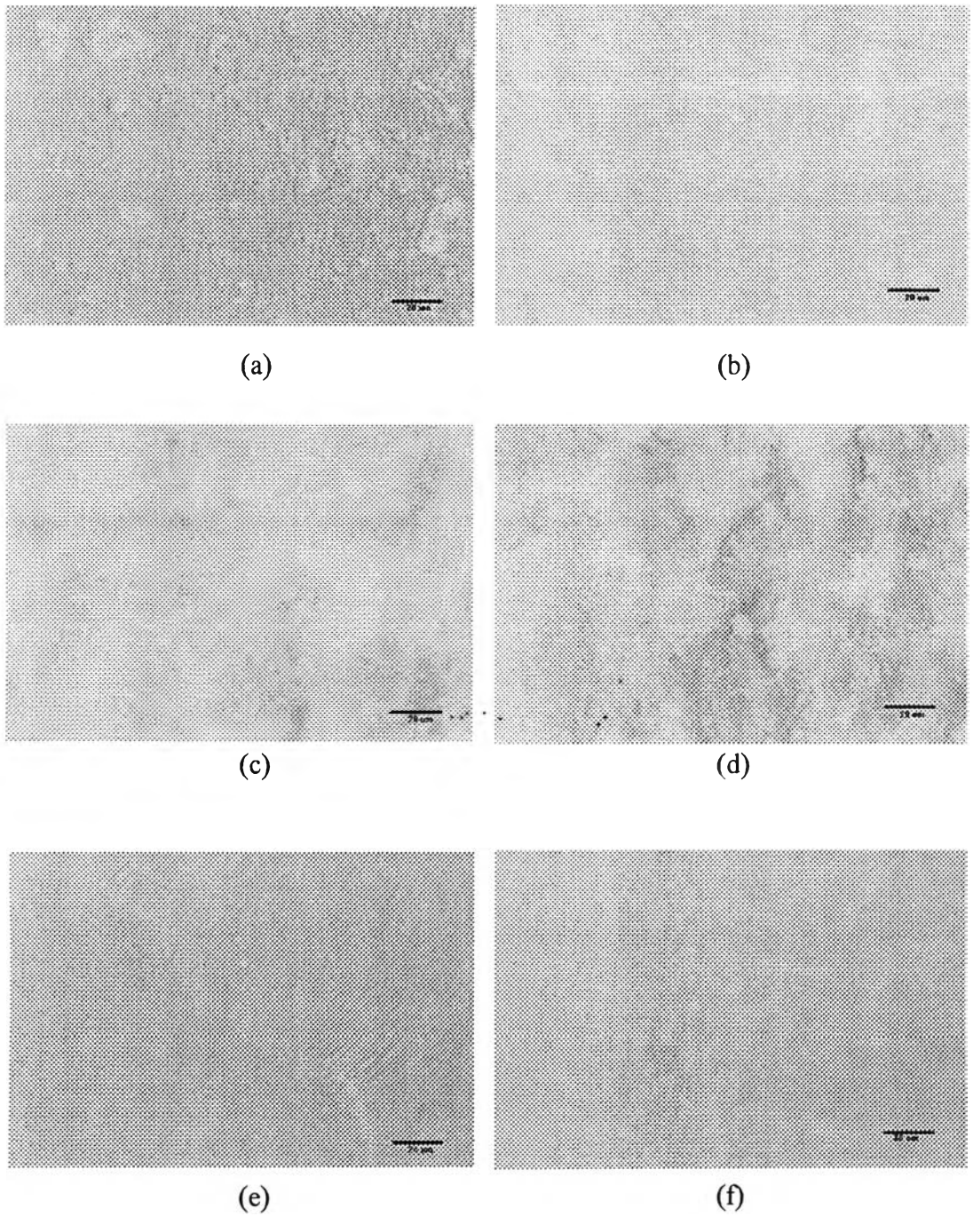

Figure D4 The morphology of SIS films prepared from 5% (w/v) SIS in toluene of: (a) D1114P (19 %wt PS, top view); (b) D1114P (19 %wt PS, side view); (c) D1164P (29 %wt PS, top view); (d) D1164P (29 %wt PS, side view); (e) D1162P (44 %wt PS, top view); (f) D1162P (44 %wt PS, side view), at 500 times magnification.

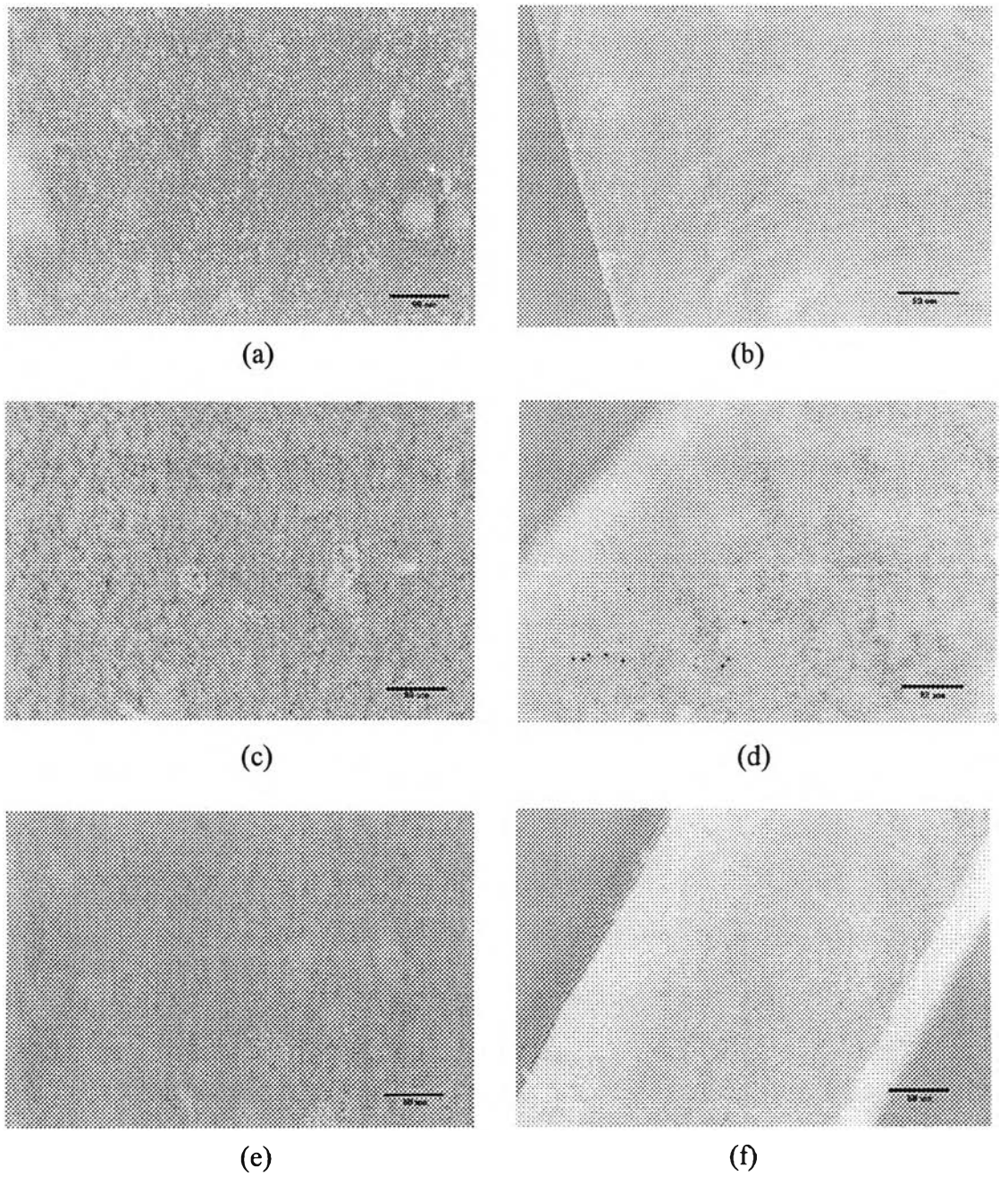

Figure D5 The morphology of SIS films prepared from 10% (w/v) SIS in toluene of: (a) D1114P (19 %wt PS, top view); (b) D1114P (19 %wt PS, side view); (c) D1164P (29 %wt PS, top view); (d) D1164P (29 %wt PS, side view); (e) D1162P (44 %wt PS, top view); (f) D1162P (44 %wt PS, side view), at 200 times magnification.

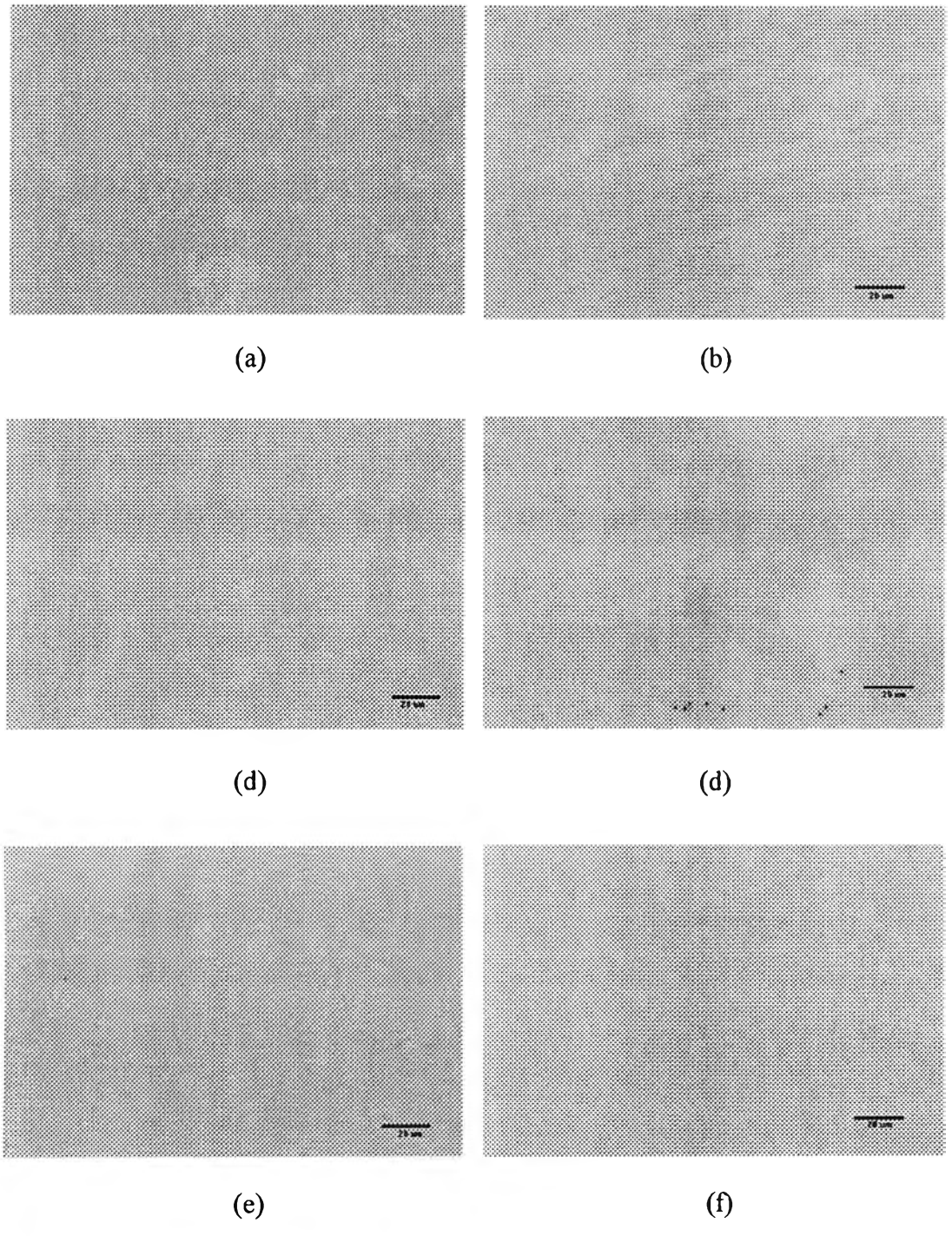

Figure D6 The morphology of SIS films prepared from 10% (w/v) SIS in toluene of: (a) D1114P (19 %wt PS, top view); (b) D1114P (19 %wt PS, side view); (c) D1164P (29 %wt PS, top view); (d) D1164P (29 %wt PS, side view); (e) D1162P (44 %wt PS, top view); (f) D1162P (44 %wt PS, side view), at 500 times magnification.

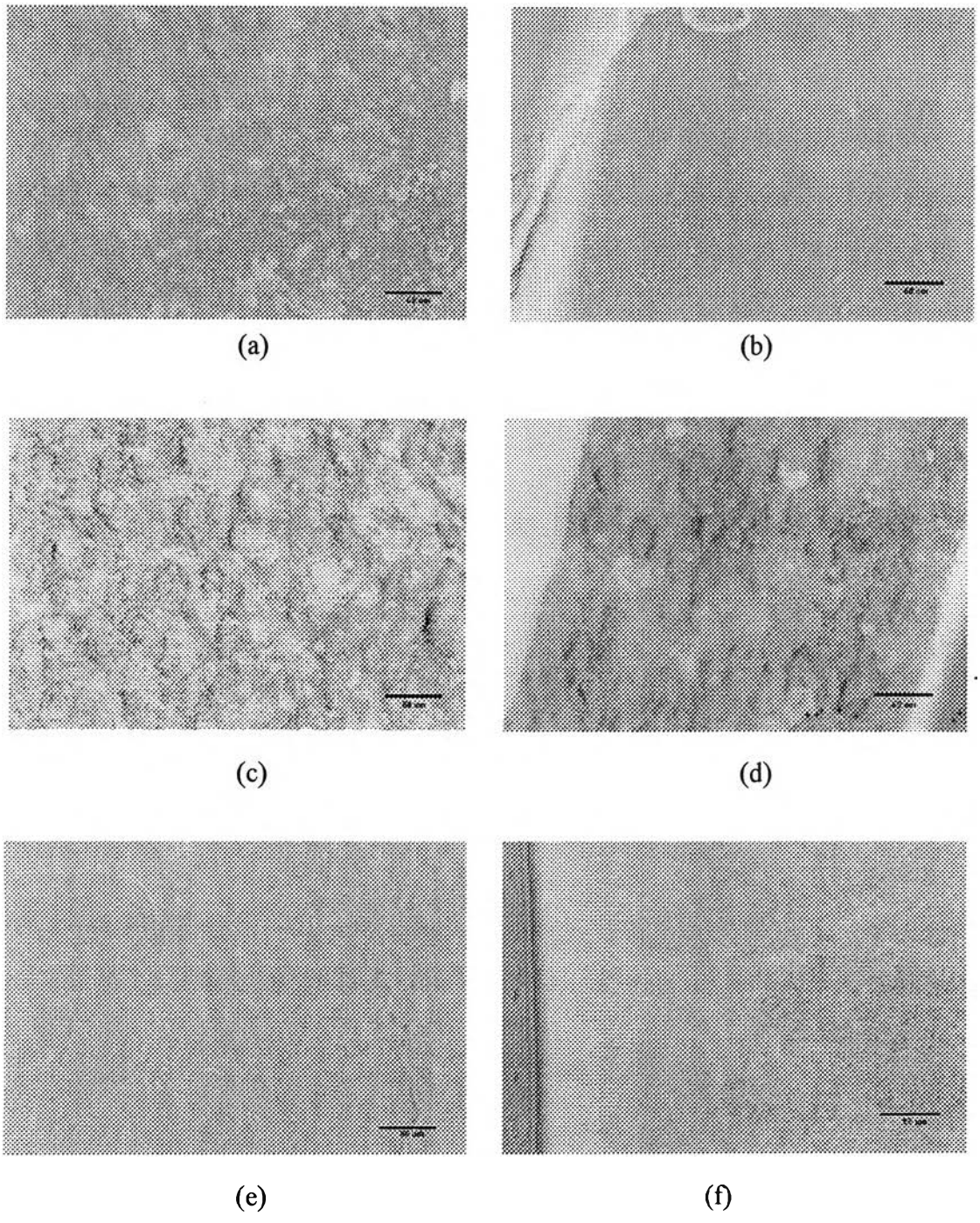

Figure D7 The morphology of SIS films prepared from 15% (w/v) SIS in toluene of: (a) D1114P (19 %wt PS, top view); (b) D1114P (19 %wt PS, side view); (c) D1164P (29 %wt PS, top view); (d) D1164P (29 %wt PS, side view); (e) D1162P (44 %wt PS, top view); (f) D1162P (44 %wt PS, side view), at 200 times magnification.

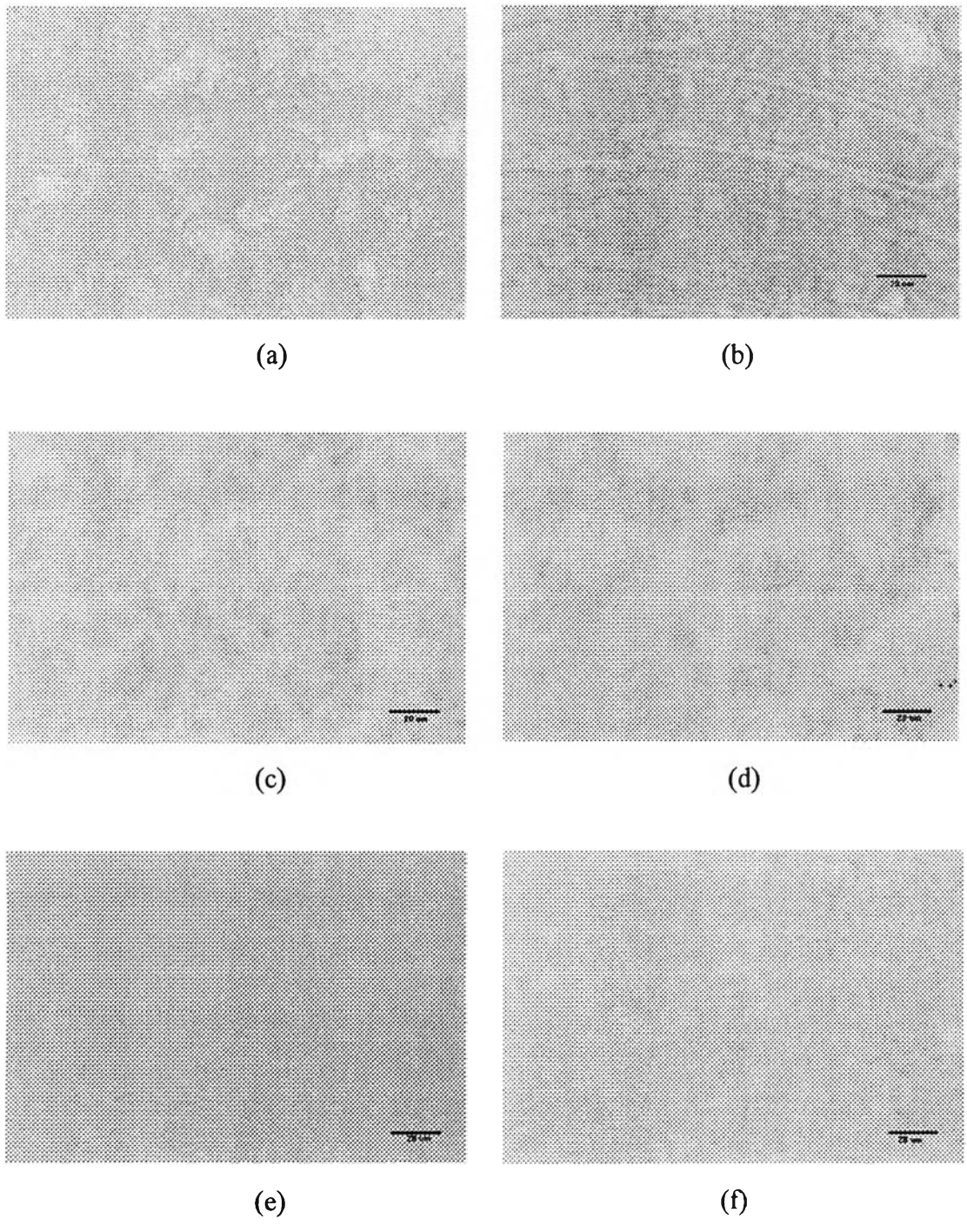

Figure D8 The morphology of SIS films prepared from 15% (w/v) SIS in toluene of: (a) D1114P (19 %wt PS, top view); (b) D1114P (19 %wt PS, side view); (c) D1164P (29 %wt PS, top view); (d) D1164P (29 %wt PS, side view); (e) D1162P (44 %wt PS, top view); (f) D1162P (44 %wt PS, side view), at 500 times magnification.

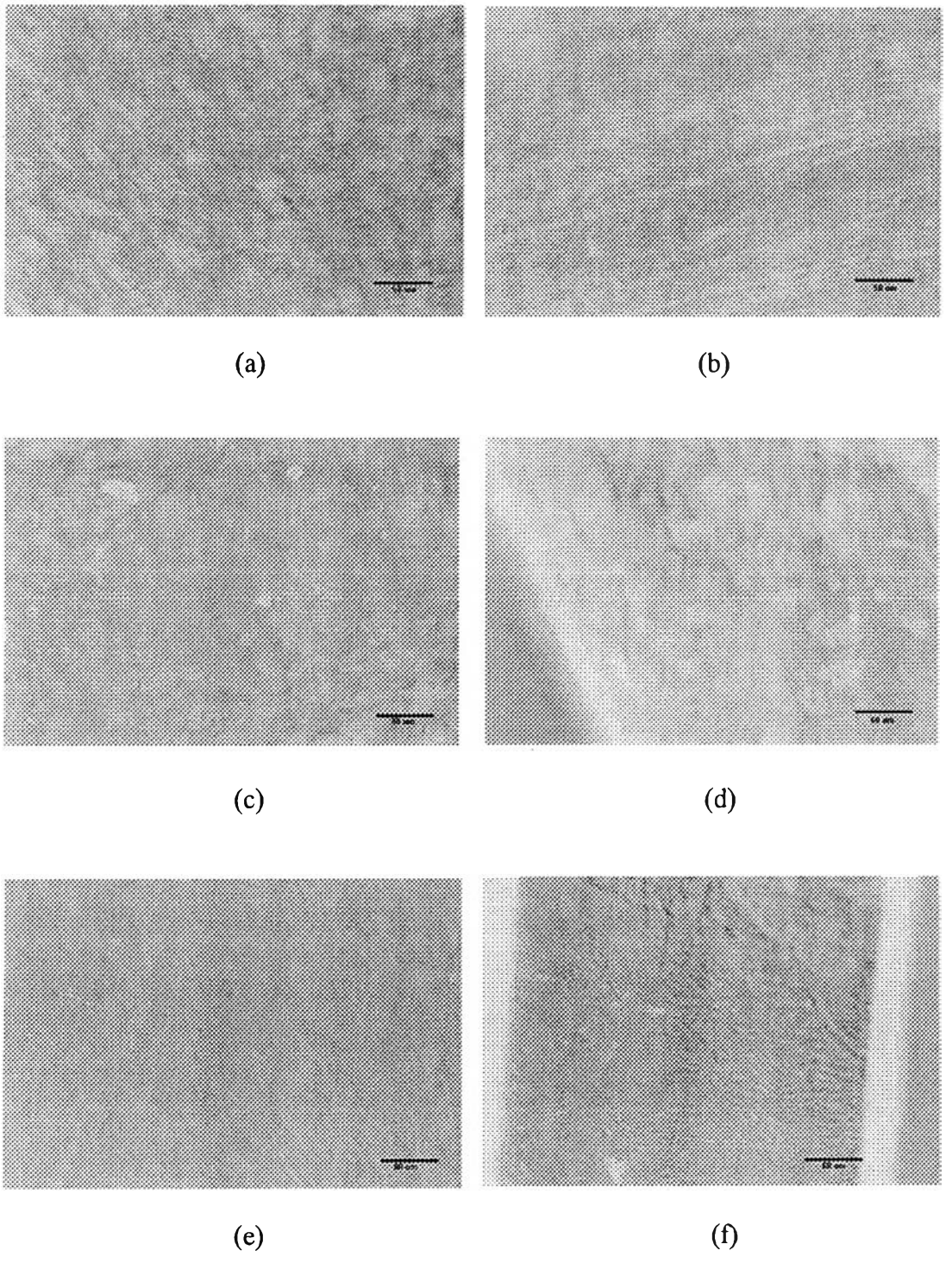

Figure D9 The morphology of SIS films prepared from 20% (w/v) SIS in toluene of: (a) D1114P (19 %wt PS, top view); (b) D1114P (19 %wt PS, side view); (c) D1164P (29 %wt PS, top view); (d) D1164P (29 %wt PS, side view); (e) D1162P (44 %wt PS, top view); (f) D1162P (44 %wt PS, side view), at 200 times magnification.

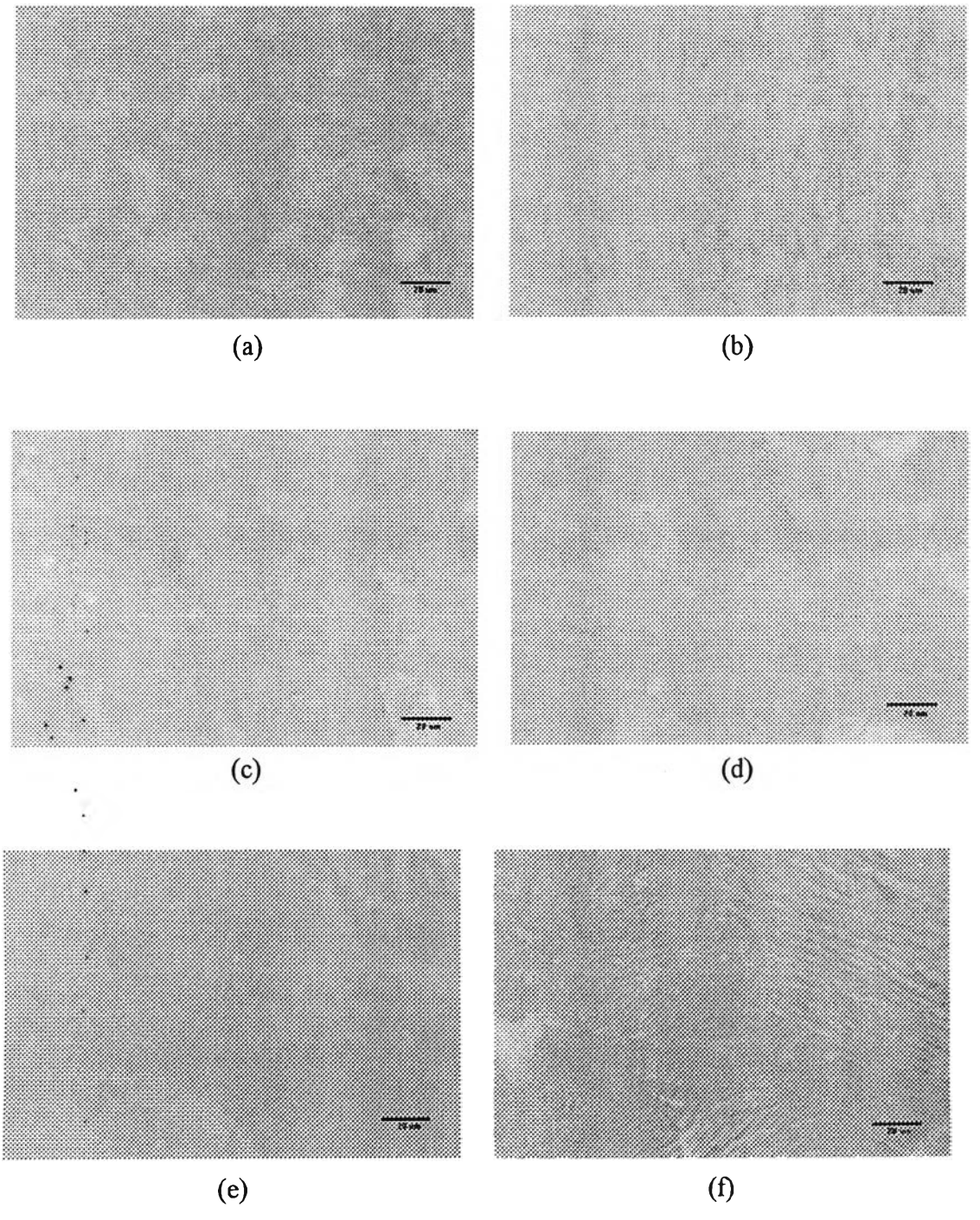

Figure D10 The morphology of SIS films prepared from 20% (w/v) SIS in toluene of: (a) D1114P (19 %wt PS, top view); (b) D1114P (19 %wt PS, side view); (c) D1164P (29 %wt PS, top view); (d) D1164P (29 %wt PS, side view); (e) D1162P (44 %wt PS, top view); (f) D1162P (44 %wt PS, side view), at 500 times magnification.

Appendix E Correction Factor (K) Measurement

A two point probe meter connected with a source power supplier (Keithley/ Model 6517A) was employed to determine the electrical conductivity of materials. A constant voltage was applied and the current was simultaneously measured.

According to the geometric effects of the probe, the geometrical correction factor depends on the configuration and probe tip spacing:

$$K = w/l \tag{E.1}$$

where K is the geometric correction factor, w is the probe width or the tip spacing (cm), and l is the probe length (cm).

The geometric correction factor can be determined by using standard materials whose specific resistivity values are known. In our case, silicon wafer chips were used as the standard materials. The resistance was measured by using our custom-made. two-point probe, obtained by applying various voltages and simultaneously measuring currents. The geometric correction factor was calculated via the equation:

$$K = \rho/R \times t = I \times \rho/V \times t \tag{E.2}$$

where ρ is the resistivity of a standard silicon wafer (Ω.cm), R is the resistance of film (Ω), t is the film thickness (cm), I is the measured current (A) and V is the applied voltage (V).

Table E1 Voltage-current data of the probe number 1 calibration with Si-wafer whose sheet resistivity of 107.373 Ω/sq, 25°C, 60-65 %RH

V			I			K=I/V*ρ/t		
1	2	3	1	2	3	1	2	3
0.2	0.2	0.2	1.07E-07	1.01E-07	9.8E-08	5.76E-05	5.44E-05	5.26E-05
0.3	0.3	0.3	2.33E-07	2.3E-07	2.37E-07	8.35E-05	8.24E-05	8.49E-05
0.5	0.5	0.5	6.67E-07	6.64E-07	6.65E-07	1.43E-04	1.43E-04	1.43E-04
0.7	0.7	0.7	1.12E-06	1.14E-06	1.16E-06	1.72E-04	1.75E-04	1.78E-04
1	1	1	1.88E-06	1.88E-06	1.87E-06	2.02E-04	2.01E-04	2.01E-04
2	2	2	4.05E-06	4.07E-06	4.05E-06	2.18E-04	2.18E-04	2.17E-04
3	3	3	6.32E-06	6.3E-06	6.3E-06	2.26E-04	2.26E-04	2.25E-04
4	4	4	8.4E-06	8.48E-06	8.43E-06	2.25E-04	2.28E-04	2.26E-04
5	5	5	1.04E-05	1.05E-05	1.05E-05	2.23E-04	2.25E-04	2.26E-04
6	6	6	1.25E-05	1.27E-05	1.27E-05	2.23E-04	2.28E-04	2.26E-04
7	7	7	1.56E-05	1.52E-05	1.47E-05	2.39E-04	2.33E-04	2.26E-04
8	8	8	1.77E-05	1.81E-05	1.8E-05	2.38E-04	2.43E-04	2.42E-04
9	9	9	2.17E-05	2.17E-05	2.11E-05	2.59E-04	2.58E-04	2.52E-04
10	10	10	2.42E-05	2.45E-05	2.4E-05	2.59E-04	2.63E-04	2.58E-04

Correction factor (K)				
1	2	3	Avg.	SD
1.98E-04	1.98E-04	1.97E-04	1.98E-04	6.11E-05

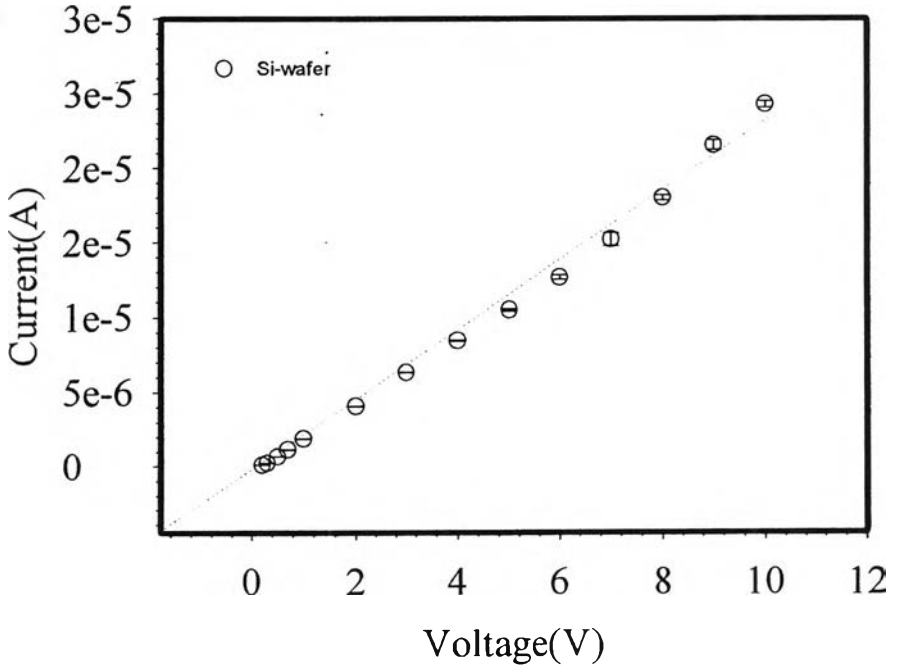

Figure E1 Voltage vs. current data of the probe number 1 calibration with Si-wafer whose sheet resistivity of 107.373 Ω/sq, 25°C, 60-65 %RH.

Appendix F Conductivity Measurement

The electrical conductivity (σ) can be measured by using the two-point probe mater connected with a voltage supplier (Keithley, 6517A) whose constant voltage can be varied and the current is measured. The conductivity measurement was performed under atmospheric pressure, 40-60 %RH and at 25-27°C. The regime where responsive current is linearly proportional to the applied voltage is called the linear Ohmic regime which can be identified by plotting the applied voltage against with the current. The voltage and the current in the regime were converted to the electrical conductivity by following equation:

$$\sigma = 1/\rho = 1/(R \times t) = I/(R_s \times V \times t) \quad \text{(F.1)}$$

where σ is the specific conductivity (S/cm), ρ is the specific resistivity (Ω.cm), R_s is the sheet resistance (Ω/sq), t is the thickness of sample pellet (cm), V is the applied voltage (Voltage drop)(V), I is the measured current (A), and K is the geometric correction factor of the two-point probe meter. All sample thicknesses were measured by using a thickness gauge.

Table F1 The specific conductivity (S/cm) of De_PDPA, D_PDPA with various doping levels, SIS D1114, SIS D1164, and SIS D1162

Samples	Specific conductivity(S/cm)
De_PDPA	$(2.89\pm0.315)\times10^{-6}$
D_PDPA200:1	$(2.35\pm0.214)\times10^{-4}$
D_PDPA100:1	$(6.31\pm0.234)\times10^{-5}$
D_PDPA10:1	$(9.46\pm0.349)\times10^{-6}$
D_PDPA1:1	$(3.32\pm0.229)\times10^{-6}$
D_PDPA1:10	$(2.65\pm0.118)\times10^{-6}$
D_PDPA1:100	$(3.13\pm0.167)\times10^{-6}$
SIS D1114	$(1.28\pm0.158)\times10^{-19}$
SIS D1164	$(2.69\pm0.326)\times10^{-17}$
SIS D1162	$(1.17\pm0.100)\times10^{-17}$
5% De_PDPA/D1114P	$(2.24\pm0.106)\times10^{-16}$
10% DePDPA/D1114P	$(2.65\pm0.141)\times10^{-15}$
20% DePDPA/D1114P	$(2.25\pm0.536)\times10^{-14}$
30% DePDPA/D1114P	$(4.80\pm0.830)\times10^{-14}$

Polydiphenylamine

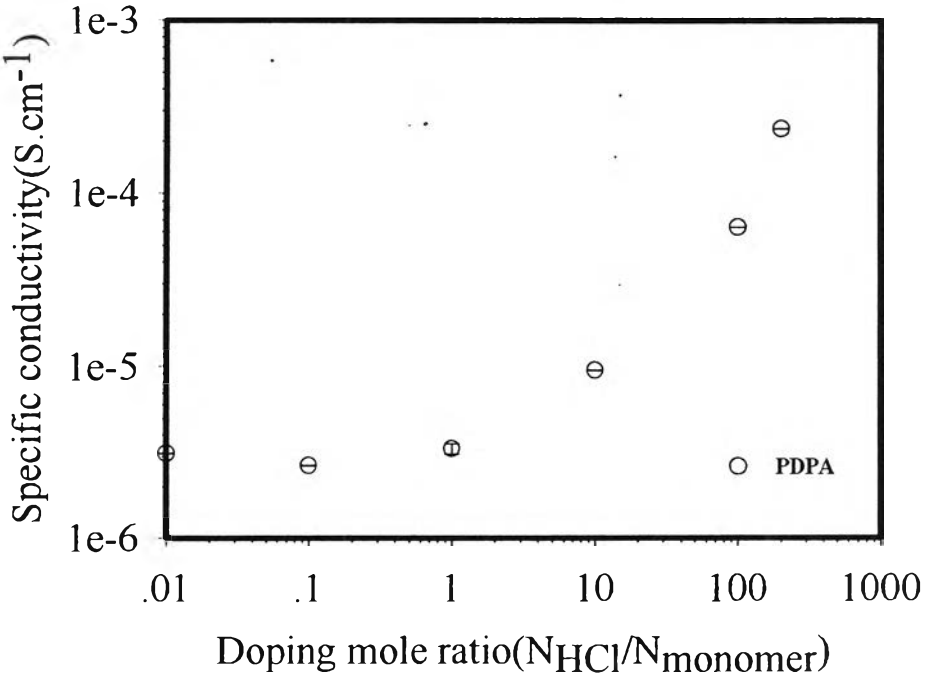

Figure F1 Specific conductivity versus doping moles ratio ($N_{HCl}/N_{monomer}$) of PDPA.

Table F2 Voltage-current data in linear regime of De_PDPA at 25°C, 60-65 %RH

Voltage(V)			Current(A)			Specific conductivity(S/cm)		
1	2	3	1	2	3	1	2	3
1	1	1	1.06E-11	1.03E-11	1.1E-11	2.12E-06	2.05E-06	2.20E-06
2	2	2	2.37E-11	2.34E-11	2.36E-11	2.37E-06	2.34E-06	2.36E-06
3	3	3	4.24E-11	4.32E-11	4.25E-11	2.82E-06	2.88E-06	2.83E-06
4	4	4	5.88E-11	5.93E-11	5.9E-11	2.94E-06	2.97E-06	2.95E-06
5	5	5	7.24E-11	7.26E-11	7.29E-11	2.90E-06	2.90E-06	2.92E-06
6	6	6	8.75E-11	8.8E-11	8.75E-11	2.91E-06	2.93E-06	2.92E-06
7	7	7	1.06E-10	1.04E-10	1.05E-10	3.02E-06	2.96E-06	3.00E-06
8	8	8	1.26E-10	1.25E-10	1.25E-10	3.14E-06	3.12E-06	3.12E-06
9	9	9	1.41E-10	1.4E-10	1.4E-10	3.13E-06	3.11E-06	3.10E-06
10	10	10	1.55E-10	1.55E-10	1.54E-10	3.10E-06	3.09E-06	3.09E-06
11	11	11	1.68E-10	1.66E-10	1.68E-10	3.05E-06	3.02E-06	3.06E-06
12	12	12	1.92E-10	1.93E-10	1.9E-10	3.19E-06	3.21E-06	3.16E-06

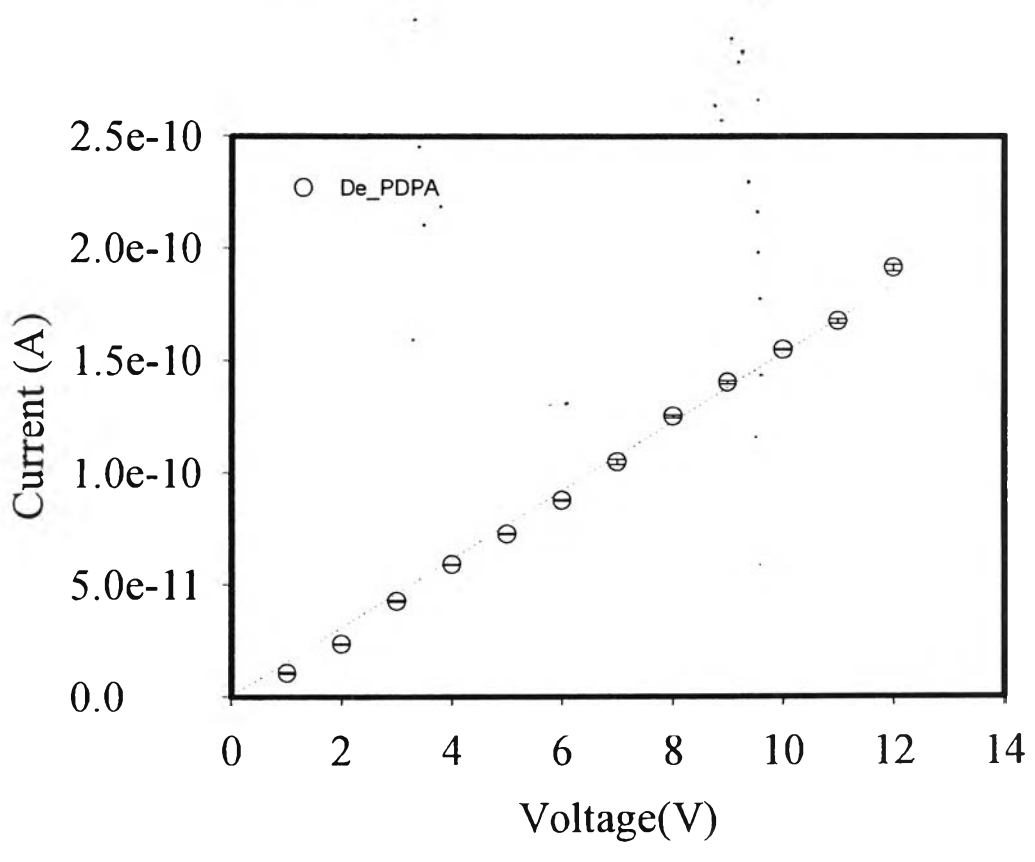

Figure F2 The Ohmic regime of De_PDPA at thickness = 0.0253 cm, 25°C, 60-65 %RH.

Table F3 Voltage-current data in linear regime of D_PDPA 1:100 at 25°C, 60-65 %RH

Voltage(V)			Current(A)			Specific conductivity(S/cm)		
1	2	3	1	2	3	1	2	3
1	1	1	1.3E-11	1.3E-11	1.32E-11	2.67E-06	2.67E-06	2.71E-06
2	2	2	2.96E-11	2.95E-11	2.96E-11	3.03E-06	3.03E-06	3.04E-06
3	3	3	4.6E-11	4.58E-11	4.6E-11	3.15E-06	3.13E-06	3.15E-06
4	4	4	6.19E-11	6.13E-11	6.22E-11	3.18E-06	3.14E-06	3.19E-06
5	5	5	7.55E-11	7.59E-11	7.63E-11	3.10E-06	3.12E-06	3.13E-06
6	6	6	9.47E-11	9.47E-11	9.42E-11	3.24E-06	3.24E-06	3.22E-06
7	7	7	1.13E-10	1.12E-10	1.13E-10	3.30E-06	3.29E-06	3.31E-06
8	8	8	1.22E-10	1.23E-10	1.23E-10	3.14E-06	3.17E-06	3.16E-06
9	9	9	1.41E-10	1.4E-10	1.39E-10	3.22E-06	3.19E-06	3.17E-06
10	10	10	1.57E-10	1.58E-10	1.59E-10	3.23E-06	3.25E-06	3.26E-06

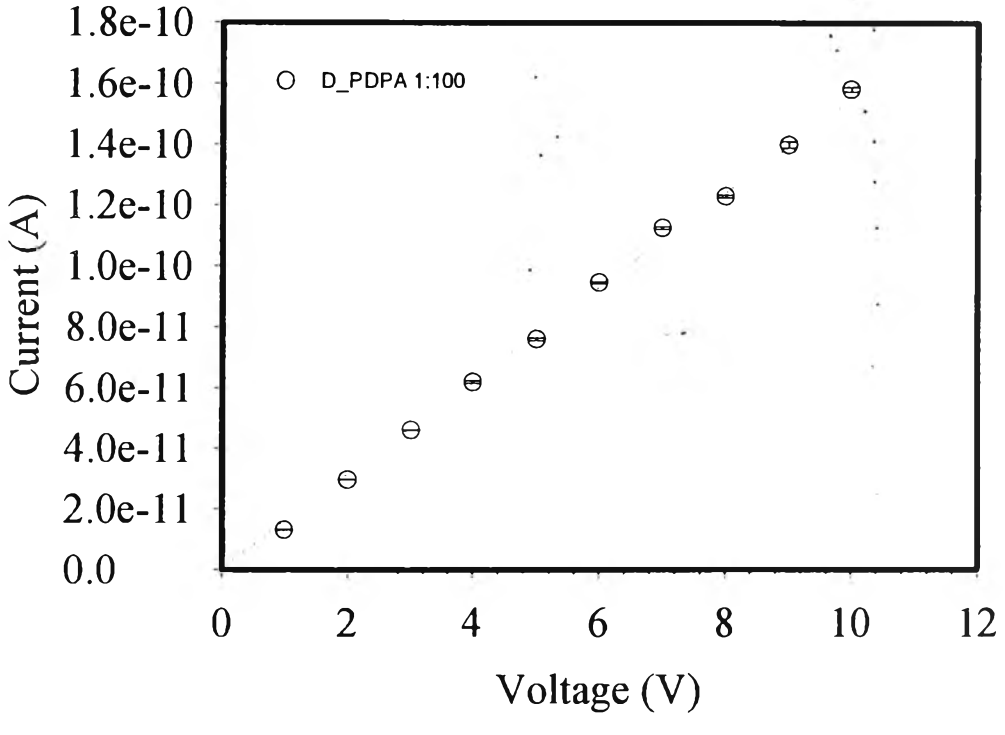

Figure F3 The Ohmic regime of D_PDPA 1:100 at thickness = 0.0246 cm, 25°C, 60-65 %RH.

Table F4 Voltage-current data in linear regime of D_PDPA 1:10 at 25°C, 60-65 %RH

Voltage(V)			Current(A)			Specific conductivity(S/cm)		
1	2	3	1	2	3	1	2	3
1	1	1	1.3E-11	1.34E-11	1.35E-11	2.34E-06	2.43E-06	2.43E-06
2	2	2	2.74E-11	2.72E-11	2.76E-11	2.47E-06	2.46E-06	2.49E-06
3	3	3	4.39E-11	4.31E-11	4.44E-11	2.64E-06	2.60E-06	2.67E-06
4	4	4	5.92E-11	5.84E-11	5.9E-11	2.67E-06	2.64E-06	2.67E-06
5	5	5	7.45E-11	7.52E-11	7.47E-11	2.69E-06	2.72E-06	2.70E-06
6	6	6	8.91E-11	8.93E-11	8.83E-11	2.68E-06	2.69E-06	2.66E-06
7	7	7	1.05E-10	1.05E-10	1.05E-10	2.72E-06	2.71E-06	2.72E-06
8	8	8	1.17E-10	1.2E-10	1.17E-10	2.65E-06	2.71E-06	2.65E-06
9	9	9	1.31E-10	1.33E-10	1.32E-10	2.63E-06	2.66E-06	2.65E-06
10	10	10	1.53E-10	1.54E-10	1.52E-10	2.76E-06	2.77E-06	2.75E-06
11	11	11	1.72E-10	1.72E-10	1.71E-10	2.82E-06	2.83E-06	2.81E-06

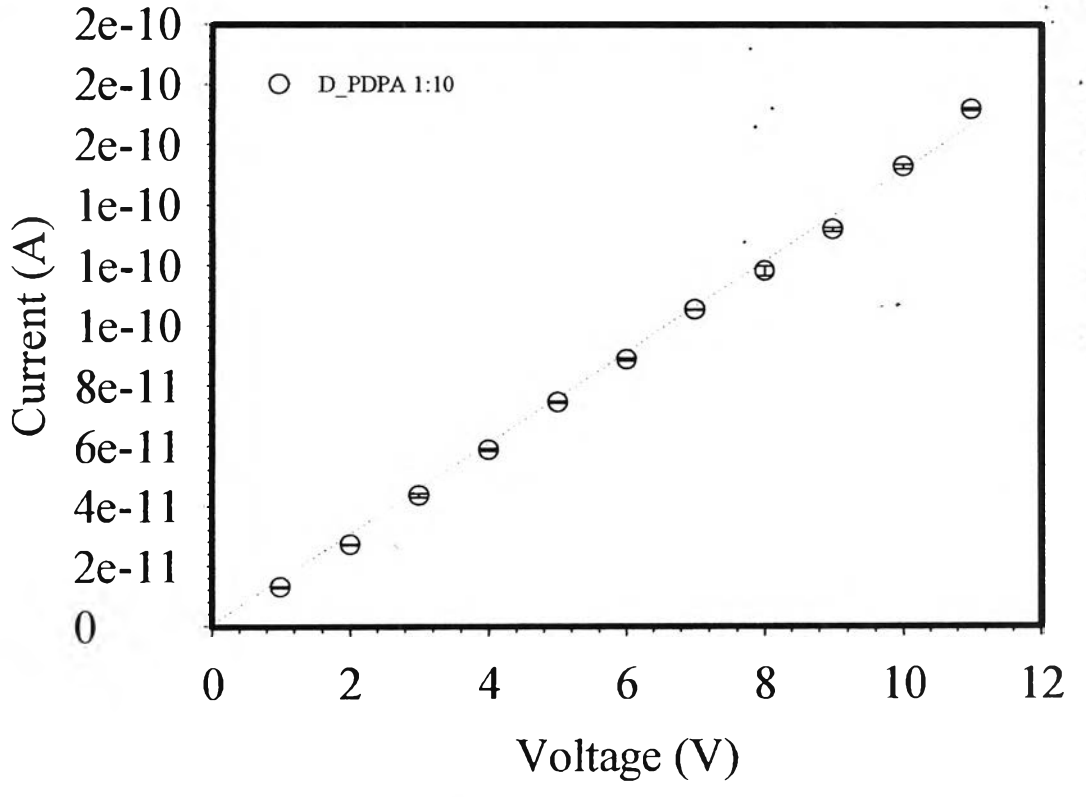

Figure F4 The Ohmic regime of D_PDPA 1:10 at thickness = 0.0280 cm, 25°C, 60-65 %RH.

Table F5 Voltage-current data in linear regime of D_PDPA 1:1 at 25°C, 60-65 %RH

Voltage(V)			Current(A)			Specific conductivity(S/cm)		
1	2	3	1	2	3	1	2	3
1	1	1	1.54E-11	1.55E-11	1.56E-11	3.05E-06	3.07E-06	3.09E-06
2	2	2	3.39E-11	3.37E-11	3.42E-11	3.05E-06	3.34E-06	3.38E-06
3	3	3	5.15E-11	5.15E-11	5.1E-11	3.049E-06	3.40E-06	3.37E-06
4	4	4	6.84E-11	6.92E-11	6.91E-11	3.049E-06	3.42E-06	3.42E-06
5	5	5	8.99E-11	8.91E-11	8.94E-11	3.049E-06	3.53E-06	3.54E-06
6	6	6	1.08E-10	1.08E-10	1.08E-10	3.049E-06	3.58E-06	3.57E-06
7	7	7	1.24E-10	1.24E-10	1.23E-10	3.049E-06	3.50E-06	3.47E-06
8	8	8	1.4E-10	1.4E-10	1.41E-10	3.049E-06	3.47E-06	3.48E-06
9	9	9	1.61E-10	1.63E-10	1.63E-10	3.049E-06	3.58E-06	3.60E-06
10	10	10	1.82E-10	1.83E-10	1.82E-10	3.049E-06	3.62E-06	3.60E-06

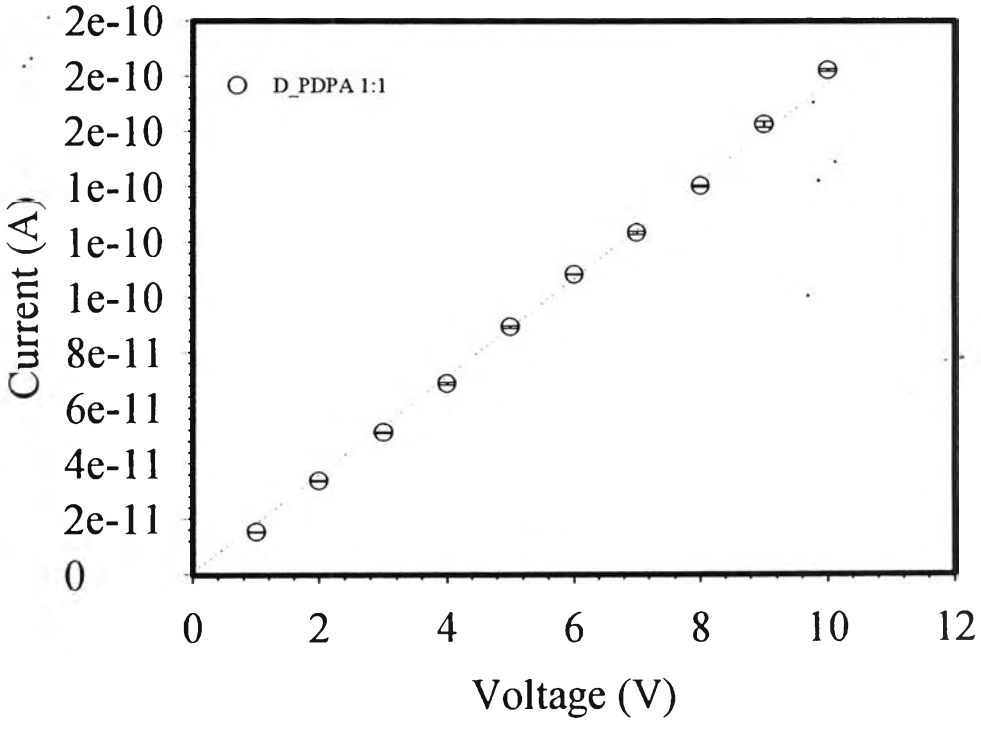

Figure F5 The Ohmic regime of D_PDPA 1:1 at thickness = 0.0255 cm, 25°C, 60-65 %RH.

Table F6 Voltage-current data in linear regime of D_PDPA 10:1 at 25°C, 60-65 %RH

Voltage(V)			Current(A)			Specific conductivity(S/cm)		
1	2	3	1	2	3	1	2	3
1	1	1	4.89E-11	4.88E-11	4.95E-11	8.66E-06	8.64E-06	8.76E-06
2	2	2	1.04E-10	1.05E-10	1.04E-10	9.24E-06	9.26E-06	9.22E-06
3	3	3	1.62E-10	1.61E-10	1.62E-10	9.58E-06	9.49E-06	9.53E-06
4	4	4	2.06E-10	2.02E-10	2.05E-10	9.14E-06	8.96E-06	9.08E-06
5	5	5	2.65E-10	2.61E-10	2.62E-10	9.40E-06	9.25E-06	9.27E-06
6	6	6	3.24E-10	3.23E-10	3.23E-10	9.57E-06	9.54E-06	9.53E-06
7	7	7	3.77E-10	3.75E-10	3.79E-10	9.54E-06	9.48E-06	9.57E-06
8	8	8	4.44E-10	4.42E-10	4.44E-10	9.82E-06	9.77E-06	9.82E-06
9	9	9	4.98E-10	4.86E-10	4.95E-10	9.80E-06	9.55E-06	9.74E-06
10	10	10	5.56E-10	5.52E-10	5.55E-10	9.84E-06	9.77E-06	9.82E-06
11	11	11	6.06E-10	6.12E-10	6.11E-10	9.76E-06	9.86E-06	9.84E-06

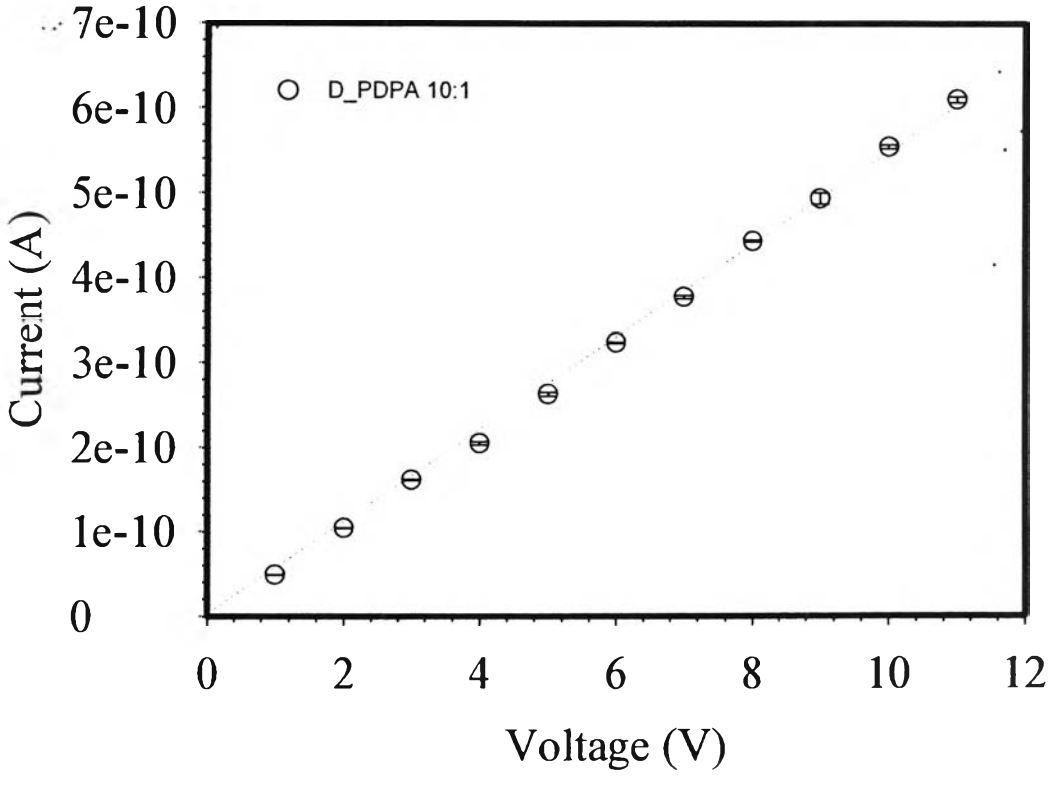

Figure F6 The Ohmic regime of D_PDPA 10:1 at thickness = 0.0286 cm, 25°C, 60-65 %RH.

Table F7 Voltage-current data in linear regime of D_PDPA 100:1 at 25°C, 60-65 %RH

Voltage(V)			Current(A)			Specific conductivity(S/cm)		
1	2	3	1	2	3	1	2	3
2	2	2	6.51E-10	6.55E-10	6.52E-10	5.81E-05	5.84E-05	5.81E-05
3	3	3	1.02E-09	1.02E-09	1.01E-09	6.08E-05	6.04E-05	6.02E-05
4	4	4	1.37E-09	1.37E-09	1.38E-09	6.10E-05	6.12E-05	6.13E-05
5	5	5	1.74E-09	1.73E-09	1.73E-09	6.21E-05	6.17E-05	6.17E-05
6	6	6	2.11E-09	2.11E-09	2.12E-09	6.27E-05	6.28E-05	6.29E-05
7	7	7	2.5E-09	2.5E-09	2.5E-09	6.37E-05	6.36E-05	6.36E-05
8	8	8	2.88E-09	2.88E-09	2.88E-09	6.42E-05	6.41E-05	6.41E-05
9	9	9	3.26E-09	3.27E-09	3.31E-09	6.46E-05	6.48E-05	6.55E-05
10	10	10	3.66E-09	3.65E-09	3.66E-09	6.52E-05	6.51E-05	6.52E-05
11	11	11	4.06E-09	4.05E-09	4.04E-09	6.57E-05	6.56E-05	6.55E-05
12	12	12	4.43E-09	4.4E-09	4.41E-09	6.58E-05	6.54E-05	6.56E-05

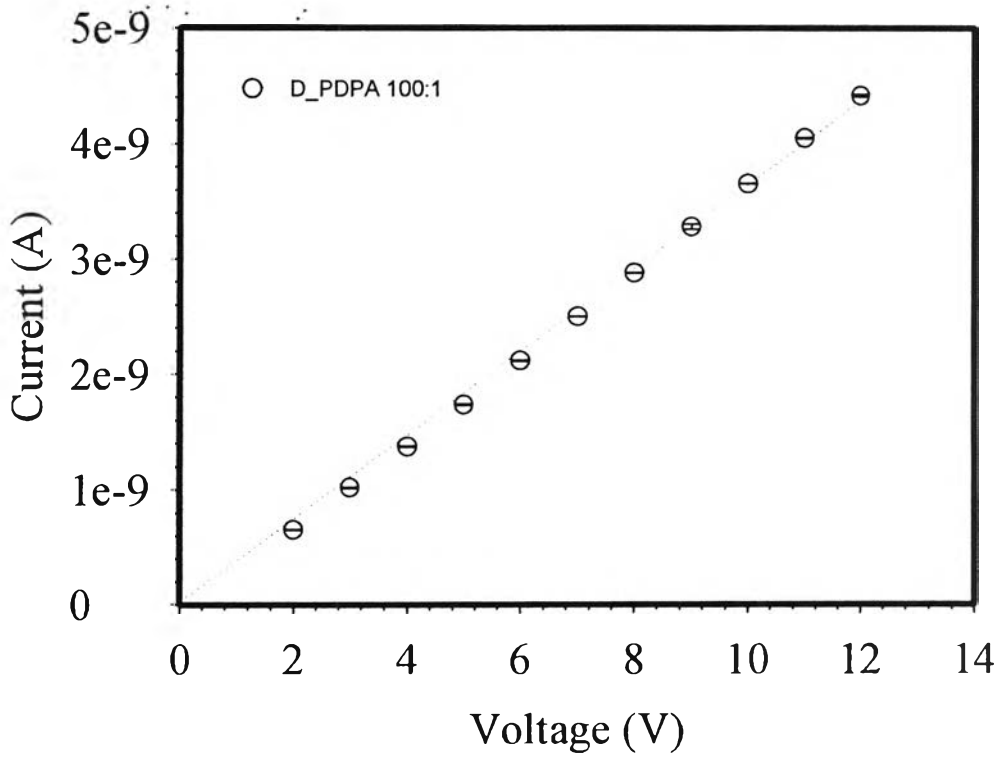

Figure F7 The Ohmic regime of D_PDPA 100:1 at thickness = 0.0284 cm, 25°C, 60-65 %RH.

Table F8 Voltage-current data in linear regime of D_PDPA 200:1 at 25°C, 60-65 %RH

Voltage(V)			Current(A)			Specific conductivity(S/cm)		
1	2	3	1	2	3	1	2	3
1	1	1	6.17E-10	6.24E-10	6.02E-10	1.86E-04	1.88E-04	1.81E-04
2	2	2	1.36E-09	1.37E-09	1.37E-09	2.04E-04	2.05E-04	2.06E-04
3	3	3	2.22E-09	2.2E-09	2.24E-09	2.23E-04	2.21E-04	2.25E-04
4	4	4	3.02E-09	3.07E-09	3.04E-09	2.28E-04	2.31E-04	2.29E-04
5	5	5	3.9E-09	3.92E-09	3.9E-09	2.35E-04	2.36E-04	2.35E-04
6	6	6	4.74E-09	4.77E-09	4.74E-09	2.38E-04	2.39E-04	2.38E-04
7	7	7	5.66E-09	5.65E-09	5.67E-09	2.43E-04	2.43E-04	2.44E-04
8	8	8	6.55E-09	6.54E-09	6.56E-09	2.46E-04	2.46E-04	2.47E-04
9	9	9	7.49E-09	7.47E-09	7.5E-09	2.51E-04	2.50E-04	2.51E-04
10	10	10	8.39E-09	8.36E-09	8.39E-09	2.53E-04	2.52E-04	2.53E-04
11	11	11	9.35E-09	9.36E-09	9.36E-09	2.56E-04	2.56E-04	2.56E-04
12	12	12	1.03E-08	1.03E-08	1.03E-08	2.59E-04	2.58E-04	2.59E-04

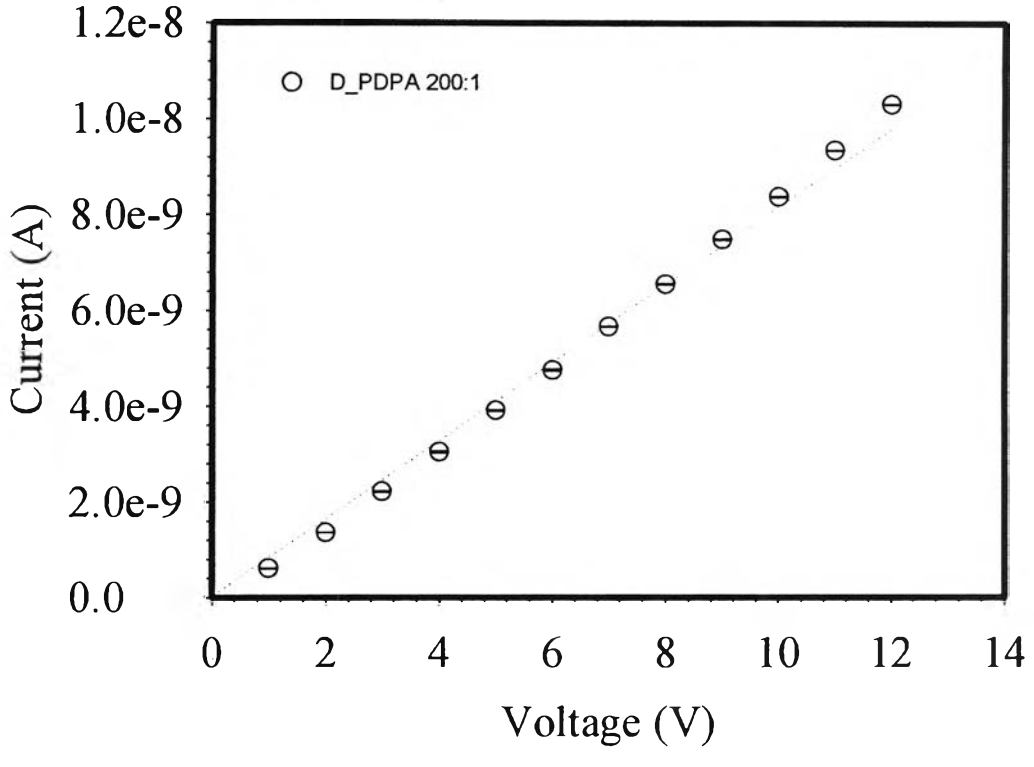

Figure F8 The Ohmic regime of D_PDPA 200:1 at thickness = 0.0168 cm, 25°C, 60-65 %RH.

Pure SIS films

Table F8 Voltage-current data in linear regime of SIS D1114P at 25°C, 60-65 %RH

Voltage(V)			Current(A)			Specific conductivity(S/cm)		
1	2	3	1	2	3	1	2	3
200	200	200	2.09E-14	1.9E-14	2.38E-14	1.06E-19	9.66E-20	1.21E-19
250	250	250	4.11E-14	4.18E-14	4.03E-14	1.67E-19	1.70E-19	1.64E-19
300	300	300	3.57E-14	3.93E-14	3.43E-14	1.21E-19	1.33E-19	1.16E-19
350	350	350	4.67E-14	4.95E-14	4.46E-14	1.36E-19	1.44E-19	1.30E-19
400	400	400	5.18E-14	4.9E-14	5.26E-14	1.32E-19	1.25E-19	1.34E-19
450	450	450	5.6E-14	5.6E-14	5.46E-14	1.27E-19	1.26E-19	1.23E-19
500	500	500	6.24E-14	5.77E-14	5.74E-14	1.27E-19	1.17E-19	1.17E-19
550	550	550	7.05E-14	6.83E-14	6.87E-14	1.30E-19	1.26E-19	1.27E-19
600	600	600	7.16E-14	7.24E-14	7.33E-14	1.21E-19	1.23E-19	1.24E-19
650	650	650	7.6E-14	7.6E-14	7.7E-14	1.19E-19	1.19E-19	1.20E-19

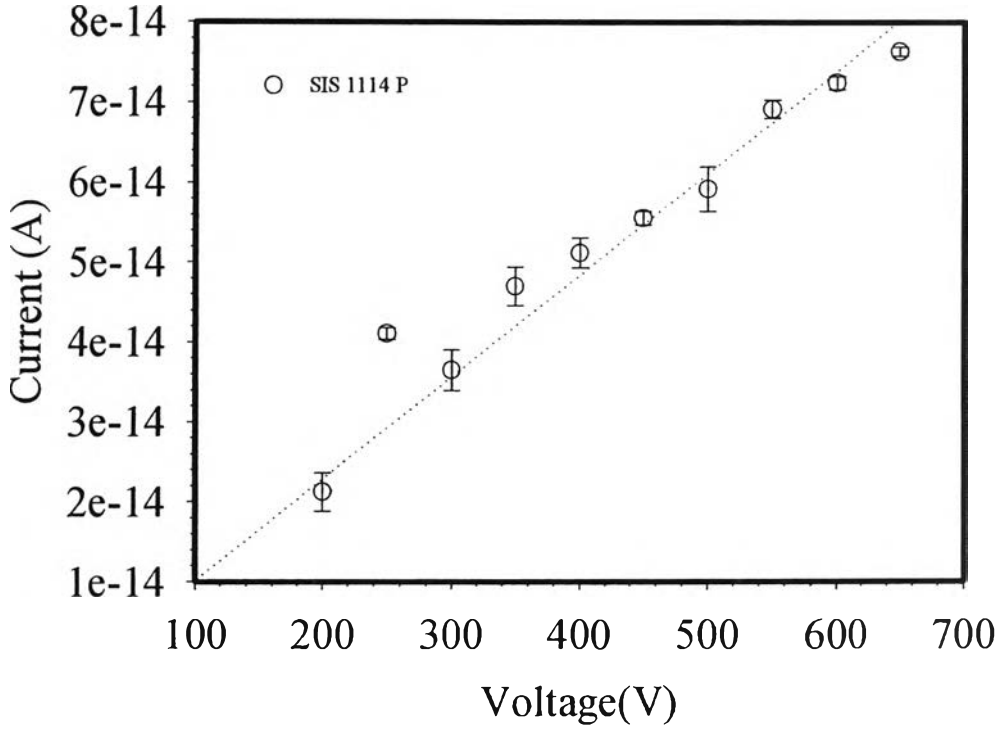

Figure F8 The Ohmic regime of SIS 1114P at thickness = 0.02327 cm, 25°C, 60-65 %RH.

Table F9 Voltage-current data in linear regime of SIS D1164P at 25°C, 60-65 %RH

Voltage(V)			Current(A)			Specific conductivity(S/cm)		
1	2	3	1	2	3	1	2	3
200	200	200	4.3E-12	3.9E-12	4E-12	1.99E-17	1.80E-17	1.85E-17
230	230	230	5.49E-12	5.69E-12	5.29E-12	2.21E-17	2.29E-17	2.13E-17
250	250	250	5.89E-12	6.17E-12	5.86E-12	2.18E-17	2.29E-17	2.17E-17
270	270	270	6.34E-12	6.45E-12	6.14E-12	2.17E-17	2.21E-17	2.10E-17
300	300	300	6.78E-12	6.95E-12	6.85E-12	2.09E-17	2.14E-17	2.11E-17
350	350	350	8.54E-12	8.96E-12	8.14E-12	2.26E-17	2.37E-17	2.15E-17
400	400	400	9.58E-12	1.07E-11	1.05E-11	2.22E-17	2.47E-17	2.44E-17
450	450	450	1.28E-11	1.34E-11	1.33E-11	2.63E-17	2.75E-17	2.73E-17
500	500	500	1.45E-11	1.48E-11	1.47E-11	2.68E-17	2.75E-17	2.72E-17
550	550	550	1.57E-11	1.62E-11	1.61E-11	2.64E-17	2.72E-17	2.71E-17
600	600	600	1.82E-11	1.83E-11	1.85E-11	2.81E-17	2.82E-17	2.86E-17
650	650	650	2.07E-11	2.09E-11	2.06E-11	2.94E-17	2.98E-17	2.93E-17

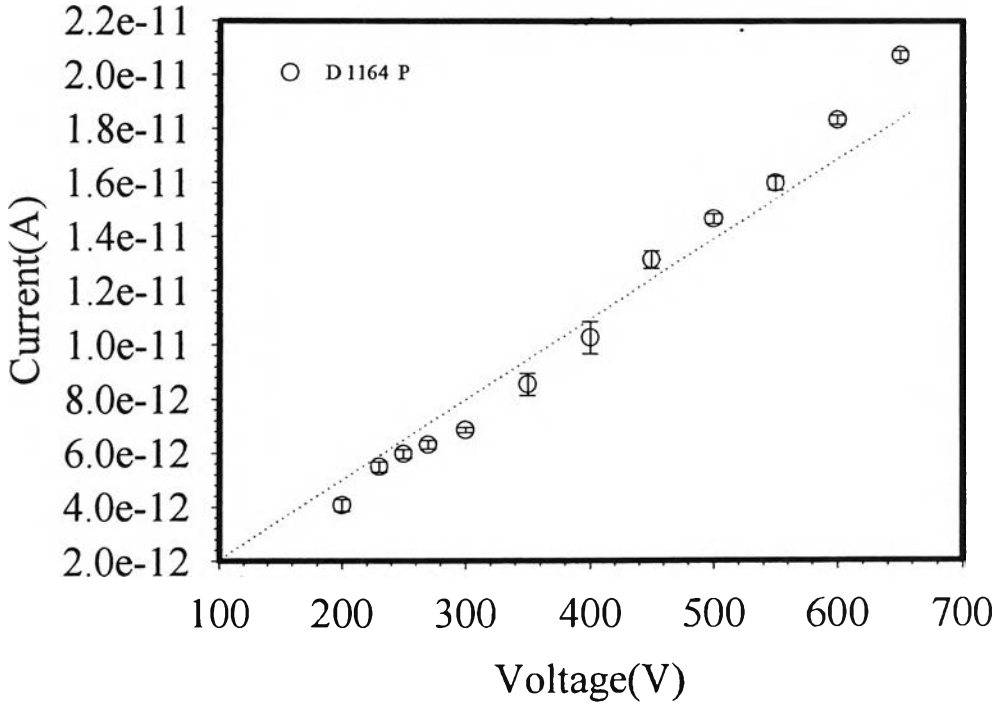

Figure F9 The Ohmic regime of SIS D1164P at thickness = 0.02120 cm, 25°C, 60-65 %RH.

Table F10 Voltage-current data in linear regime of SIS D1162P at 25°C, 60-65 %RH

Voltage(V)			Current(A)			Specific conductivity(S/cm)		
1	2	3	1	2	3	1	2	3
200	200	200	2.67E-12	2.53E-12	2.65E-12	1.32E-17	1.24E-17	1.31E-17
230	230	230	3.60E-12	2.86E-12	3.19E-12	1.54E-17	1.22E-17	1.37E-17
250	250	250	2.87E-12	2.72E-12	2.83E-12	1.13E-17	1.07E-17	1.11E-17
270	270	270	2.64E-12	2.77E-12	3.16E-12	9.63E-18	1.01E-17	1.15E-17
300	300	300	3.53E-12	3.35E-12	3.32E-12	1.16E-17	1.10E-17	1.09E-17
330	330	330	3.79E-12	3.82E-12	3.73E-12	1.13E-17	1.14E-17	1.11E-17
350	350	350	3.93E-12	4.46E-12	3.87E-12	1.11E-17	1.26E-17	1.09E-17
370	370	370	4.52E-12	4.32E-12	4.26E-12	1.20E-17	1.15E-17	1.13E-17
400	400	400	4.91E-12	4.72E-12	4.52E-12	1.21E-17	1.16E-17	1.11E-17
430	430	430	5.55E-12	5.40E-12	5.34E-12	1.27E-17	1.24E-17	1.22E-17
450	450	450	5.13E-12	5.26E-12	5.17E-12	1.12E-17	1.15E-17	1.13E-17
470	470	470	5.45E-12	5.49E-12	5.77E-12	1.14E-17	1.15E-17	1.21E-17
500	500	500	6.46E-12	5.75E-12	5.8E-12	1.27E-17	1.13E-17	1.14E-17

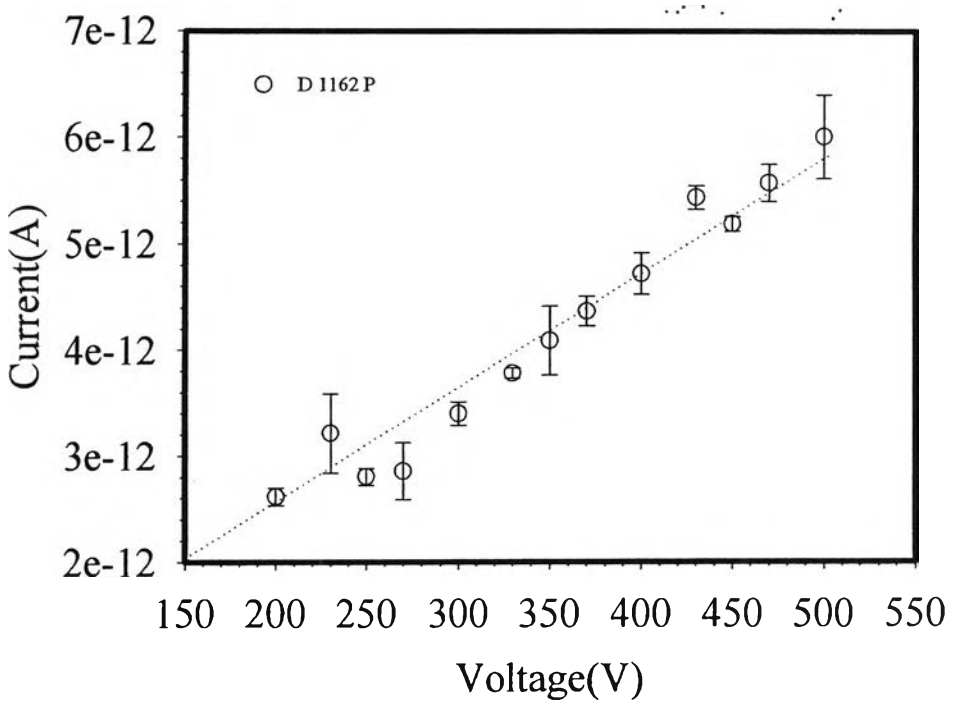

Figure F10 The Ohmic regime of SIS 1162P at thickness = 0.02253 cm, 25°C, 60-65 %RH.

Dedoped polydiphenylamine (De_PDPA)/D1114P blends

Table F11 Voltage-current data in linear regime of 5 % De_PDPA/D1114P at thickness = 0.0343 cm, 25°C, 60-65 %RH

Voltage(V)			Current(A)			Specific conductivity(S/cm)		
1	2	3	1	2	3	1	2	3
200	200	200	2.72E-11	3.05E-11	2.87E-11	2.04E-16	2.29E-16	2.15E-16
230	230	230	3.11E-11	3.13E-11	3.46E-11	2.03E-16	2.04E-16	2.25E-16
250	250	250	3.58E-11	3.82E-11	3.88E-11	2.15E-16	2.29E-16	2.33E-16
280	280	280	4.08E-11	4.03E-11	4.55E-11	2.18E-16	2.16E-16	2.44E-16
300	300	300	4.42E-11	4.83E-11	4.69E-11	2.21E-16	2.41E-16	2.34E-16
330	330	330	4.99E-11	4.78E-11	5.07E-11	2.27E-16	2.17E-16	2.30E-16
350	350	350	5.32E-11	5.39E-11	5.5E-11	2.28E-16	2.31E-16	2.35E-16
380	380	380	5.67E-11	5.92E-11	6.02E-11	2.24E-16	2.34E-16	2.37E-16
400	400	400	5.56E-11	5.9E-11	6.34E-11	2.09E-16	2.21E-16	2.38E-16
430	430	430	6.52E-11	6.44E-11	6.51E-11	2.27E-16	2.25E-16	2.27E-16
450	450	450	6.47E-11	6.65E-11	6.5E-11	2.15E-16	2.21E-16	2.17E-16

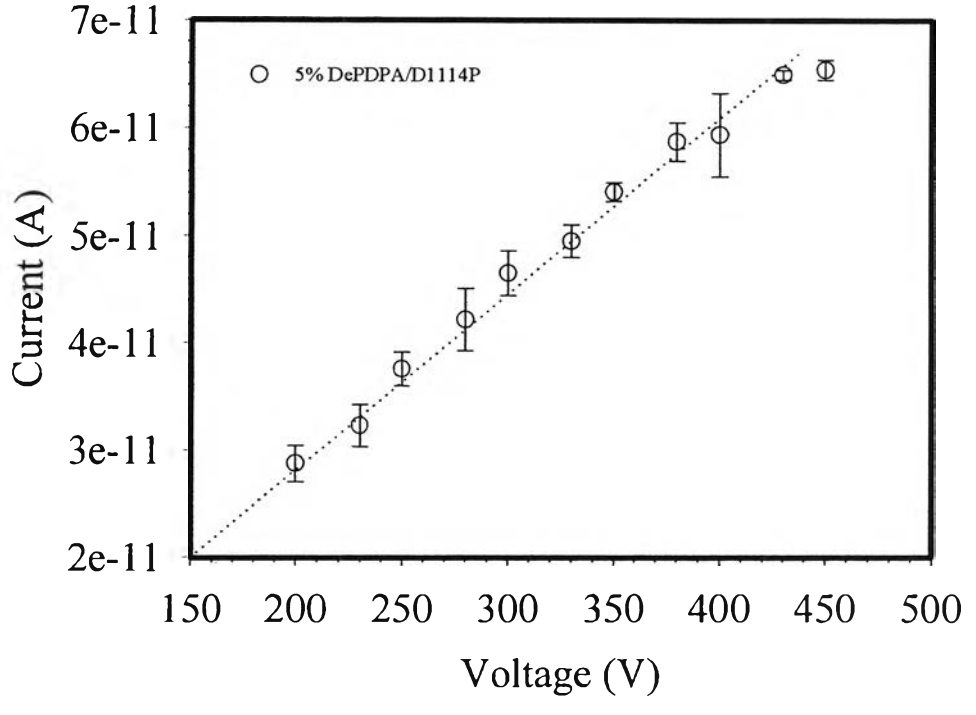

Figure F11 The Ohmic regime of 5 % De_PDPA/D1114P at thickness = 0.0343 cm, 25°C, 60-65 %RH.

Table F12 Voltage-current data in linear regime of 10 % De_PDPA/D1114P at thickness = 0.0310 cm, 25°C, 60-65 %RH

Voltage(V)			Current(A)			Specific conductivity(S/cm)		
1	2	3	1	2	3	1	2	3
200	200	200	3.72E-10	3.51E-10	3.59E-10	2.52E-15	2.38E-15	2.43E-15
230	230	230	4.58E-10	4.5E-10	4.23E-10	2.70E-15	2.65E-15	2.49E-15
250	250	250	5.03E-10	5.19E-10	5.14E-10	2.72E-15	2.81E-15	2.79E-15
280	280	280	5.29E-10	5.25E-10	5.27E-10	2.56E-15	2.54E-15	2.55E-15
300	300	300	6.4E-10	6.33E-10	6.56E-10	2.89E-15	2.86E-15	2.96E-15
330	330	330	6.67E-10	6.43E-10	6.32E-10	2.74E-15	2.64E-15	2.59E-15
350	350	350	6.86E-10	7.12E-10	6.75E-10	2.65E-15	2.75E-15	2.61E-15
380	380	380	7.09E-10	7.54E-10	7.18E-10	2.53E-15	2.68E-15	2.56E-15
400	400	400	8.15E-10	8.11E-10	7.62E-10	2.76E-15	2.75E-15	2.58E-15

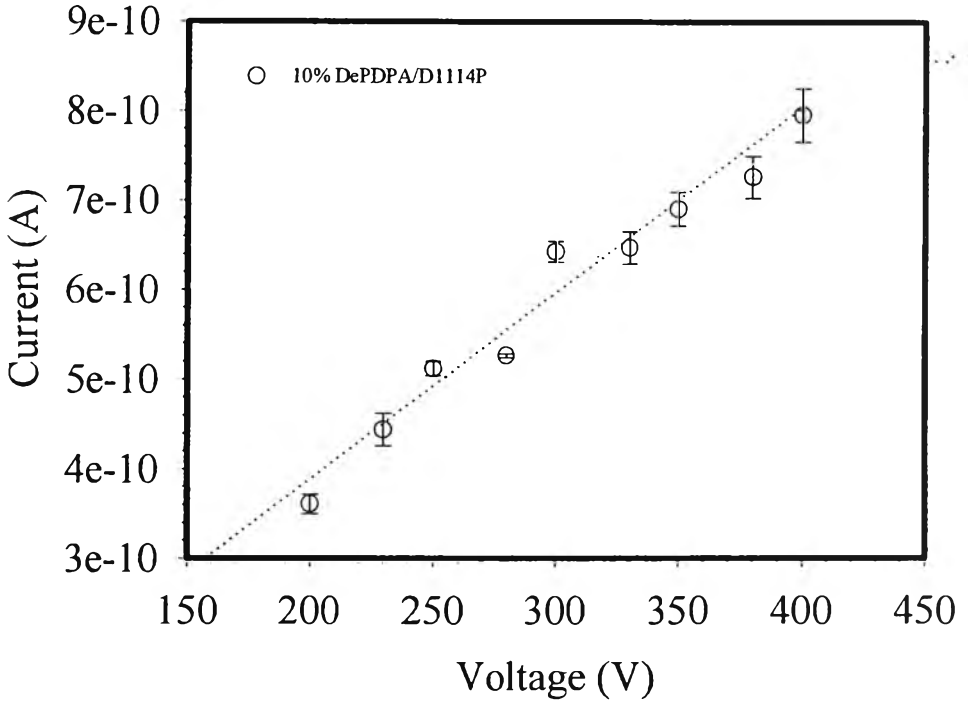

Figure F12 The Ohmic regime of 10 % De_PDPA/D1114P at thickness = 0.0310 cm, 25°C, 60-65 %RH.

Table F13 Voltage-current data in linear regime of 20 % De_PDPA/D1114P at thickness = 0.0313 cm, 25°C, 60-65 %RH

Voltage(V)			Current(A)			Specific conductivity(S/cm)		
1	2	3	1	2	3	1	2	3
200	200	200	2.4E-09	2.05E-09	2.09E-09	1.64E-14	1.41E-14	1.43E-14
250	250	250	2.99E-09	3.07E-09	3.03E-09	1.64E-14	1.68E-14	1.66E-14
300	300	300	3.97E-09	3.91E-09	3.96E-09	1.81E-14	1.78E-14	1.81E-14
350	350	350	5.23E-09	5.67E-09	5.25E-09	2.05E-14	2.22E-14	2.05E-14
400	400	400	6.52E-09	6.69E-09	6.4E-09	2.23E-14	2.29E-14	2.19E-14
450	450	450	7.68E-09	7.58E-09	7.62E-09	2.34E-14	2.31E-14	2.32E-14
500	500	500	9.76E-09	9.53E-09	9.9E-09	2.67E-14	2.61E-14	2.71E-14
550	550	550	1.16E-08	1.16E-08	1.16E-08	2.89E-14	2.87E-14	2.89E-14
600	600	600	1.37E-08	1.36E-08	1.36E-08	3.12E-14	3.11E-14	3.09E-14

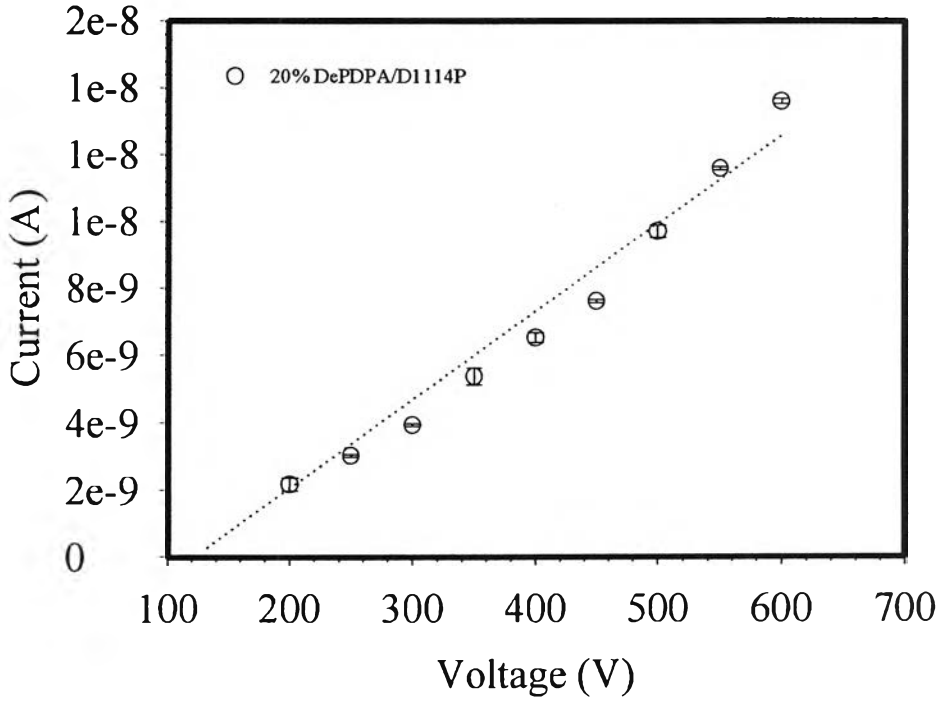

Figure F13 The Ohmic regime of 20 % De_PDPA/D1114P at thickness = 0.0313 cm, 25°C, 60-65 %RH.

Table F14 Voltage-current data in linear regime of 30 % De_PDPA/D1114P at thickness = 0.0330 cm, 25°C, 60-65 %RH

Voltage(V)			Current(A)			Specific conductivity(S/cm)		
1	2	3	1	2	3	1	2	3
150	150	150	3.59E-09	3.74E-09	3.73E-09	3.45E-14	3.59E-14	3.59E-14
200	200	200	5.19E-09	5.32E-09	5.23E-09	3.74E-14	3.83E-14	3.77E-14
250	250	250	7.65E-09	7.26E-09	7E-09	4.41E-14	4.19E-14	4.04E-14
300	300	300	9.92E-09	9.96E-09	9.95E-09	4.76E-14	4.78E-14	4.78E-14
350	350	350	1.17E-08	1.18E-08	1.16E-08	4.82E-14	4.86E-14	4.79E-14
400	400	400	1.47E-08	1.48E-08	1.45E-08	5.30E-14	5.34E-14	5.23E-14
450	450	450	1.52E-08	1.53E-08	1.5E-08	4.86E-14	4.91E-14	4.81E-14
500	500	500	1.97E-08	2.07E-08	2E-08	5.68E-14	5.97E-14	5.75E-14
550	550	550	2.35E-08	2.29E-08	2.35E-08	6.15E-14	6.01E-14	6.15E-14

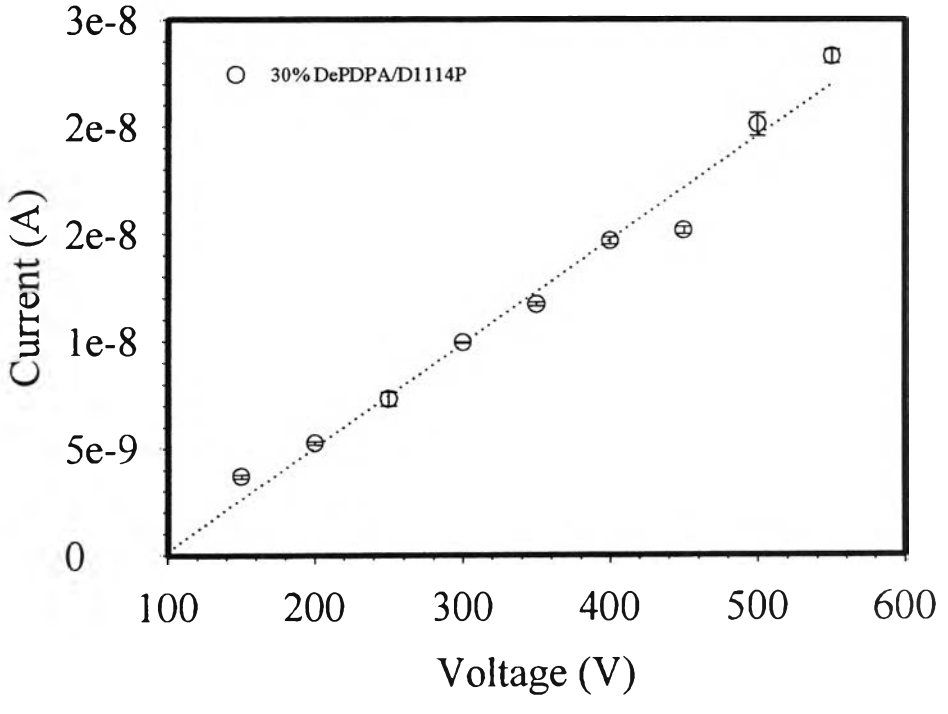

Figure F14 The Ohmic regime of 30 % De_PDPA/D1114P at thickness = 0.0330 cm, 25°C, 60-65 %RH.

Appendix G Scanning Electron Microscopy (SEM)

Scanning Electron Microscopy (SEM): pure SIS films

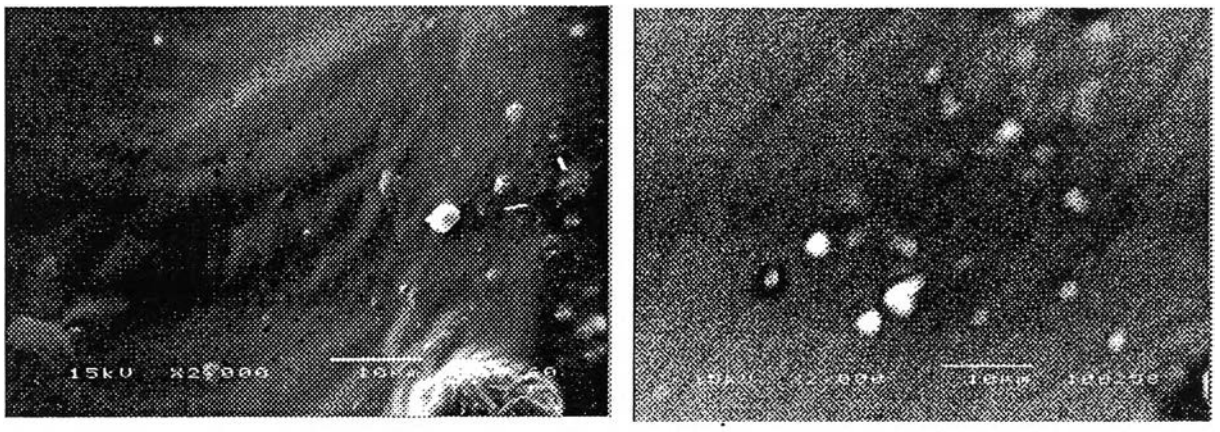

a) b)

Figure G1 SEM micrograms of SIS D1114 P film at magnification ×2000, 15kV: a) long section; b) cross section.

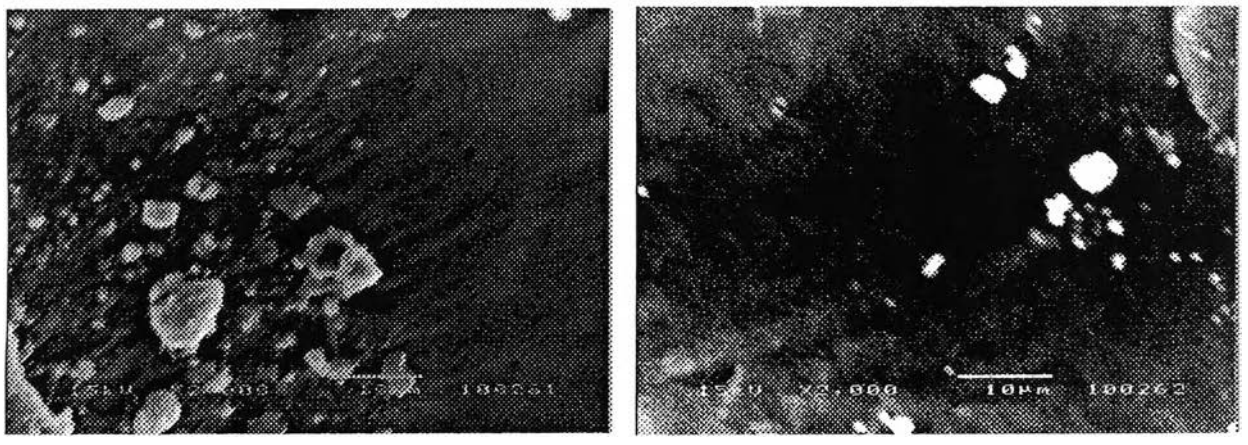

a) b)

Figure G2 SEM micrograms of SIS D1164 P film at magnification ×2000, 15kV: a) long section; b) cross section.

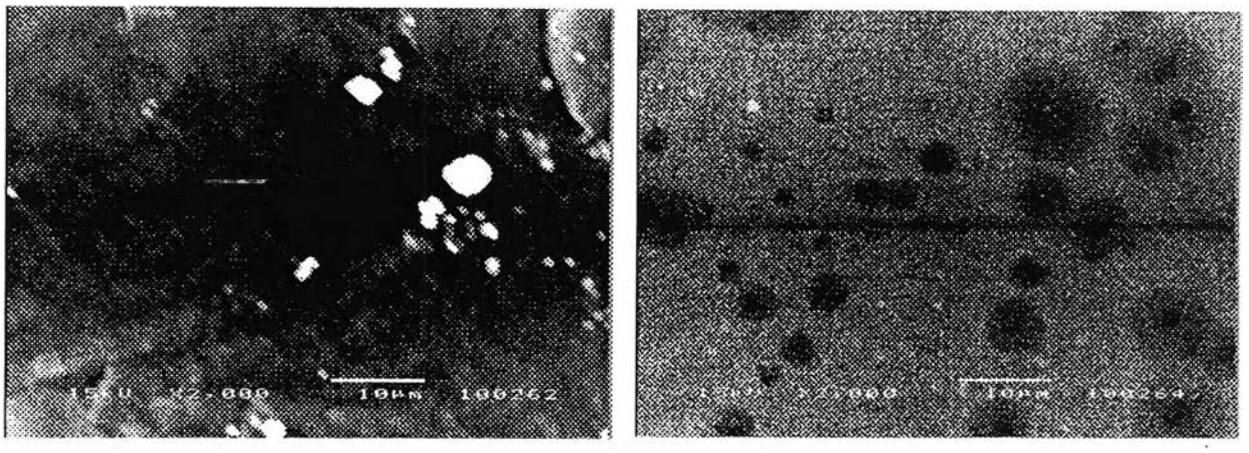

a) b)

Figure G3 SEM micrograms of SIS D1162 P film at magnification ×2000, 15kV: a) long section; b) cross section.

Scanning Electron Microscopy (SEM); polydiphenylamine (PDPA)

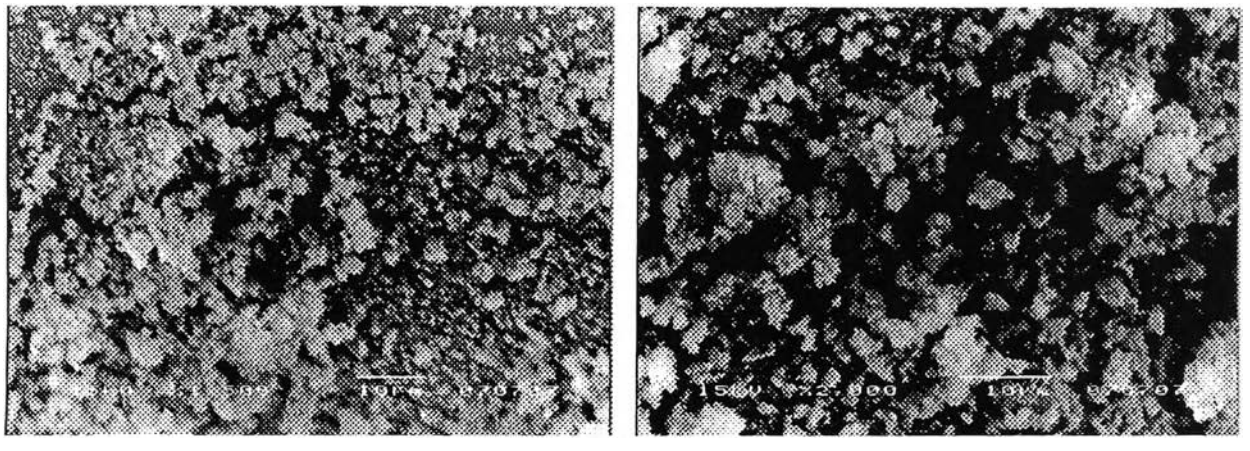

a) b)

Figure G4 SEM micrograms of Dedoped-PDPA at magnifications of a) magnification ×1500, 15 kV; b) magnification ×2000, 15 kV.

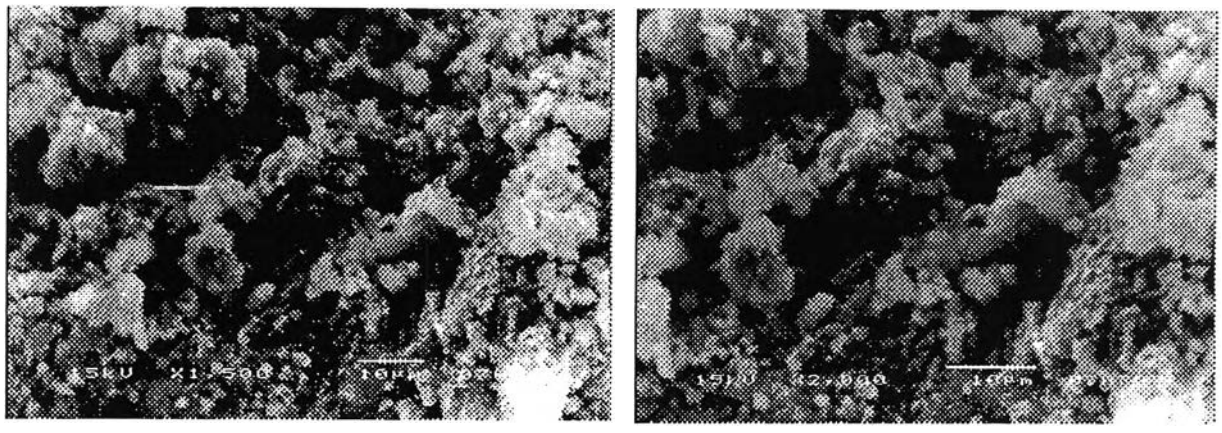

a) b)

Figure G5 SEM micrograms of Doped-PDPA at magnifications: a) magnification×1500, 15 kV; b) magnification×2000, 15 kV.

Scanning Electron Microscopy (SEM): dedoped polydiphenylamine (De-PDPA)/D1114P blends

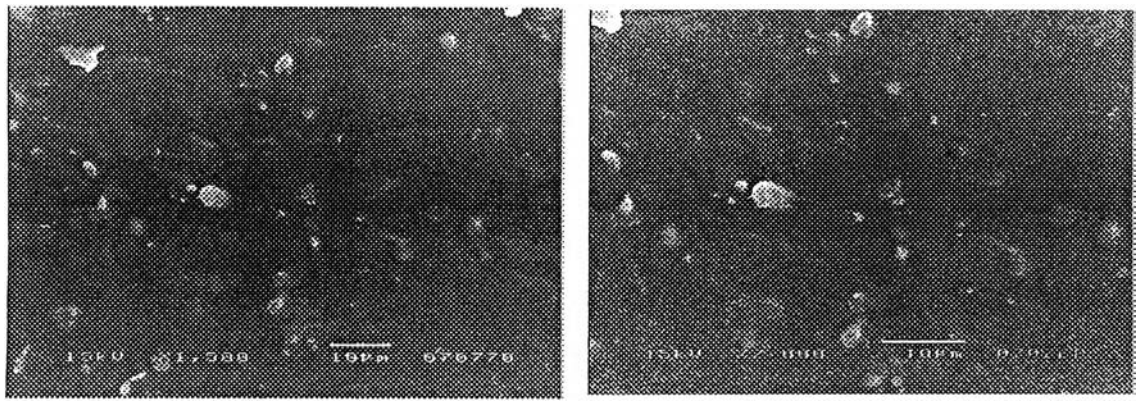

a) b)

Figure G6 SEM Micrograms of 5% DePDPA/D1114 P film: a) magnification of 1500, 15 kV; b) magnification of 2000, 15 kV.

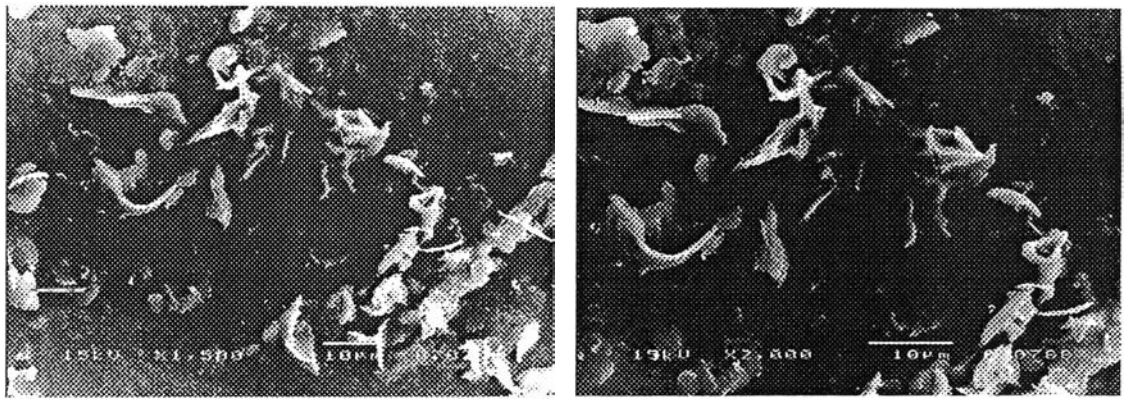

a) b)

Figure G7 SEM Micrograms of 10% DePDPA/D1114 P film: a) magnification of 1500, 15 kV; b) magnification of 2000, 15 kV.

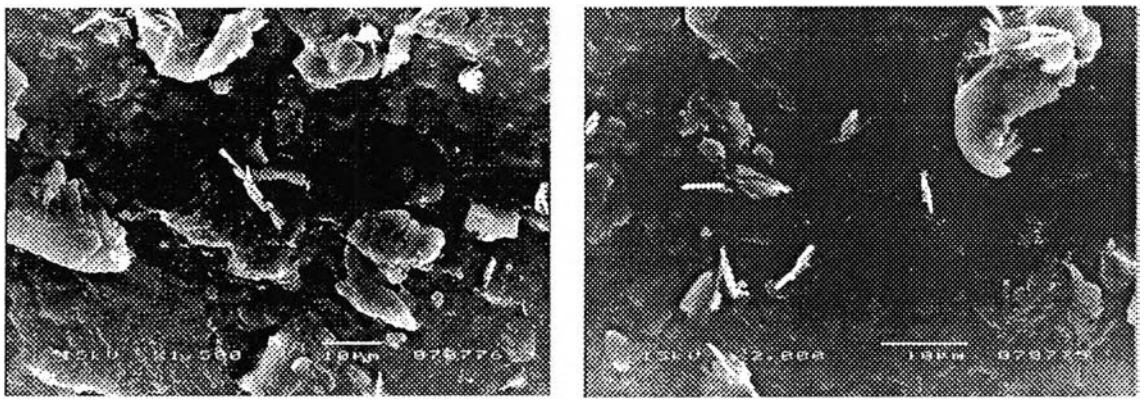

a) b)

Figure G8 SEM Micrograms of 15% DePDPA/D1114 P film: a) magnification of 1500, 15 kV; b) magnification of 2000, 15 kV.

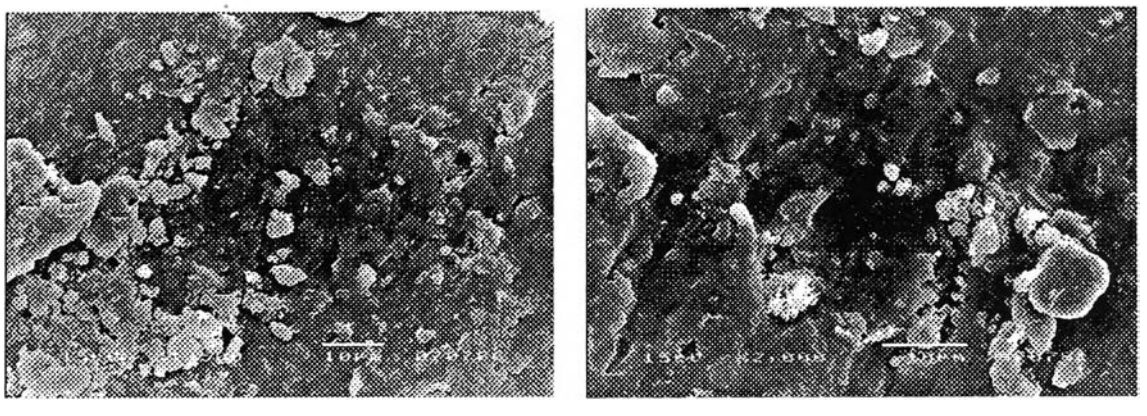

a) b)

Figure G9 SEM Micrograms of 20% DePDPA/D1114 P film: a) magnification of 1500, 15 kV; b) magnification of 2000, 15 kV.

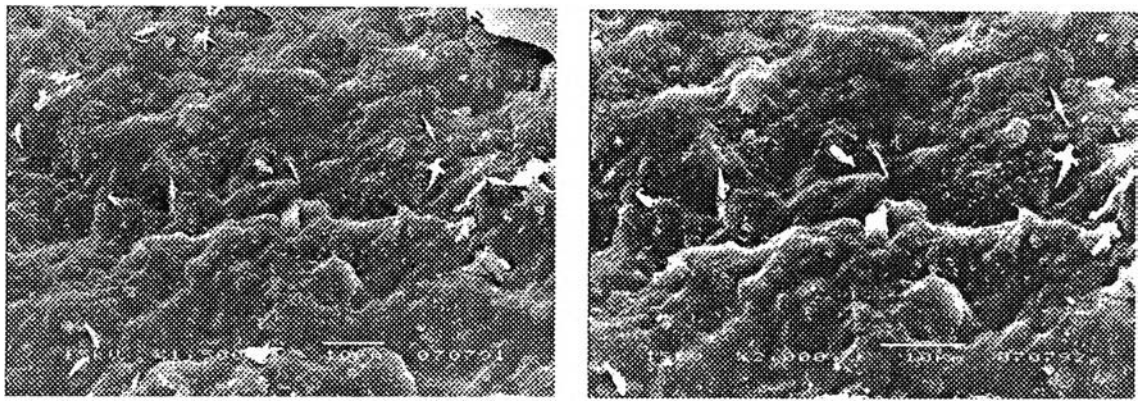

a) b)

Figure G10 SEM Micrograms of 20% DePDPA/D1114 P film: a) magnification of 1500, 15 kV; b) magnification of 2000, 15 kV.

Appendix H Electrorheological Properties Measurement

Temporal response: pure SIS film by using stretch fixture

The temporal response of pure SIS films with different morphology; D1114P; D1164P; and D1162P were investigated by the rheometer (Rheometric Scientific, ARES). It was fitted with a custom-built stretch fixture, gap = 30 mm. A DC voltage was applied with a DC power supply (Gold Sun 3000, GPS 3003D) work with high voltage power supply (Gamma High Voltage, UC5-30P), which can deliver electric field strength up to 1 kV/mm. A digital multimeter was used to monitor the voltage input. In the temporal response testing, the dynamic strain was applied and the dynamic moduli (G' and G") were measured as functions of time and electric field strength. Dynamic strain sweep test were first carried out to determine suitable strains to measured G' and G" in linear viscoelastic regime, as following figures (Figure H1, H2, and H3). The appropriate strains were determined to be 0.2 % for the pure films.

Table H1 Storage modulus and loss modulus data, obtained from dynamic strain sweep test of D1114P (19%wt PS), stretch fixture, gap = 30 mm, film thickness = 0.296 mm, film width = 7.0mm, electric field (E) = 0 V/mm, 25°C

%Strain	G'(Pa)	G"(Pa)	%Strain	G'(Pa)	G"(Pa)
0.00052	3848200	1018500	0.03139	3552800	272620
0.00075	5.77E+08	1.79E+09	0.04981	3490100	248430
0.00120	5408500	1603300	0.07897	3478000	308420
0.00194	4349500	-396600	0.12515	3470800	253900
0.00308	3720100	-61935	0.19840	3474900	263180
0.00491	3583800	162710	0.31435	3466400	271930
0.00781	3843100	496320	0.49896	3472800	282620
0.01241	3490000	195770	0.79096	3454800	293890
0.01968	3446200	274750			

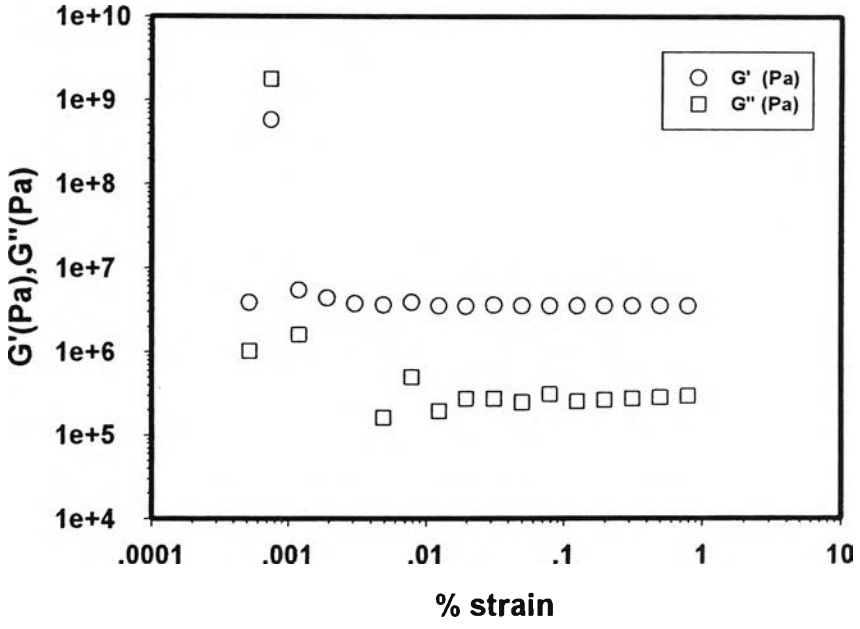

Figure H1 Storage modulus and loss modulus versus strain (%) obtained from dynamic strain sweep test of D1114P (19%wt PS), stretch fixture, gap = 30 mm, film thickness = 0.296 mm, film width = 7.0mm, electric field (E) = 0 V/mm, 25°C.

Table H2 Storage modulus and loss modulus data, obtained from dynamic strain sweep test of D1164P (29%wt PS), stretch fixture, gap = 30 mm, film thickness = 0.429 mm, film width = 7.0 mm, electric field (E) = 0 V/mm, 25°C

%Strain	G' (Pa)	G"(Pa)	%Strain	G' (Pa)	G"(Pa)
0.000521	6763900	1286200	0.03131	6202400	299210
0.000784	6478300	2051300	0.0497	6200400	283480
0.0012	5151900	-317500	0.07878	6206800	279410
0.00194	6543600	220160	0.12488	6208400	295300
0.00307	6118800	-43724	0.19795	6183900	299260
0.0049	6186800	323830	0.31369	6168000	296560
0.0078	6366500	317020	0.49798	6061700	290080
0.01239	6205400	323590	0.7895	5861900	294200
0.01964	6299700	270320			

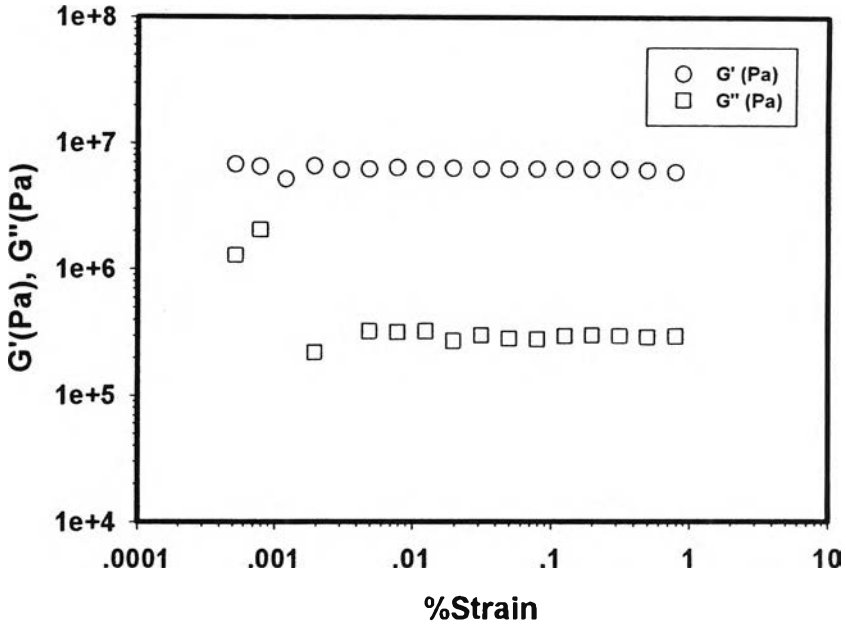

Figure H2 Storage modulus and loss modulus versus strain (%) obtained from dynamic strain sweep test of D1164P (29%wt PS), stretch fixture, gap = 30 mm, film thickness = 0.429 mm, film width = 7.0 mm, electric field (E) = 0 V/mm, 25°C.

Table H3 Storage modulus and loss modulus data, obtained from dynamic strain sweep test of D1162P (44%wt PS), stretch fixture, gap = 30 mm, film thickness = 0.351 mm, film width = 6.5 mm, electric field (E) = 0 V/mm, 25°C

%Strain	G'(Pa)	G"(Pa)	%Strain	G'(Pa)	G"(Pa)
0.0005	82172000	-1.9E+07	0.01951	26086000	1077800
0.00077	31531000	-1.1E+07	0.0311	26364000	1538300
0.00119	32876000	104230	0.04939	26050000	1340100
0.00191	36891000	6658700	0.07826	25684000	1419800
0.00305	28085000	5029300	0.12407	25505000	1348900
0.00486	28051000	2270900	0.19672	25704000	1453500
0.00774	26553000	-21676	0.31143	27275000	1541200
0.01231	26649000	1699200			

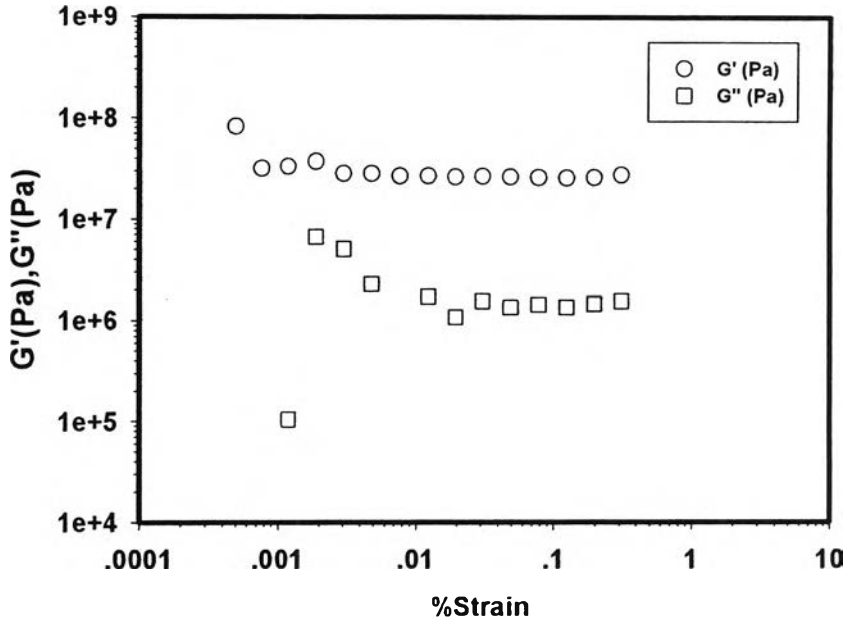

Figure H3 Storage modulus and loss modulus versus strain (%) obtained from dynamic strain sweep test of D1162P (44%wt PS), stretch fixture, gap = 30 mm, film thickness = 0.351 mm, film width = 6.5 mm, electric field (E) = 0 V/mm, 25°C.

The time sweep test was carried out with electric field applied on and off, alternatively. The G'of each film was investigated to measure time that each film response reach to steady state and there response under electric field stimulation. Figure H4 shows G' of D1114P was steady state after 2600 s of measurement. Moreover, the film is not affected stimulated by electric field (1 kV/mm), it is stress free system. In the case of, Figure H5 and H6, D1164P and D1162P were steady state after 4200 s and 2600 s, respectively. There also shows the similar response under electric field as the D1114P film.

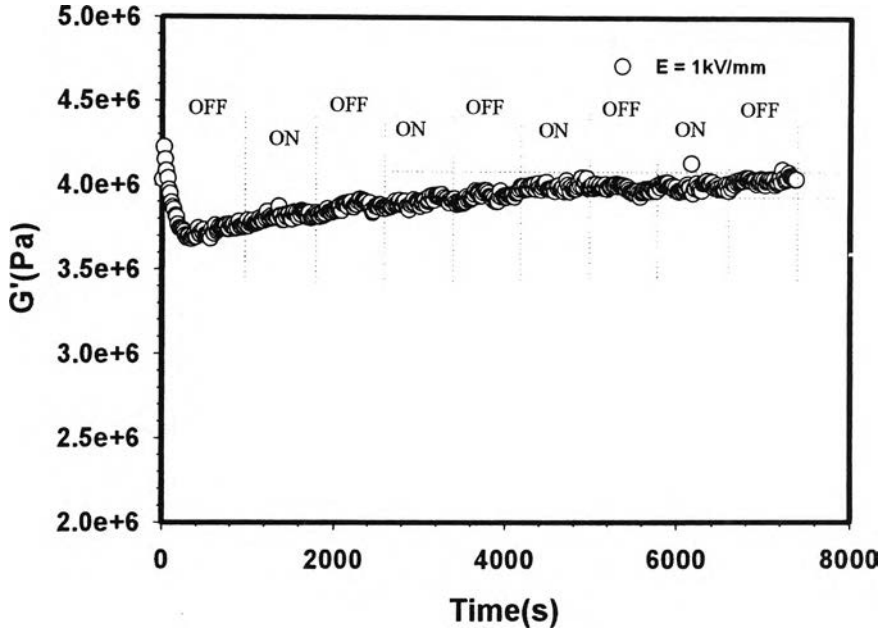

Figure H4 Temporal response testing of storage modulus (G') of D1114P (19 %wt PS), stretch fixture, strain 0.2 %, gap 30 mm, film thickness 0.296 mm, film width 7.0 mm, freguency 1.0 rad/s, electric field (E) 1 kV/mm, 25°C.

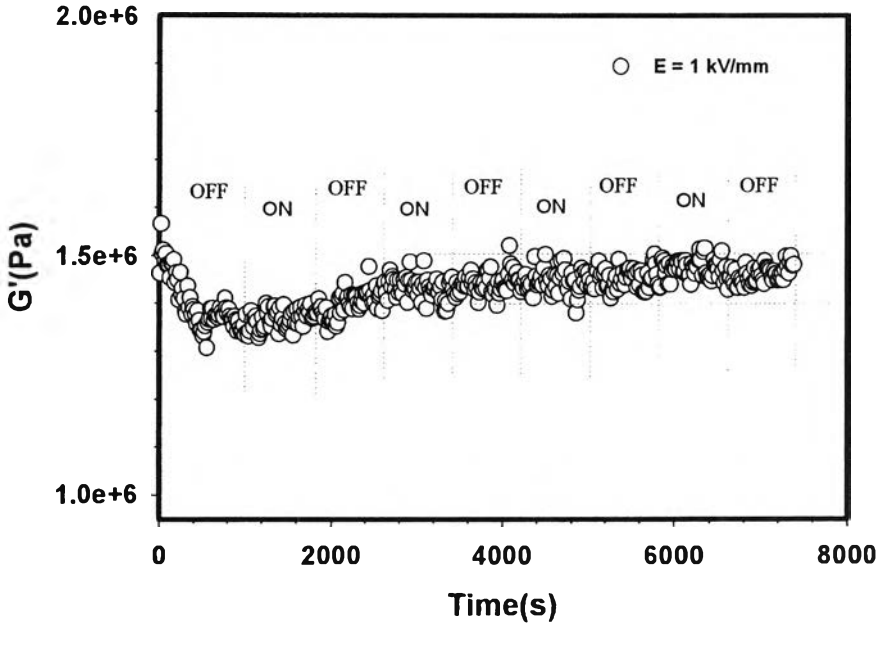

Figure H5 Temporal response testing of storage modulus (G') of D1164P (29 %wt PS), stretch fixture, strain 0.2 %, gap 30 mm, film thickness 0.429 mm, film width 7.0 mm, frequency 1.0 rad/s, electric field (E) 1 kV/mm, 25°C.

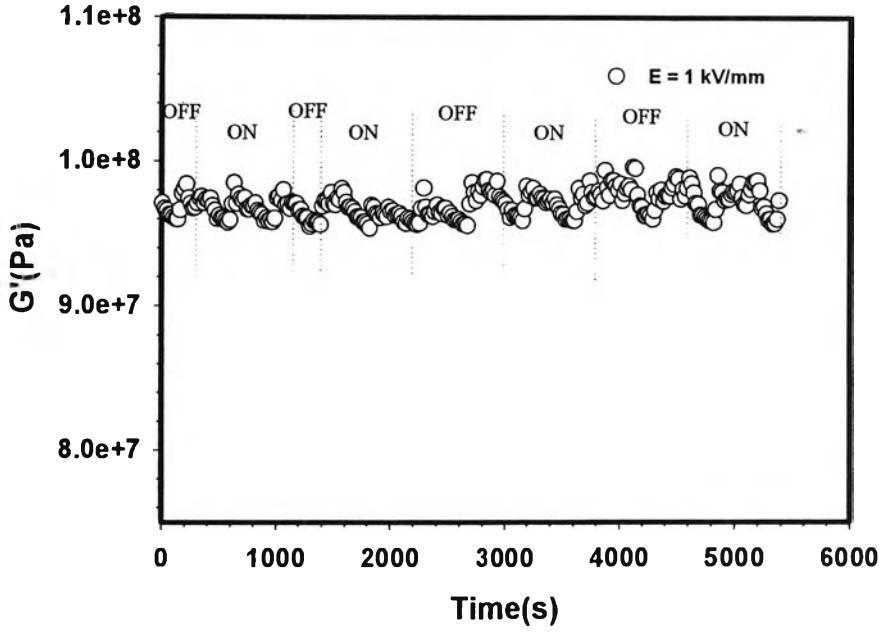

Figure H6 Temporal response testing of storage modulus of D1162P (44 %wt PS), stretch fixture, strain 0.2 %, gap 30 mm, film thickness 0.351 mm, film width 6.5 mm, frequency 1.0 rad/s, electric field (E) 1 kV/mm, 25°C.

Temporal response: pure SIS film by using parallel plates

The temporal response of pure SIS films with different morphology; D1114P; D1164P; and D1162P were carried out by melt rheometer meter (Rheometric Scientific, ARES). It was fitted with a custom-built copper parallel plates fixture, diameter 25 mm. A DC voltage was applied by DC power supply (Instek, GFG 8216A), which can deliver electric field strength to 2 kV/mm. A digital multimeter was used to monitor the voltage input. For temporal responses testing, oscillate shear strain was applied and the dynamic moduli (G' and G") were investigated as a function of time and electric field strength. Dynamic strain sweep test were first carried out to determine appropriate strains by measured G' and G" in linear viscoelastic regime. The following figures, Figure H7, H9, and H11, show linear viscoelastic regimes of pure SIS films: D1114P; D1164P; and D1162P; respectively, without electric field strength (0 V/mm). Besides, Figure H8, H10, and H12, show

the linear viscoelastic regimes of pure SIS films in the influence of electric field strength at 2 kV/mm.

Table H4 Storage modulus and loss modulus data, obtained from dynamic strain sweep test of D1114P (19 %wt PS), parallel plate, gap = 1.076 mm, film diameter = 25 mm, electric field (E) = 0 V/mm, 27°C

%strain	G'(Pa)	G'(Pa)	%strain	G'(Pa)	G'(Pa)
0.01023	116000	2049.67	0.92277	96270.6	4787.6
0.01502	107600	-8568.9	1.46737	91966.4	7628.91
0.0234	108130	4101.55	2.34038	85078.3	10459.3
0.03549	117080	4666.33	3.73553	76377.9	13090
0.05709	105460	-4140.3	5.97161	66530.4	14652.3
0.09042	106620	-1791.7	9.54458	55993.9	16293.8
0.14412	101310	-291.53	15.2586	42352.2	16542.3
0.229	99550.3	161.313	24.4096	32231.2	16827.7
0.36358	99049.5	820.602	38.9474	23962.4	15667.6
0.58143	98528.3	2057.9			

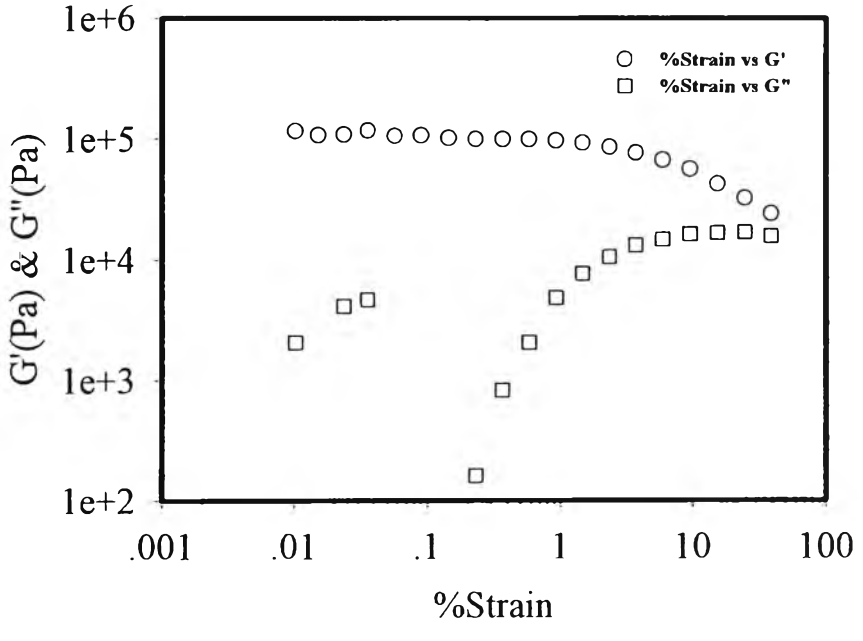

Figure H7 Storage modulus and loss modulus versus strain (%) obtained from dynamic strain sweep test of D1114P (19 %wt PS), parallel plate, gap = 1.076 mm, film diameter = 25 mm, electric field (E) = 0 V/mm, 27°C.

Table H5 Storage modulus and loss modulus data, obtained from dynamic strain sweep test of D1114P (19 %wt PS), parallel plate, gap = 1.076 mm, film diameter = 25 mm, electric field (E) = 2 kV/mm, 27°C

%strain	G'(Pa)	G"(Pa)	%strain	G'(Pa)	G"(Pa)
0.00855	110430	16927.1	0.93808	78434	13961.4
0.0145	101560	9037.88	1.50038	67114.7	14954.9
0.02181	112580	9360.45	2.39911	55965.1	15411.7
0.03465	117080	2957.13	3.83452	45263.5	15258.3
0.05638	117010	7505.94	6.12914	35320.8	14708.6
0.09038	113140	4006.18	9.78612	25652.8	14593.5
0.14429	108950	7706.24	15.6188	17449.4	13782.3
0.22984	104620	8279.27	24.8812	11662.1	12006.8
0.36543	97772.9	10747.7	39.5257	7886.6	10219.9
0.58649	88865.2	12944.8			

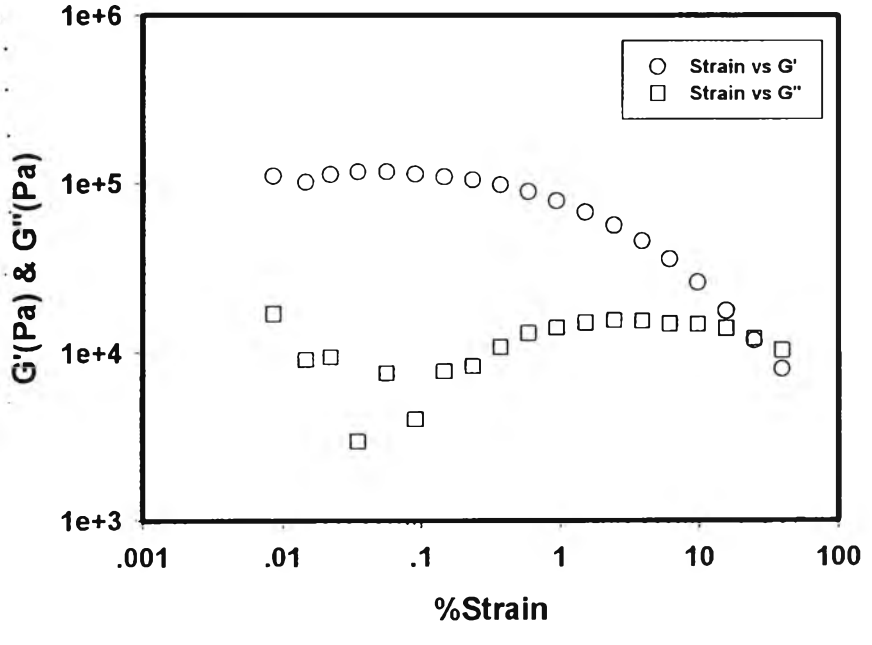

Figure H8 Storage modulus and loss modulus versus strain (%) obtained from dynamic strain sweep test of D1114P (19 %wt PS), parallel plate, gap = 1.076 mm, film diameter = 25 mm, electric field (E) = 2 kV/mm, 27°C.

Table H6 Storage modulus and loss modulus data, obtained from dynamic strain sweep test of D1164P (29 %wt PS), parallel plate, gap = 1.058 mm, film diameter = 25 mm, electric field (E) = 0 V/mm, 27°C

%strain	G'(Pa)	G''(Pa)	%strain	G'(Pa)	G''(Pa)
0.00986	72081.9	15745.3	0.94071	75485.5	5078.09
0.01544	80933.2	-872.62	1.49873	69331.1	7035.75
0.02363	89837.8	8616.06	2.39105	60316	8715.13
0.03629	91645.7	1551.3	3.81471	52340.6	10005.6
0.05757	93063.7	785.434	6.07859	45224	10339.3
0.092	89339.2	20.5974	9.68972	38645.4	9916.83
0.14623	86515.2	1656.88	15.4408	30380.3	8947.22
0.23266	84229	2889.68	24.6075	23858.9	9578.74
0.37035	81297.9	2842.42	39.2263	16755.8	8556.08
0.59185	78638.1	3918.13			

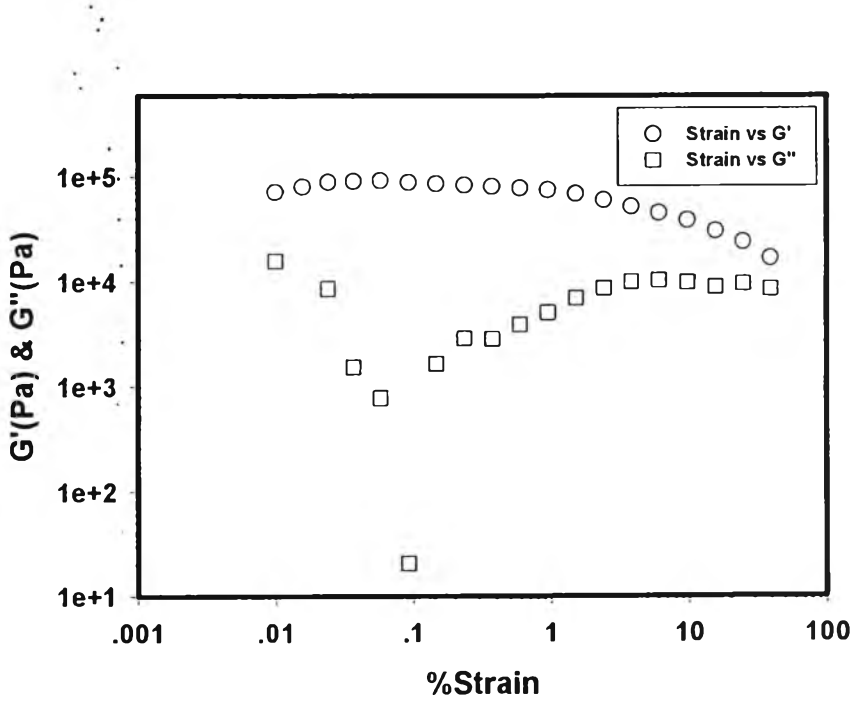

Figure H9 Storage modulus and loss modulus versus strain (%) obtained from dynamic strain sweep test of D1164P (29 %wt PS), parallel plate, gap = 1.058 mm, film diameter = 25 mm, electric field (E) = 0 V/mm, 27°C.

Table H7 Storage modulus and loss modulus data, obtained from dynamic strain sweep test of D1164P (29 %wt PS), parallel plate, gap = 1.058 mm, film diameter = 25 mm, electric field (E) = 2 kV/mm, 27°C

%strain	G'(Pa)	G"(Pa)	%strain	G'(Pa)	G"(Pa)
0.01014	58853.1	12275	0.96662	39650.3	2412.99
0.01566	53514.9	9034.08	1.5291	42634.3	-93.531
0.02422	54632	3320.67	2.42363	43939.6	430.709
0.03727	54218.3	2328.23	3.84395	42670.6	2075.43
0.05945	55262.7	4026.62	6.11441	39919.1	3808.96
0.09456	50751.7	3858.58	9.71386	33742.3	5321.26
0.15053	48436.2	3501.11	15.4603	28704.3	6430.25
0.23997	44908.4	4616.84	24.6438	23001.1	6557.42
0.38119	42448.8	4724.8	39.166	18579.8	6539.68
0.6103	39723.6	4295.75			

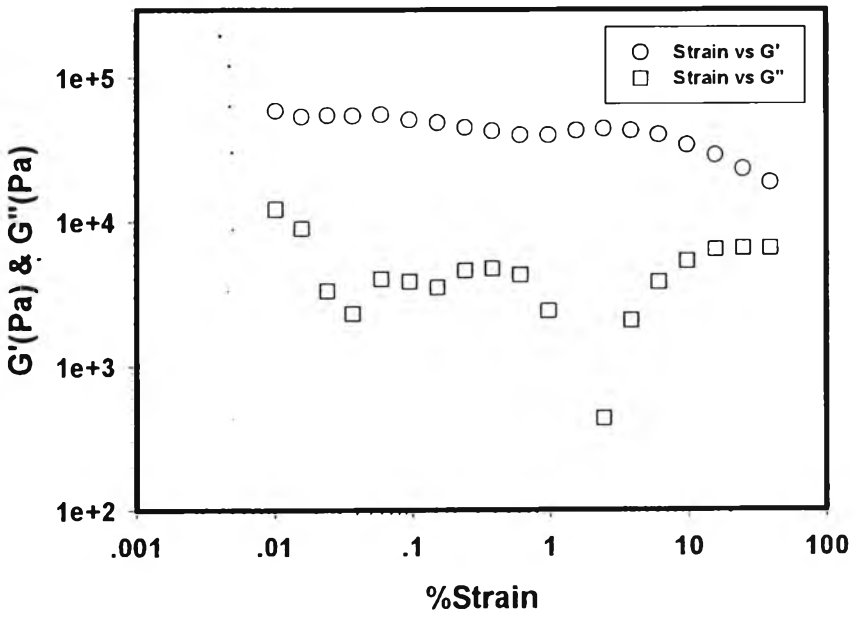

Figure H10 Storage modulus and loss modulus versus strain (%) obtained from dynamic strain sweep test of D1164P (29 %wt PS), parallel plate, gap = 1.058 mm, film diameter = 25 mm, electric field (E) = 2 kV/mm, 27°C.

Table H8 Storage modulus and loss modulus data, obtained from dynamic strain sweep test of D1162P (44 %wt PS), parallel plate, gap = 0.896 mm, film diameter = 25 mm, electric field (E) = 0 V/mm, 27°C

%strain	G'(Pa)	G"(Pa)	%strain	G'(Pa)	G"(Pa)
0.00895	227870	23324.3	0.91088	99325.2	33451.4
0.0134	257690	14143.2	1.48129	70384.7	34165.8
0.02021	254430	42494.4	2.42525	34441.3	30008.5
0.03188	245560	29801.7	3.91003	16830.8	19071.7
0.05035	233210	29783.7	6.26344	7002.08	9972.04
0.08104	223350	32534.9	9.94667	4266.69	6757.11
0.12923	206960	31206.4	15.8031	2389.71	4853.73
0.20929	186750	32543.9	25.0746	1348.3	3438.97
0.34028	162590	35142.6	39.758	732.628	2386.48
0.55343	132390	34943			

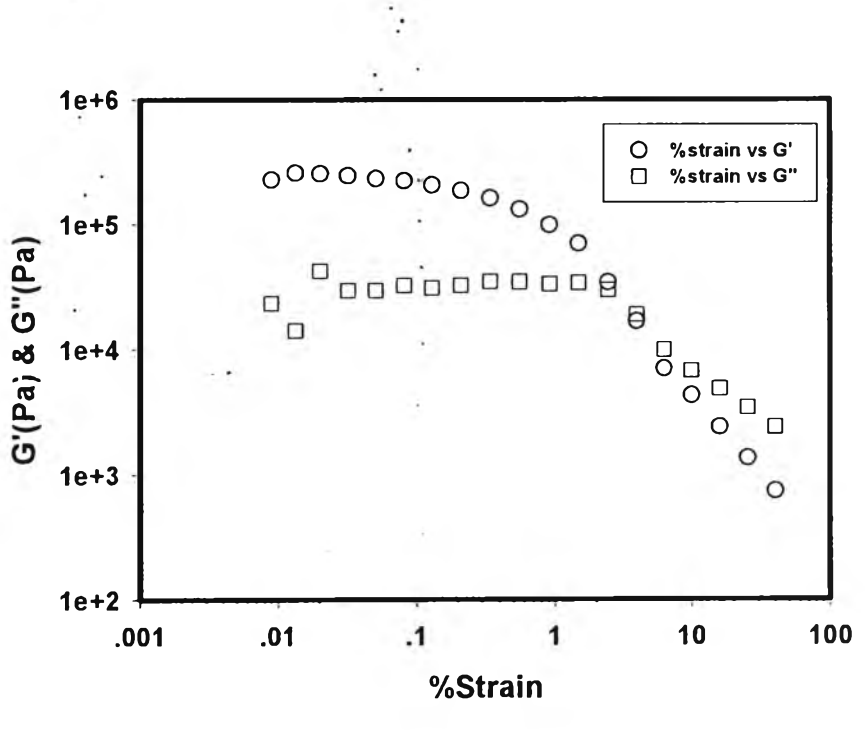

Figure H11 Storage modulus and loss modulus versus strain (%) obtained from dynamic strain sweep test of D1162P (44 %wt PS), parallel plate, gap = 0.861 mm, film diameter = 25 mm, electric field (E) = 0 V/mm, 27°C.

Table H9 Storage modulus and loss modulus data, obtained from dynamic strain sweep test of D1162P (44 %wt PS), parallel plate, gap = 0.896 mm, film diameter = 25 mm, electric field (E) = 2 kV/mm, 27°C

%strain	G'(Pa)	G"(Pa)	%strain	G'(Pa)	G"(Pa)
0.00779	392670	14834.2	0.79797	254110	60421.6
0.01186	387430	50521.2	1.34314	180630	64328.6
0.01751	406090	-2827.1	2.25848	110970	64499.2
0.02799	389650	39655	3.74293	61902.1	53439.1
0.04452	372630	11753.2	6.08199	35891.3	39649.1
0.0709	378610	24814.6	9.77579	21650.5	28309.9
0.11396	368950	21998.6	15.6286	13617.1	20010.5
0.18097	376190	24029.9	24.8894	8821.77	14452.6
0.28925	368240	33901.9	39.5804	5420.94	10603.8
0.47642	318250	51582.7			

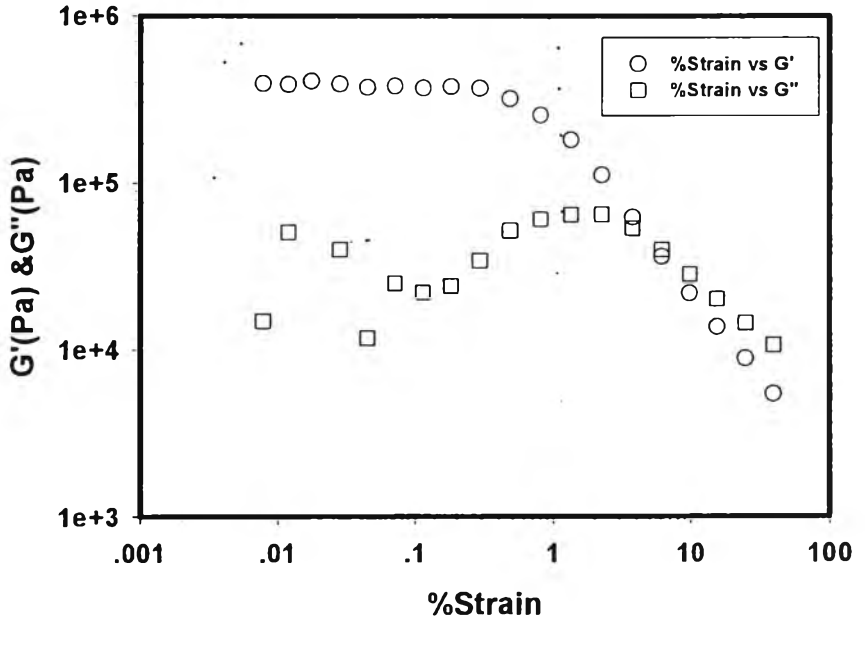

Figure H12 Storage modulus and loss modulus versus strain (%) obtained from dynamic strain sweep test of D1162P (44 %wt PS), parallel plate, gap = 0.861 mm, film diameter = 25 mm, electric field (E) = 2 kV/mm, 27°C.

The time sweep test was carried out with electric field applied on and off, alternately. The G'of each film was investigated to measure the time each film response reaches a steady state and there is no response under electric field stimulation. In Figure H13, the dynamic storage modulus (G') of D1114P was in steady state after 1000 s of measurement, without electric field strength. After that, the electric field was alternately applied. From the figure, D1114P could not be stimulated by electric field at 2 kV/mm. Similar result to D1114P, pure SIS D1164P reached a steady state after 1000 s of measurement in absence of electric field. But the film modulus (G') is not response to the electric filed. In the case of D1162P which reached a steady state after 1200 s, its response was similar to the first two, D1114P and D1164P. Their behaviors depend on their dielectric constant. Because they are low dielectric materials. Thus, the force generated under electric field is low. The effective actuation force is given by (Pelrine *et al., 2000*):

$$p = \varepsilon\varepsilon_0 E^2 = \varepsilon\varepsilon_0 (V/z)^2 \qquad \text{(H.1)}$$

where p is the actuation pressure, E is the electric field strength, ε is the dielectric constant, ε_0 is the permittivity of free space, V is voltage, and z is the polymer thickness.

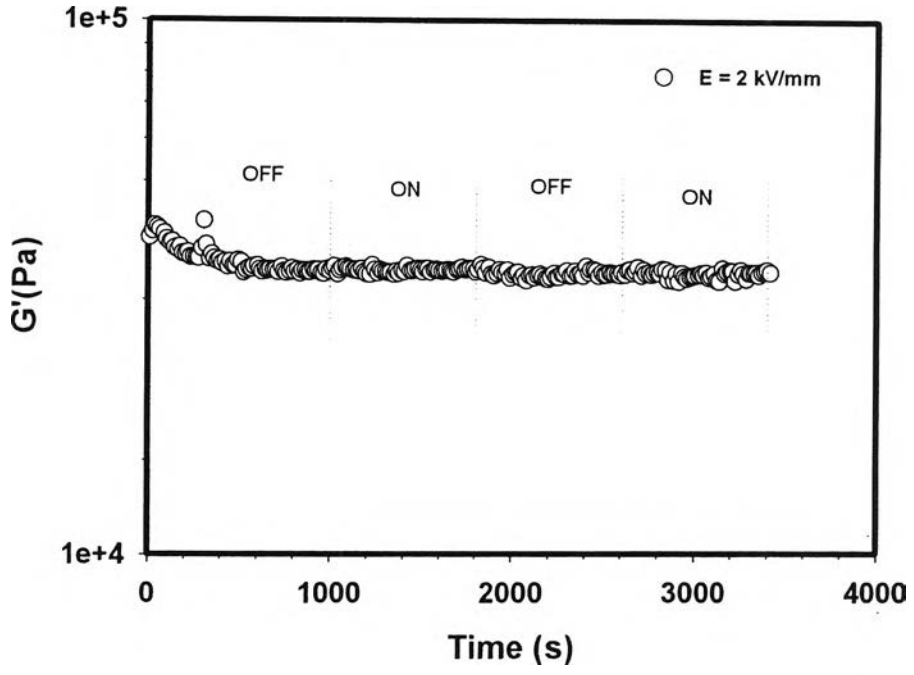

Figure H13 Temporal response testing of storage modulus (G') of D1114P (19 %wt PS), parallel plate, strain 0.2 %, gap 0.997 mm, film diameter 25 mm, freguency 1.0 rad/s, electric field (E) 2 kV/mm, 27°C.

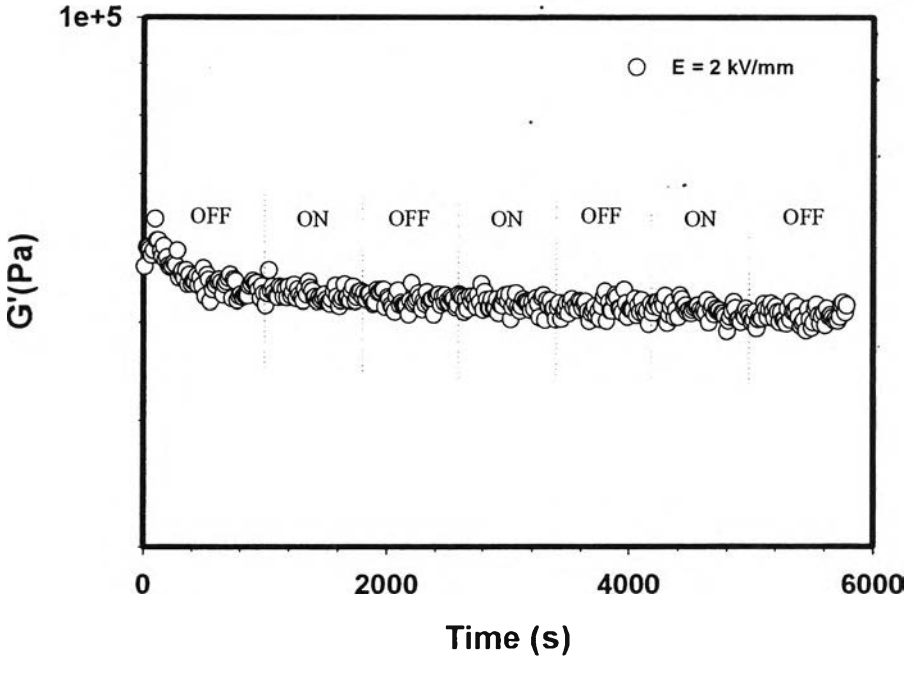

Figure H14 Temporal response testing of storage modulus (G') of D1164P (29 %wt PS), parallel plate, strain 0.1 %, gap 1.058 mm, film diameter 25 mm, freguency 1.0 rad/s, electric field (E) 2 kV/mm, 27°C.

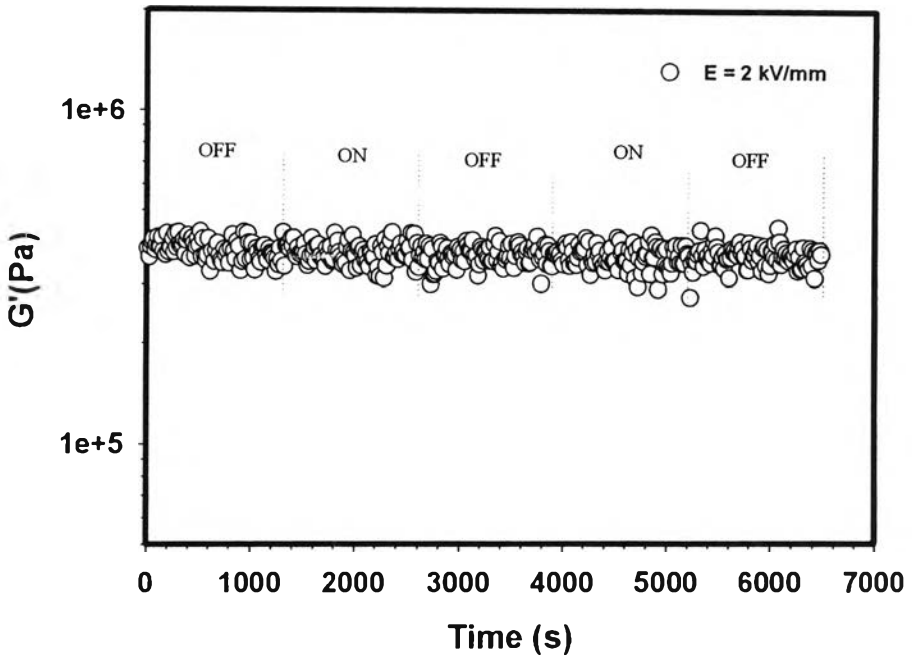

Figure H15 Temporal response testing of storage modulus (G') of D1162P (44 %wt PS), parallel plate, strain 0.02 %, gap 0.861 mm, film diameter 25 mm, freguency 1.0 rad/s, electric field (E) 2 kV/mm, 27°C.

Temporal response: dedoped PDPA/D1114P blends

5 % vol. DePDPA/D1114P

Table H10 Storage modulus and loss modulus versus strain (%) obtained from dynamic strain sweep test of 5 %vol. De_PDPA/D1114P, parallel plate, gap = 0.903 mm, film diameter = 25 mm, electric field (E) = 0 V/mm, 27°C

% strain	G'(Pa)	G"(Pa)	% strain	G'(Pa)	G"(Pa)
.0200	48031.9	5431.5	.7586	48236.4	7261.2
.0291	57623.2	7713.6	1.2068	46272.7	6898.5
.0462	56928.7	5235.9	1.9162	44175.3	7039.1
.0743	54949.0	7160.0	3.0514	39145.7	10603.3
.1174	54767.1	7527.0	4.8673	32207.1	10831.1
.1867	53502.2	7846.0	7.7107	32952.0	7860.4
.2971	52633.2	7586.0	12.2650	30949.90	7343.6
.4734	50772.7	7349.4	19.5245	25591.1	7411.0

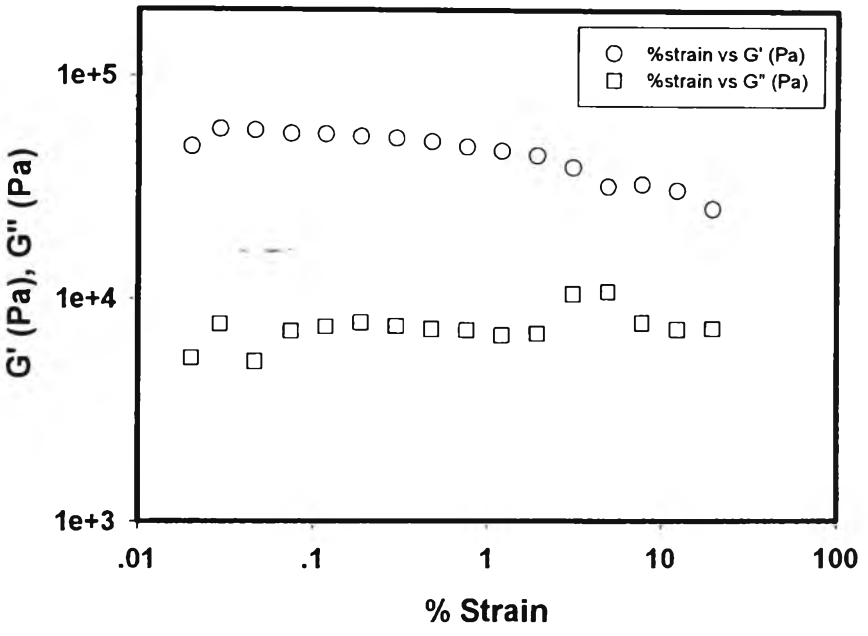

Figure H16 Storage modulus and loss modulus versus strain (%) obtained from dynamic strain sweep test of 5 %vol. De_PDPA/D1114P, parallel plate, gap = 0.903 mm, film diameter = 25 mm, electric field (E) = 0 V/mm, 27°C.

Table H11 Storage modulus and loss modulus versus strain (%) obtained from dynamic strain sweep test of 5 %vol. De_PDPA/D1114P, parallel plate, gap = 0.903 mm, film diameter = 25 mm, electric field (E) = 2 kV/mm, 27°C

% strain	G'(Pa)	G"(Pa)	% strain	G'(Pa)	G"(Pa)
.0194	38808.1	2720.9	.7716	30254.2	4306.6
.0298	37169.2	5939.4	1.2253	29239.9	4136.2
.0463	37925.3	3907.37	1.9428	28399.1	3945.0
.0747	35839.1	4918.9	3.0843	27453.3	4002.3
.1193	35309.4	4224.2	4.8953	26128.0	4765.4
.1904	34218.4	4542.1	7.7962	22134.6	7130.8
.3033	32695.5	4404.3	12.3755	20862.6	6036.5
.4823	31454.6	4447.2	19.6251	19450.9	5479.4

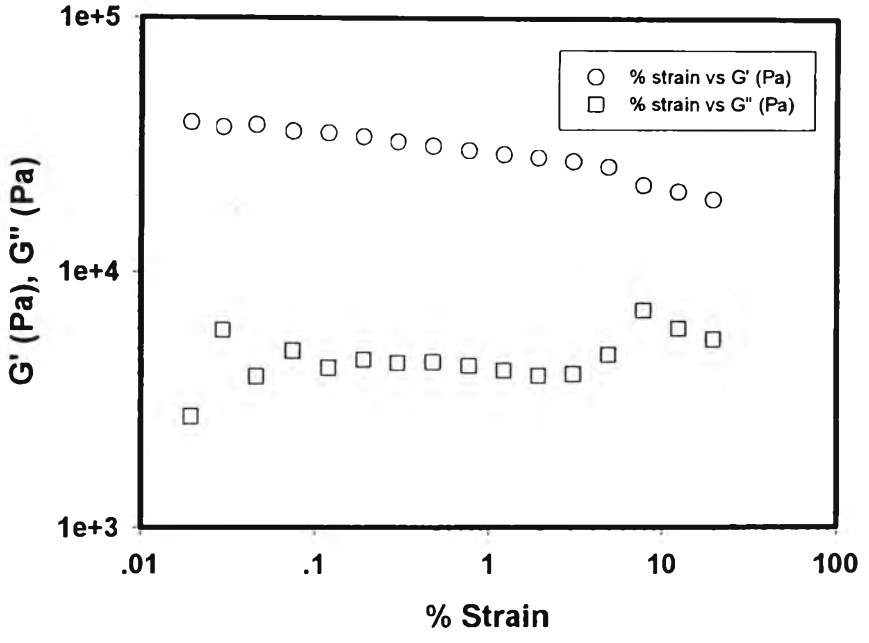

Figure H17 Storage modulus and loss modulus versus strain (%) obtained from dynamic strain sweep test of 5 %vol. De_PDPA/D1114P, parallel plate, gap = 0.903 mm, film diameter = 25 mm, electric field (E) = 2 kV/mm, 27°C.

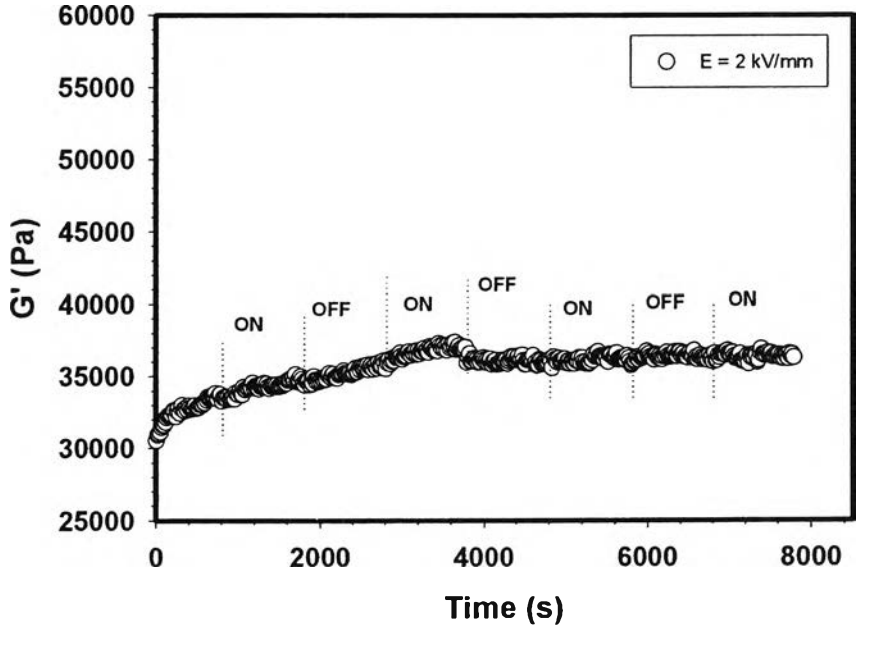

Figure H18 Temporal response testing of storage modulus (G') of 5 %vol. De_PDPA/D1114P, parallel plate, strain 0.2 %, gap 0.900 mm, film diameter 25 mm, freguency 1.0 rad/s, electric field (E) 2 kV/mm, 27°C.

10 % vol. DePDPA/D1114P

Table H12 Storage modulus and loss modulus versus strain (%) obtained from dynamic strain sweep test of 10 %vol. De_PDPA/D1114P, parallel plate, gap = 0.854 mm, film diameter = 25 mm, electric field (E) = 0 V/mm, 27°C

% strain	G'(Pa)	G"(Pa)	% strain	G'(Pa)	G"(Pa)
.0200	33186.8	10783.8	.7709	28850.5	4800.8
.0301	36422.3	4824.8	1.2249	26705.7	5146.0
.0463	37580.1	2965.7	1.9475	24665.7	5030.8
.0744	33538.4	4118.7	3.0943	22727.0	4843.8
.1193	32890.2	4537.9	4.9113	21259.8	5060.1
.1907	32363.7	4869.7	7.8037	19834.6	4698.5
.3030	31484.6	4593.0	12.3737	18961.3	4612.7
.4820	30356.7	4316.5	19.5887	20877.6	4922.0

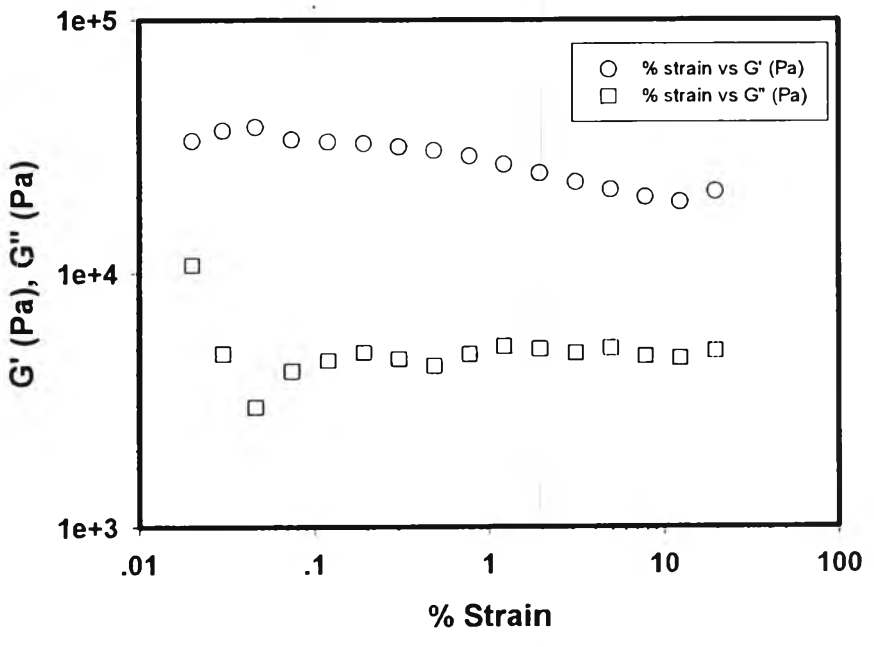

Figure H19 Storage modulus and loss modulus versus strain (%) obtained from dynamic strain sweep test of 10 %vol. De_PDPA/D1114P, parallel plate, gap = 0.854 mm, film diameter = 25 mm, electric field (E) = 0 V/mm, 27°C.

Table H13 Storage modulus and loss modulus versus strain (%) obtained from dynamic strain sweep test of 10 % vol. De_PDPA/D1114P, parallel plate, gap = 0.854 mm, film diameter = 25 mm, electric field (E) = 2 kV/mm, 27°C

% strain	G'(Pa)	G"(Pa)	% strain	G'(Pa)	G"(Pa)
.0172	42903.5	-1578.1	.7667	34380.3	4559.8
.0280	35854.3	-5358.5	1.2188	32064.9	5211.2
.0452	40442.5	2063.9	1.9382	29972.7	5226.6
.0730	38901.7	2629.0	3.0774	28093.2	5081.2
.1175	38235.6	3210.9	4.8911	25662.5	6346.0
.1891	36339.8	3758.33	7.7858	22615.8	6143.9
.3011	35749.4	3671.0	12.3302	23097.4	5029.6
.4796	35409.7	3710.9	19.5161	24993.9	5502.5

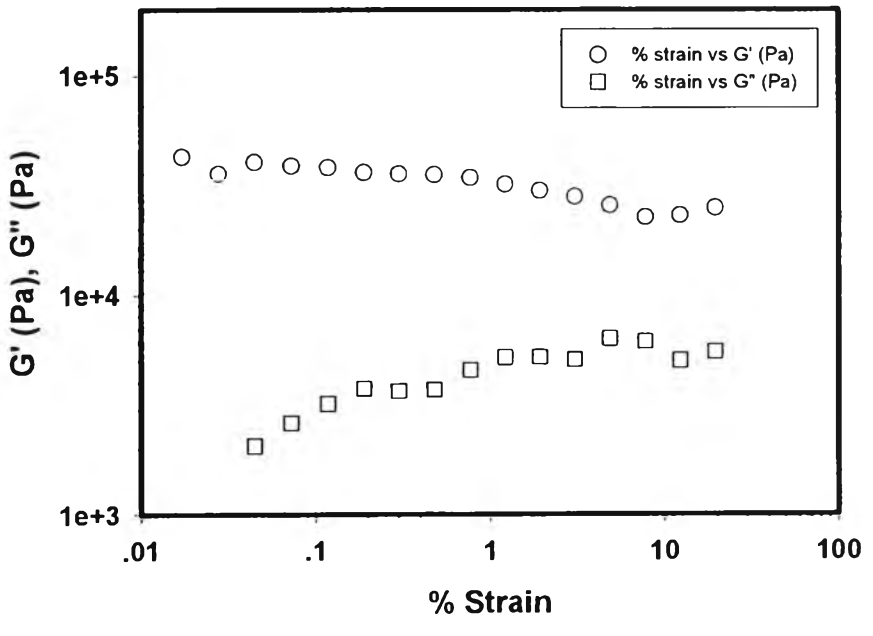

Figure H20 Storage modulus and loss modulus versus strain (%) obtained from dynamic strain sweep test of 10 %vol. De_PDPA/D1114P, parallel plate, gap = 0.854 mm, film diameter = 25 mm, electric field (E) = 2 kV/mm, 27°C.

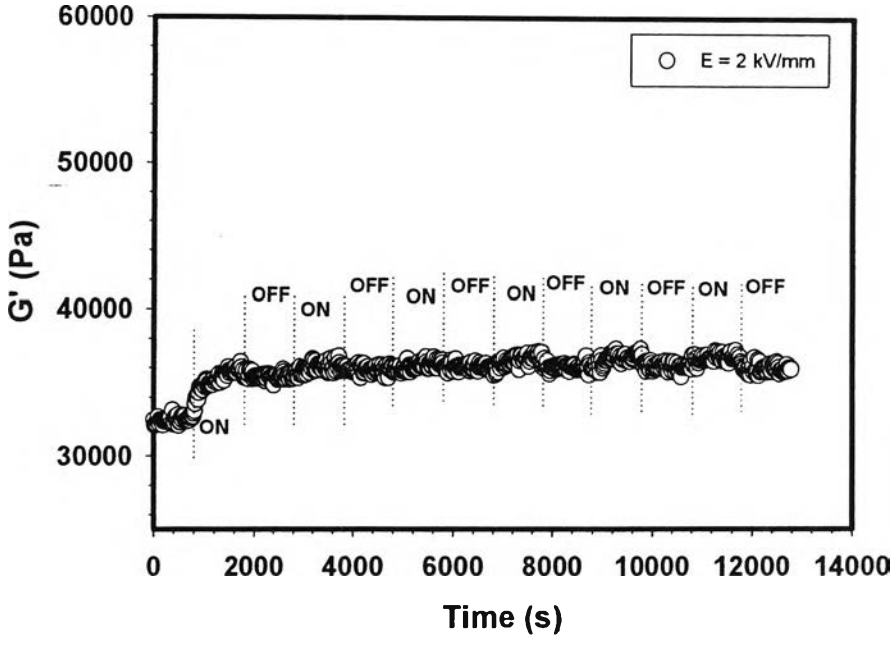

Figure H21 Temporal response testing of storage modulus (G') of 10 %vol. De_PDPA/D1114P, parallel plate, strain 0.3 %, gap 0.854 mm, film diameter 25 mm, freguency 1.0 rad/s, electric field (E) 2 kV/mm, 27°C.

20 % vol. DePDPA/D1114P

Table H14 Storage modulus and loss modulus versus strain (%) obtained from dynamic strain sweep test of 20 %vol. De_PDPA/D1114P, parallel plate, gap = 0.988 mm, film diameter = 25 mm, electric field (E) = 0 V/mm, 27°C

% Strain	G'(Pa)	G"(Pa)	% Strain	G'(Pa)	G"(Pa)
0.01844	115430	21698.4	0.76232	48111.3	21785.4
0.02737	117870	27891.2	1.22191	35211.7	17381.8
0.04402	112370	18753.4	1.95031	26965.9	12860.6
0.07067	108100	22809.4	3.1065	21603	10431
0.11299	103040	20922	4.95336	14278	8271.58
0.18184	94664.8	20539.2	7.89593	9154.91	6753.66
0.29145	85314.4	20355.8	12.5559	5065.99	5948.5
0.46816	71765.6	20846.5	19.937	2916.2	4688.62

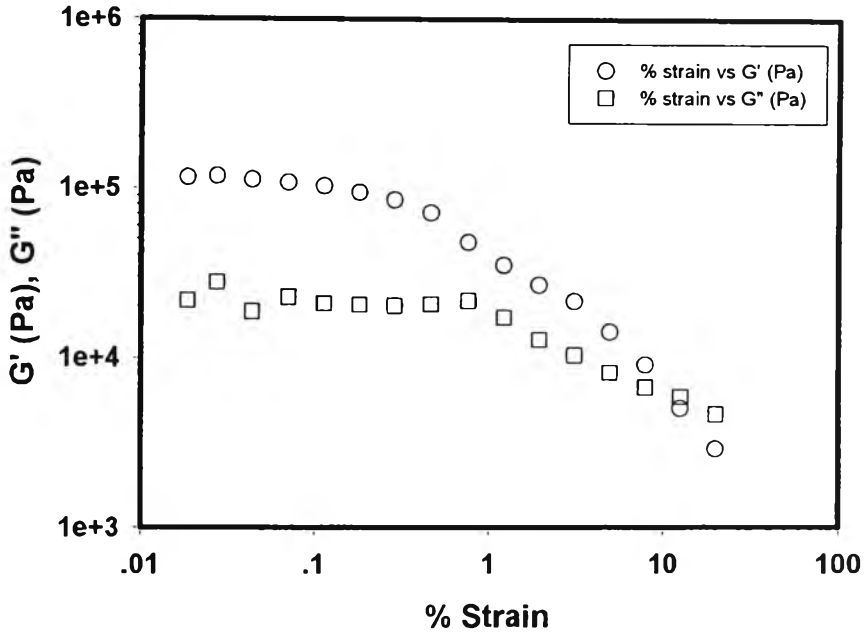

Figure H22 Storage modulus and loss modulus versus strain (%) obtained from dynamic strain sweep test of 20 %vol. De_PDPA/D1114P, parallel plate, gap = 0.988 mm, film diameter = 25 mm, electric field (E) = 0 V/mm, 27°C.

Table H15 Storage modulus and loss modulus versus strain (%) obtained from dynamic strain sweep test of 20 %vol. De_PDPA/D1114P, parallel plate, gap = 0.988 mm, film diameter = 25 mm, electric field (E) = 2 kV/mm, 27°C

% Strain	G'(Pa)	G"(Pa)	% Strain	G'(Pa)	G"(Pa)
0.0174	159480	59329.4	0.75902	50455.4	35563
0.02605	177250	43244.2	1.21944	37120.1	26673.6
0.04143	176130	42956.4	1.94611	29068.2	19690.2
0.06679	173860	38548.4	3.09916	23675	15395.2
0.10831	158390	44922.2	4.93566	18546.2	13396.5
0.17636	133610	48674.9	7.85451	13557.4	12257.3
0.28761	101860	50371.4	12.52	8607.17	10902.2
0.46796	71277.1	44698.4	19.9059	4944.99	8408.33

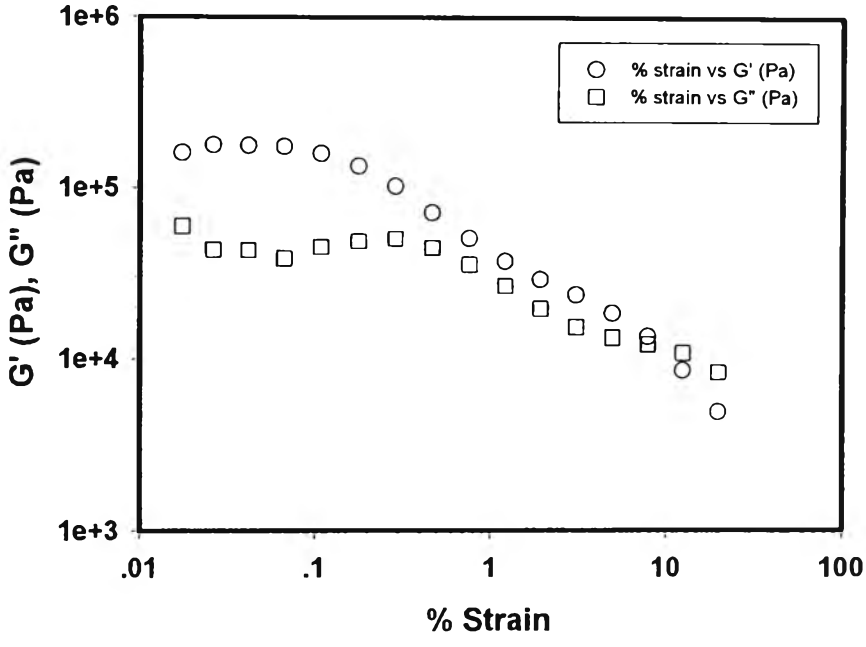

Figure H23 Storage modulus and loss modulus versus strain (%) obtained from dynamic strain sweep test of 20 %vol. De_PDPA/D1114P, parallel plate, gap = 0.988 mm, film diameter = 25 mm, electric field (E) = 2 kV/mm, 27°C.

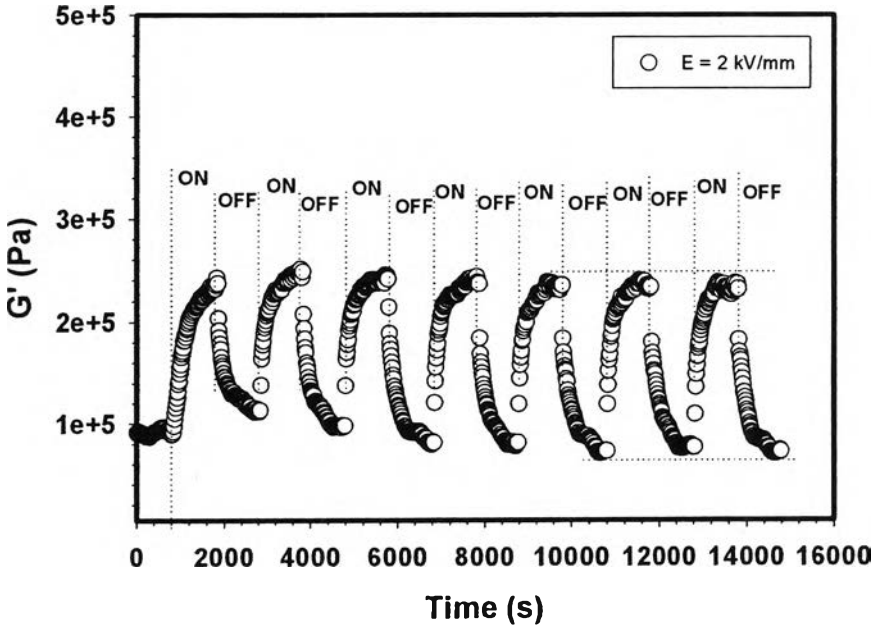

Figure H24 Temporal response testing of storage modulus (G') of 20 %vol. De_PDPA/D1114P, parallel plate, strain 0.1 %, gap 0.980 mm, film diameter 25 mm, freguency 1.0 rad/s, electric field (E) 2 kV/mm, 27°C.

30 % vol. DePDPA/D1114P

Table H16 Storage modulus and loss modulus versus strain (%) obtained from dynamic strain sweep test of 30 % vol. De_PDPA/D1114P, parallel plate, gap = 0.984 mm, film diameter = 25 mm, electric field (E) = 0 V/mm, 27°C

% Strain	G'(Pa)	G"(Pa)	% Strain	G'(Pa)	G"(Pa)
0.01802	200930	42952.2	0.6948	167120	58509.1
0.02588	224050	44937.7	1.1899	64955.5	70461.5
0.04057	219220	47075.7	1.94608	28959.6	47602.1
0.06536	215810	46448.7	3.12954	12347.7	28865.6
0.1043	216440	46825.5	4.99206	5335.45	17490.6
0.16699	209680	47258.2	7.9416	2464.82	11000.1
0.26636	204240	45736.3	12.5882	1169.38	7046.63
0.42651	193470	47406.4	19.9842	542.721	4562.1

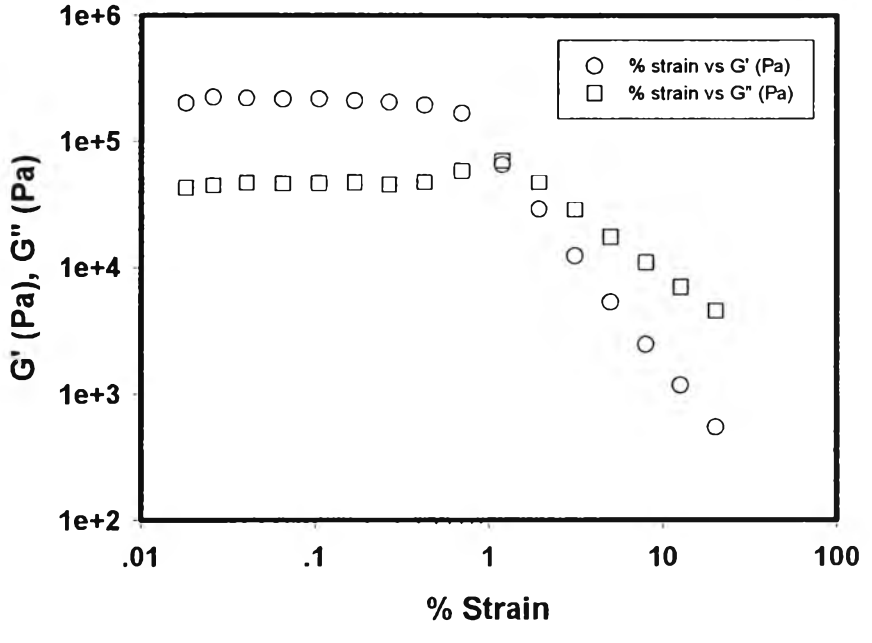

Figure H25 Storage modulus and loss modulus versus strain (%) obtained from dynamic strain sweep test of 30 %vol. De_PDPA/D1114P, parallel plate, gap = 0.984 mm, film diameter = 25 mm, electric field (E) = 0 V/mm, 27°C.

Table H17 Storage modulus and loss modulus versus strain (%) obtained from dynamic strain sweep test of 30 % vol. De_PDPA/D1114P, parallel plate, gap = 0.984 mm, film diameter = 25 mm, electric field (E) = 2 kV/mm, 27°C

% Strain	G'(Pa)	G"(Pa)	% Strain	G'(Pa)	G"(Pa)
0.0141	412810	63683	0.66426	219990	139080
0.02144	419480	83970.1	1.15249	101820	110070
0.03515	415120	52265.2	1.91297	47416	76089.7
0.05652	418500	70927.4	3.09601	24463.3	45811
0.09021	418660	64372.6	4.96144	12058.1	29541.8
0.14381	425660	64726.4	7.87373	6026.37	19501.5
0.22884	424810	72413.4	12.5688	3140.44	12733.4
0.37076	393990	88622.7	19.9545	1733.65	8519.68

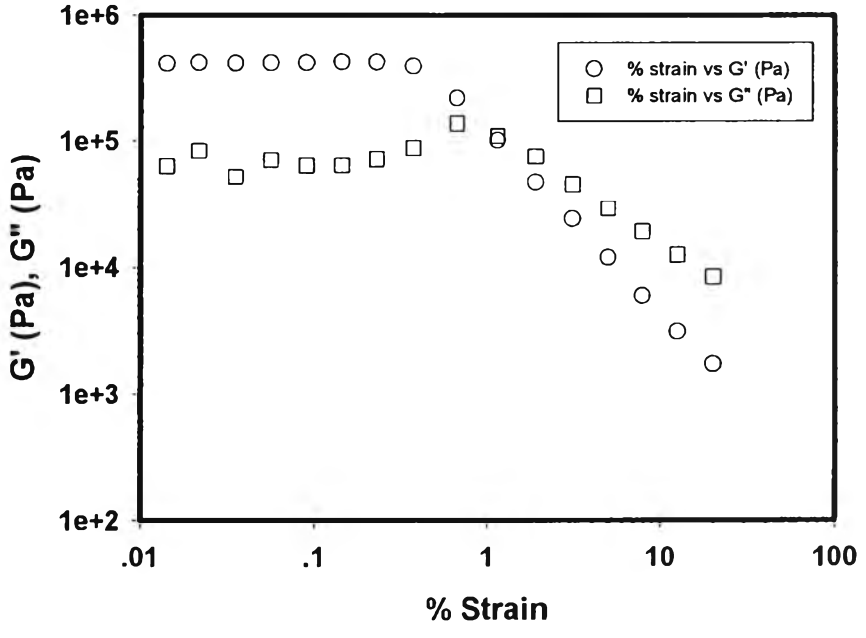

Figure H26 Storage modulus and loss modulus versus strain (%) obtained from dynamic strain sweep test of 30 %vol. De_PDPA/D1114P, parallel plate, gap = 0.984 mm, film diameter = 25 mm, electric field (E) = 2 kV/mm, 27°C.

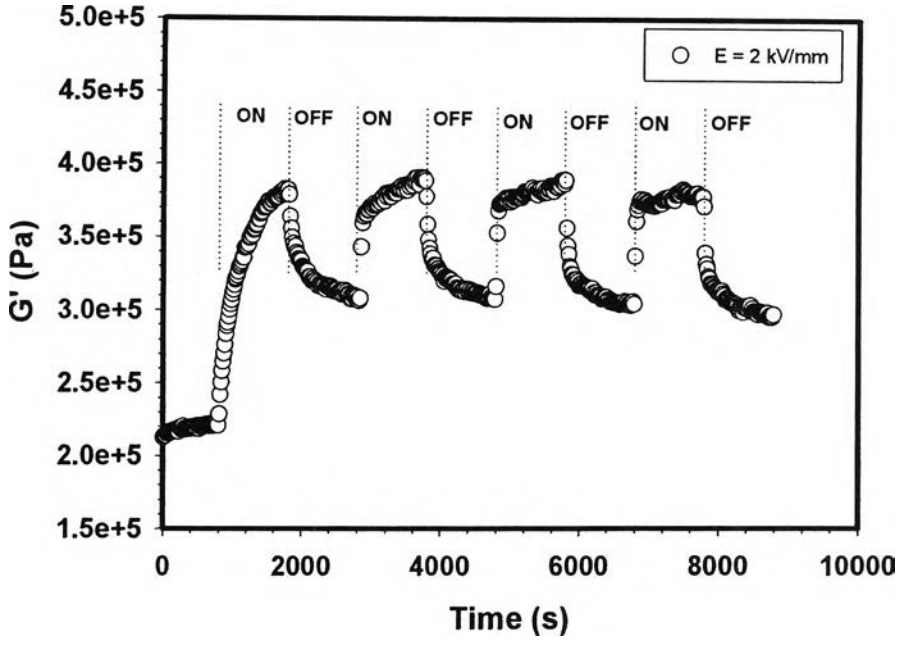

Figure H27 Temporal response testing of storage modulus (G') of 30 %vol. De_PDPA/D1114P, parallel plate, strain 0.3 %, gap 0.978 mm, film diameter 25 mm, freguency 1.0 rad/s, electric field (E) 2 kV/mm, 27°C.

Appendix I Density Determination by Pycnometer

The density of dedoped-Polydiphenylamine and the doped-polymers with various doping mole ratios was determined by using Ultrapycnometer (Ultrapycnometer 1000, V 2.4) with small cell size. The polymers were firstly vacuum-dried for 24 hr and then weighted at ambient temperature, loaded the sample to the cell. Density determination was carried out 10 time for each sample for a run under flow purge mode, target gas pressure 17 psi, and calibration volumes: V_{added} 12.4159 cm^3; V_{cell} 20.8093 cm^3.

Table I1 Density data of dedoped-polydiphenylamine (De_PDPA) measured at 27 °C, sample weight 0.2515 g

Run	Volume (cm^3)	Density (g/cm^3)
1	0.1857	1.1756
2	0.1843	1.1732
3	0.1869	1.1703
4	0.1891	1.1743
5	0.1886	1.1857
6	0.1912	1.1685
7	0.1923	1.1734
8	0.191	1.1807
9	0.1914	1.1814
10	0.191	1.1886

Average Volume	0.1912 cm^3
Average Density	1.3156 g/cm^3
Standard Deviation	0.00061 g/cm^3

Table I2 Density data of doped-polydiphenylamine at doping mole ratio $N_{HCl}:N_{monomer}$, 200:1 (D_PDPA 200:1) measured at 27.1 °C, sample weight 0.2349 g

Run	Volume (cm^3)	Density (g/cm^3)
1	0.1975	1.1893
2	0.1959	1.1992
3	0.1962	1.1973
4	0.1956	1.2008
5	0.1953	1.2026
6	0.1948	1.2057
7	0.1959	1.1994
8	0.1959	1.1989
9	0.1971	1.1915
10	0.1973	1.1905

Average Volume	0.1968 cm^3
Average Density	1.1936 g/cm^3
Standard Deviation	0.0038 g/cm^3

Table I3 Density data of doped-polydiphenylamine at doping mole ratio $N_{HCl}:N_{monomer}$, 100:1 (D_PDPA 100:1) measured at 29.2 °C, sample weight 0.2257 g

Run	Volume (cm3)	Density (g/cm3)
1	0.1816	1.2426
2	0.181	1.2471
3	0.1789	1.2617
4	0.1828	1.2349
5	0.1829	1.2337
6	0.1819	1.2406
7	0.1832	1.2319
8	0.1821	1.2393
9	0.1833	1.2314
10	0.1819	1.2409

Average Volume	0.1824 cm^3
Average Density	1.2372 g/cm^3
Standard Deviation	0.0042 g/cm^3

Table I4 Density data of doped-polydiphenylamine at doping mole ratio $N_{HCl}:N_{monomer}$, 10:1 (D_PDPA 10:1) measured at 26.1°C, sample weight 0.2239 g

Run	Volume (cm3)	Density (g/cm3)
1	0.1905	1.1756
2	0.1909	1.1732
3	0.1913	1.1703
4	0.1907	1.1743
5	0.1888	1.1857
6	0.1916	1.1685
7	0.1908	1.1734
8	0.1896	1.1807
9	0.1895	1.1814
10	0.1884	1.1886

Average Volume	0.1892 cm^3
Average Density	1.1836 g/cm^3
Standard Deviation	0.0036 g/cm^3

Appendix J Frequency sweep test; various electric fields and temperature

Frequency test of D1114P

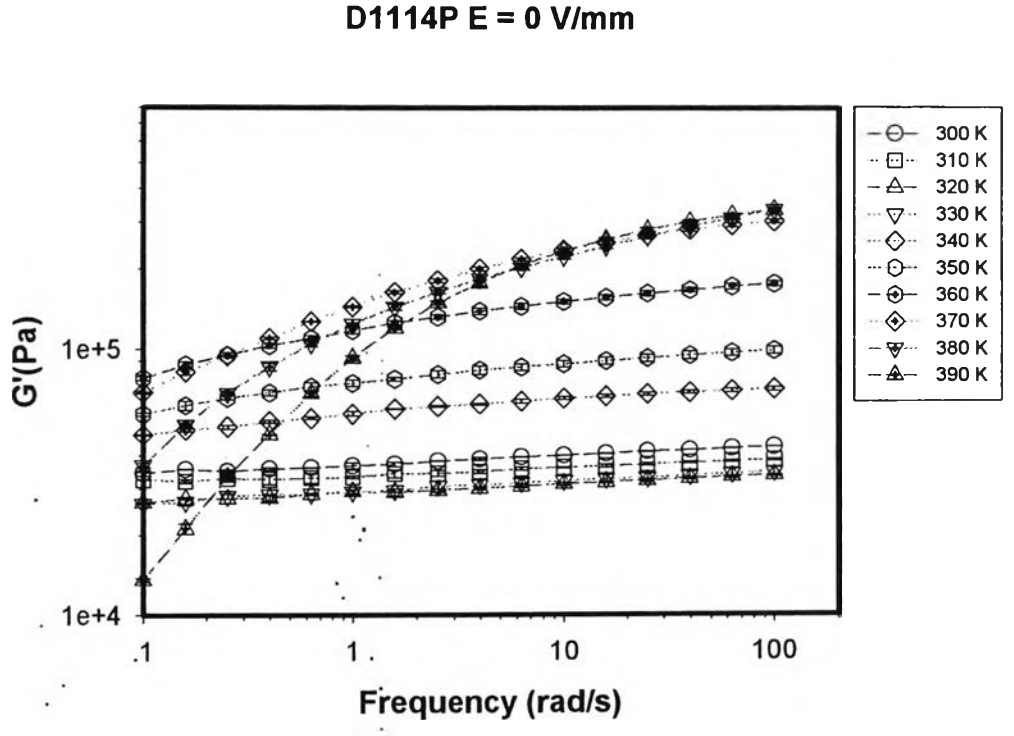

(a)

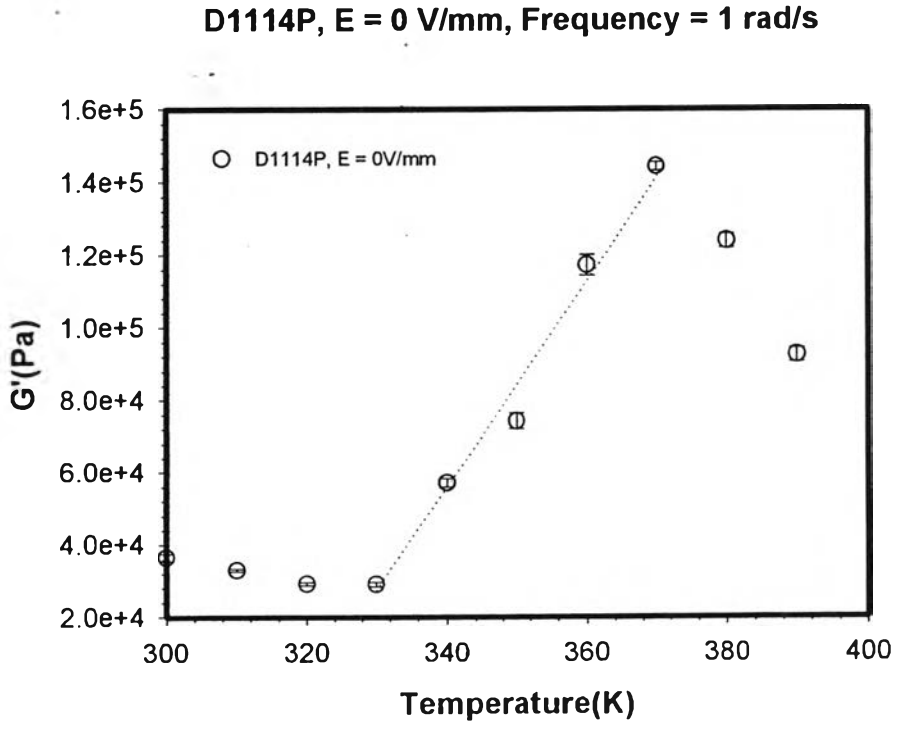

(b)

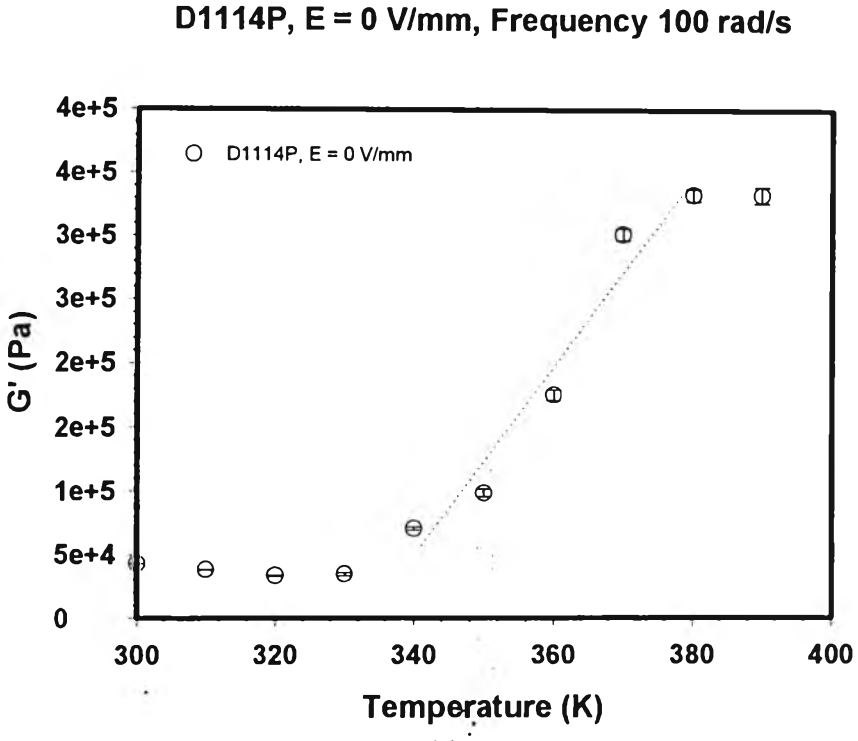

(c)

Figure J1 D1114P at E = 0V/mm, strain 0.2 % (a) frequency sweep test at various temperatures; (b) storage modulus (G') versus temperature at frequency 1 rad/s; (c) storage modulus (G') versus temperature at frequency 100 rad/s.

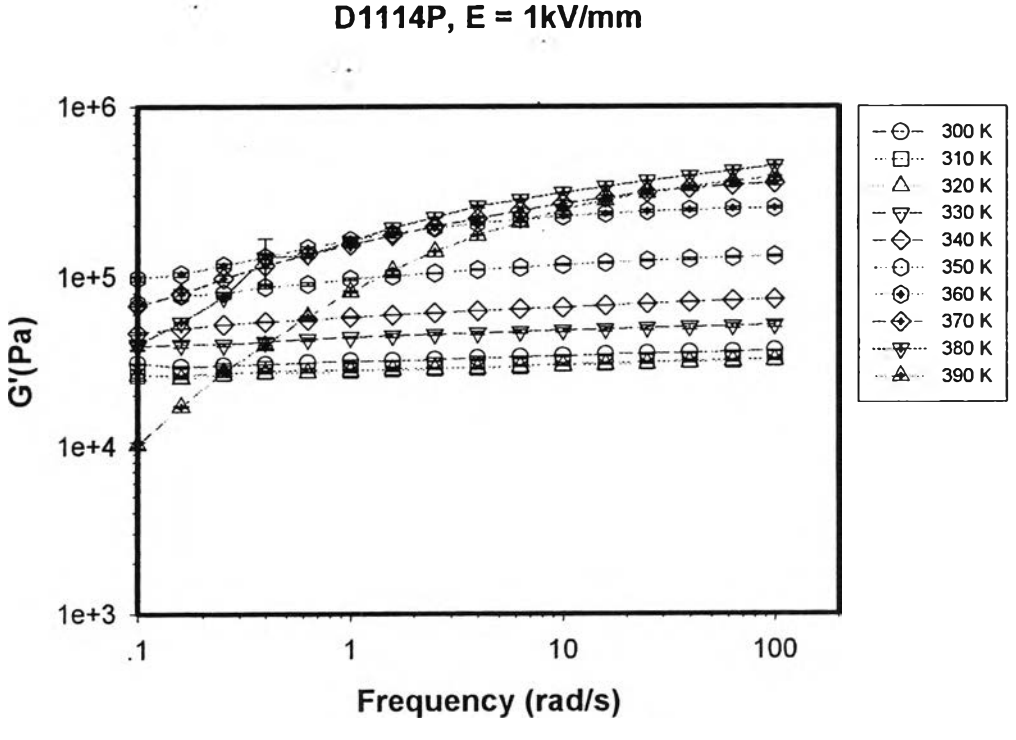

(a)

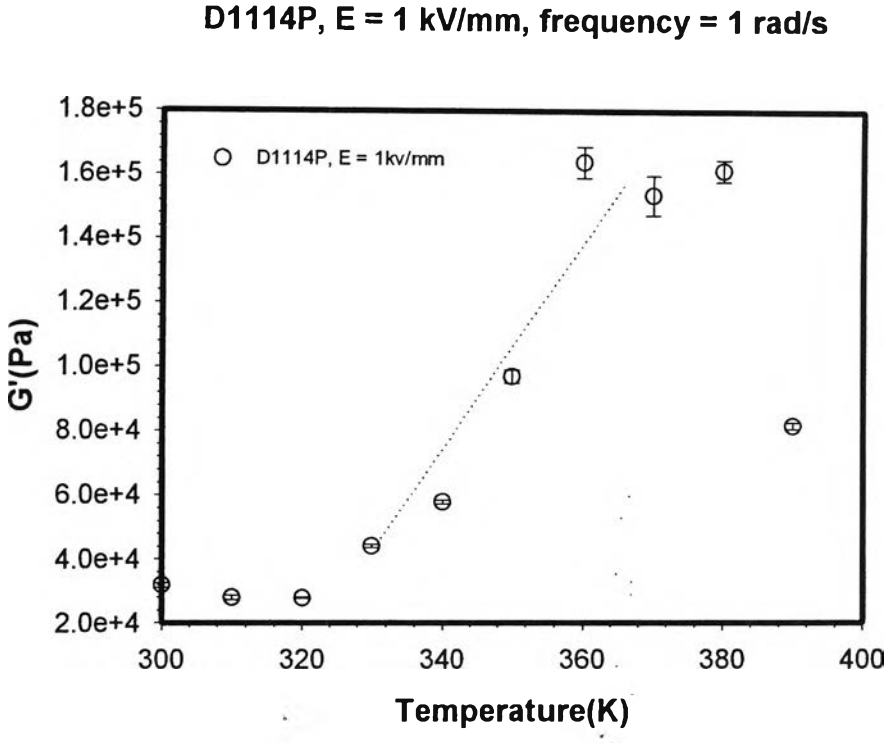

(b)

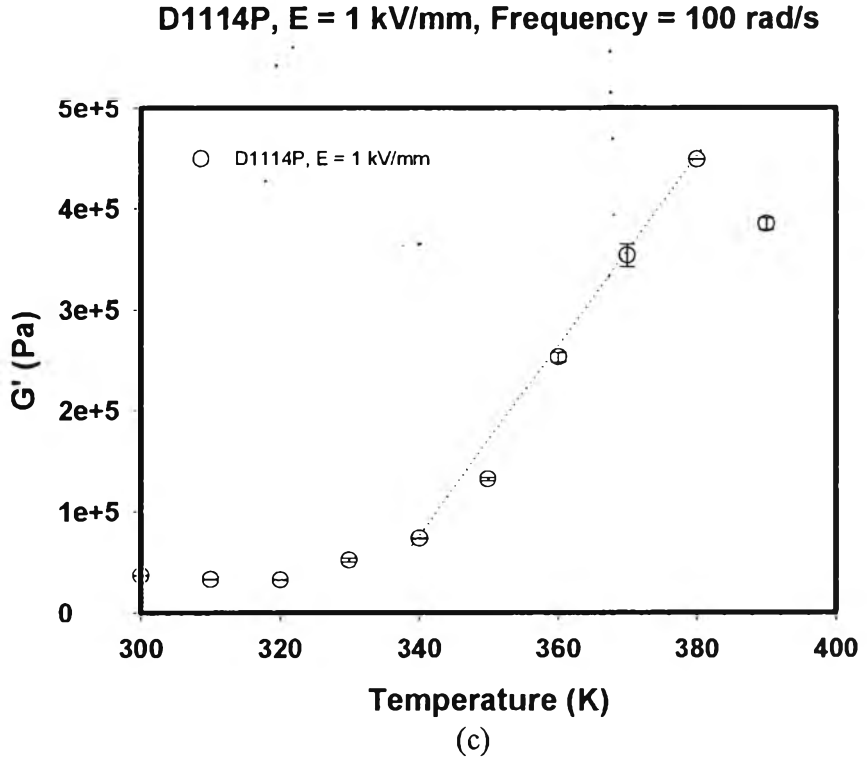

(c)

Figure J2 D1114P at E = 1 kV/mm, strain 0.2 %: (a) frequency sweep test at various temperatures; (b) storage modulus (G') versus temperature at frequency 1 rad/s; (c) storage modulus (G') versus temperature at frequency 100 rad/s.

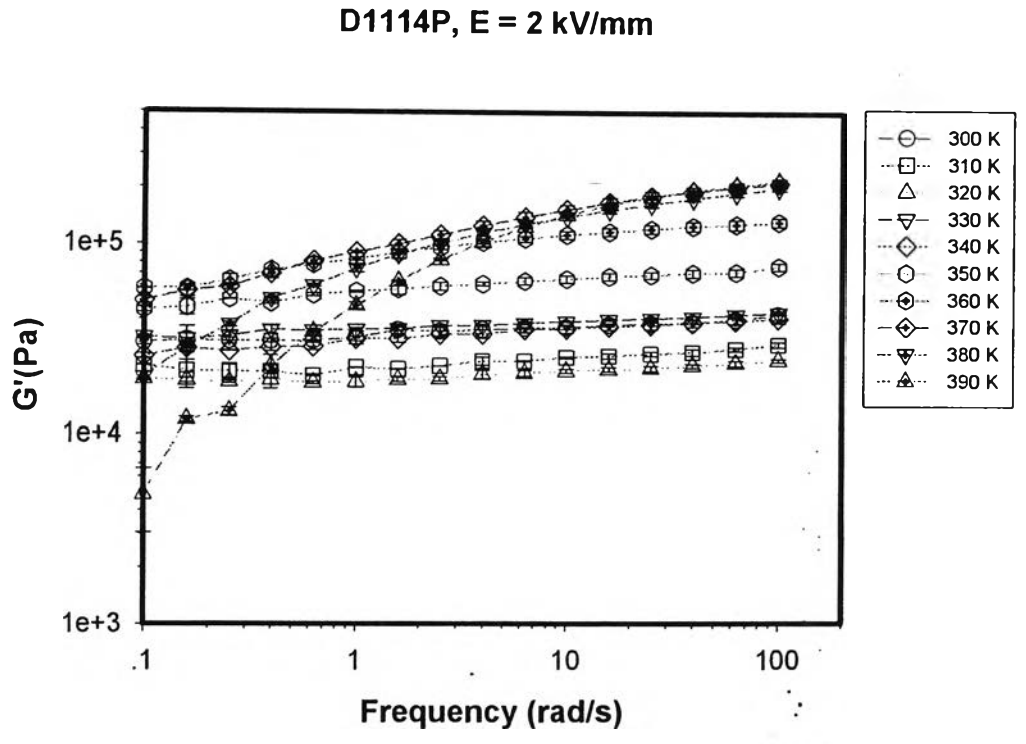
D1114P, E = 2 kV/mm
G'(Pa)
1e+5
1e+4
1e+3
.1
1
10
100
Frequency (rad/s)
300 K
310 K
320 K
330 K
340 K
350 K
360 K
370 K
380 K
390 K

(a)

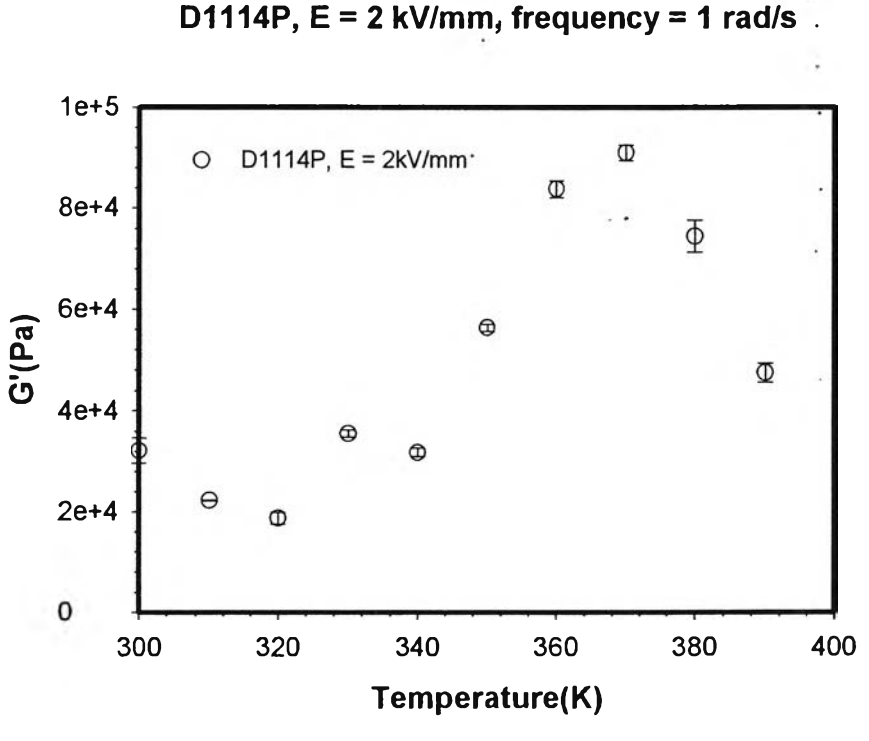
D1114P, E = 2 kV/mm, frequency = 1 rad/s
G'(Pa)
1e+5
8e+4
6e+4
4e+4
2e+4
0
D1114P, E = 2kV/mm
300
320
340
360
380
400
Temperature(K)

(b)

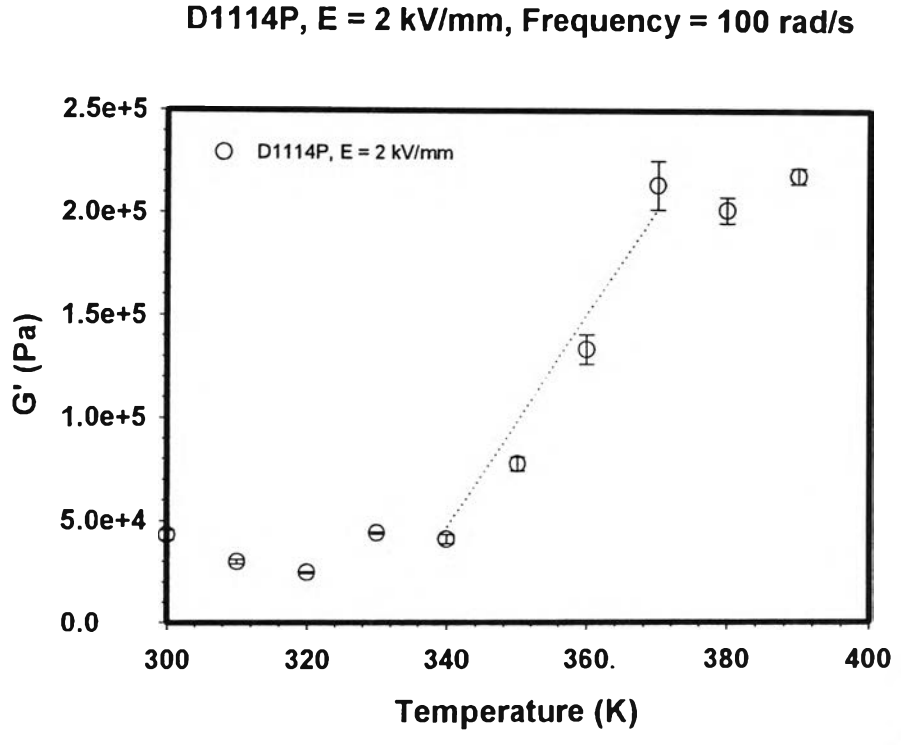

(c)

Figure J3 D1114P at E = 2 kV/mm, strain 0.2 %; (a) frequency sweep test at various temperatures; (b) storage modulus (G') versus temperature at frequency 1 rad/s; (c) storage modulus (G') versus temperature at frequency 100 rad/s.

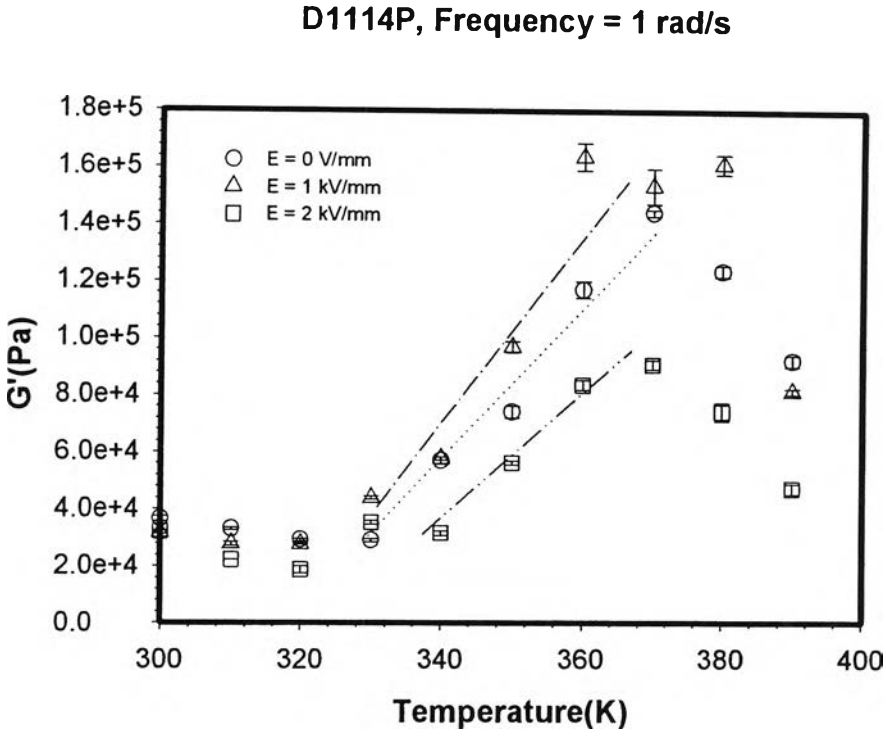

Figure J4 Comparison of D1114P's storage modulus exhibited at different temperatures under various electric fields, frequency 1 rad/s, and strain 0.2 %.

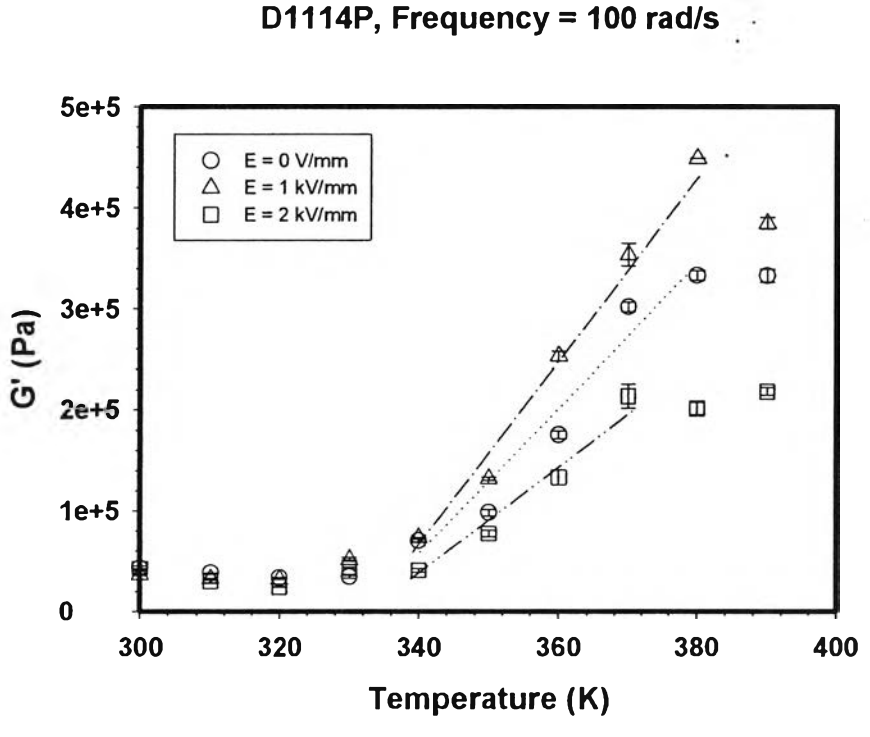

Figure J5 Comparison of D1114P's storage modulus exhibited at different temperatures under various electric fields, frequency 100 rad/s, and strain 0.2 %.

Frequency test of D1164P

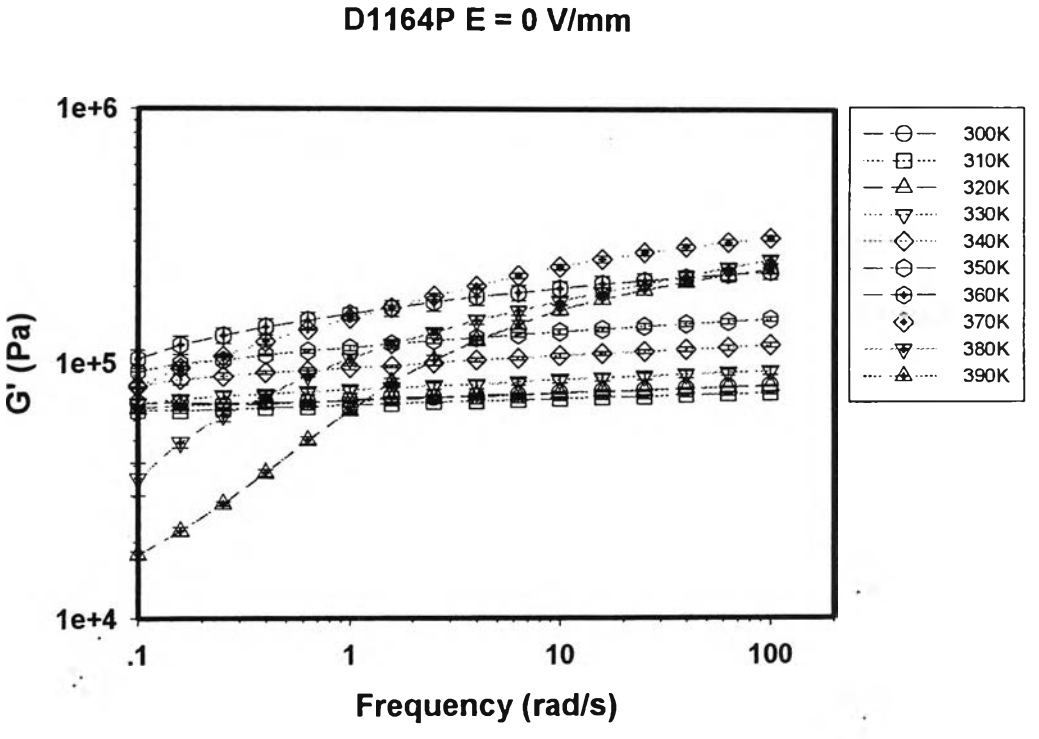

(a)

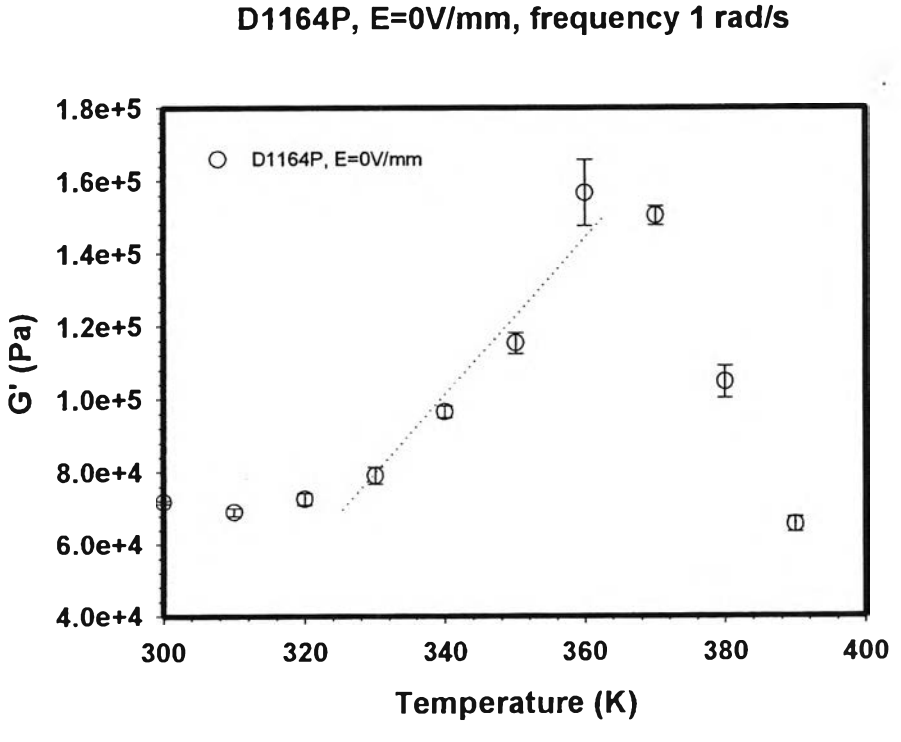

(b)

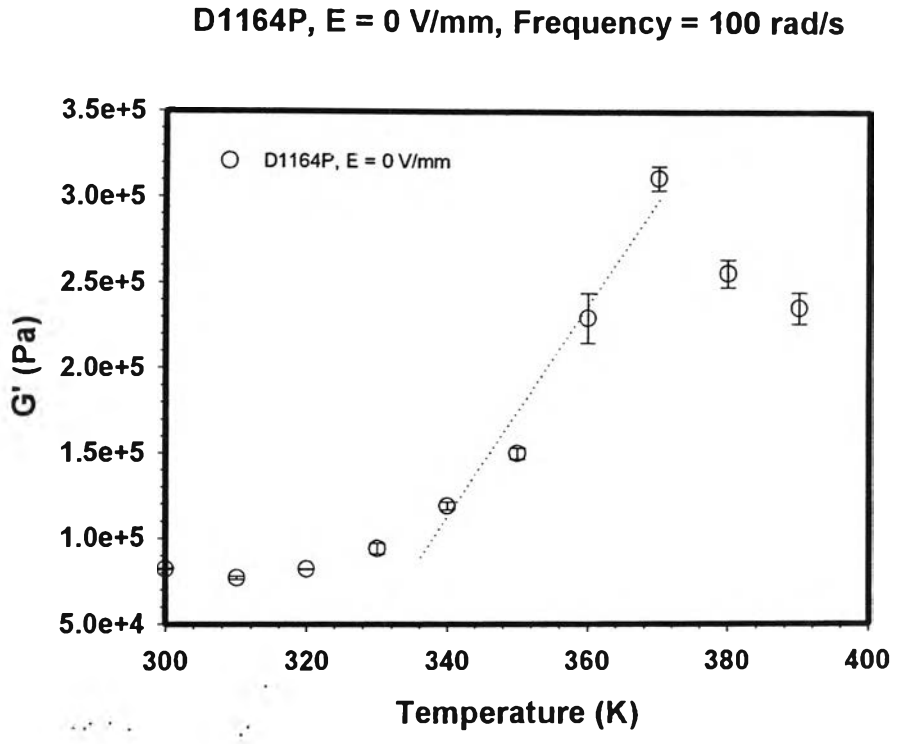

(c)

Figure J6 D1164P at E = 0 V/mm, strain 0.1 %: (a) frequency sweep test at various temperatures; (b) storage modulus (G') versus temperature at frequency 1 rad/s; (c) storage modulus (G') versus temperature at frequency 100 rad/s.

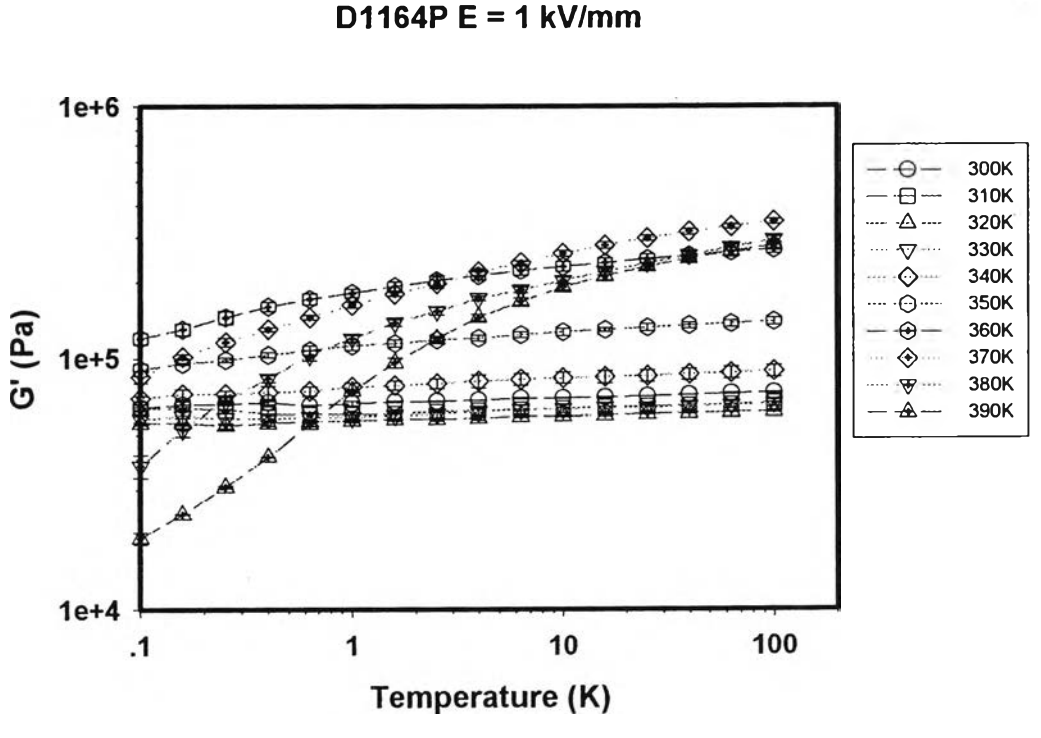

(a)

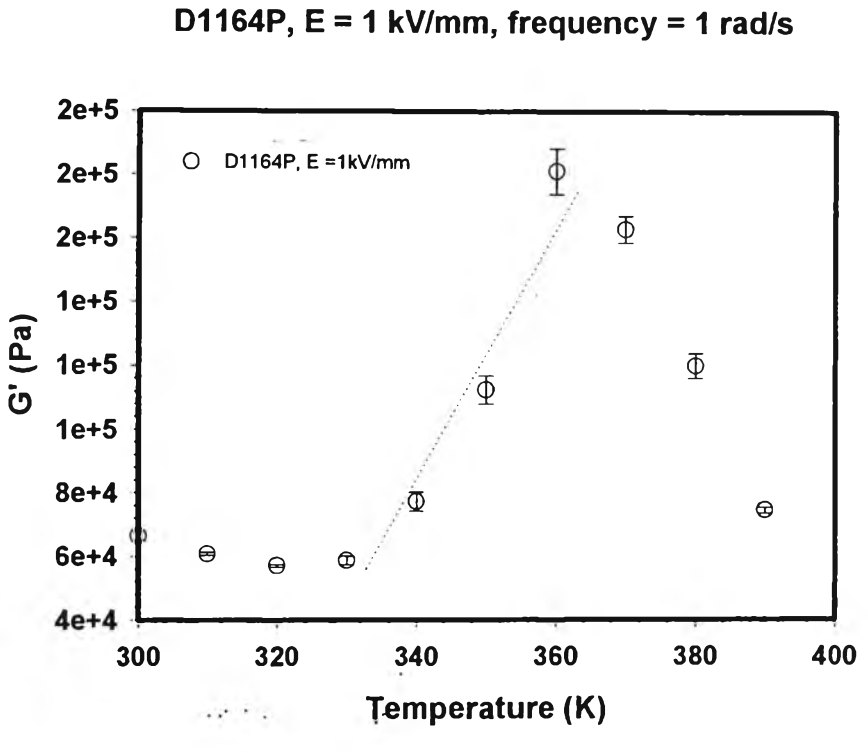
D1164P, E = 1 kV/mm, frequency = 1 rad/s
D1164P, E =1kV/mm
G' (Pa)
2e+5
2e+5
2e+5
1e+5
1e+5
1e+5
8e+4
6e+4
4e+4
300
320
340
360
380
400
Temperature (K)

(b)

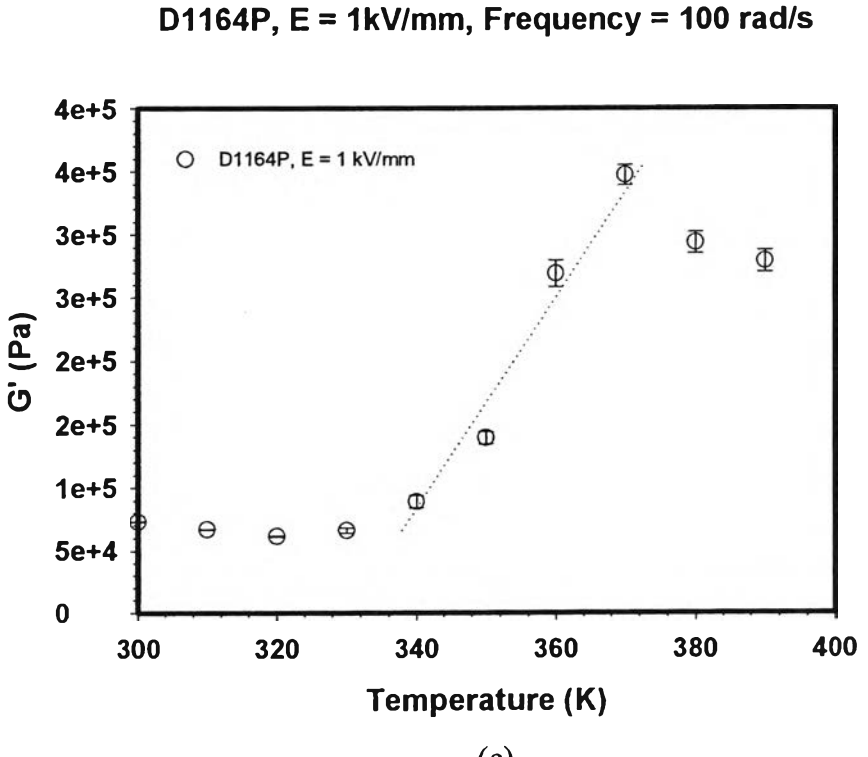
D1164P, E = 1kV/mm, Frequency = 100 rad/s
D1164P, E = 1 kV/mm
G' (Pa)
4e+5
4e+5
3e+5
3e+5
2e+5
2e+5
1e+5
5e+4
0
300
320
340
360
380
400
Temperature (K)

(c)

Figure J7 D1164P at E = 1 kV/mm, strain 0.1 %: (a) frequency sweep test at various temperatures; (b) storage modulus (G') versus temperature at frequency 1 rad/s; (c) storage modulus (G') versus temperature at frequency 100 rad/s.

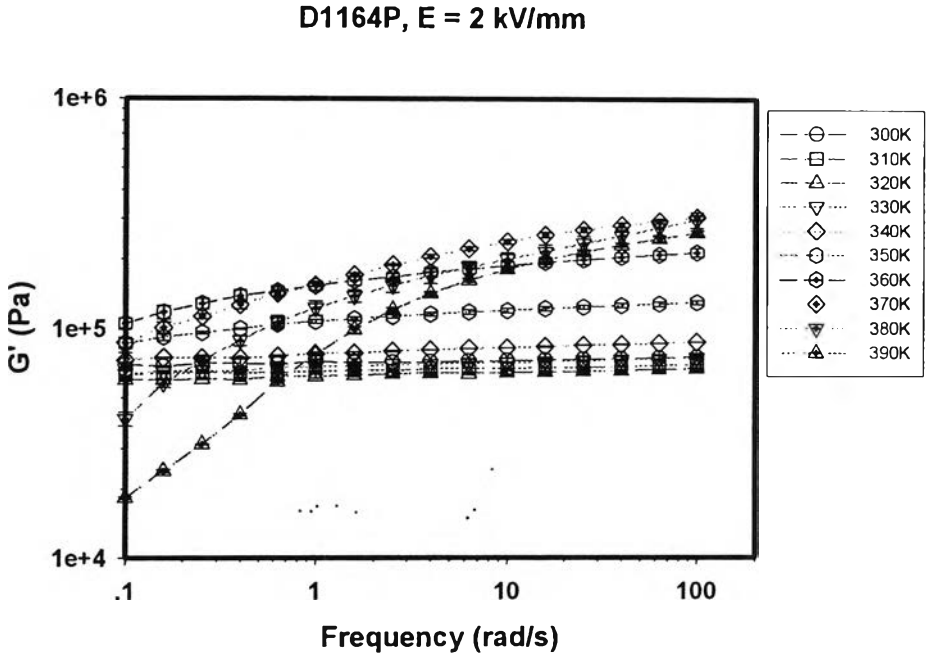

(a)

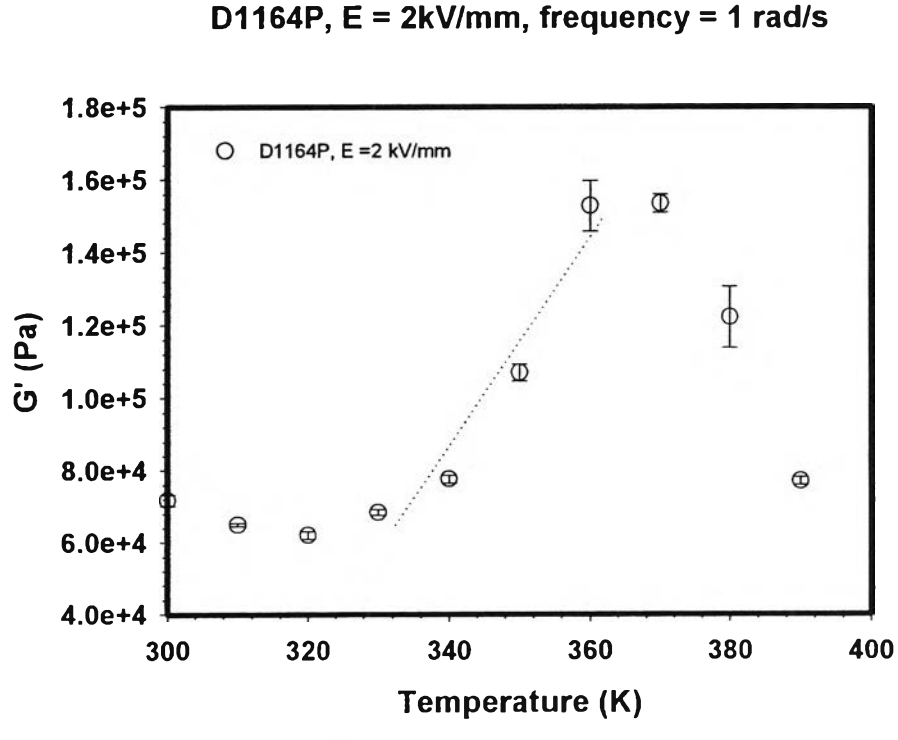

(b)

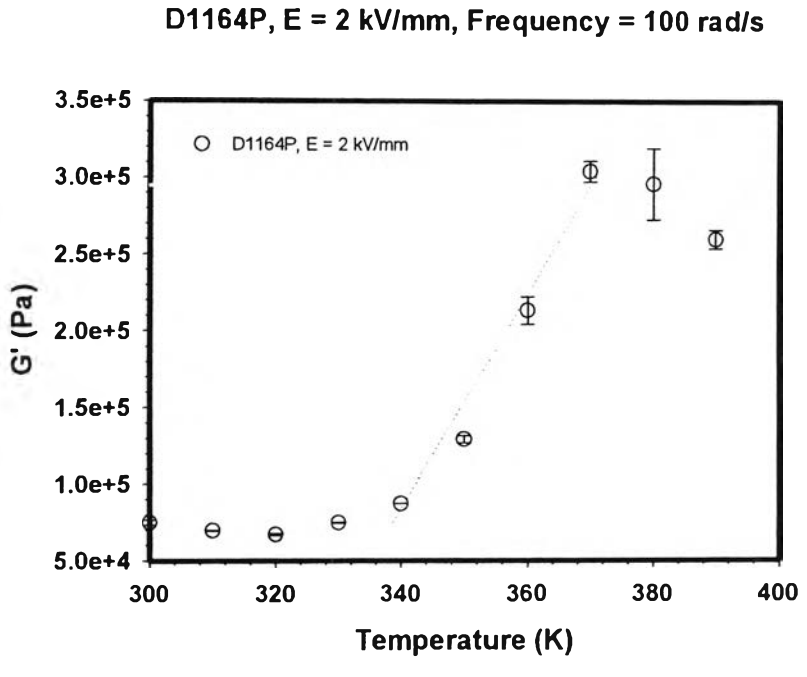

(c)

Figure J8 D1164P at E = 2 kV/mm, strain 0.1 %: (a) frequency sweep test at various temperatures; (b) storage modulus (G') versus temperature at frequency 1 rad/s; (c) storage modulus (G') versus temperature at frequency 100 rad/s.

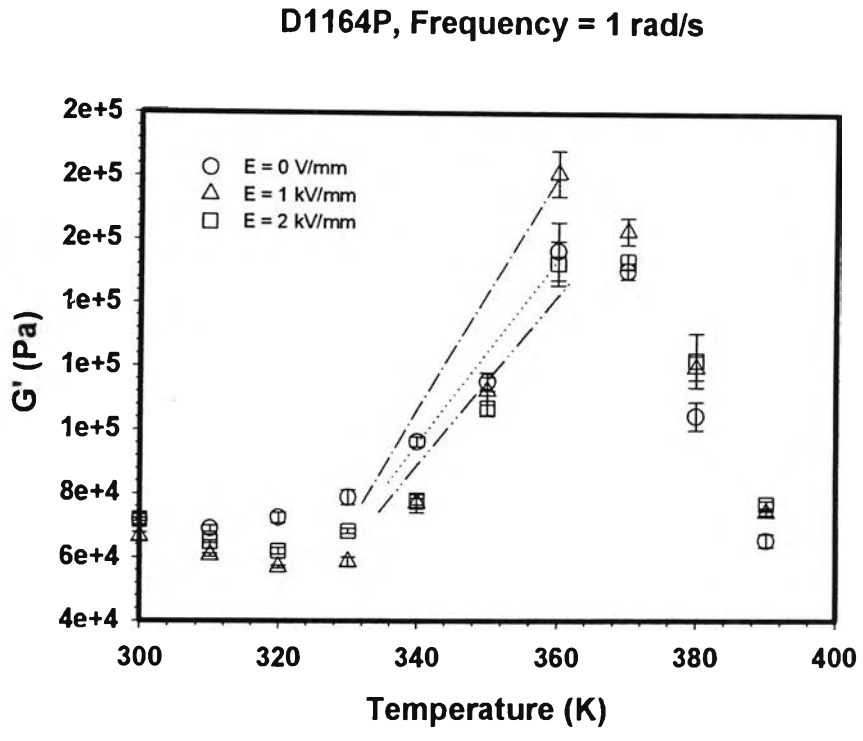

Figure J9 Comparison of D1164P's storage modulus exhibited at different temperatures under various electric fields, frequency 1 rad/s, and strain 0.1 %.

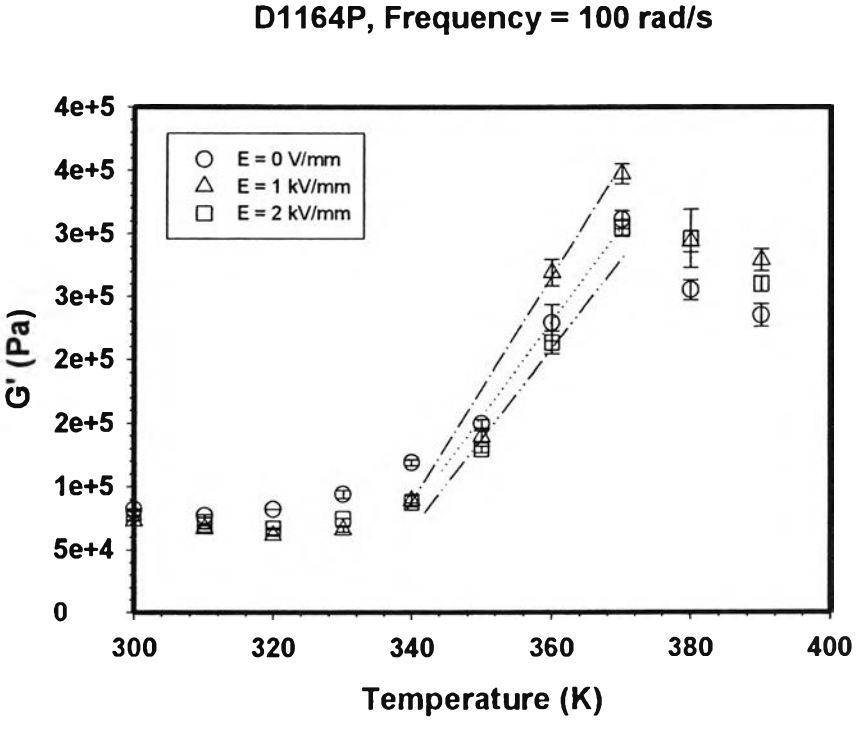

Figure J10 Comparison of D1164P's storage modulus exhibited at different temperatures under various electric fields, frequency 100 rad/s, and strain 0.1 %.

Frequency test of D1162P

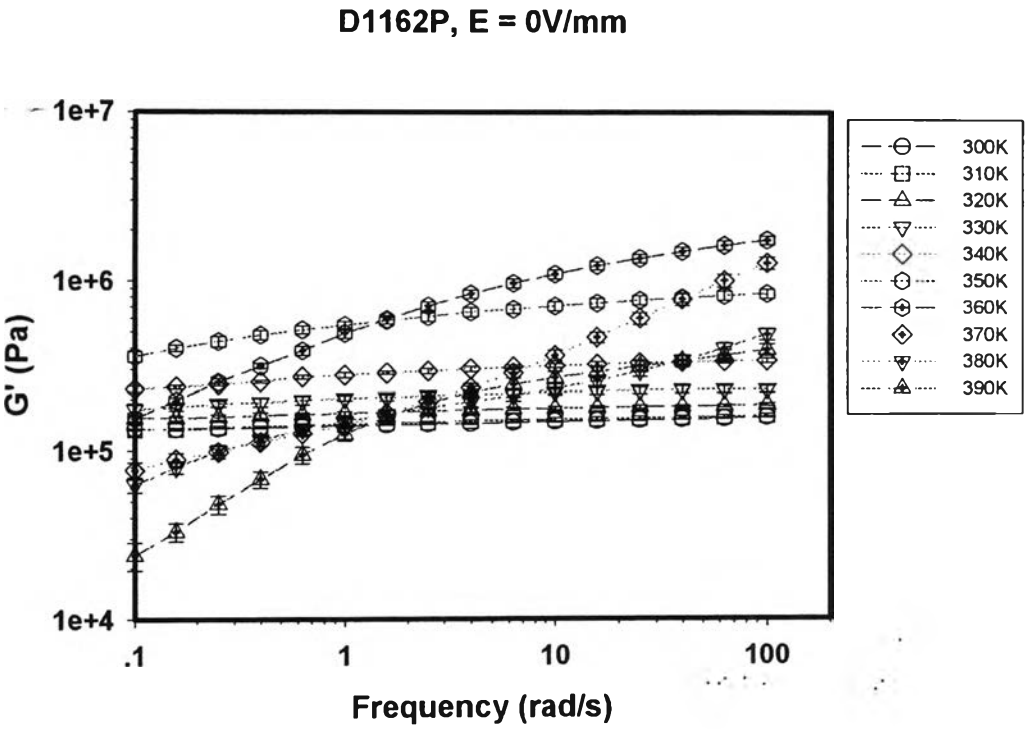

(a)

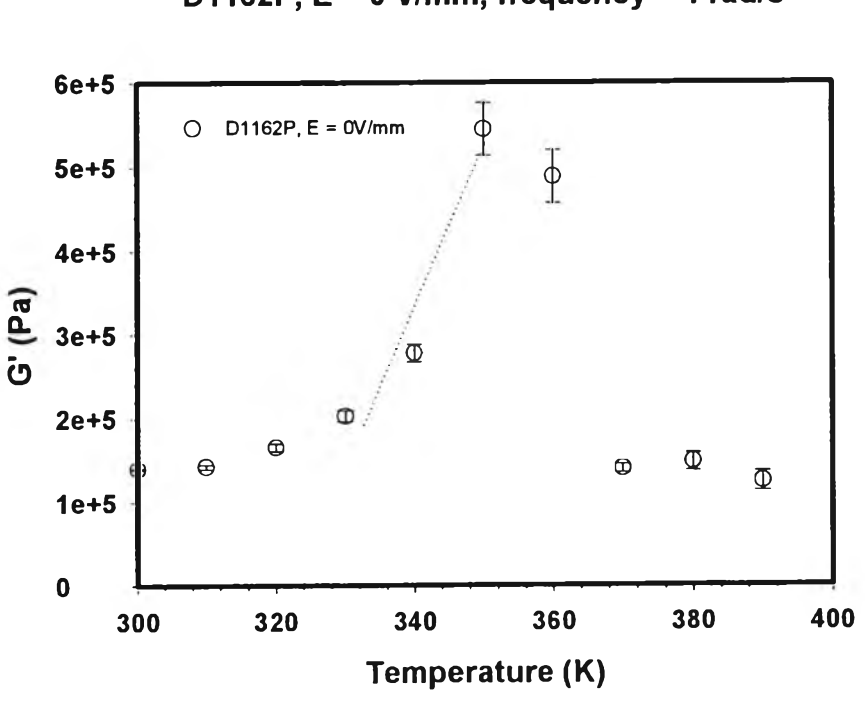

(b)

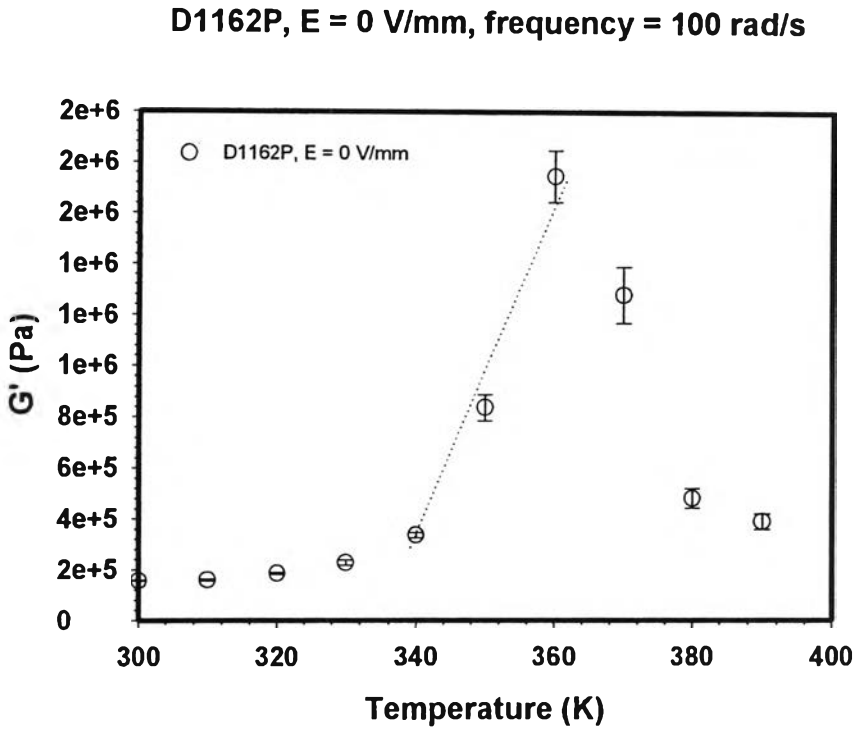

(c)

Figure J11 D1162P at E = 0 V/mm, strain 0.2 %: (a) frequency sweep test at various temperatures; (b) storage modulus (G') versus temperature at frequency 1 rad/s; (c) storage modulus (G') versus temperature at frequency 100 rad/s.

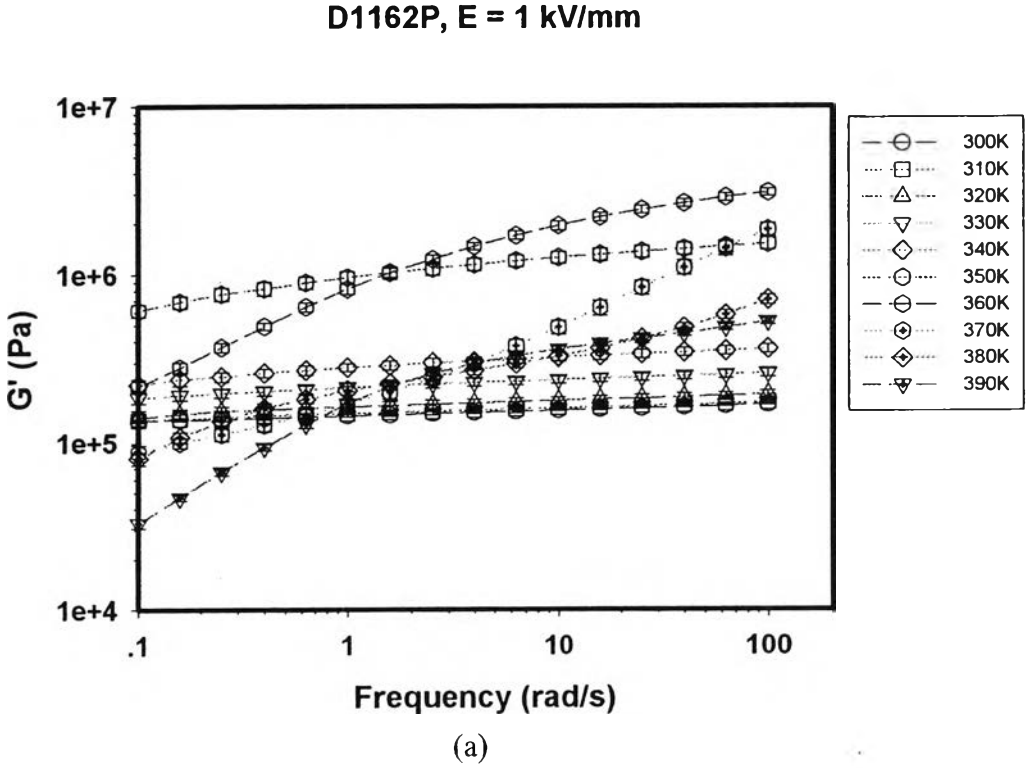

(a)

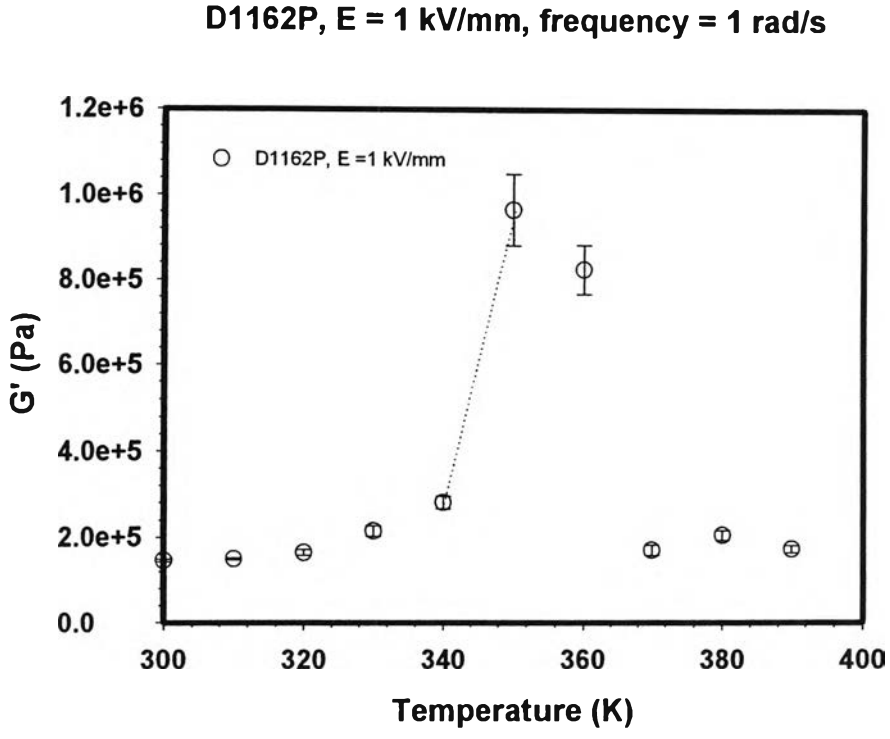

(b)

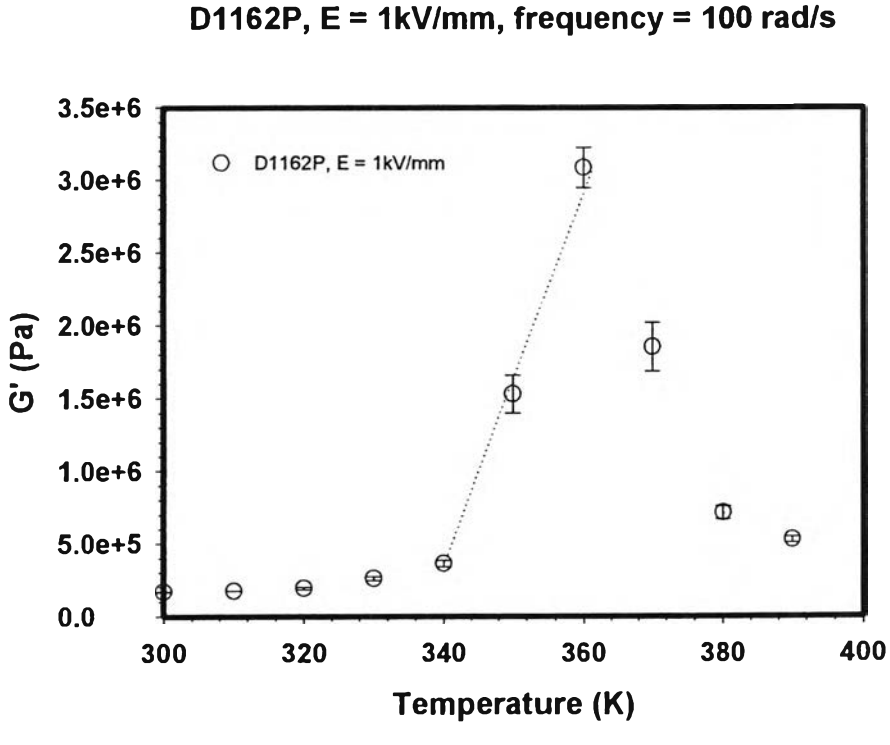

(c)

Figure J12 D1162P at E = 1 kV/mm, strain 0.2 %: (a) frequency sweep test at various temperatures; (b) storage modulus (G') versus temperature at frequency 1 rad/s; (c) storage modulus (G') versus temperature at frequency 100 rad/s.

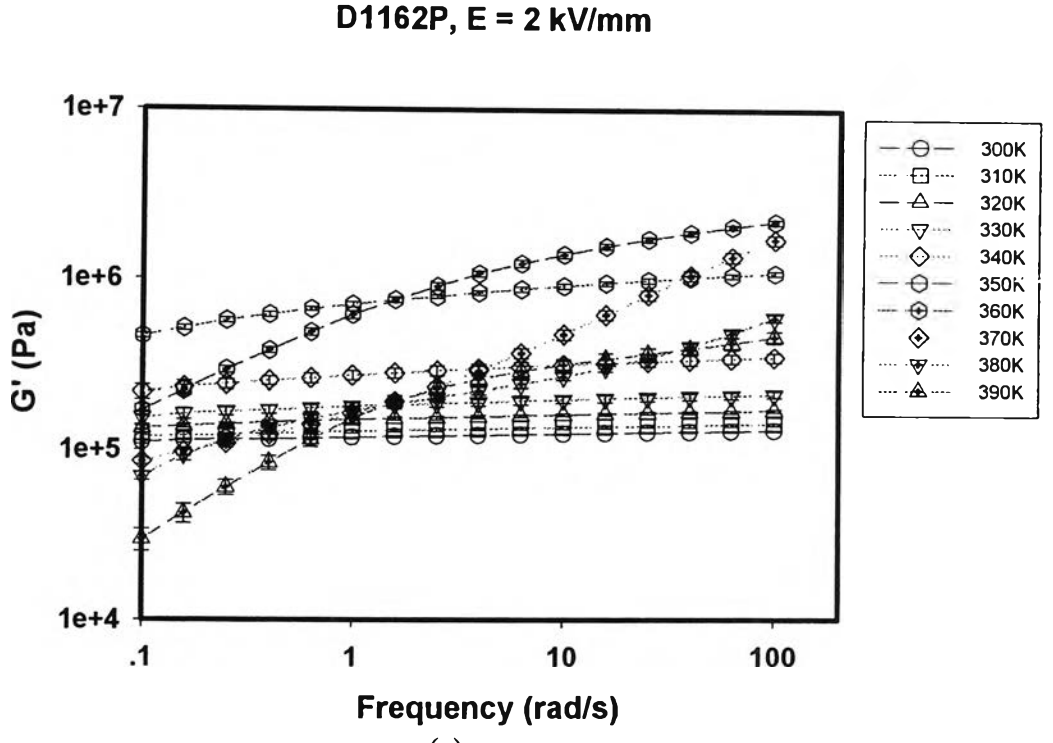
D1162P, E = 2 kV/mm
1e+7
1e+6
1e+5
1e+4
G' (Pa)
.1
1
10
100
Frequency (rad/s)
300K
310K
320K
330K
340K
350K
360K
370K
380K
390K

(a)

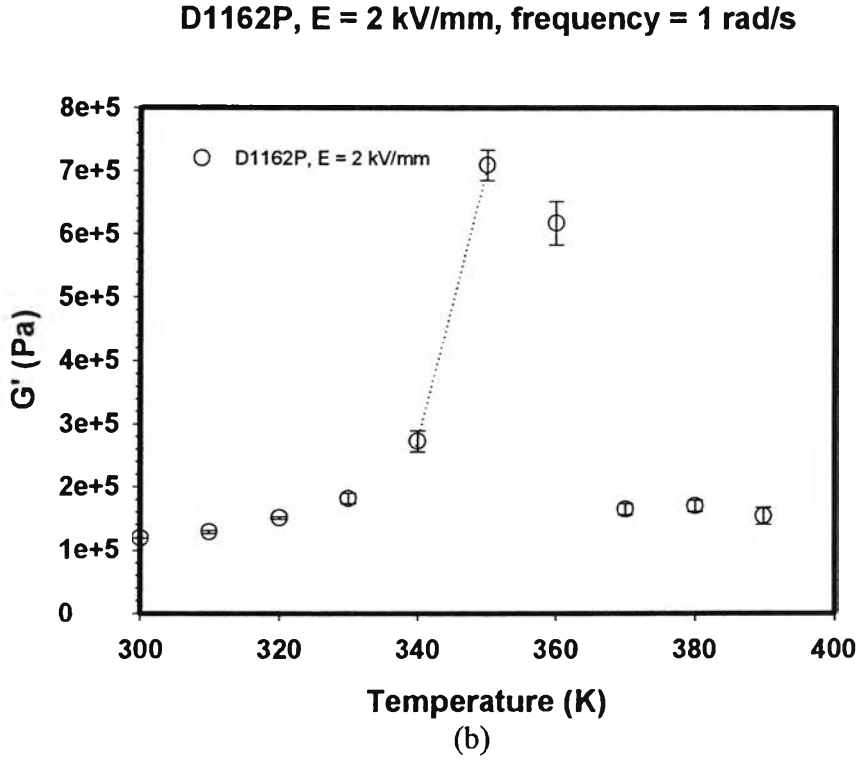
D1162P, E = 2 kV/mm, frequency = 1 rad/s
8e+5
7e+5
6e+5
5e+5
4e+5
3e+5
2e+5
1e+5
0
G' (Pa)
D1162P, E = 2 kV/mm
300
320
340
360
380
400
Temperature (K)

(b)

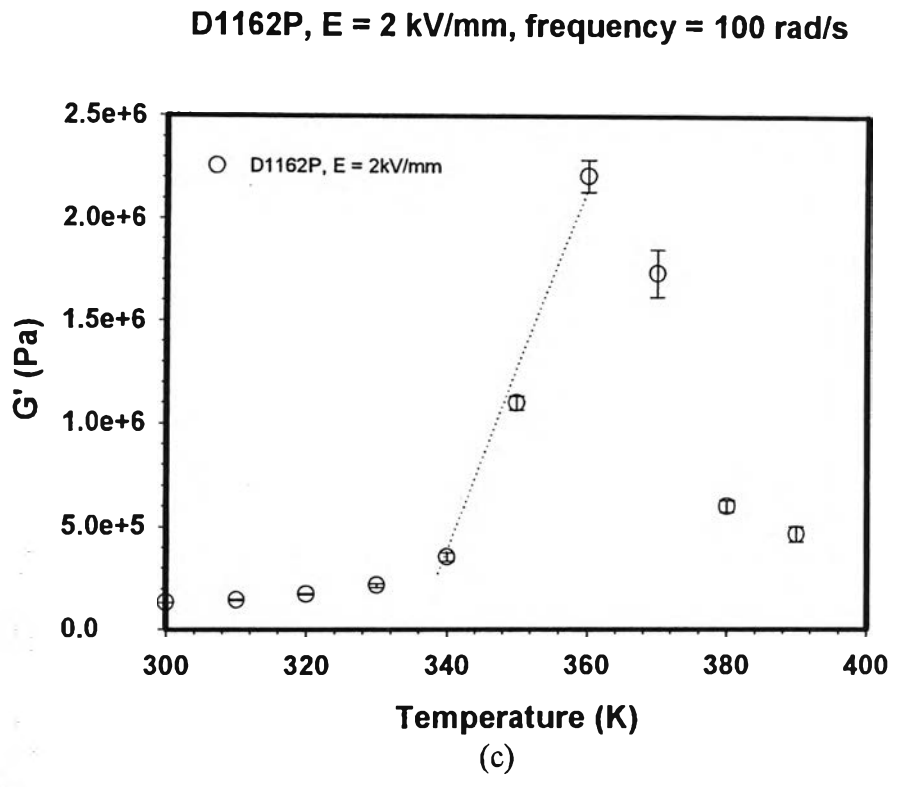

(c)

Figure J12 D1162P at E = 2 kV/mm, strain 0.2 %: (a) frequency sweep test at various temperatures; (b) storage modulus (G') versus temperature at frequency 1 rad/s; (c) storage modulus (G') versus temperature at frequency 100 rad/s.

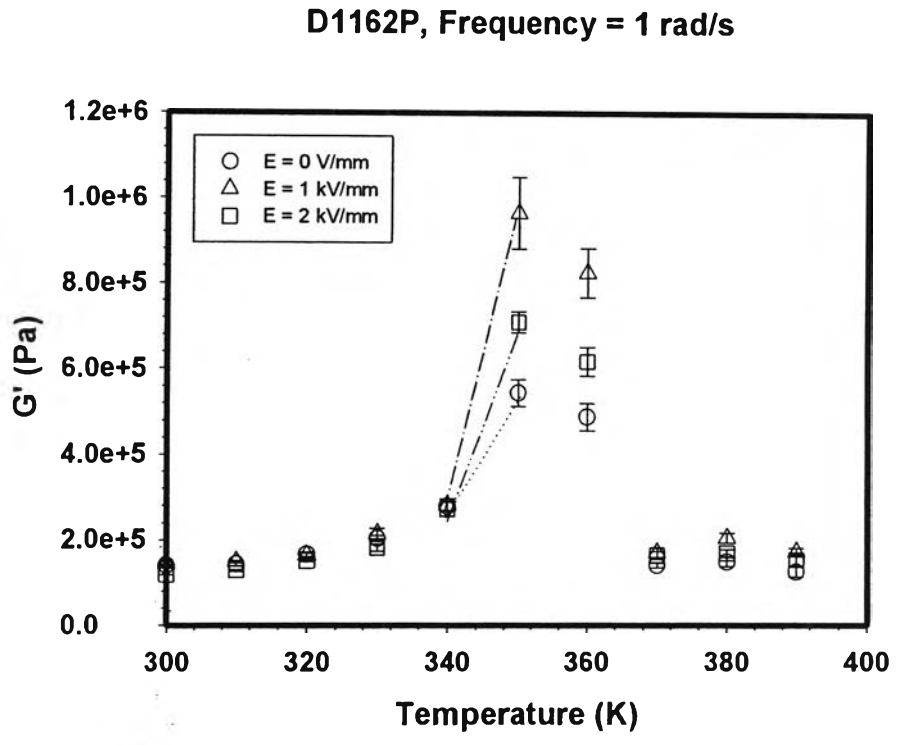

Figure J13 Comparison of D1162P's storage modulus exhibited at different temperatures under various electric fields, frequency 1 rad/s, and strain 0.2 %.

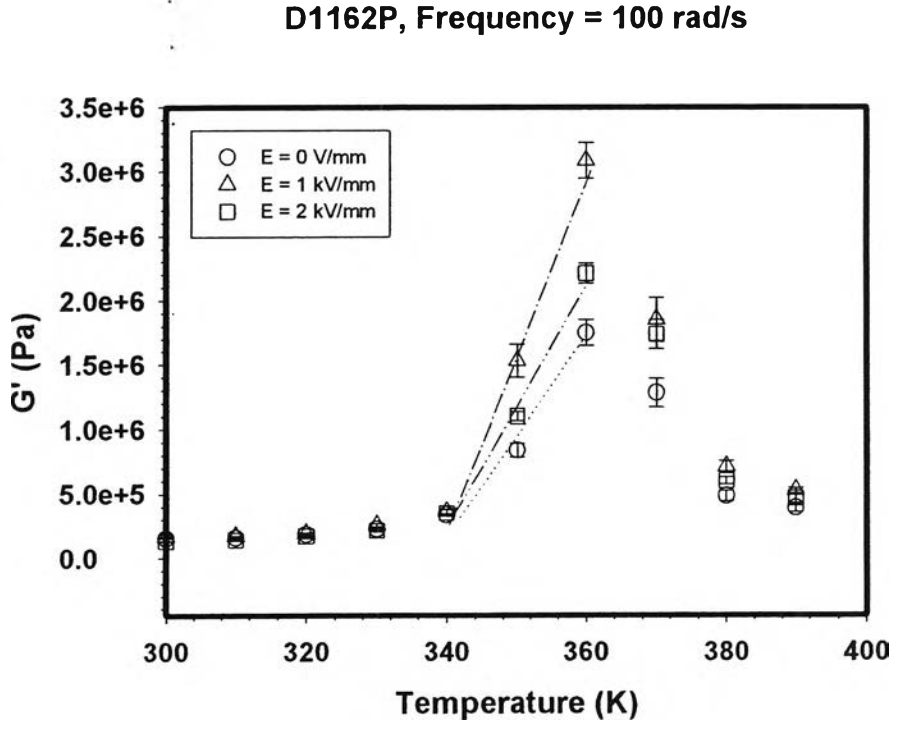

Figure J14 Comparison of D1162P's storage modulus exhibited at different temperatures under various electric fields, frequency 100 rad/s, and strain 0.2 %.

Table J1 Number of electrical strand (ν_e) of the plot between storage modulus of D1114P, D1164P, and D1162P at various electric fields strength versus temperature

Sample	Applied electric field (kV/mm)	Strain (%)	ν_e (cm^{-3}) at frequency 1 rad/s	ν_e (cm^{-3}) at frequency 100 rad/s
D1114P	0	0.2	2.10×10^{21}	5.58×10^{21}
	1	0.2	2.89×10^{21}	7.05×10^{21}
	2	0.2	1.89×10^{21}	4.15×10^{21}
D1164P	0	0.1	1.82×10^{21}	3.94×10^{21}
	1	0.1	2.91×10^{21}	6.54×10^{21}
	2	0.1	2.05×10^{21}	5.32×10^{21}
D1162P	0	0.2	1.93×10^{22}	5.11×10^{22}
	1	0.2	4.95×10^{22}	9.86×10^{22}
	2	0.2	3.16×10^{22}	6.72×10^{22}

5 vol% De_PDPA/D1114P

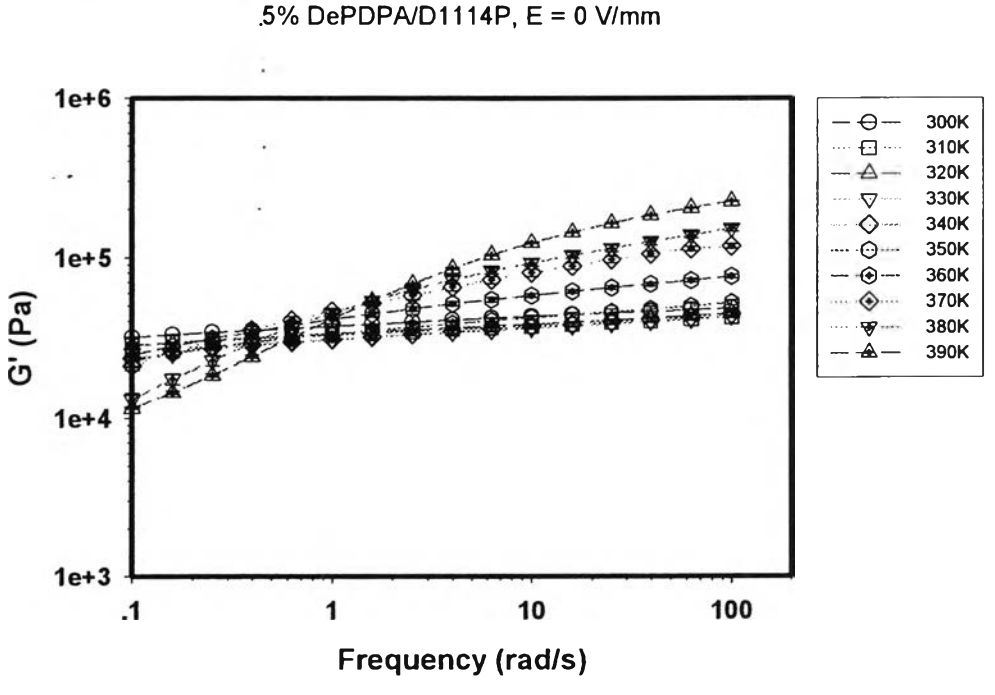

(a)

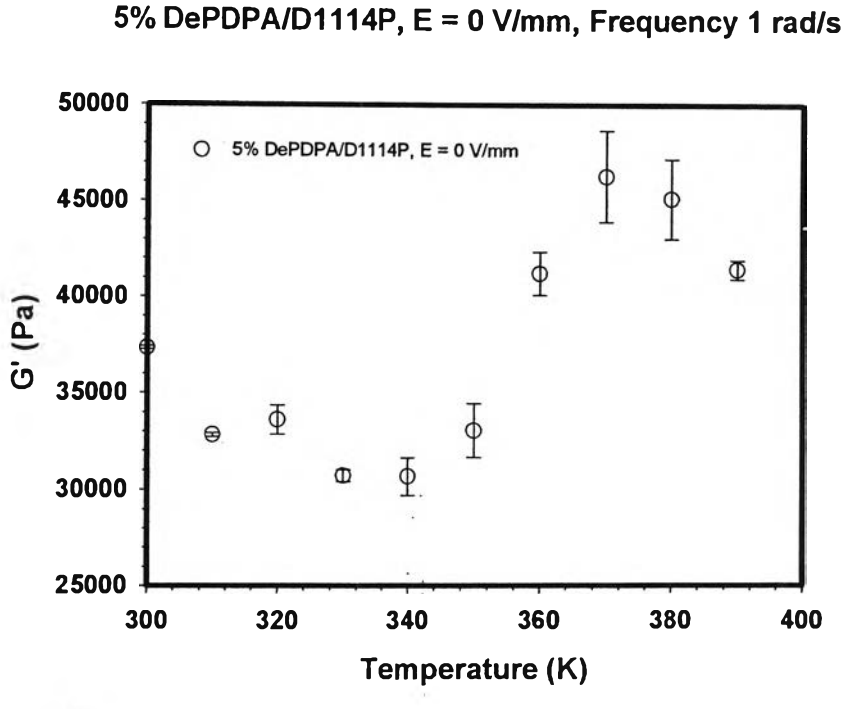

(b)

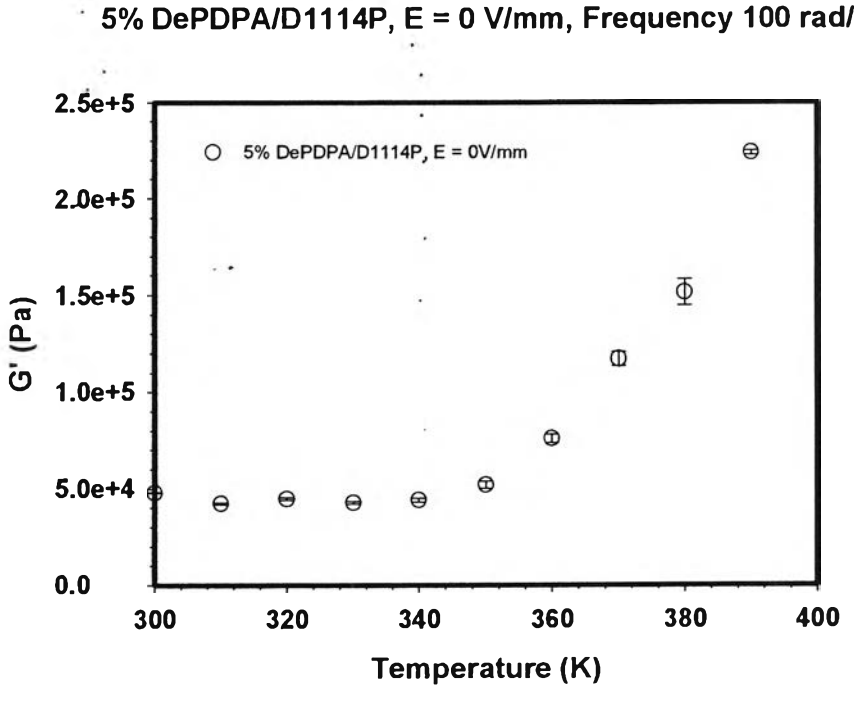

(c)

Figure J15 5% De_PDPA/D1114P_at E = 0V/mm, strain 0.2 % (a) frequency sweep test at various temperatures; (b) storage modulus (G') versus temperature at frequency 1 rad/s; (c) storage modulus (G') versus temperature at frequency 100 rad/s.

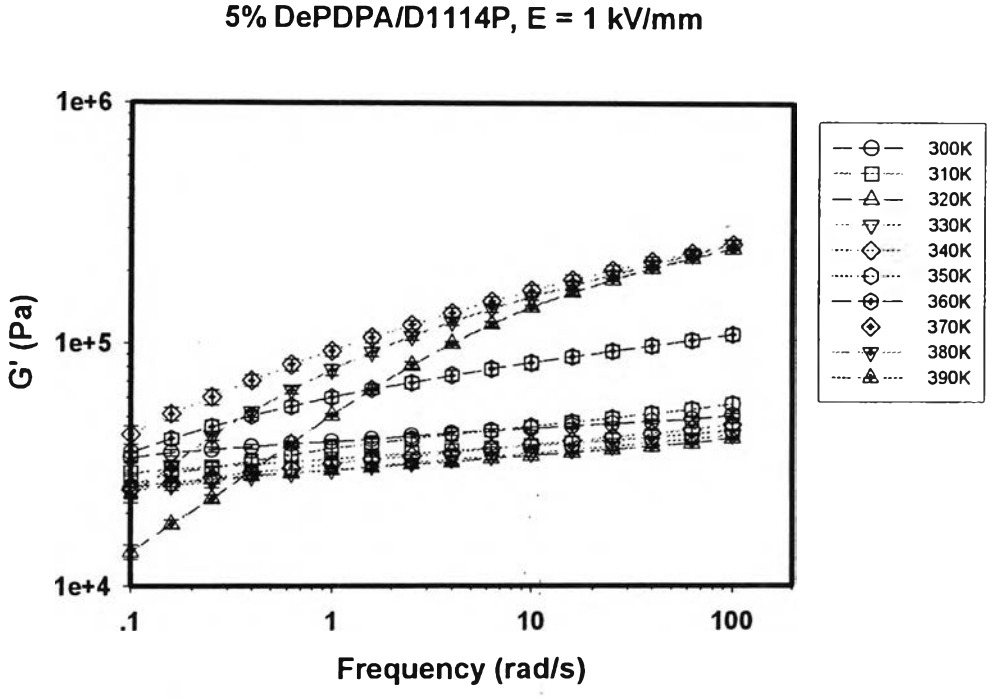
5% DePDPA/D1114P, E = 1 kV/mm
1e+6
1e+5
1e+4
G' (Pa)
.1
1
10
100
Frequency (rad/s)
300K
310K
320K
330K
340K
350K
360K
370K
380K
390K

(a)

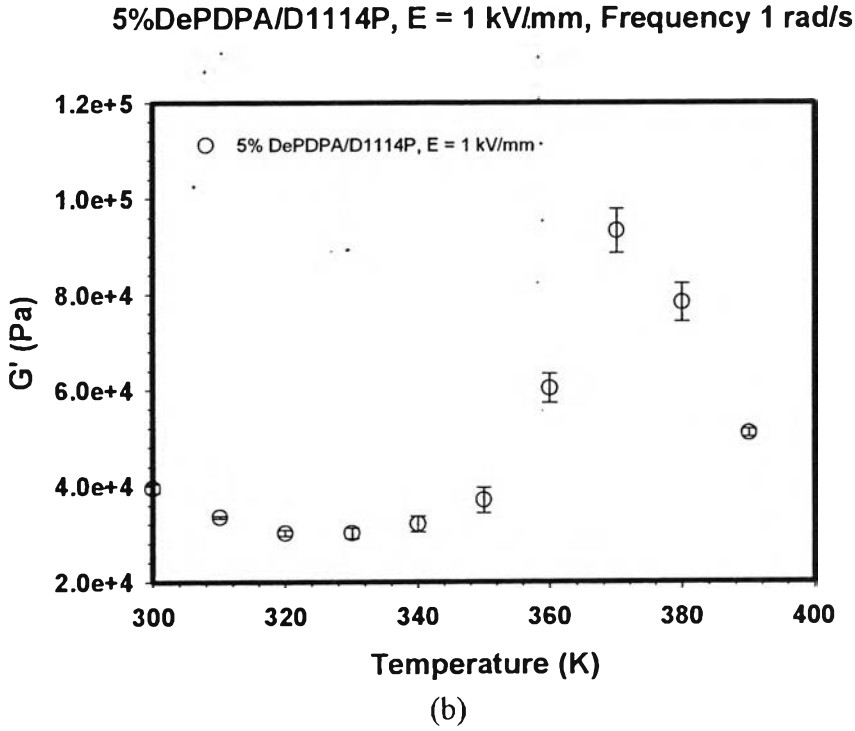
5%DePDPA/D1114P, E = 1 kV/mm, Frequency 1 rad/s
5% DePDPA/D1114P, E = 1 kV/mm
1.2e+5
1.0e+5
8.0e+4
6.0e+4
4.0e+4
2.0e+4
G' (Pa)
300
320
340
360
380
400
Temperature (K)

(b)

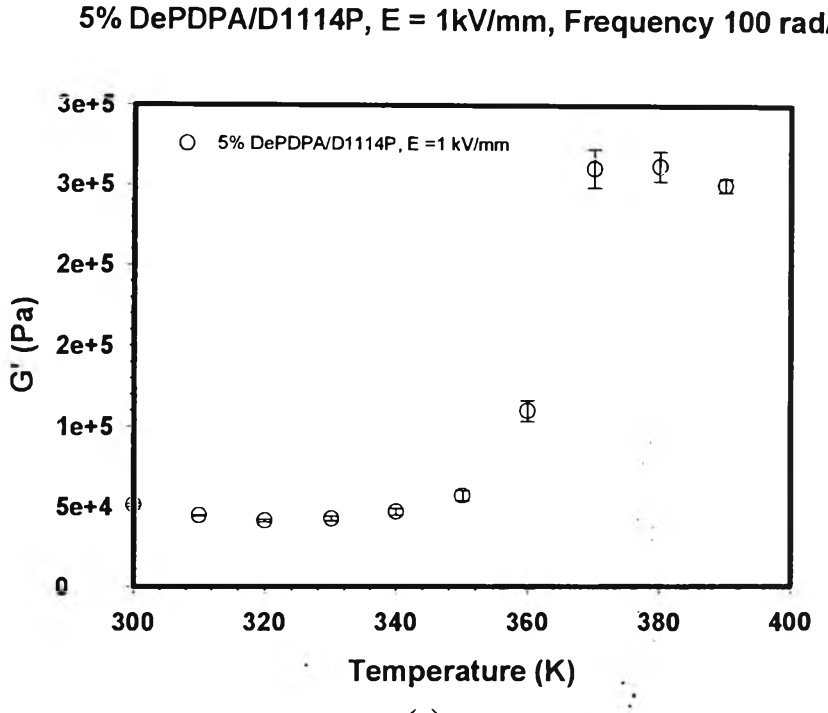

(c)

Figure J16 5% De_PDPA/D1114P_at E = 1 kV/mm, strain 0.2 % (a) frequency sweep test at various temperatures; (b) storage modulus (G') versus temperature at frequency 1 rad/s; (c) storage modulus (G') versus temperature at frequency 100 rad/s.

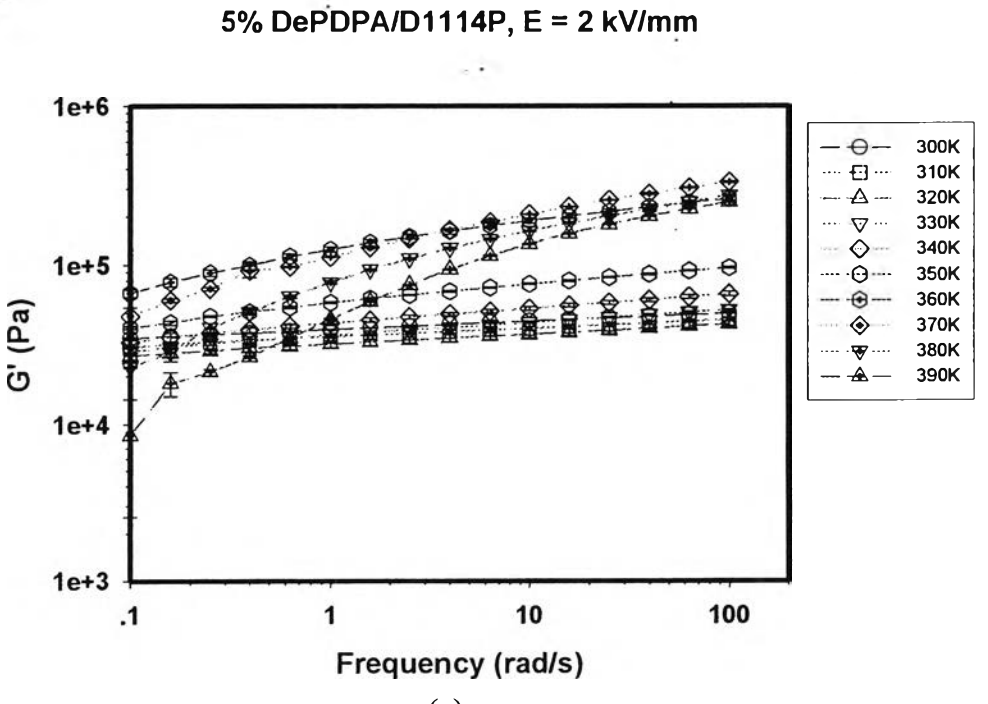

(a)

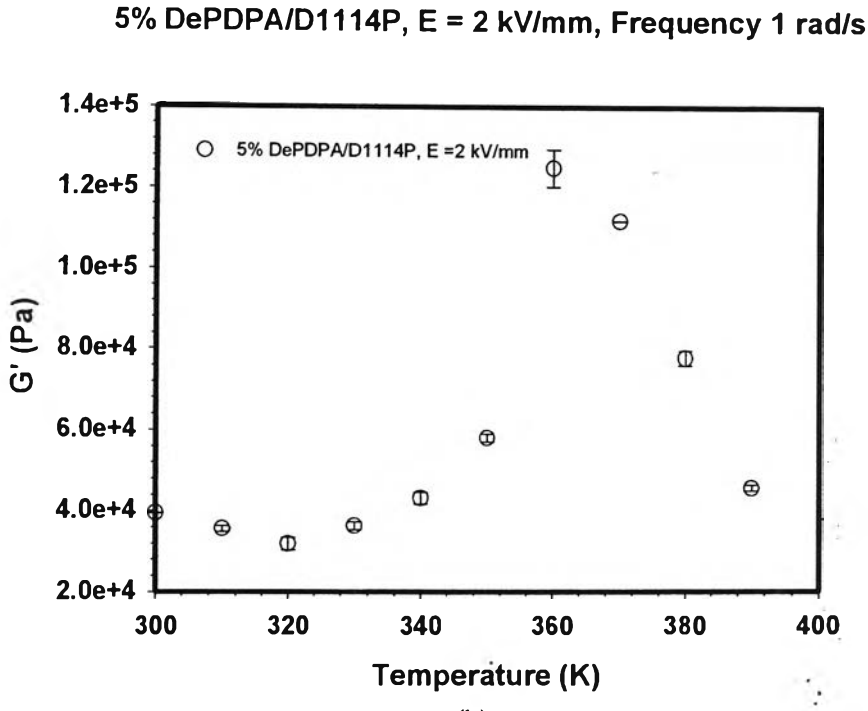

(b)

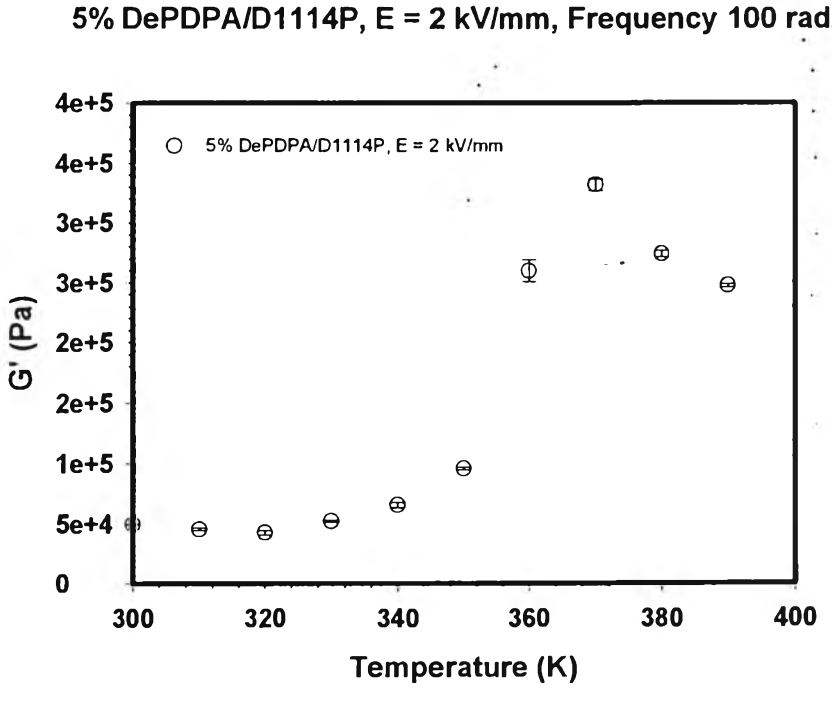

(c)

Figure J17 5% De_PDPA/D1114P at E = 2 kV/mm, strain 0.2 % (a) frequency sweep test at various temperatures; (b) storage modulus (G') versus temperature at frequency 1 rad/s; (c) storage modulus (G') versus temperature at frequency 100 rad/s.

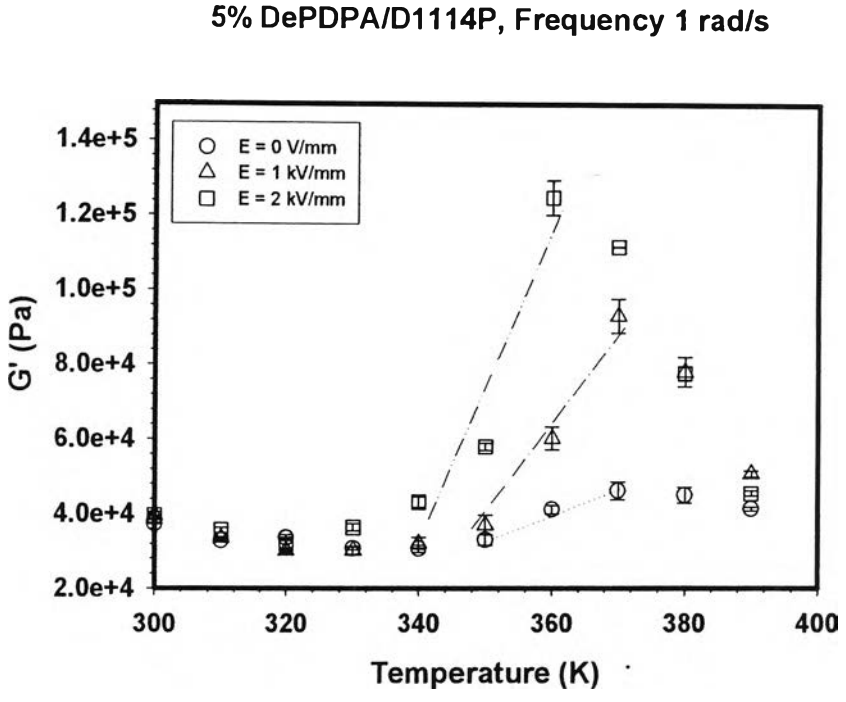

Figure J18 Comparison of 5% De_PDPA/D1114P's storage modulus exhibited at different temperatures under various electric fields, frequency 1 rad/s, and strain 0.2 %.

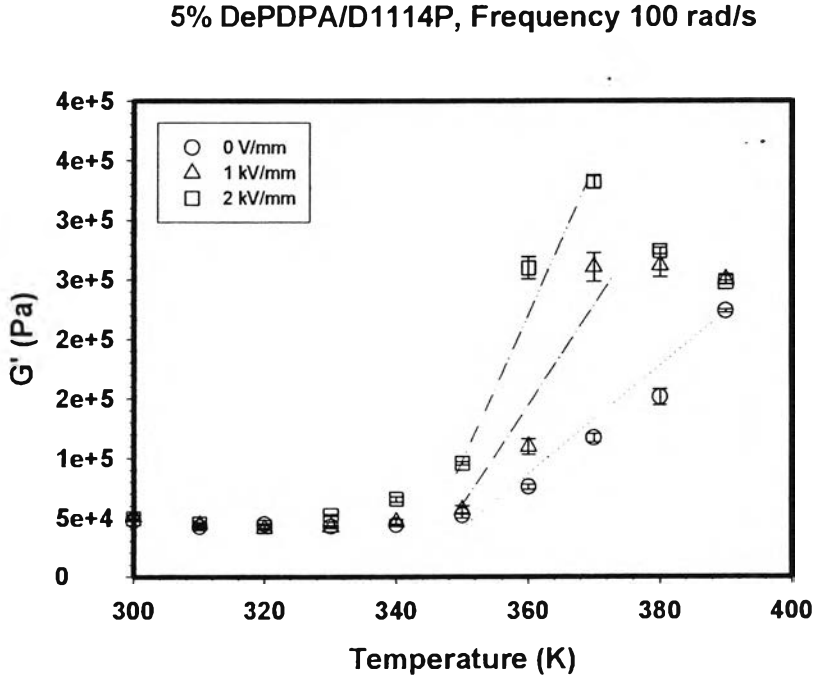

Figure J19 Comparison of 5% De_PDPA/D1114P's storage modulus exhibited at different temperatures under various electric fields, frequency 100 rad/s, and strain 0.2 %.

10 vol% De_PDPA/D1114P

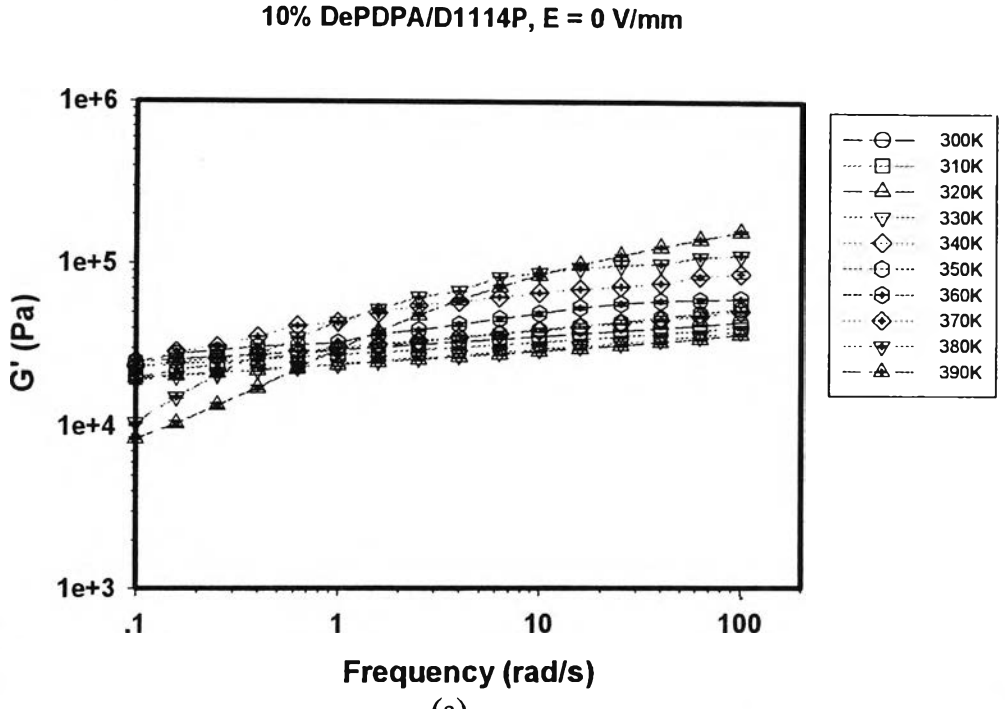

(a)

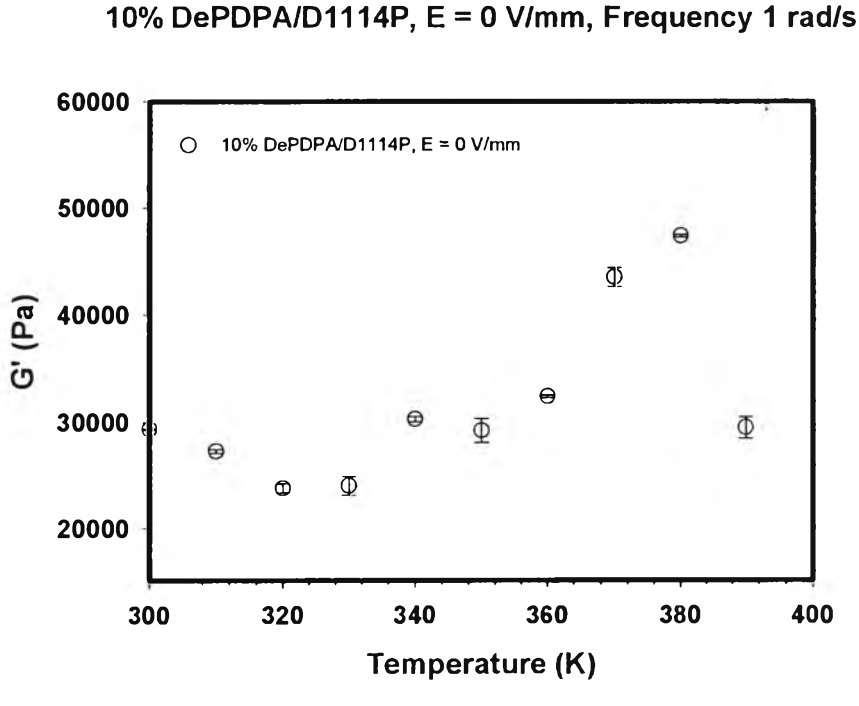

(b)

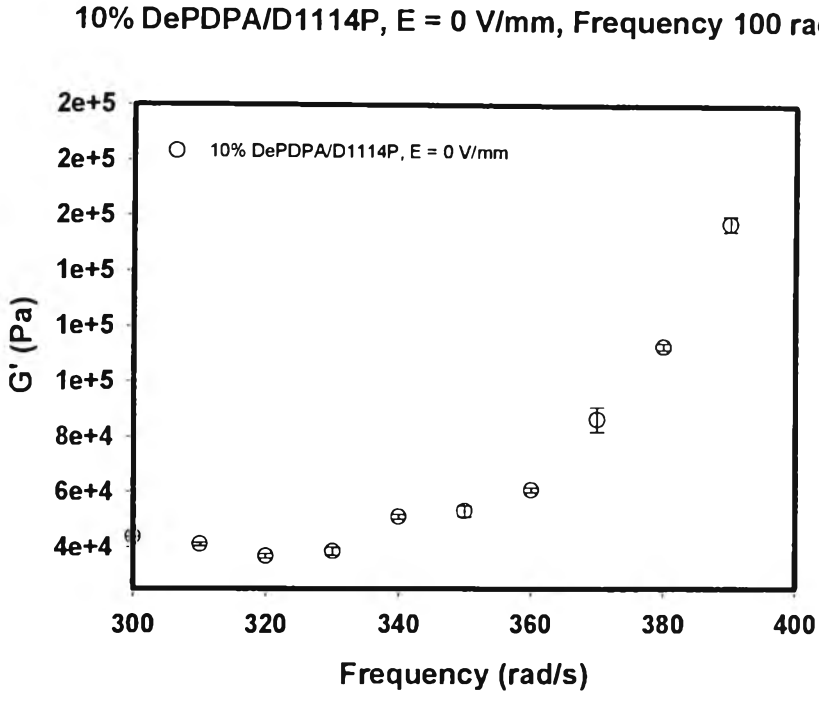

(c)

Figure J20 10% De_PDPA/D1114P at E = 0 V/mm, strain 0.3 % (a) frequency sweep test at various temperatures; (b) storage modulus (G') versus temperature at frequency 1 rad/s; (c) storage modulus (G') versus temperature at frequency 100 rad/s.

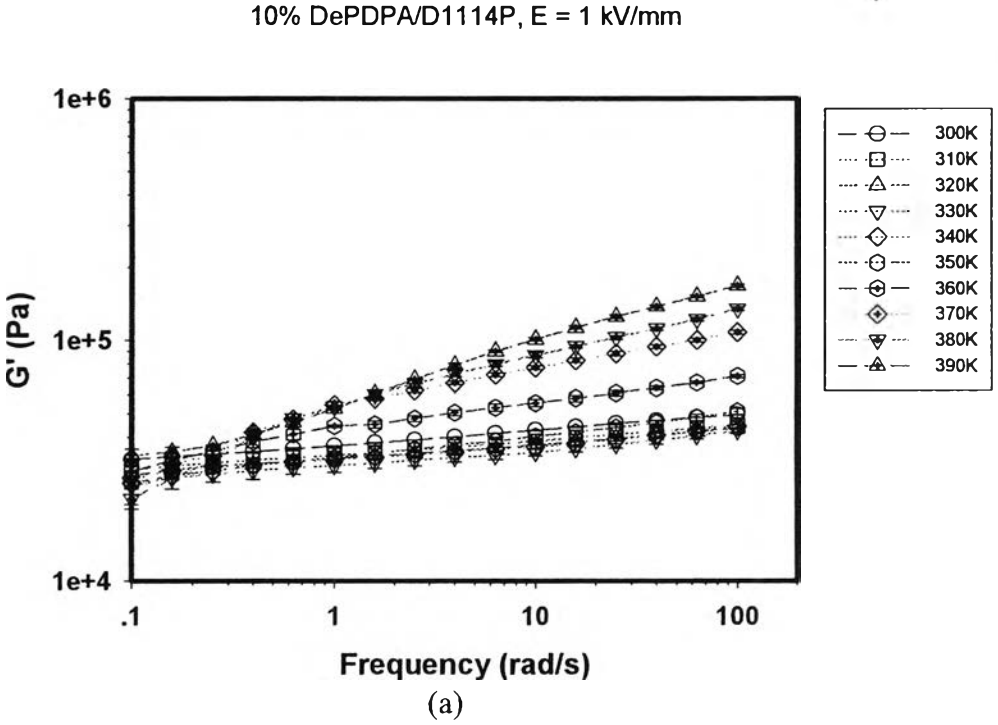

(a)

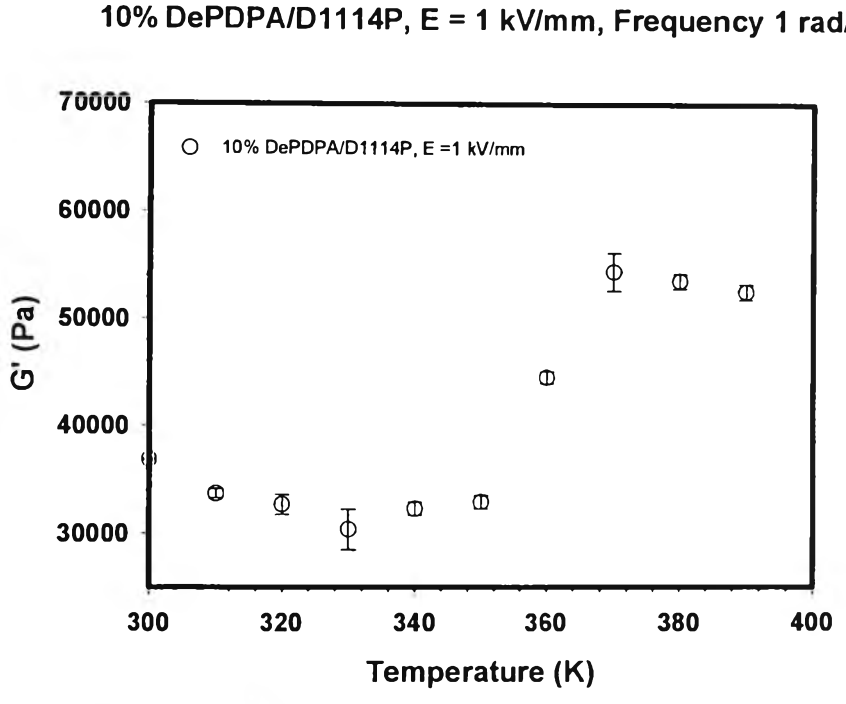

(b)

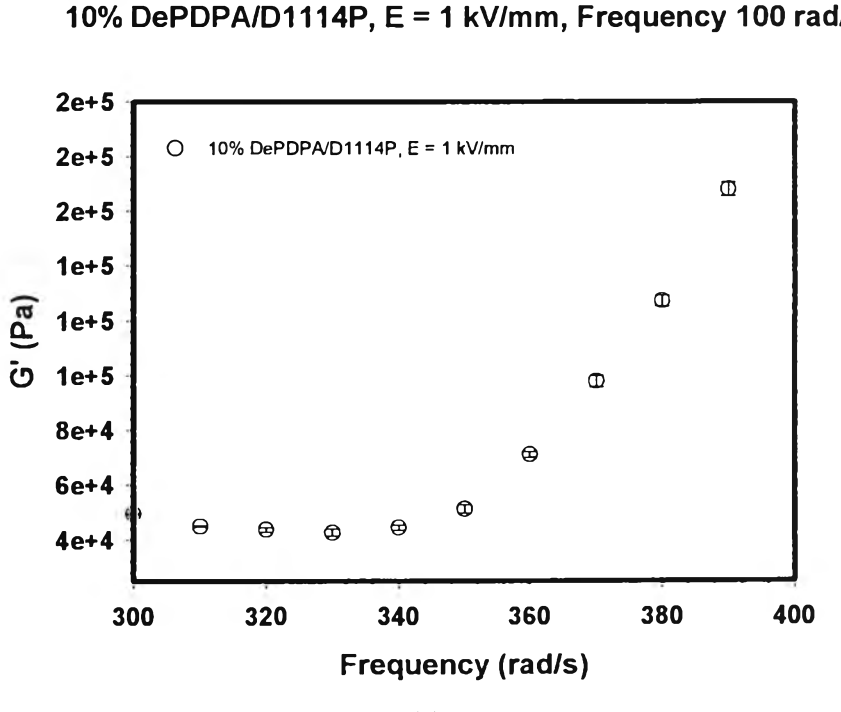

(c)

Figure J21 10% De_PDPA/D1114P at E = 1 kV/mm, strain 0.3 % (a) frequency sweep test at various temperatures; (b) storage modulus (G') versus temperature at frequency 1 rad/s; (c) storage modulus (G') versus temperature at frequency 100 rad/s.

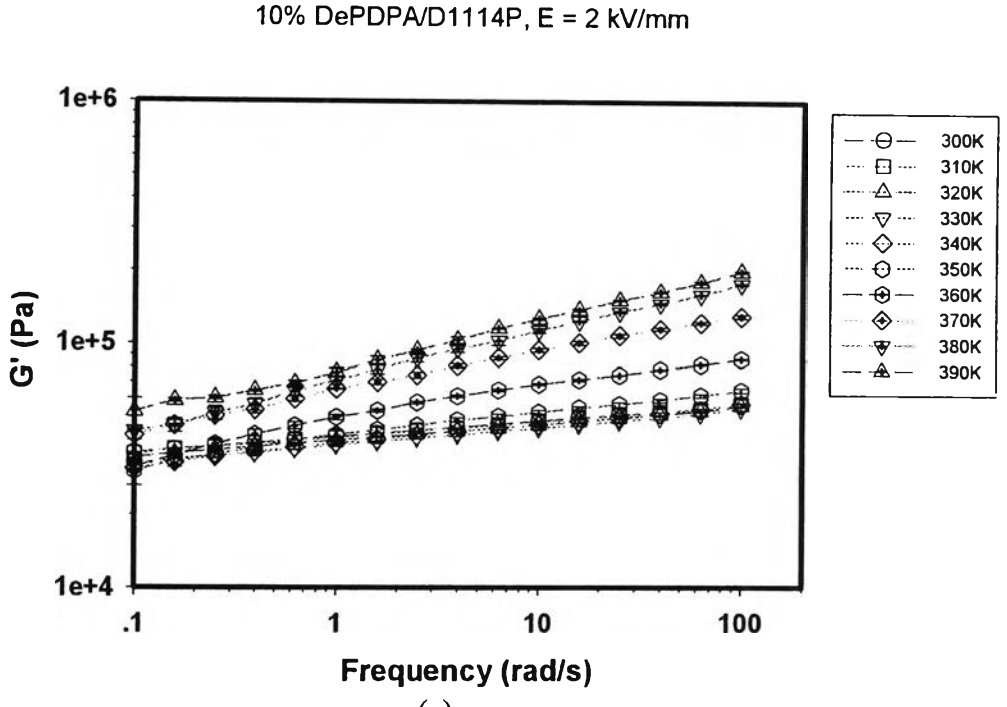
10% DePDPA/D1114P, E = 2 kV/mm
1e+6
1e+5
1e+4
G' (Pa)
.1
1
10
100
Frequency (rad/s)
300K
310K
320K
330K
340K
350K
360K
370K
380K
390K

(a)

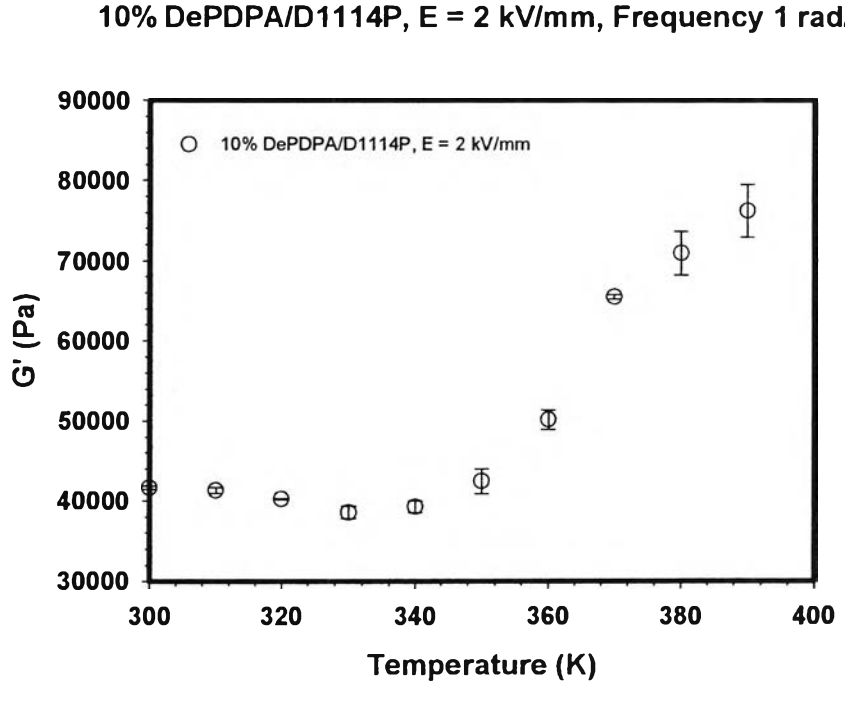
10% DePDPA/D1114P, E = 2 kV/mm, Frequency 1 rad/s
10% DePDPA/D1114P, E = 2 kV/mm
90000
80000
70000
60000
50000
40000
30000
G' (Pa)
300
320
340
360
380
400
Temperature (K)

(b)

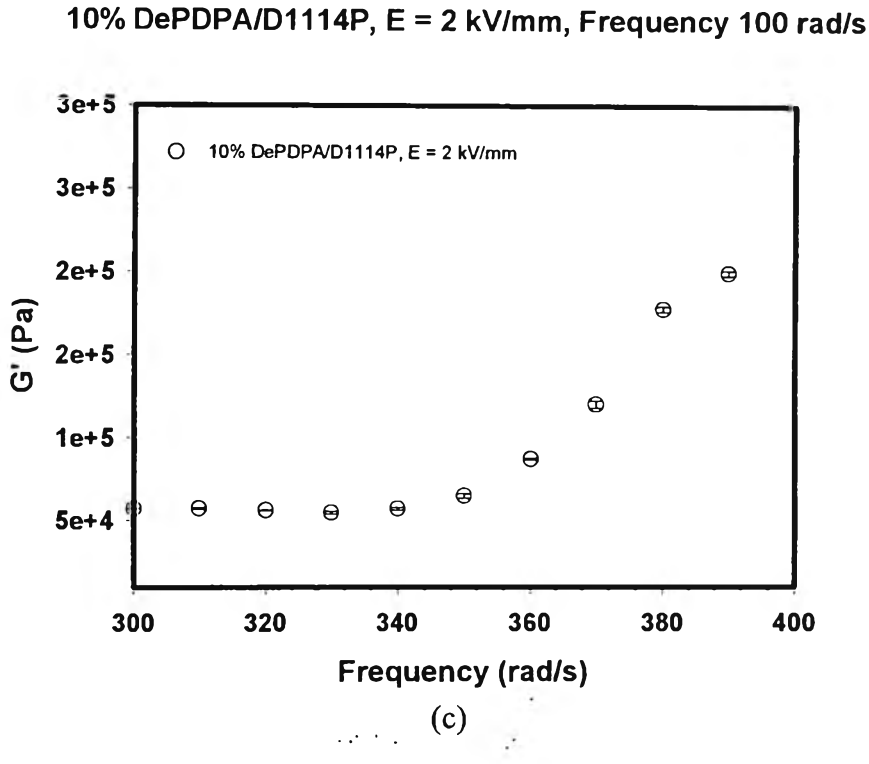

(c)

Figure J22 10% De_PDPA/D1114P at E = 2 kV/mm, strain 0.3 % (a) frequency sweep test at various temperatures; (b) storage modulus (G') versus temperature at frequency 1 rad/s; (c) storage modulus (G') versus temperature at frequency 100 rad/s.

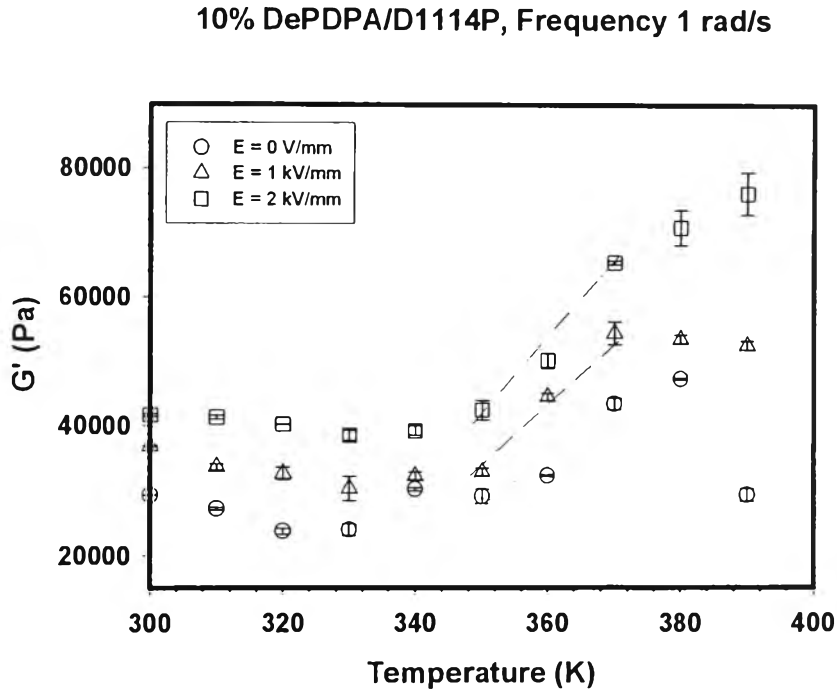

Figure J23 Comparison of 10% De_PDPA/D1114P's storage modulus exhibited at different temperatures under various electric fields, frequency 1 rad/s, and strain 0.3 %.

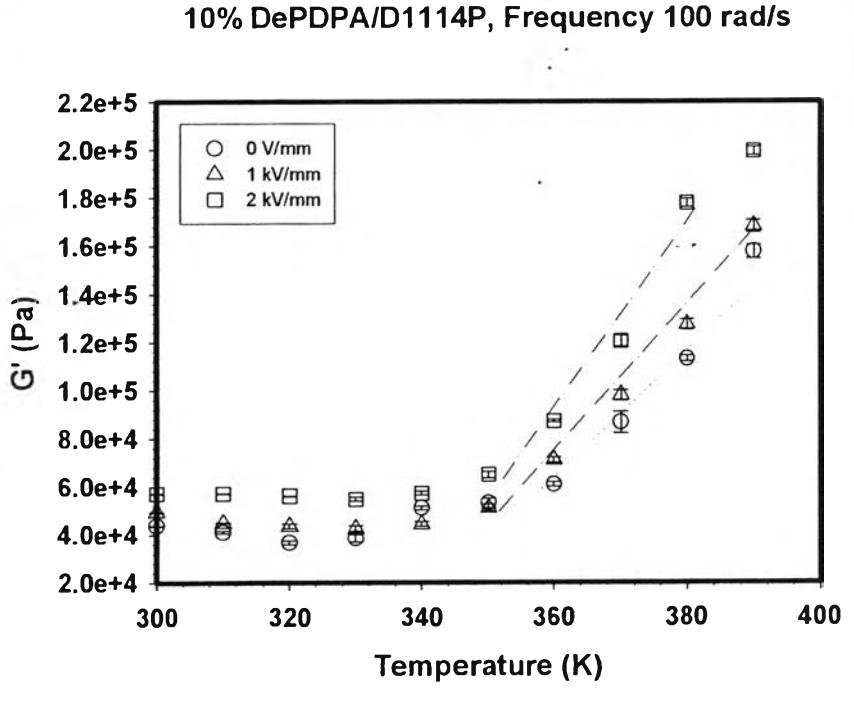

Figure J24 Comparison of 10% De_PDPA/D1114P's storage modulus exhibited at different temperatures under various electric fields, frequency 100 rad/s, and strain 0.3 %.

20 vol% De_PDPA/D1114P

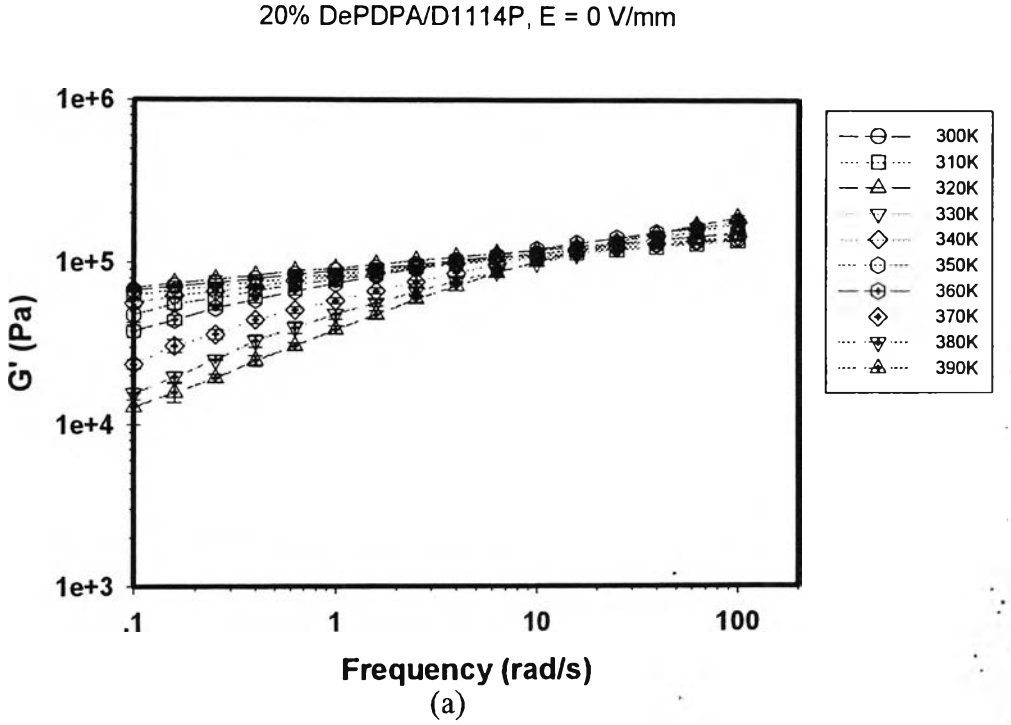

(a)

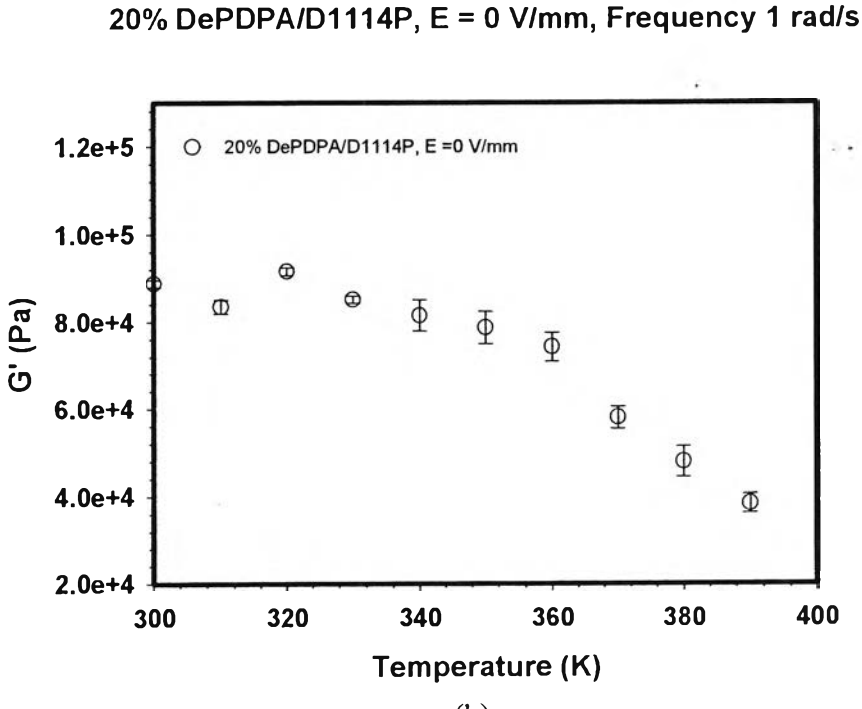

(b)

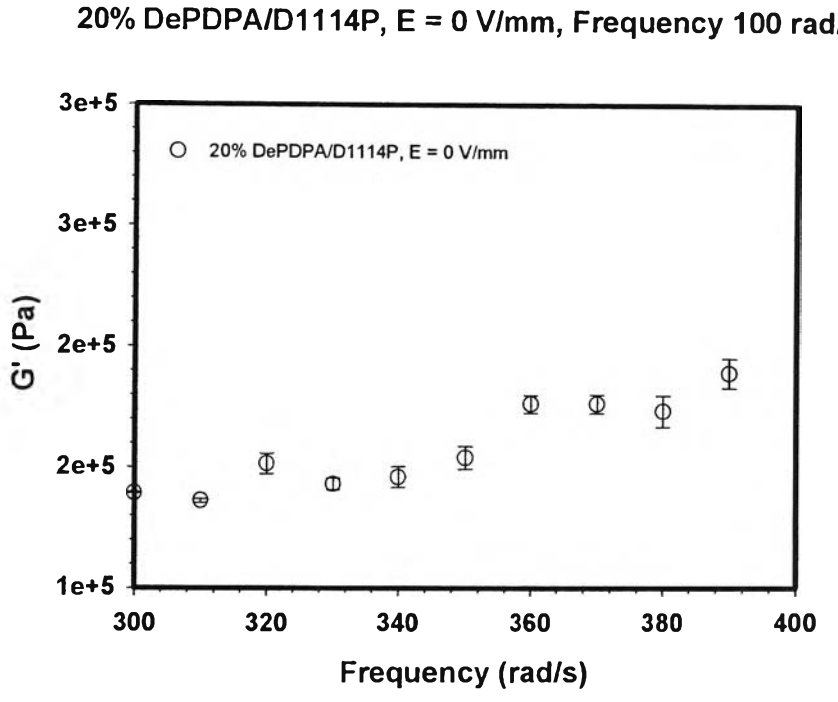

(c)

Figure J25 20% De_PDPA/D1114P at E = 0 V/mm, strain 0.1 % (a) frequency sweep test at various temperatures; (b) storage modulus (G') versus temperature at frequency 1 rad/s; (c) storage modulus (G') versus temperature at frequency 100 rad/s.

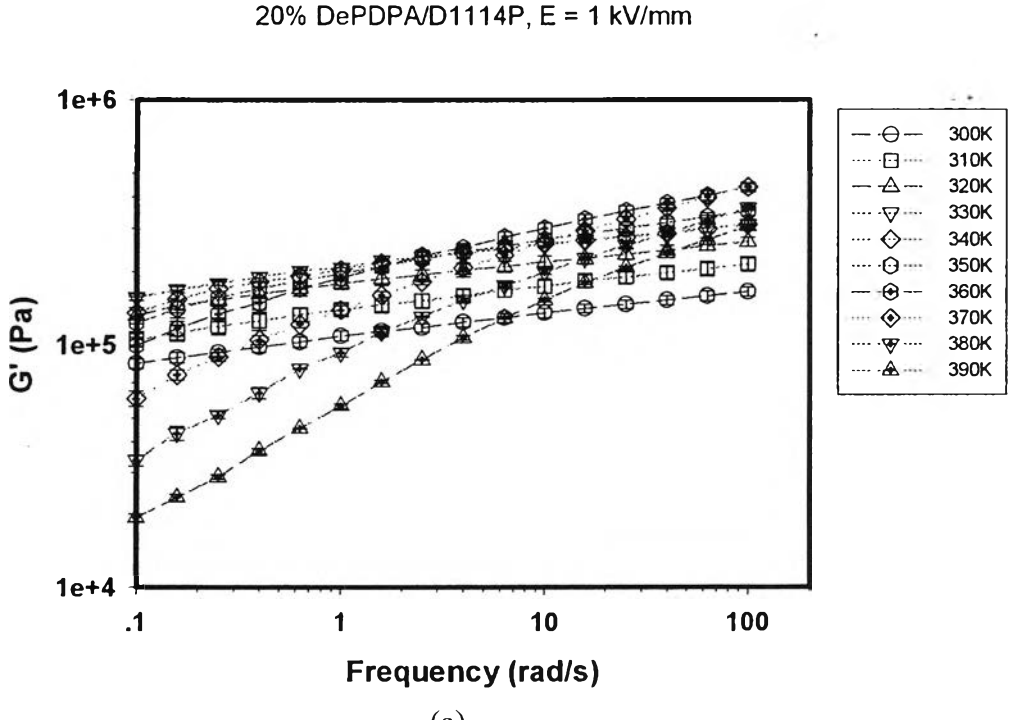

(a)

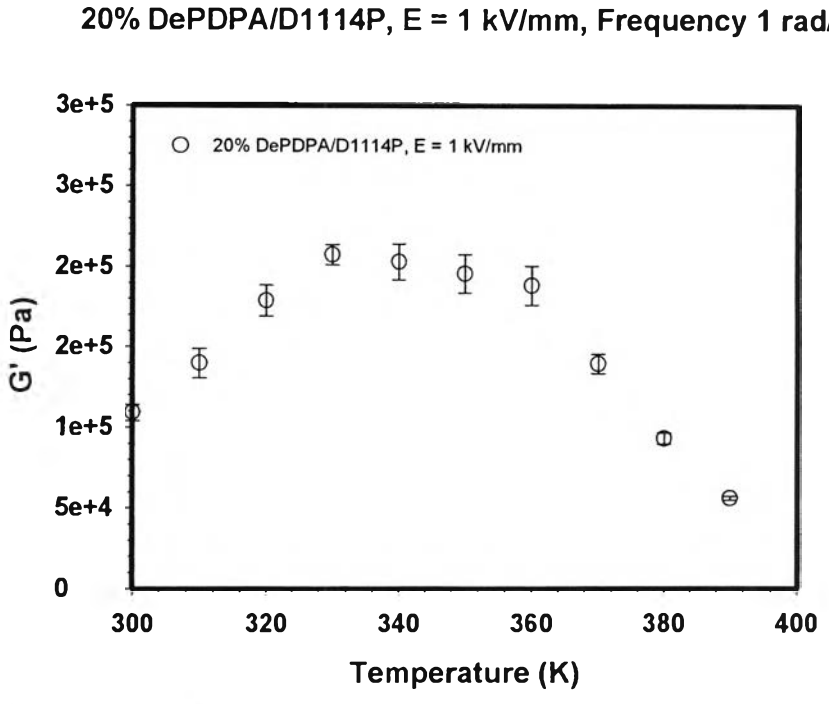

(b)

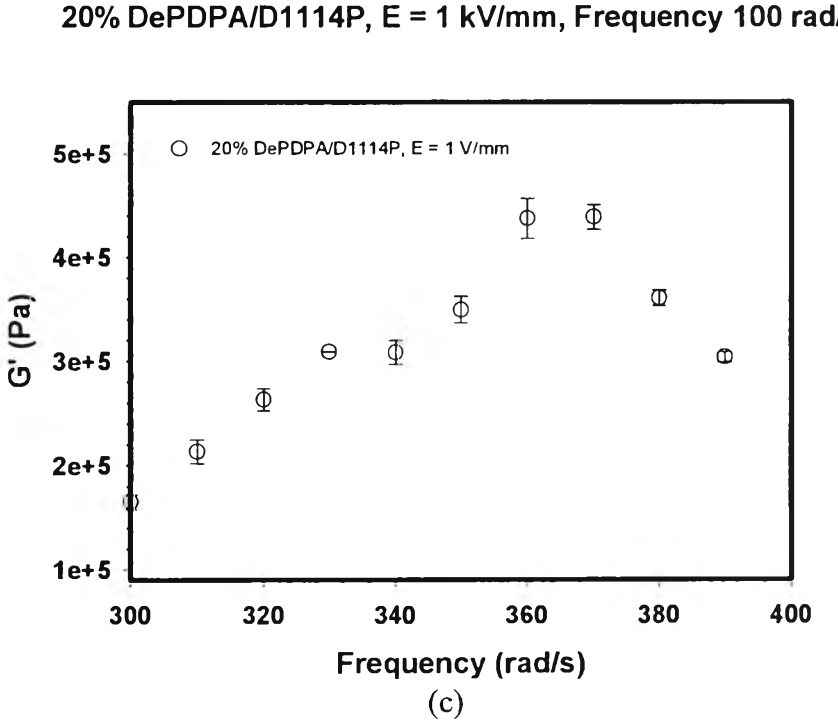

(c)

Figure J26 20% De_PDPA/D1114P at E = 1 kV/mm, strain 0.1 % (a) frequency sweep test at various temperatures; (b) storage modulus (G') versus temperature at frequency 1 rad/s; (c) storage modulus (G') versus temperature at frequency 100 rad/s.

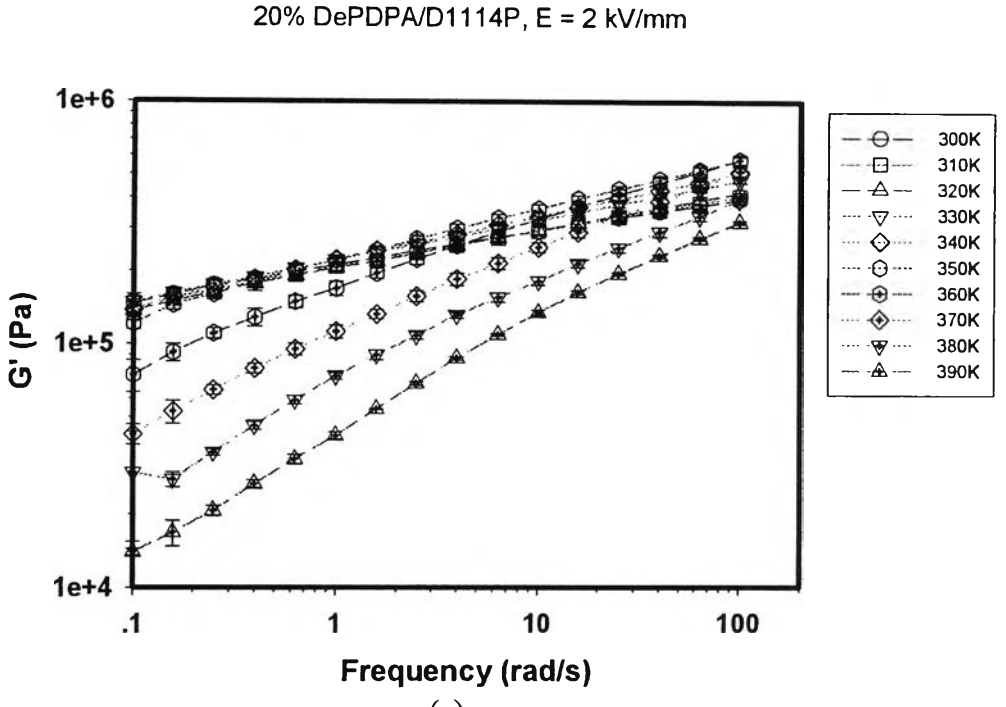
20% DePDPA/D1114P, E = 2 kV/mm
1e+6
1e+5
1e+4
G' (Pa)
.1
1
10
100
Frequency (rad/s)
300K
310K
320K
330K
340K
350K
360K
370K
380K
390K

(a)

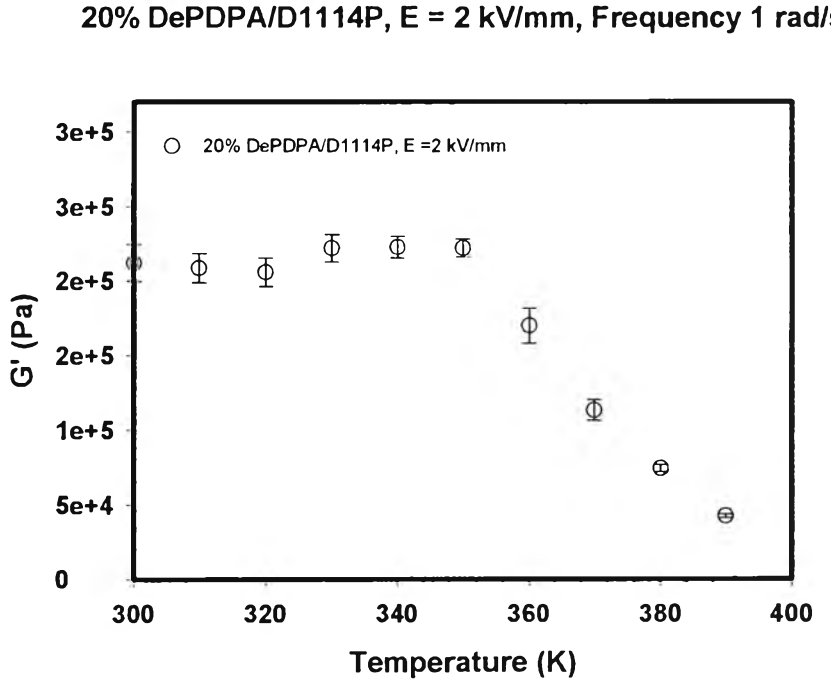
20% DePDPA/D1114P, E = 2 kV/mm, Frequency 1 rad/s
20% DePDPA/D1114P, E =2 kV/mm
3e+5
3e+5
2e+5
2e+5
1e+5
5e+4
0
G' (Pa)
300
320
340
360
380
400
Temperature (K)

(b)

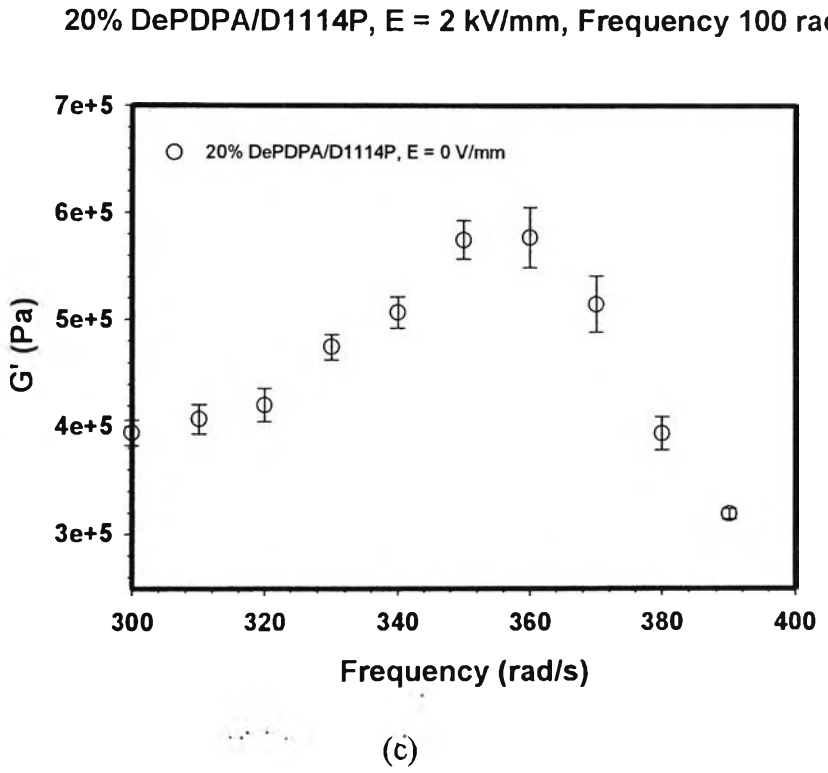

(c)

Figure J27 20% De_PDPA/D1114P at E = 2 kV/mm, strain 0.1 % (a) frequency sweep test at various temperatures; (b) storage modulus (G') versus temperature at frequency 1 rad/s; (c) storage modulus (G') versus temperature at frequency 100 rad/s.

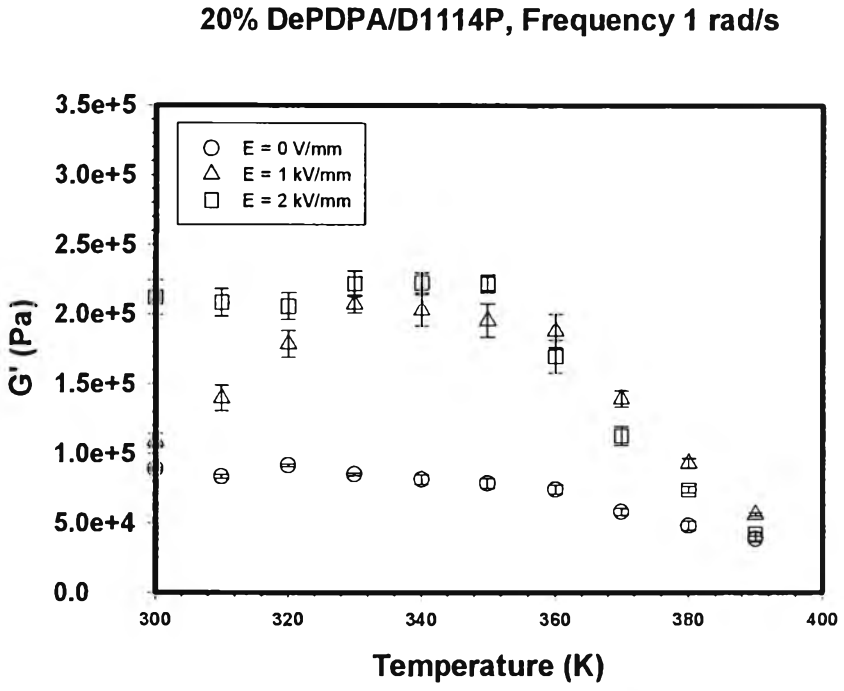

Figure J28 Comparison of 20% De_PDPA/D1114P's storage modulus exhibited at different temperatures under various electric fields, frequency 1 rad/s, and strain 0.1 %.

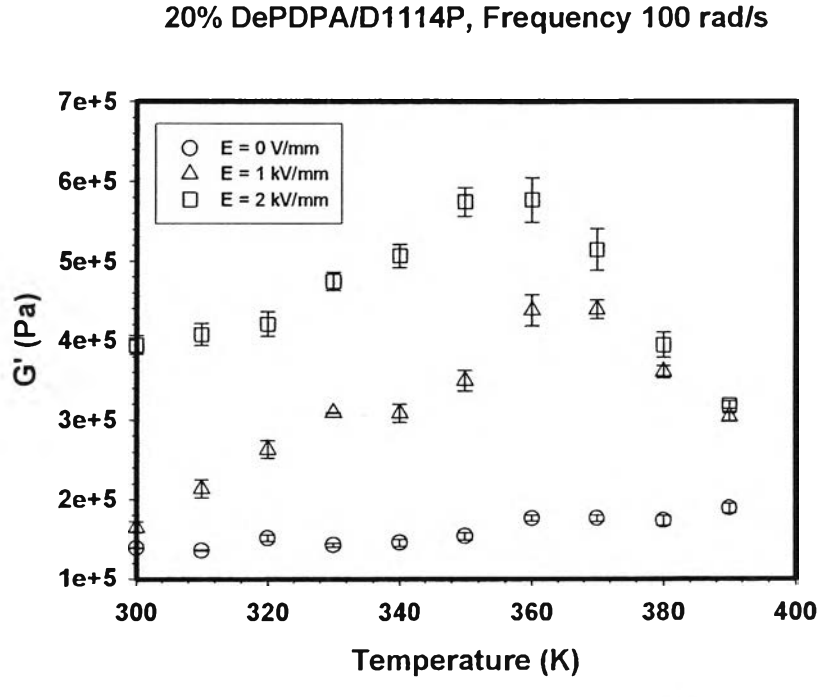

Figure J29 Comparison of 20% De_PDPA/D1114P's storage modulus exhibited at different temperatures under various electric fields, frequency 100 rad/s, and strain 0.1 %.

30 vol% De_PDPA/D1114P

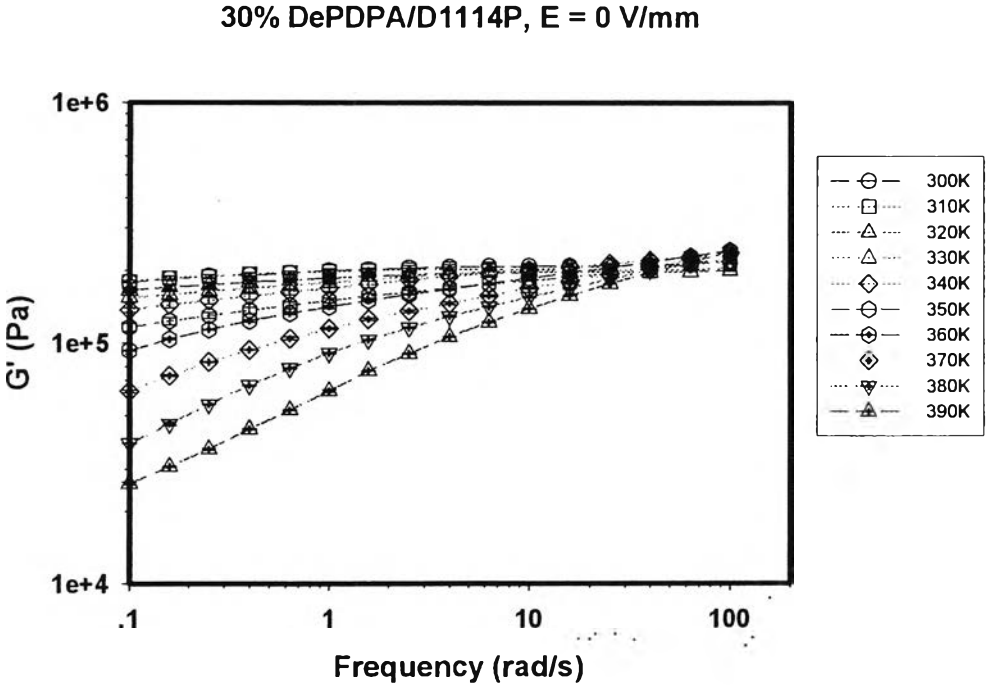

(a)

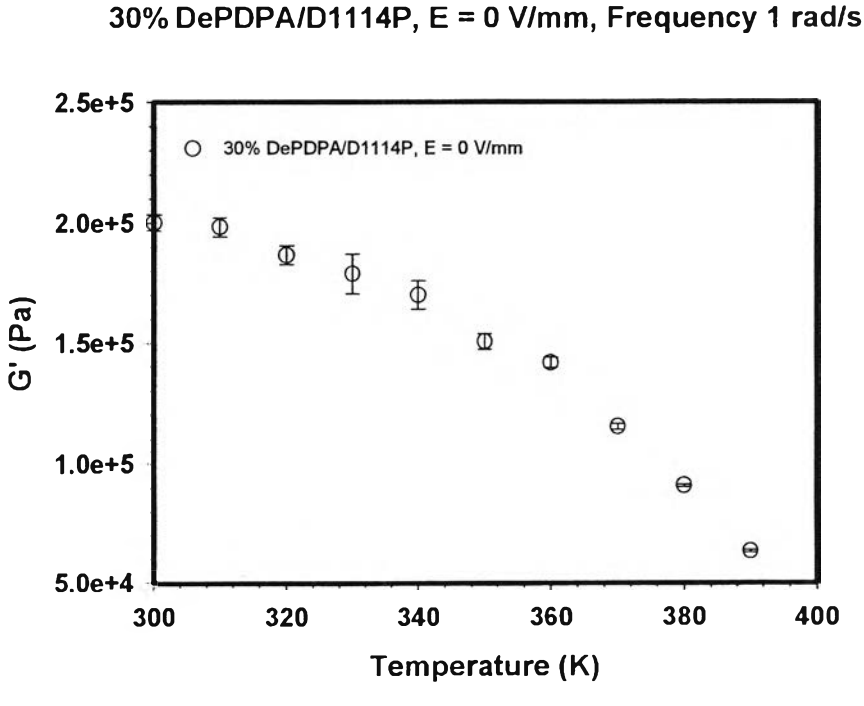

(b)

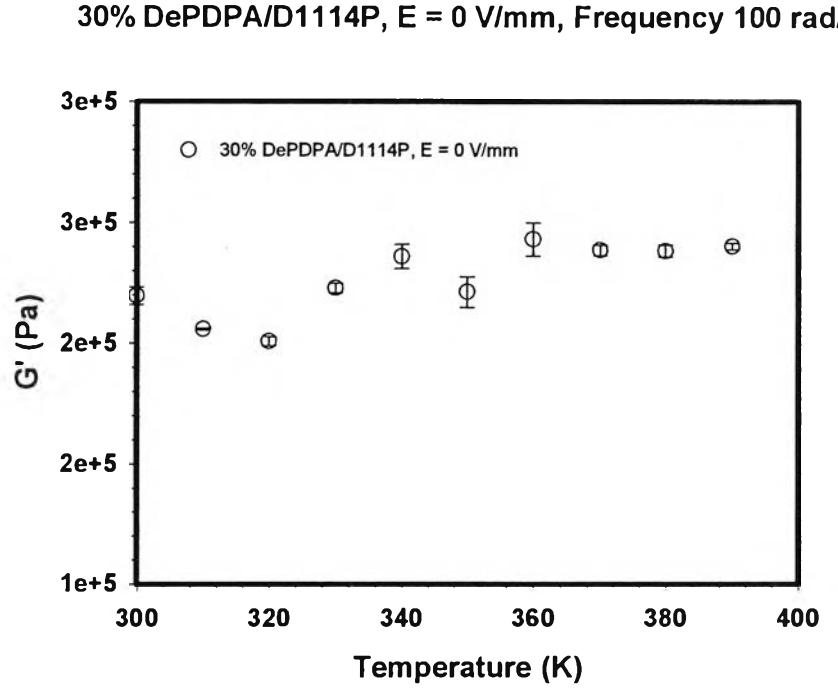

(c)

Figure J30 30% De_PDPA/D1114P_at E = 0 V/mm, strain 0.3 % (a) frequency sweep test at various temperatures; (b) storage modulus (G') versus temperature at frequency 1 rad/s; (c) storage modulus (G') versus temperature at frequency 100 rad/s.

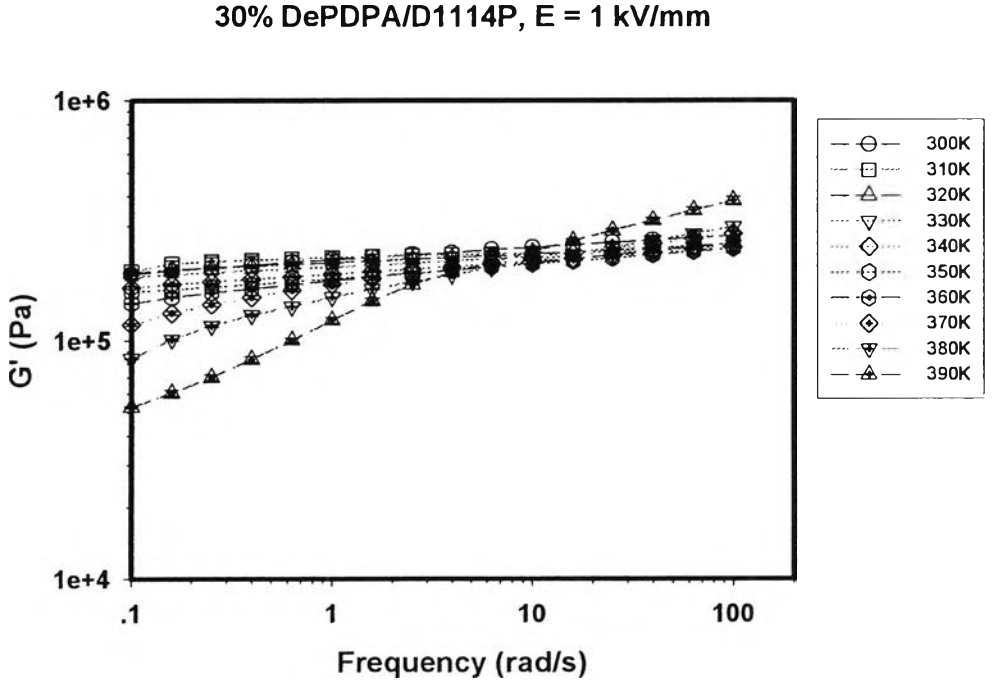

(a)

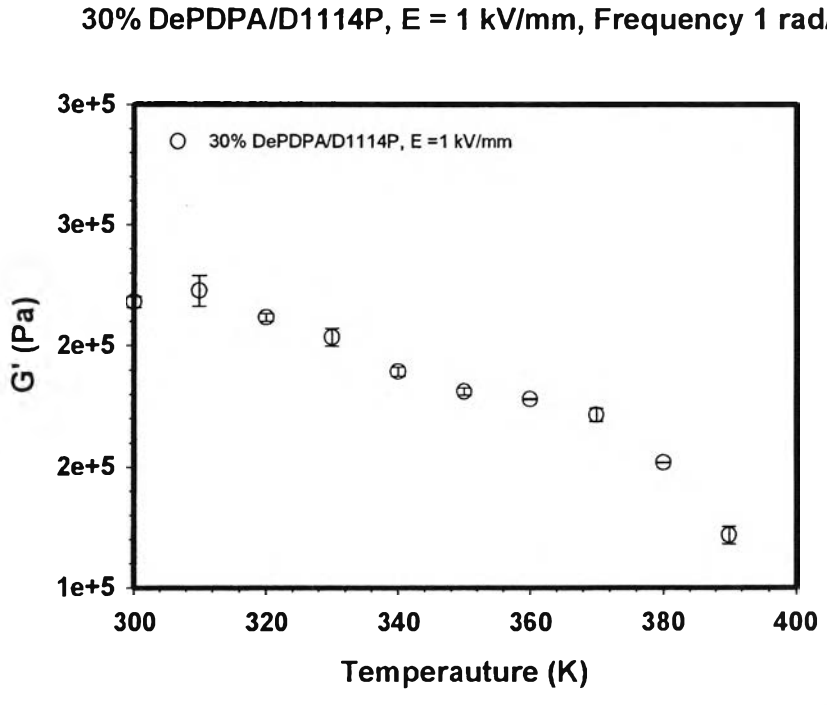

(b)

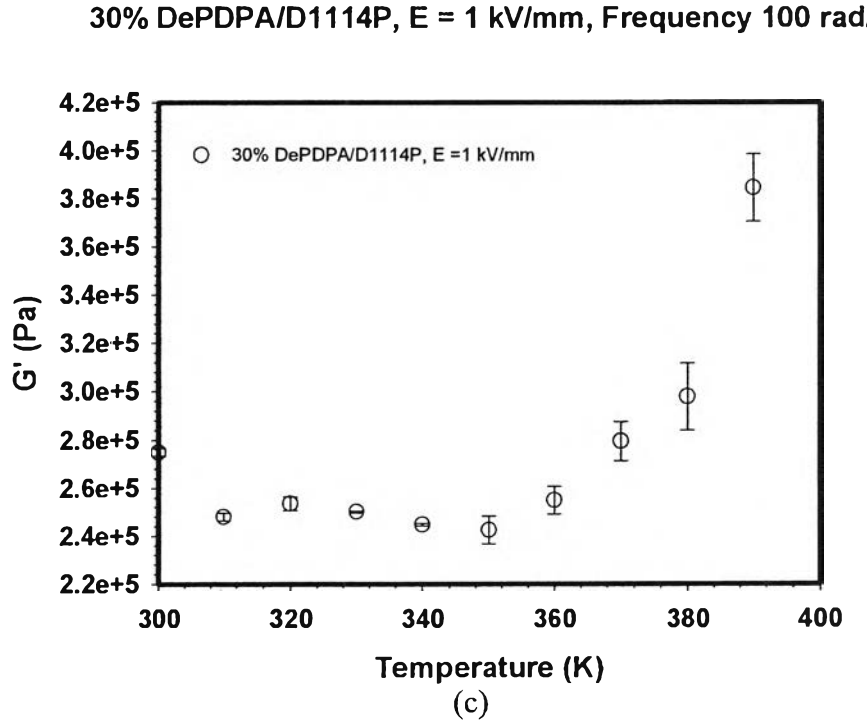

(c)

Figure J31 30% De_PDPA/D1114P_at E = 1 kV/mm, strain 0.3 % (a) frequency sweep test at various temperatures; (b) storage modulus (G') versus temperature at frequency 1 rad/s; (c) storage modulus (G') versus temperature at frequency 100 rad/s.

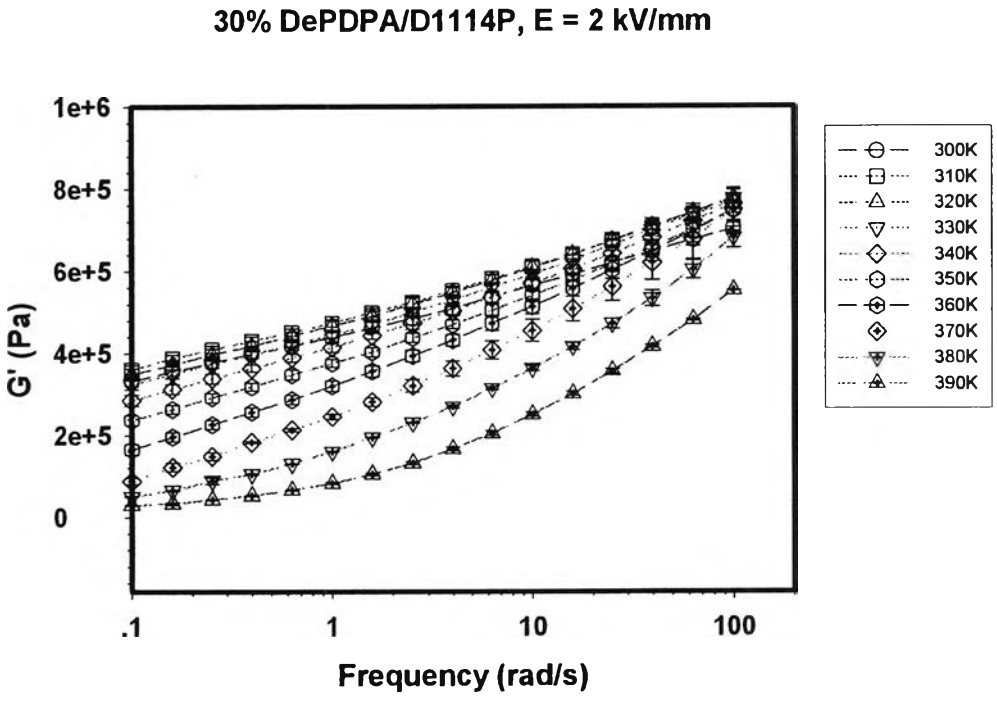
30% DePDPA/D1114P, E = 2 kV/mm
1e+6
8e+5
6e+5
4e+5
2e+5
0
G' (Pa)
.1
1
10
100
Frequency (rad/s)
300K
310K
320K
330K
340K
350K
360K
370K
380K
390K

(a)

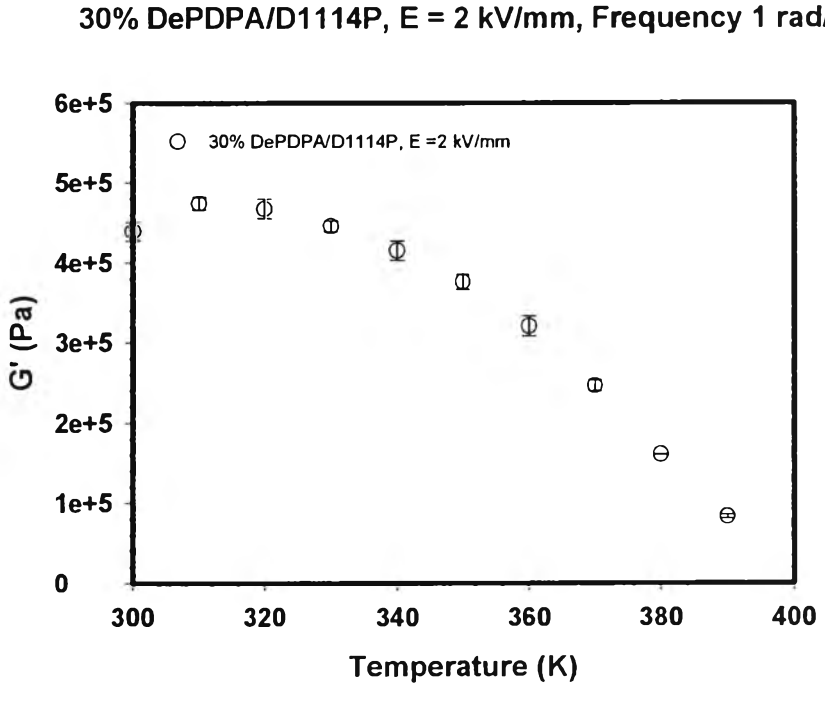
30% DePDPA/D1114P, E = 2 kV/mm, Frequency 1 rad/s
30% DePDPA/D1114P, E =2 kV/mm
6e+5
5e+5
4e+5
3e+5
2e+5
1e+5
0
G' (Pa)
300
320
340
360
380
400
Temperature (K)

(b)

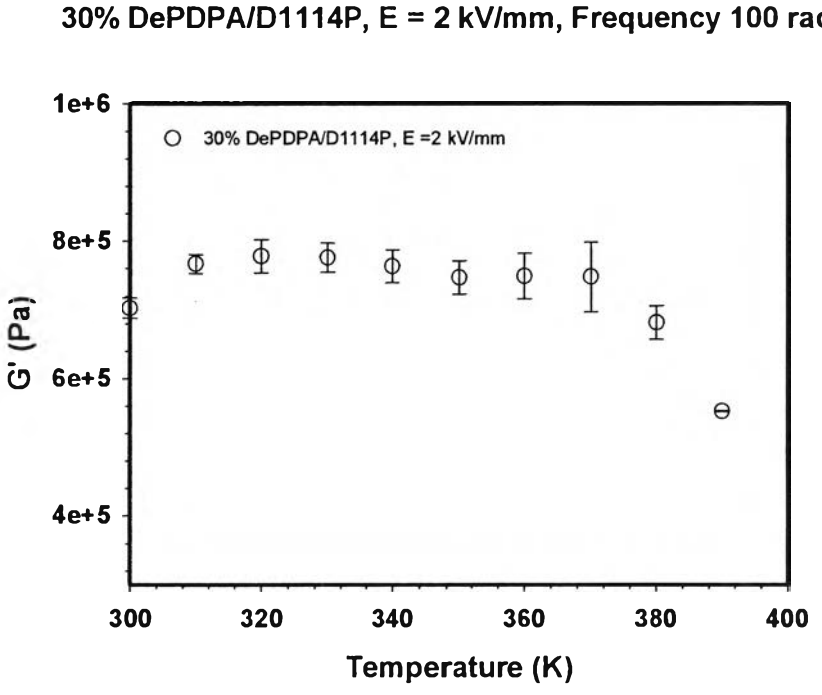

(c)

Figure J32 30% De_PDPA/D1114P_at E = 2 kV/mm, strain 0.3 % (a) frequency sweep test at various temperatures; (b) storage modulus (G') versus temperature at frequency 1 rad/s; (c) storage modulus (G') versus temperature at frequency 100 rad/s.

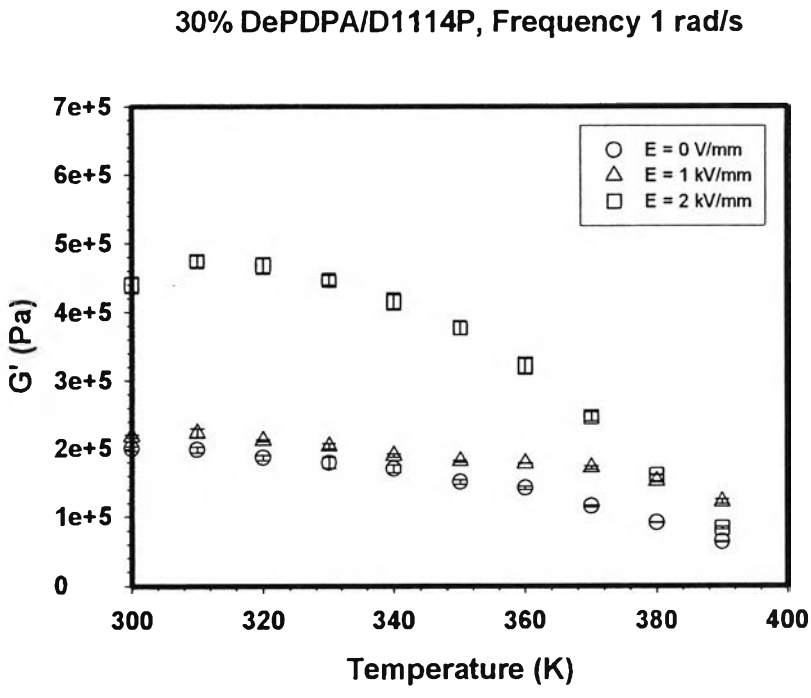

Figure J33 Comparison of 30% De_PDPA/D1114P's storage modulus exhibited at different temperatures under various electric fields, frequency 1 rad/s, and strain 0.3 %.

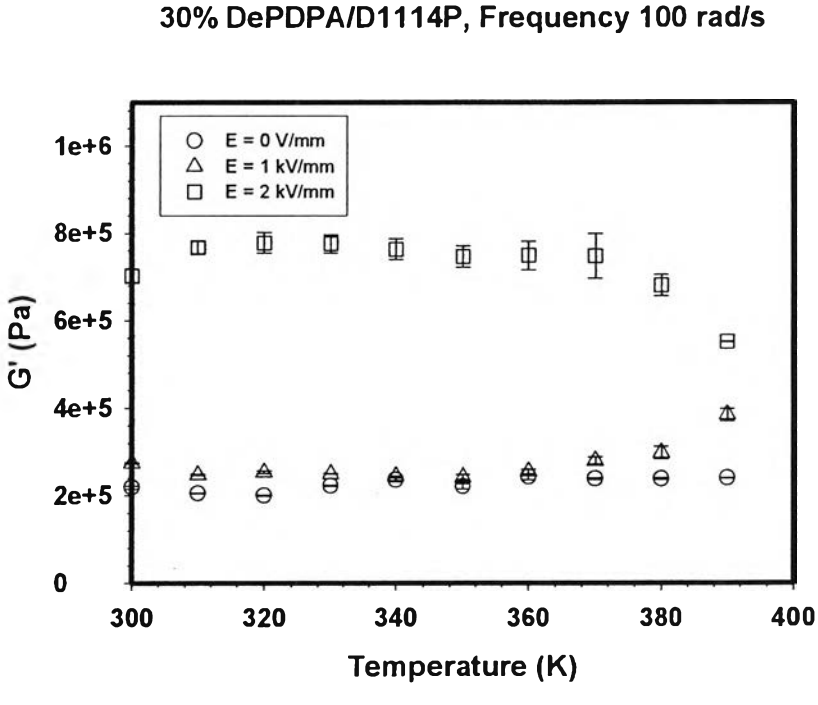

Figure J34 Comparison of 30% De_PDPA/D1114P's storage modulus exhibited at different temperatures under various electric fields, frequency 100 rad/s, and strain 0.3 %.

Appendix K Analysis of deflection force of pure SIS films

Deflection of SIS films; D1114P (19%wt PS), D1164P (29%wt PS), and D1162P were carried out under various applied-electric strengths. For each of SIS films, one end of the sample was fixed with tong vertically in the chamber, which consisted of two electrodes and poly(dimethylsiloxane). The input DC field was generated by a DC power supply (Gold Sun 3000, GPS 3003D) and a high voltage power supply (Gamma High Voltage, UC5-30P) which delivered to the electrodes various electric fields (25, 50, 75, 100, 125, 150, 175, 200, 225, 250, 275, 300. 325, 350, 375, 400, 425, 450, 475, 500, 525, 550, 575, and 600 V/mm). A video recorder was used to record the displacement of the film made a model. The tip displacement was measured through a Scion Image (Beta 4.0.3) program.

To calculate the theoretical force of sample displacement it can be regarded as a cantilever beam. It is assumed that the sample is symmetric with respect to the longitudinal direction and that a concentrated load is acting at the tip of an actuator. Then, the relation between tip displacements (d) and force (Fe) are calculate from the linear deflection and non-linear deflection models depending on their bending characteristic (Figure K1), as the following:

(Linear deflection) $$Fe = \frac{3dEI}{l^3} \quad \text{(K.1)}$$

(Non-linear deflection) $$Fe = \frac{dEI}{l^3} \quad \text{(K.2)}$$

where E is the modulus of elasticity (Pa), d is displacement distance in x axis (mm), I is the moment of inertia (m^4), and l is the deflection distance in y axis (mm), which are shown in Figure K1.

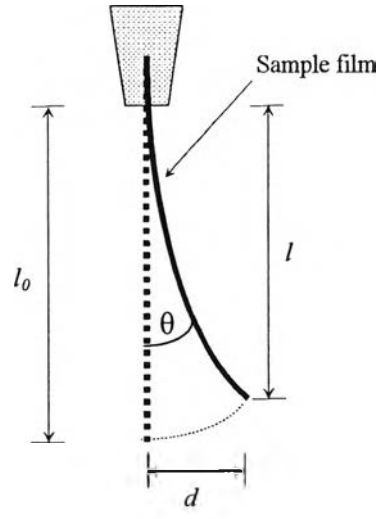

Figure K1 deflection of one free end sample beam.

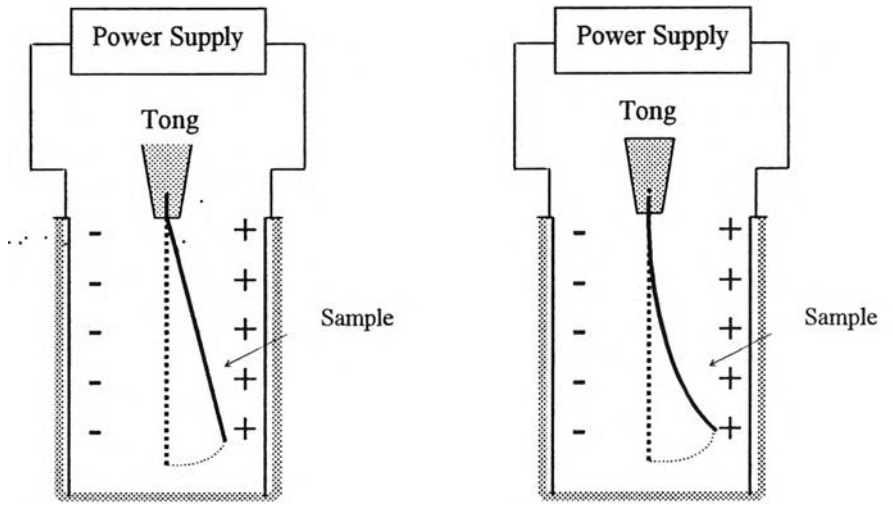

Figure K2 (a) Linear deflection and (b) Non-linear deflection of the sample under electric field.

But, the absolute vertical deflection force at the free end of the sample does not only depend on Elastic force (*Fe*), but also depend on weight in deflection direction, (*mg sin(θ)*). Thus, the absolute deflection force of free end of sample beam or dielectrophoretic force is the sum of the elastic force (*Fe*) and *mg sin(θ)*, as in the following equation:

(Dielectrophoretic force) $$Fd = Fe + mg\sin\theta \qquad \text{(K.3)}$$

Table K1 Electromechanical responses of pure SIS D1114 P at various electric field strengths

E (V/mm)	d (mm)	l (mm)	θ (°)	sin(θ)	mg sin(θ) (N)	F_e from linear deflection (N)	F_d from linear deflection (N)	F_e from non linear deflection (N)	F_d from non linear deflection (N)	τ_i (sec)	τ_r (sec)	Energy density (J/m3)	Force density (N/m3)
0	0	15.31	0	0	0	0	0	0	0	0	0	0	0.0
25	0	15.31	0	0	0	0	0	0	0	0	0	0	0.0
50	0	15.31	0	0	0	0	0	0	0	0	0	0	0.0
75	0	15.31	0	0	0	0	0	0	0	0	0	0	0.0
100	0	15.31	0	0	0	0	0	0	0	0	0	0	0.0
125	0	15.31	0	0	0	0	0	0	0	0	0	0	0.0
150	0	15.31	0	0	0	0	0	0	0	0	0	0	0.0
175	0.41	15.31	1.5	0.0268	4.802E-06	3.654E-07	5.168E-06	3.691E-07	5.171E-06	30	4	36.5	260.5
200	0.61	15.31	2.3	0.0398	7.144E-06	5.436E-07	7.687E-06	5.491E-07	7.693E-06	30	4	80.8	387.5
225	0.61	15.31	2.3	0.0398	7.144E-06	5.436E-07	7.687E-06	5.491E-07	7.693E-06	32	5	80.8	387.5
250	0.61	15.31	2.3	0.0398	7.144E-06	5.436E-07	7.687E-06	5.491E-07	7.693E-06	33	5	80.8	387.5
275	0.61	15.31	2.3	0.0398	7.144E-06	5.436E-07	7.687E-06	5.491E-07	7.693E-06	35	7	80.8	387.5
300	0.61	15.31	2.3	0.0398	7.144E-06	5.436E-07	7.687E-06	5.491E-07	7.693E-06	40	8	80.8	387.5
325	0.82	15.31	3.1	0.0535	9.601E-06	7.308E-07	1.033E-05	7.382E-07	1.034E-05	44	9	145.9	520.8
350	1.02	15.31	3.8	0.0666	1.194E-05	9.090E-07	1.285E-05	9.183E-07	1.286E-05	44	9	225.6	647.6
375	1.02	15.31	3.8	0.0666	1.194E-05	9.090E-07	1.285E-05	9.183E-07	1.286E-05	45	12	225.6	647.6
400	1.02	15.31	3.8	0.0666	1.194E-05	9.090E-07	1.285E-05	9.183E-07	1.286E-05	49	14	225.6	647.6
425	1.43	15.31	5.4	0.0933	1.673E-05	1.274E-06	1.8E-05	1.293E-06	1.802E-05	50	14	442.8	907.6
450	1.43	15.31	5.4	0.0933	1.673E-05	1.274E-06	1.8E-05	1.293E-06	1.802E-05	50	15	442.8	907.6
475	1.63	15.31	6.1	0.1063	1.906E-05	1.453E-06	2.051E-05	1.476E-06	2.053E-05	53	18	574.8	1034.2
500	1.63	15.31	6.1	0.1063	1.906E-05	1.453E-06	2.051E-05	1.476E-06	2.053E-05	54	17	574.8	1034.2
525	2.04	15.31	7.6	0.1329	2.383E-05	1.818E-06	2.564E-05	1.853E-06	2.568E-05	55	18	898.4	1293.4
550	2.65	15.31	9.9	0.1722	3.089E-05	2.362E-06	3.325E-05	2.447E-06	3.333E-05	54	28	1509.9	1679.0
575	2.86	15.1	10.9	0.1883	3.376E-05	2.657E-06	3.642E-05	2.651E-06	3.642E-05	56	29	1804.4	1834.2
600	2.86	15.1	10.9	0.1883	3.376E-05	2.657E-06	3.642E-05	2.651E-06	3.642E-05	55	33	1804.4	1834.2

Pure SIS D1114 P (19 %wt PS)

The weight of specimen (wt) = 0.0183 g

The length of specimen (l_0) = 15.31 mm

The initial length of specimen (L) = 22.23 mm

The thickness of specimen (t) = 0.390 mm

The width of specimen (w) = 2.29 mm

G' = 33935.8 Pa at E = 0 kV/mm, T = 300 K, strain = 1.0%, f = 1 rad/s.

d = deflection distance in x axis (mm), l= deflection distance in y axis (mm)

τ_i = induction time (sec), τ_r = recovery time (sec)

I = Moment of inertia (m^4) = $t^3w/12$

E = Modulus of elasticity (Pa)

F_e = elastic force (N) = $3dEI/l^3$ for linear deflection

F_e = elastic force (N) = dEI/l^3 for non linear deflection

F_d = dielectrophoretic force = F_e (N) + mgsinθ

Energy density = $\frac{1}{2}E\theta^2$ (J/m^3)

Force density = $\frac{F_d}{volume}$ (N/m^3)

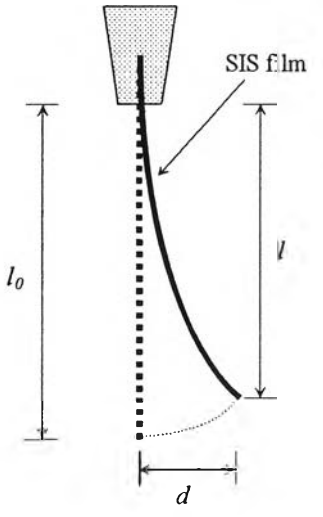

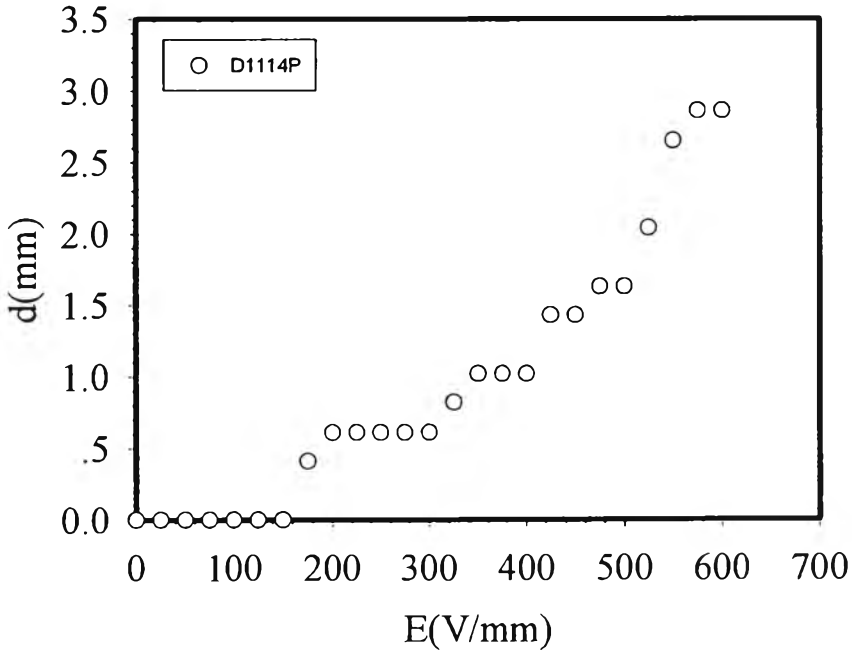
D1114P
d(mm)
3.5
3.0
2.5
2.0
1.5
1.0
.5
0.0
0
100
200
300
400
500
600
700
E(V/mm)

(a)

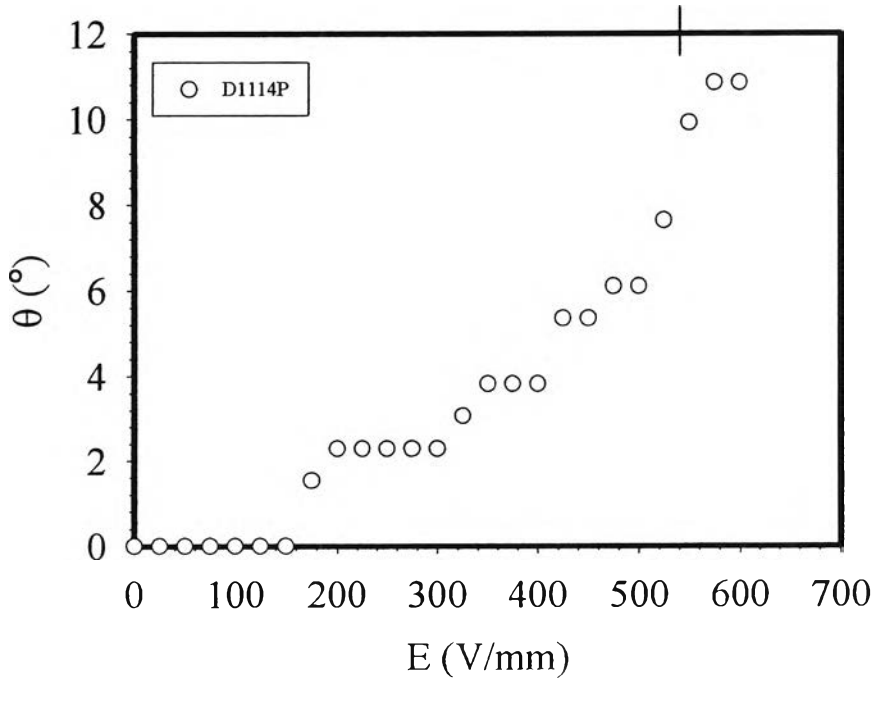
D1114P
θ (°)
12
10
8
6
4
2
0
0
100
200
300
400
500
600
700
E (V/mm)

(b)

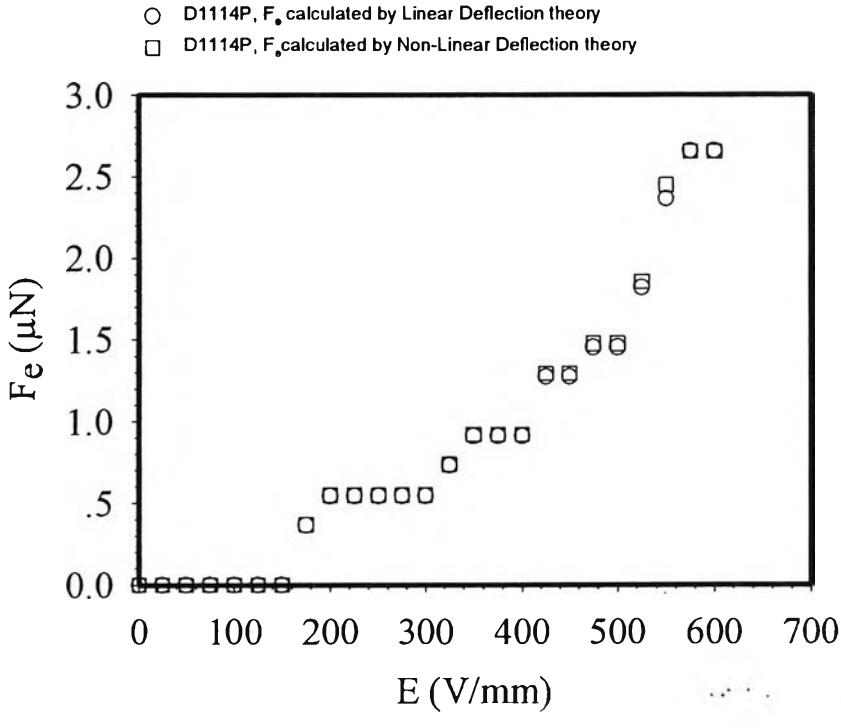
D1114P, F_e calculated by Linear Deflection theory
D1114P, $F_e$calculated by Non-Linear Deflection theory
3.0
2.5
2.0
1.5
1.0
.5
0.0
F_e (μN)
0
100
200
300
400
500
600
700
E (V/mm)

(c)

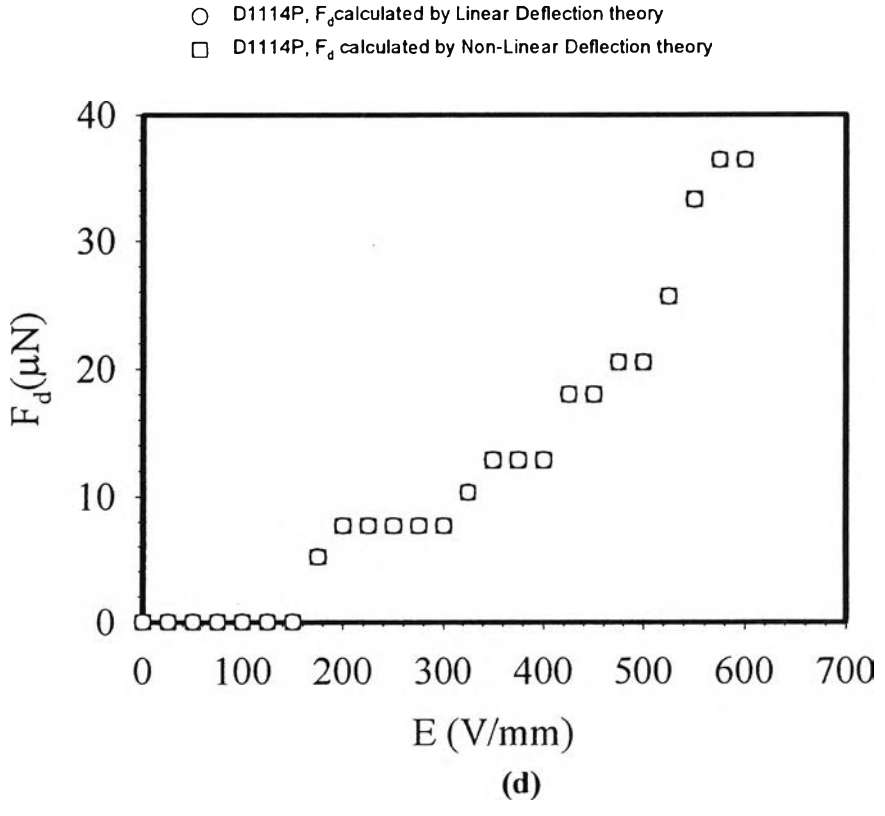
D1114P, $F_d$calculated by Linear Deflection theory
D1114P, F_d calculated by Non-Linear Deflection theory
40
30
20
10
0
F_d(μN)
0
100
200
300
400
500
600
700
E (V/mm)

(d)

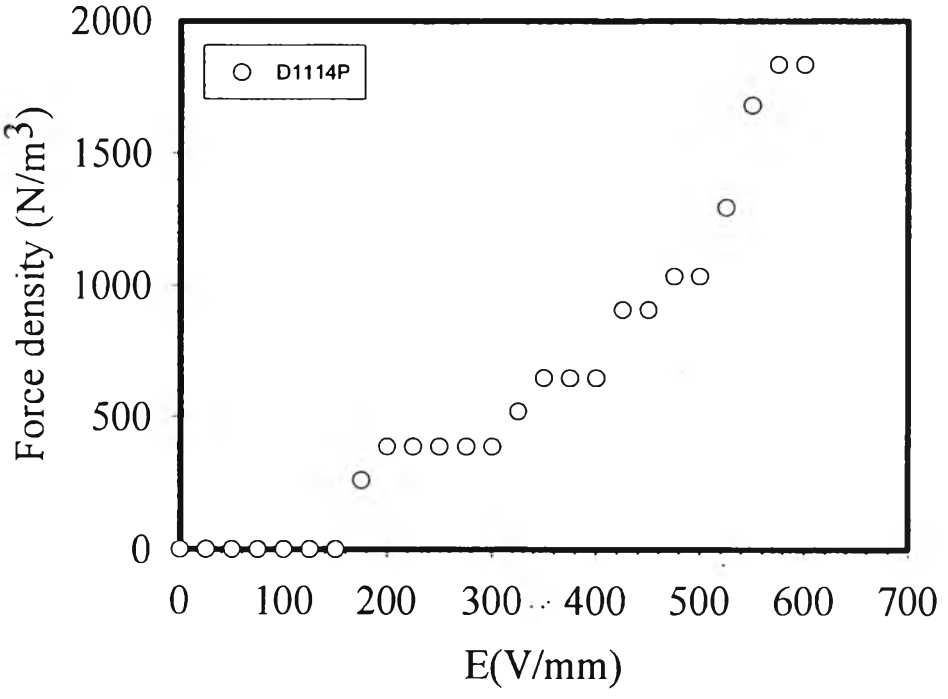
D1114P
Force density (N/m3)
2000
1500
1000
500
0
0
100
200
300
400
500
600
700
E(V/mm)

(e)

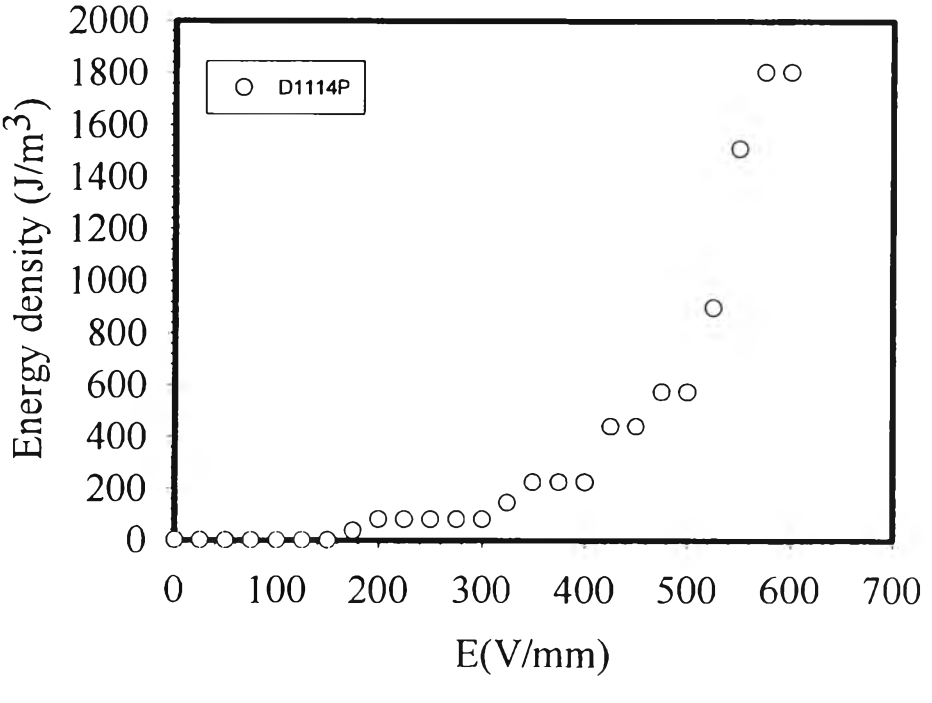
D1114P
Energy density (J/m3)
2000
1800
1600
1400
1200
1000
800
600
400
200
0
0
100
200
300
400
500
600
700
E(V/mm)

(f)

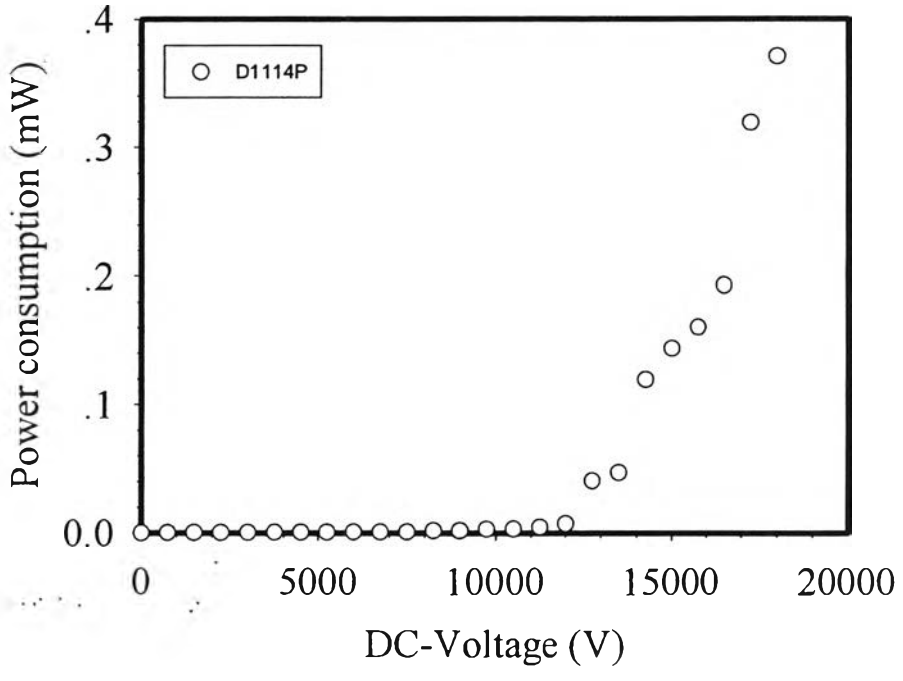

(g)

Figure K1 Electromechanical responses of pure SIS D1114P at various electric field strengths: (a) deflection lengths; (b) deflection angles; (c) elastic force (F_e); (d) dielectrophoretic forces (F_d); (e) force density; (f) energy density; (g) power consumption

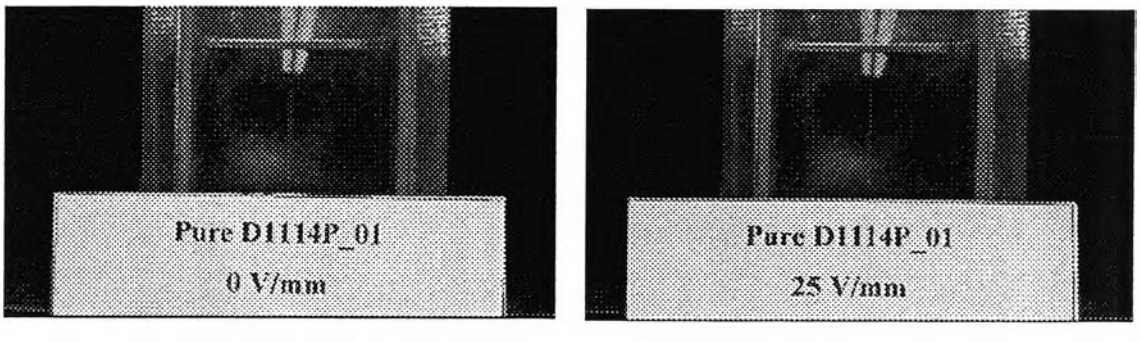

(a) **(b)**

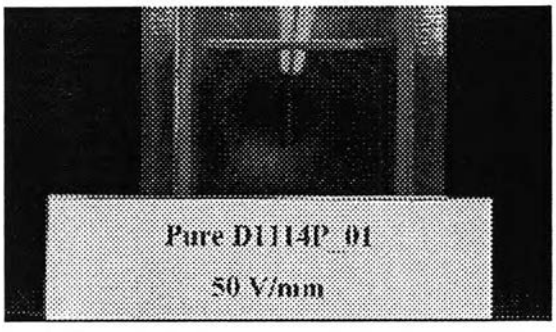
Pure D1114P_01
50 V/mm

(c)

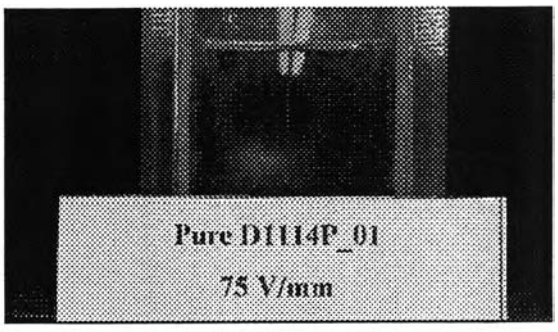
Pure D1114P_01
75 V/mm

(d)

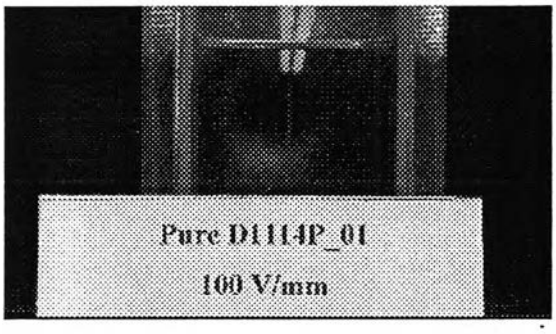
Pure D1114P_01
100 V/mm

(e)

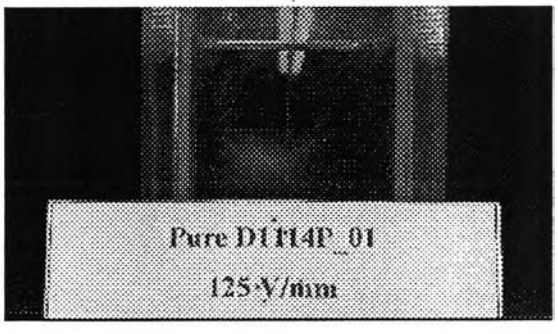
Pure D1114P_01
125 V/mm

(f)

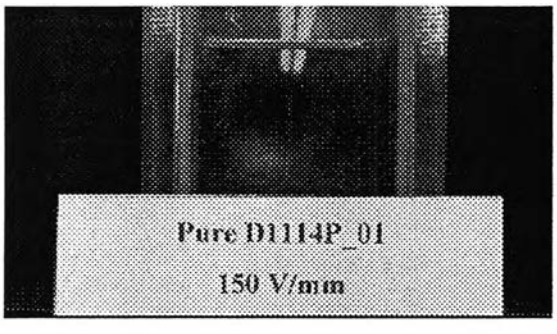
Pure D1114P_01
150 V/mm

(g)

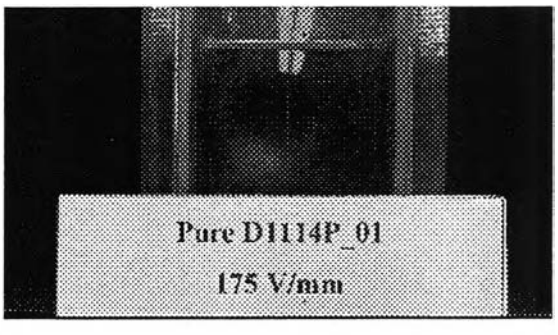
Pure D1114P_01
175 V/mm

(h)

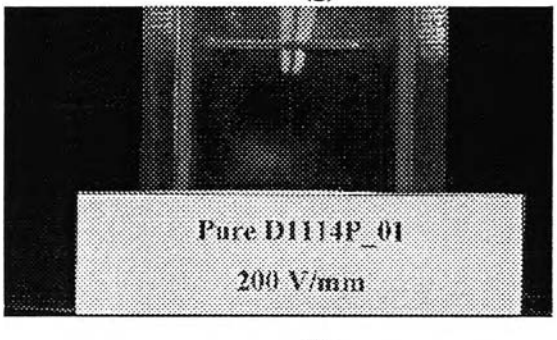
Pure D1114P_01
200 V/mm

(i)

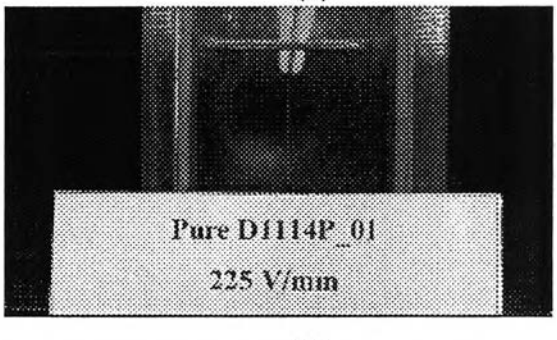
Pure D1114P_01
225 V/mm

(j)

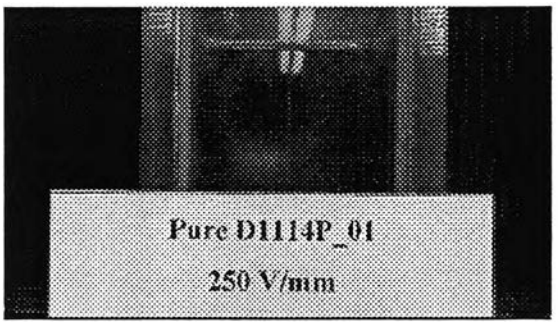
Pure D1114P_01
250 V/mm

(k)

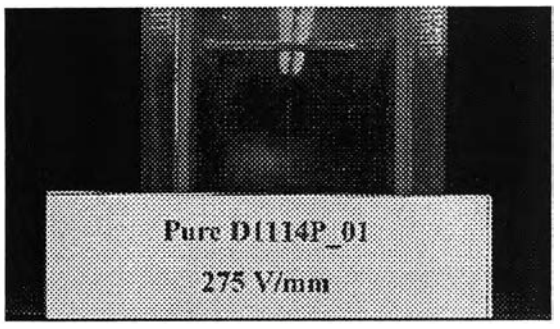
Pure D1114P_01
275 V/mm

(l)

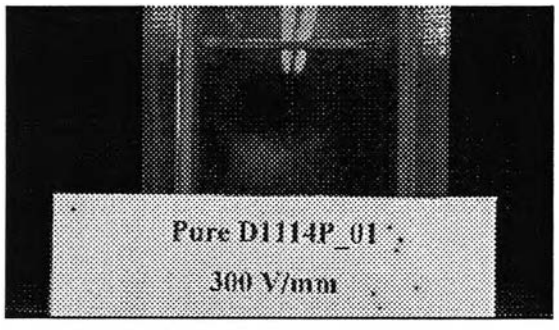
Pure D1114P_01
300 V/mm

(m)

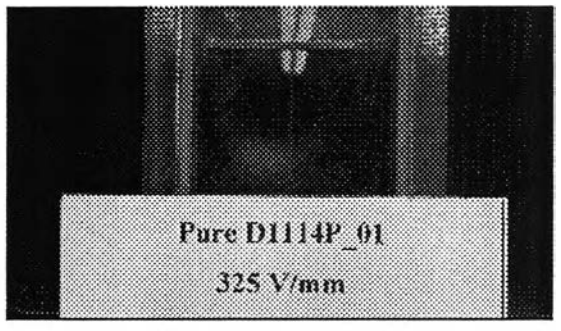
Pure D1114P_01
325 V/mm

(n)

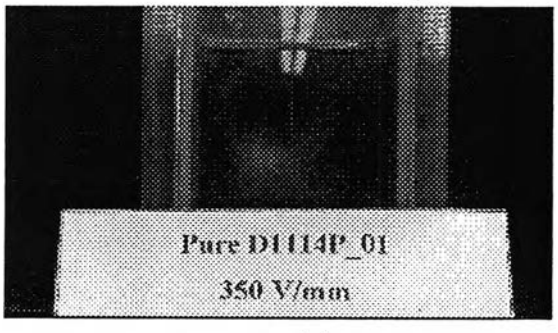
Pure D1114P_01
350 V/mm

(o)

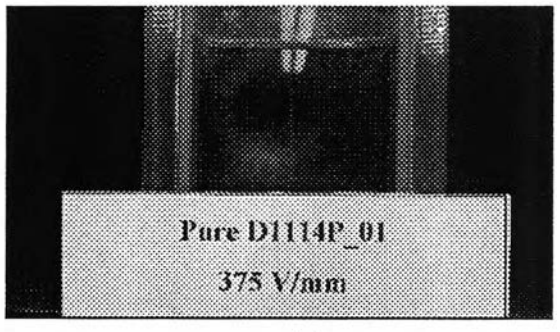
Pure D1114P_01
375 V/mm

(p)

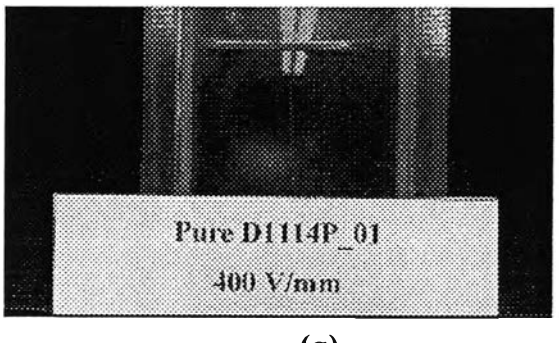
Pure D1114P_01
400 V/mm

(q)

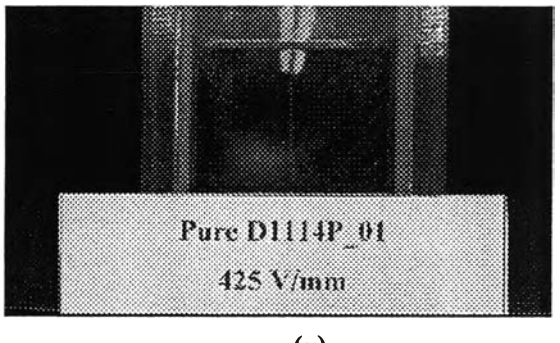
Pure D1114P_01
425 V/mm

(r)

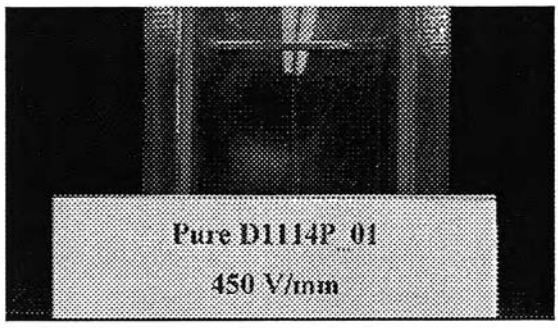
Pure D1114P_01
450 V/mm

(s)

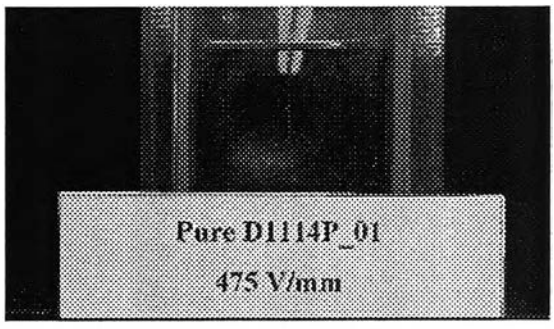
Pure D1114P_01
475 V/mm

(t)

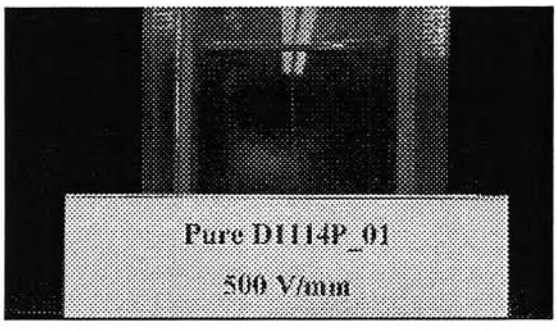
Pure D1114P_01
500 V/mm

(u)

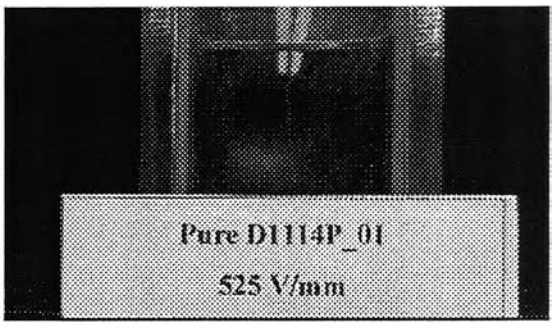
Pure D1114P_01
525 V/mm

(v)

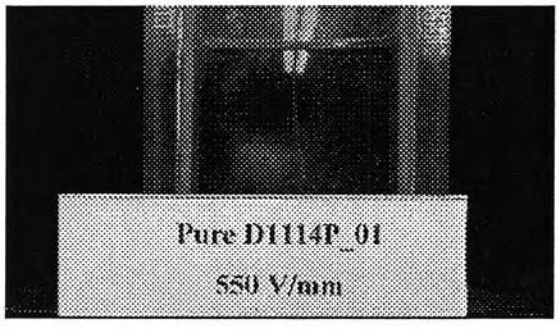
Pure D1114P_01
550 V/mm

(w)

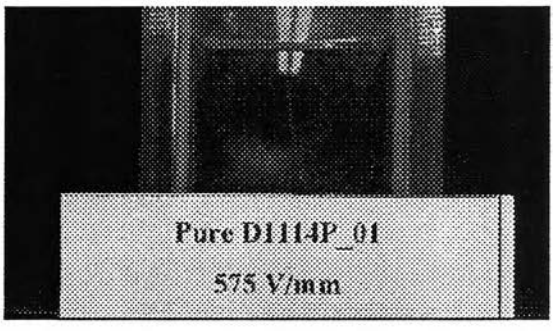
Pure D1114P_01
575 V/mm

(x)

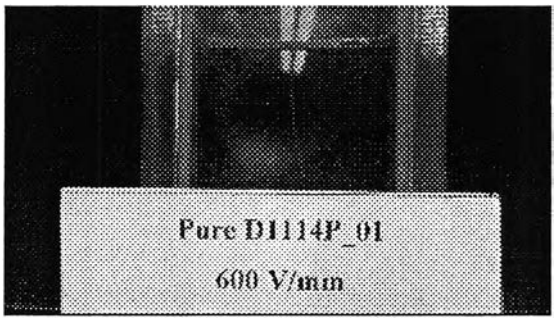
Pure D1114P_01
600 V/mm

(y)

Figure K2 Electromechanical responses of pure SIS D1114P at various electric field strengths: (a) 0 V/mm; (b) 25 V/mm; (c) V = 50 V/mm; (d) 75 V/mm; (e) 100 V/mm; (f) 125 V/mm; (g) 150 V/mm; (h) 175 V/mm; (i) 200 V/mm; (j) 225 V/mm; (k) 250 V/mm; (l) 275 V/mm; (m) 300 V/mm; (n) 325 V/mm; (o) 350 V/mm; (p) 375 V/mm; (q) 400 V/mm; (r) 425 V/mm; (s) 450 V/mm; (t) 475 V/mm; (u) 500 V/mm; (v) 525 V/mm; (w) 550 V/mm; (x) 575 V/mm; (y) 600 V/mm.

Table K2 Electromechanical responses of pure SIS D1164 P at various electric field strengths

E (V/mm)	d (mm)	l (mm)	θ (°)	sin(θ)	mg sin(θ) (N)	F_e from linear deflection (N)	F_d from linear deflection (N)	F_e from non linear deflection (N)	F_d from non linear deflection (N)	τ_i (sec)	τ_r (sec)	Energy density (J/m3)	Force density (N/m3)
0	0	14.68	0	0	0	0	0	0	0	0	0	0	0
25	0	14.68	0	0	0	0	0	0	0	0	0	0	0
50	0	14.68	0	0	0	0	0	0	0	0	0	0	0
75	0	14.68	0	0	0	0	0	0	0	0	0	0	0
100	0	14.68	0	0	0	0	0	0	0	0	0	0	0
125	0	14.68	0	0	0	0	0	0	0	0	0	0	0
150	0	14.68	0	0	0	0	0	0	0	0	0	0	0
175	0	14.68	0	0	0	0	0	0	0	0	0	0	0
200	0	14.68	0	0	0	0	0	0	0	0	0	0	0
225	0	14.68	0	0	0	0	0	0	0	0	0	0	0
250	0	14.68	0	0	0	0	0	0	0	0	0	0	0
275	0.21	14.68	0.8	0.014	2.523E-06	3.8983E-07	2.9132E-06	3.9377E-07	2.9171E-06	22	5	16.5	155
300	0.21	14.68	0.8	0.014	2.523E-06	3.8983E-07	2.9132E-06	3.9377E-07	2.9171E-06	29	6	16.5	155
325	0.21	14.68	0.8	0.014	2.523E-06	3.8983E-07	2.9132E-06	3.9377E-07	2.9171E-06	30	6	16.5	155
350	0.21	14.68	0.8	0.014	2.523E-06	3.8983E-07	2.9132E-06	3.9377E-07	2.9171E-06	30	7	16.5	155
375	0.21	14.68	0.8	0.014	2.523E-06	3.8983E-07	2.9132E-06	3.9377E-07	2.9171E-06	32	8	16.5	155
400	0.43	14.68	1.7	0.029	5.166E-06	7.9823E-07	5.9645E-06	8.0629E-07	5.9726E-06	33	10	69.3	318
425	0.64	14.68	2.5	0.044	7.688E-06	1.1881E-06	8.8761E-06	1.2001E-06	8.8881E-06	34	10	153.4	473
450	0.64	14.68	2.5	0.044	7.688E-06	1.1881E-06	8.8761E-06	1.2001E-06	8.8881E-06	39	10	153.4	473
475	0.64	14.68	2.5	0.044	7.688E-06	1.1881E-06	8.8761E-06	1.2001E-06	8.8881E-06	40	12	153.4	473
500	0.64	14.68	2.5	0.044	7.688E-06	1.1881E-06	8.8761E-06	1.2001E-06	8.8881E-06	43	13	153.4	473
525	0.64	14.68	2.5	0.044	7.688E-06	1.1881E-06	8.8761E-06	1.2001E-06	8.8881E-06	44	13	153.4	473
550	0.64	14.68	2.5	0.044	7.688E-06	1.1881E-06	8.8761E-06	1.2001E-06	8.8881E-06	45	13	153.4	473
575	1.07	14.68	4.2	0.073	1.285E-05	1.9863E-06	1.4832E-05	2.0093E-06	1.4855E-05	45	15	428.3	791
600	1.07	14.68	4.2	0.073	1.285E-05	1.9863E-06	1.4832E-05	2.0093E-06	1.4855E-05	49	16	428.3	791

D1164 P (29 %wt PS)

The weight of specimen (wt) = 0.0180 g

The length of specimen (l_0) = 14.68 mm

The initial length of specimen (L) = 21.71 mm

The thickness of specimen (t) = 0.410 mm

The width of specimen (w) = 2.11 mm

G′ = 53844.34 Pa at E = 0 kV/mm, T = 300 K, strain = 0.1%, f = 1 rad/s.

d = deflection distance in x axis (mm), l= deflection distance in y axis (mm)

τ_i = induction time (sec), τ_r = recovery time (sec)

I = Moment of inertia (m^4) = $t^3w/12$

E = Modulus of elasticity (Pa)

F_e = elastic force (N) = $3dEI/l^3$ for linear deflection

F_e = elastic force (N) = dEI/l^3 for non linear deflection

F_d = dielectrophoretic force = F_e (N) + mgsinθ

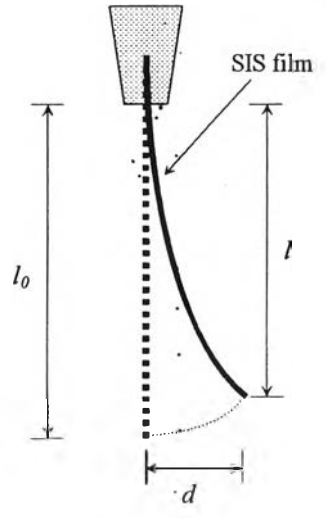

$$\text{Energy density} = \frac{1}{2}E\theta^2 \ (\text{J/m}^3)$$

$$\text{Force density} = \frac{F_d}{volume} \quad (\text{N/m}^3)$$

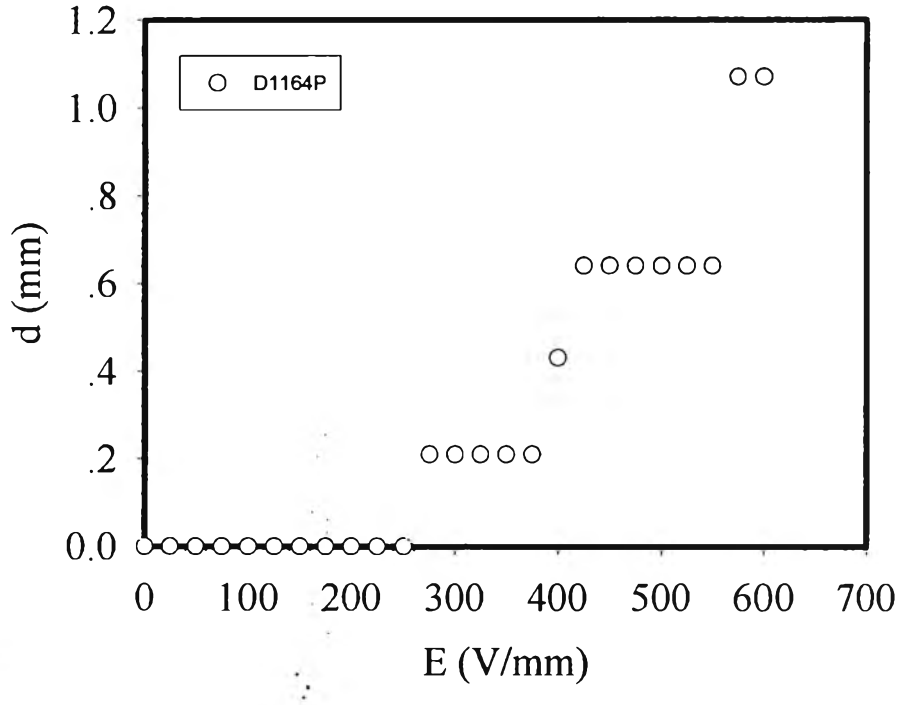
D1164P
d (mm)
1.2
1.0
.8
.6
.4
.2
0.0
0
100
200
300
400
500
600
700
E (V/mm)

(a)

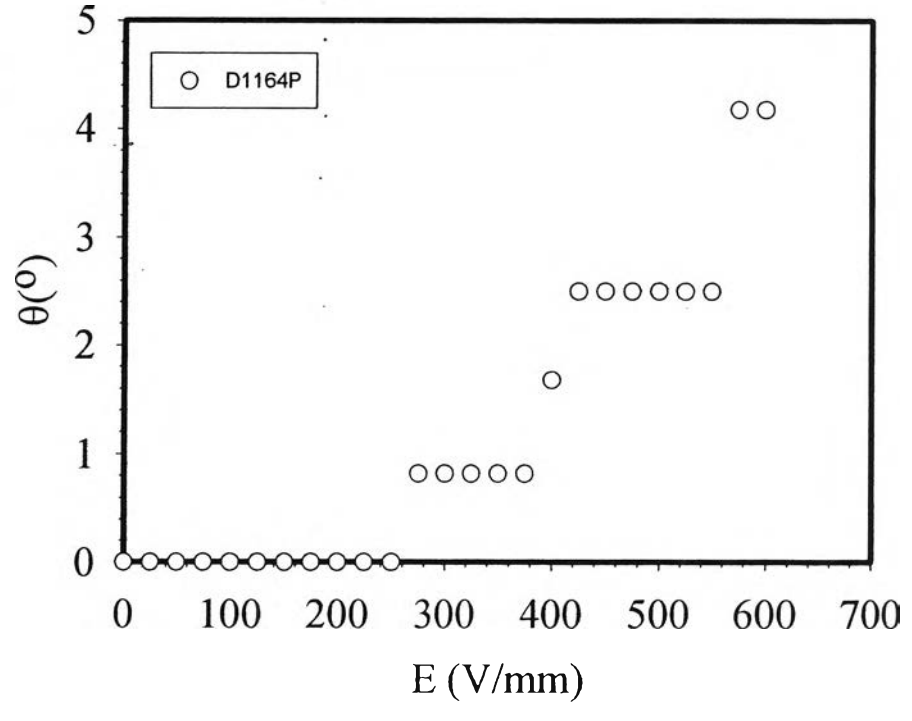
D1164P
θ(°)
5
4
3
2
1
0
0
100
200
300
400
500
600
700
E (V/mm)

(b)

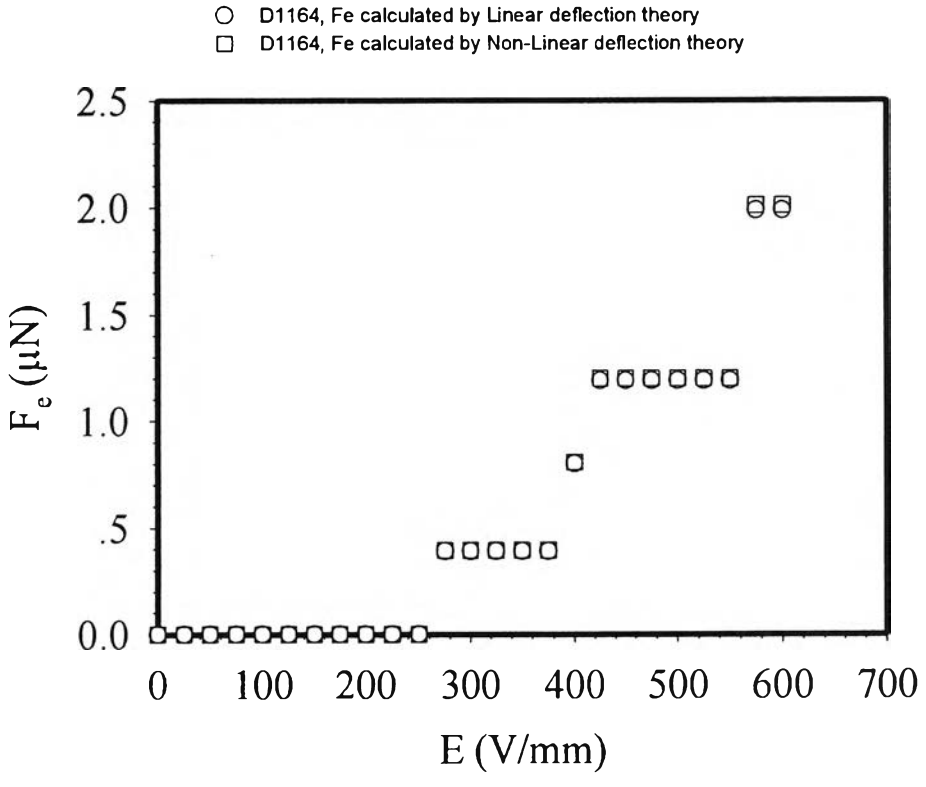
D1164, Fe calculated by Linear deflection theory
D1164, Fe calculated by Non-Linear deflection theory
2.5
2.0
1.5
1.0
.5
0.0
F_e (μN)
0
100
200
300
400
500
600
700
E (V/mm)

(c)

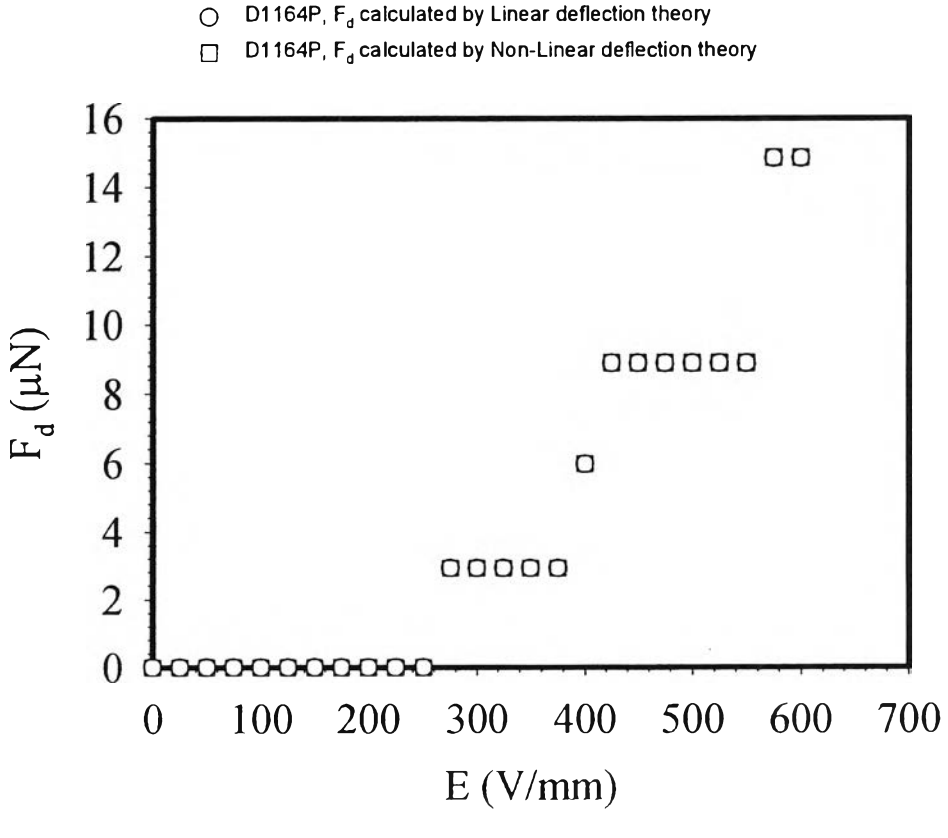
D1164P, F_d calculated by Linear deflection theory
D1164P, F_d calculated by Non-Linear deflection theory
16
14
12
10
8
6
4
2
0
F_d (μN)
0
100
200
300
400
500
600
700
E (V/mm)

(d)

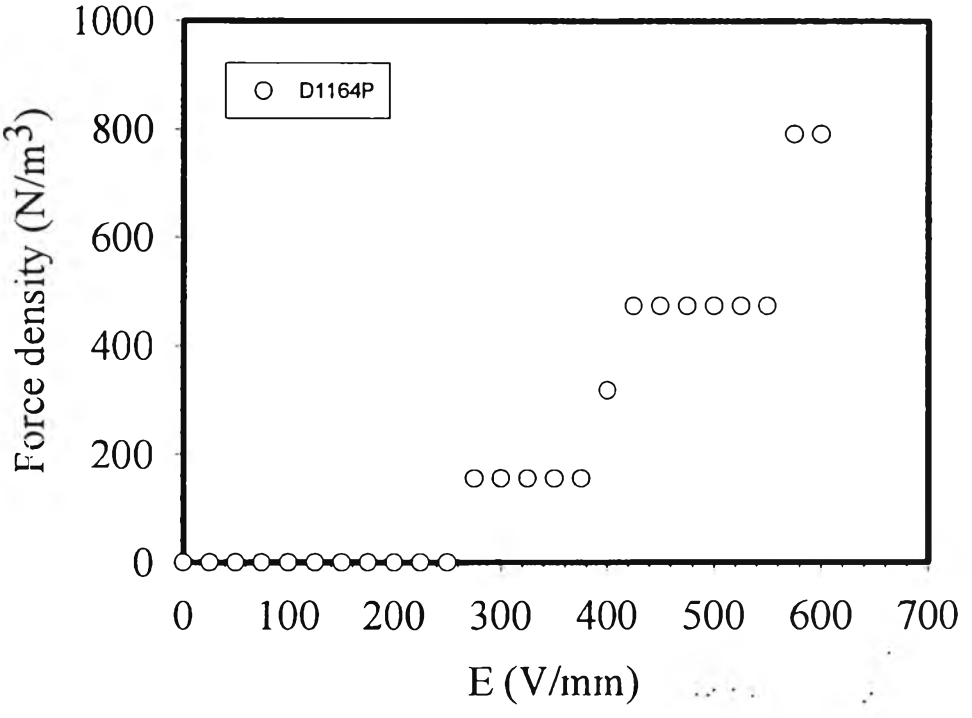
D1164P
Force density (N/m3)
1000
800
600
400
200
0
0
100
200
300
400
500
600
700
E (V/mm)

(e)

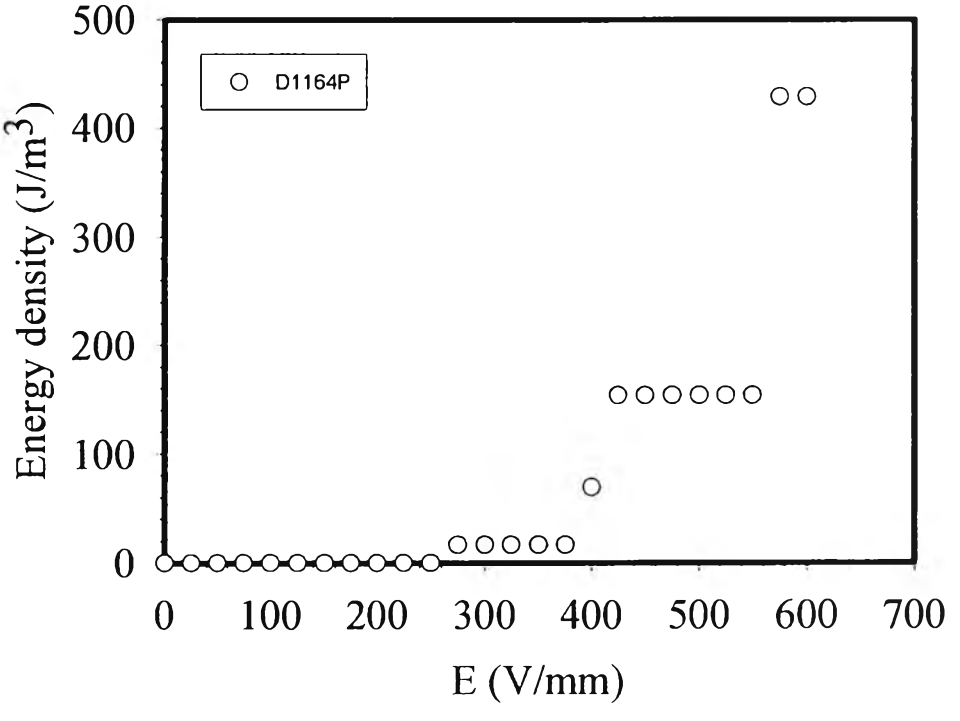
D1164P
Energy density (J/m3)
500
400
300
200
100
0
0
100
200
300
400
500
600
700
E (V/mm)

(f)

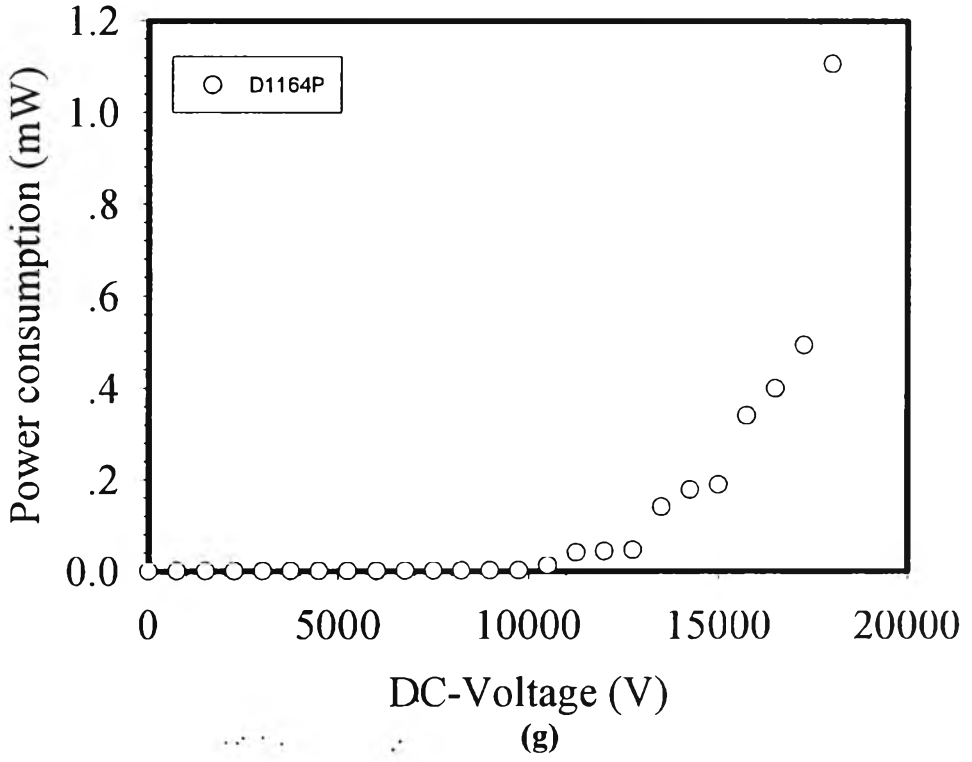

(g)

Figure K3 Electromechanical responses of pure SIS D1164P at various electric field strengths: (a) deflection lengths; (b) deflection angles; (c) elastic force (F_e); (d) dielectrophoretic forces (F_d); (e) force density; (f) energy density; (g) power consumption.

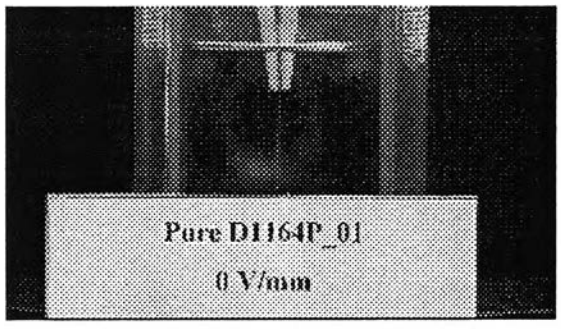
Pure D1164P_01
0 V/mm

(a)

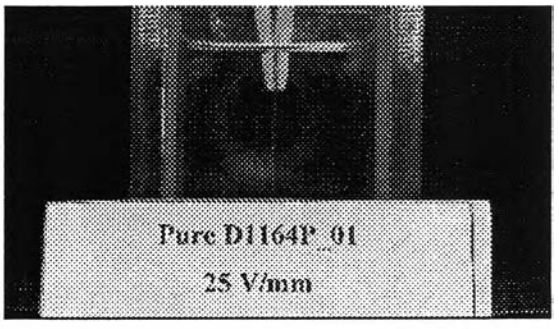
Pure D1164P_01
25 V/mm

(b)

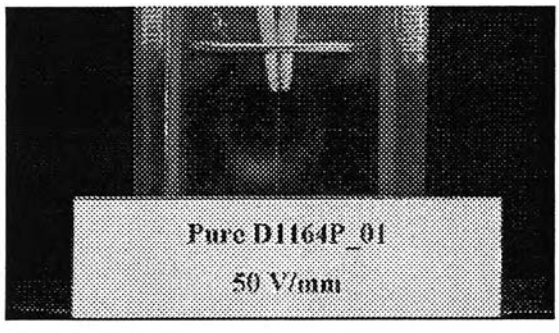
Pure D1164P_01
50 V/mm

(c)

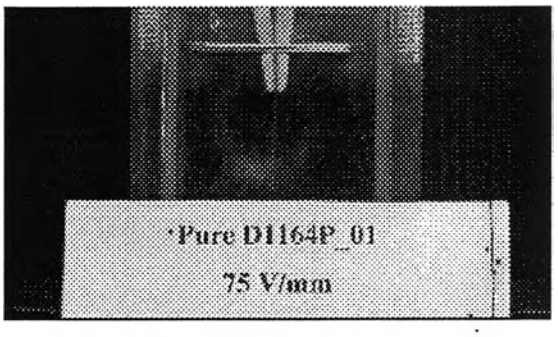
Pure D1164P_01
75 V/mm

(d)

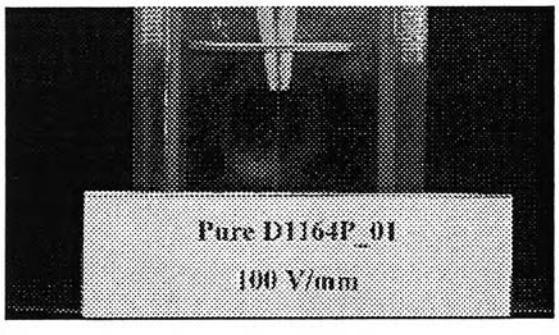
Pure D1164P_01
100 V/mm

(e)

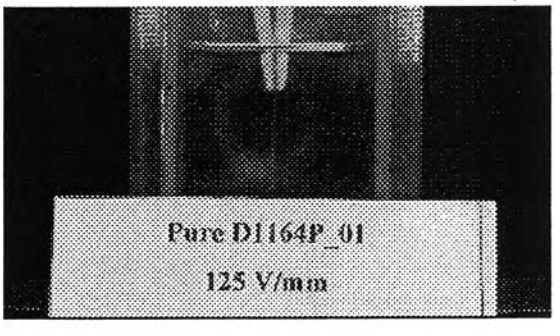
Pure D1164P_01
125 V/mm

(f)

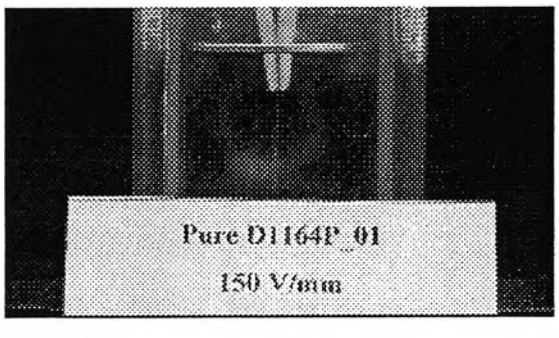
Pure D1164P_01
150 V/mm

(g)

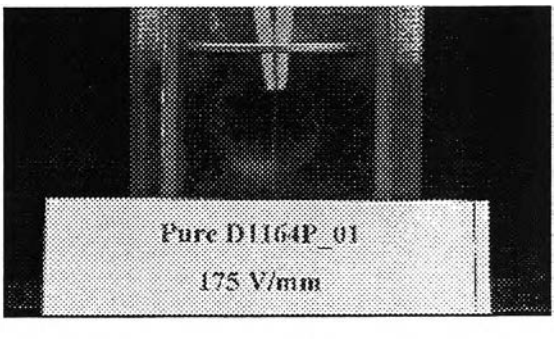
Pure D1164P_01
175 V/mm

(h)

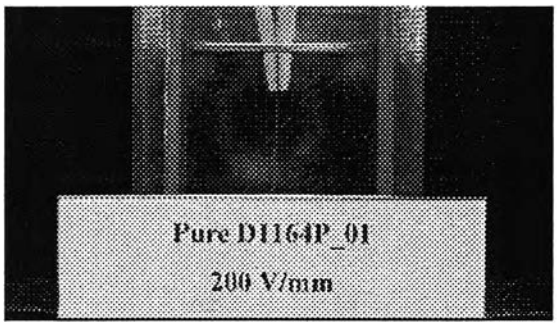
Pure D1164P_01
200 V/mm

(i)


Pure D1164P_01
225 V/mm

(j)

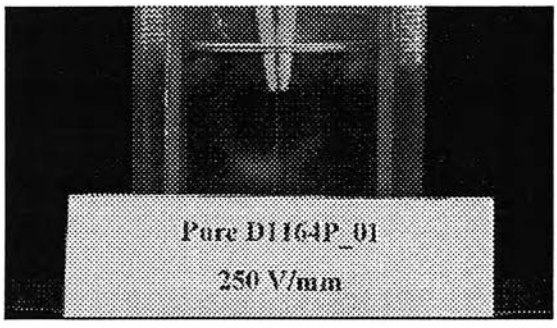
Pure D1164P_01
250 V/mm

(k)

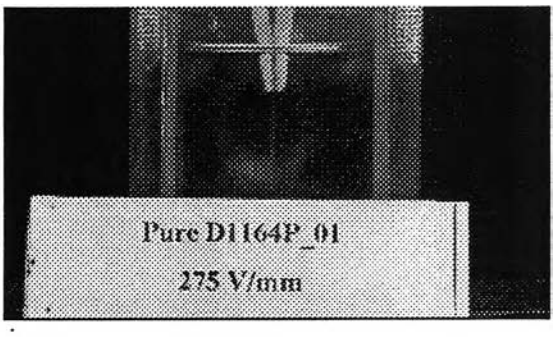
Pure D1164P_01
275 V/mm

(l)

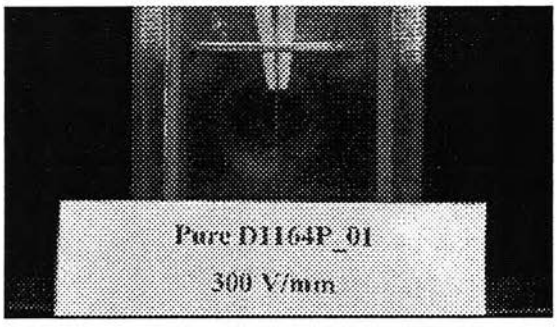
Pure D1164P_01
300 V/mm

(m)

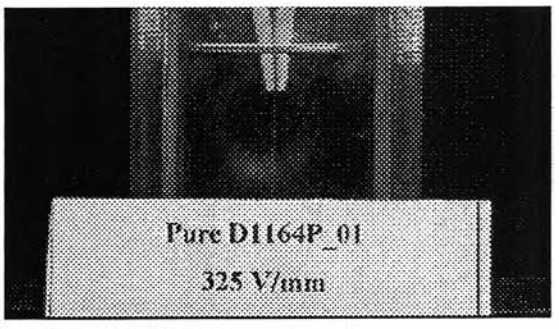
Pure D1164P_01
325 V/mm

(n)

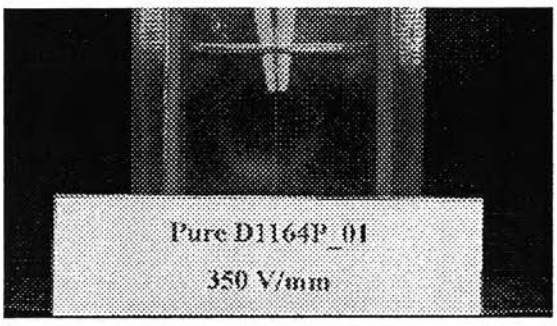
Pure D1164P_01
350 V/mm

(o)

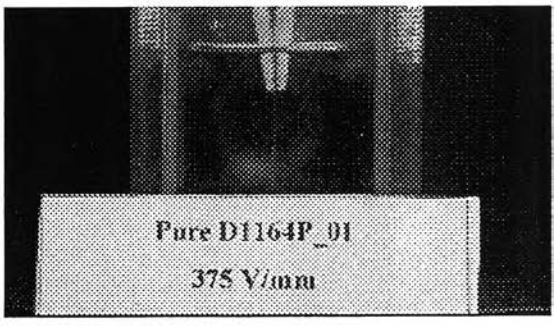
Pure D1164P_01
375 V/mm

(p)

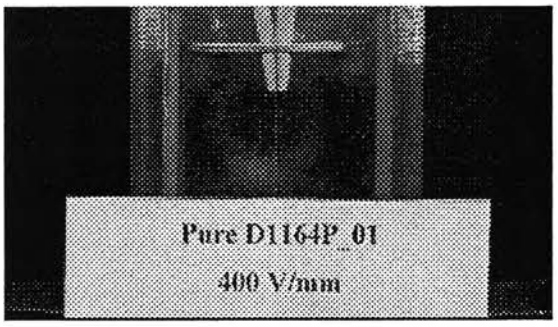
Pure D1164P_01
400 V/mm

(q)

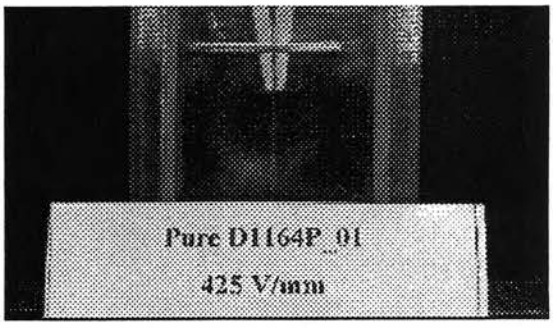
Pure D1164P_01
425 V/mm

(r)

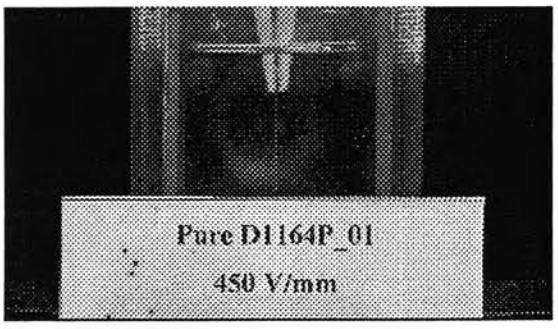
Pure D1164P_01
450 V/mm

(s)

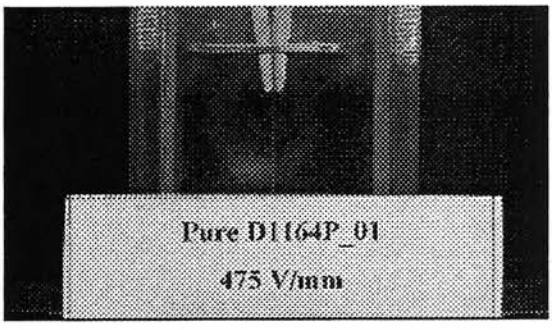
Pure D1164P_01
475 V/mm

(t)

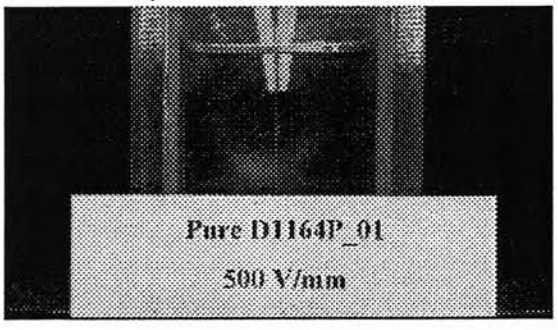
Pure D1164P_01
500 V/mm

(u)

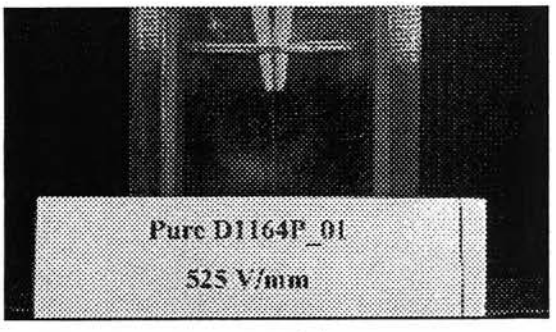
Pure D1164P_01
525 V/mm

(v)

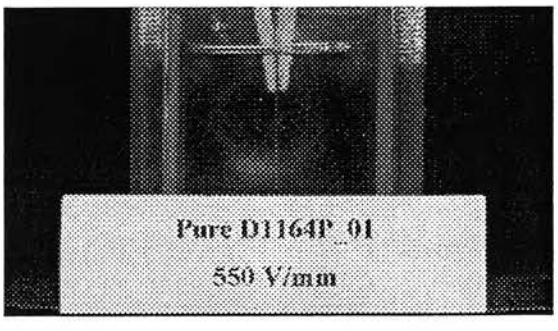
Pure D1164P_01
550 V/mm

(w)

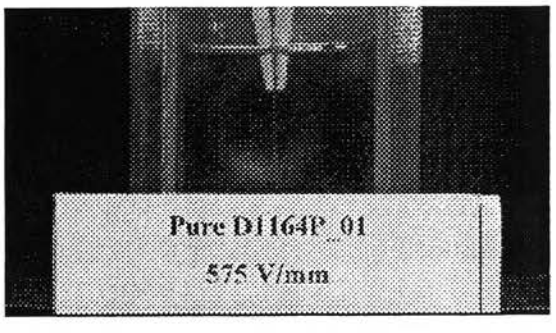
Pure D1164P_01
575 V/mm

(x)

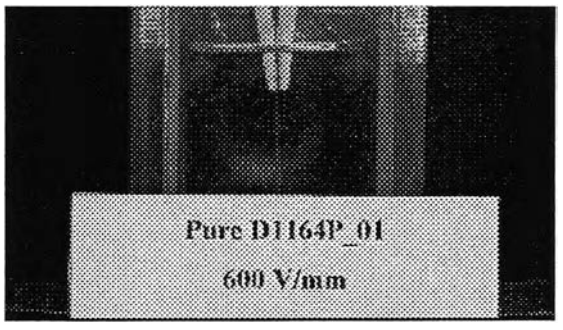

(y)

Figure K4 Electromechanical responses of pure SIS D1164P at various electric field strengths: (a) 0 V/mm; (b) 25 V/mm; (c) V = 50 V/mm; (d) 75 V/mm; (e) 100 V/mm; (f) 125 V/mm; (g) 150 V/mm; (h) 175 V/mm; (i) 200 V/mm; (j) 225 V/mm; (k) 250 V/mm; (l) 275 V/mm; (m) 300 V/mm; (n) 325 V/mm; (o) 350 V/mm; (p) 375 V/mm; (q) 400 V/mm; (r) 425 V/mm; (s) 450 V/mm; (t) 475 V/mm; (u) 500 V/mm; (v) 525 V/mm; (w) 550 V/mm; (x) 575 V/mm; (y) 600 V/mm.

Table K3 Electromechanical responses of pure SIS D1162P at various electric field strengths

E (V/mm)	d (mm)	l (mm)	θ (°)	sin(θ)	mg sin(θ) (N)	F_e from linear deflection (N)	F_d from linear deflection (N)	F_e from non linear deflection (N)	F_d from non linear deflection (N)	τ_i (sec)	τ_r (sec)	Energy density (J/m3)	Force density (N/m3)
0	0	15.53	0	0	0	0	0	0	0	0	0	0	0
25	0	15.53	0	0	0	0	0	0	0	0	0	0	0
50	0	15.53	0	0	0	0	0	0	0	0	0	0	0
75	0	15.53	0	0	0	0	0	0	0	0	0	0	0
100	0	15.53	0	0	0	0	0	0	0	0	0	0	0
125	0	15.53	0	0	0	0	0	0	0	0	0	0	0
150	0	15.53	0	0	0	0	0	0	0	0	0	0	0
175	0	15.53	0	0	0	0	0	0	0	0	0	0	0
200	0	15.53	0	0	0	0	0	0	0	0	0	0	0
225	0	15.53	0	0	0	0	0	0	0	0	0	0	0
250	0	15.53	0	0	0	0	0	0	0	0	0	0	0
275	0	15.53	0	0	0	0	0	0	0	0	0	0	0
300	0	15.53	0	0	0	0	0	0	0	0	0	0	0
325	0	15.53	0	0	0	0	0	0	0	0	0	0	0
350	0	15.53	0	0	0	0	0	0	0	0	0	0	0
375	0	15.53	0	0	0	0	0	0	0	0	0	0	0
400	0	15.53	0	0	0	0	0	0	0	0	0	0	0
425	0	15.53	0	0	0	0	0	0	0	0	0	0	0
450	0	15.53	0	0	0	0	0	0	0	0	0	0	0
475	0	15.53	0	0	0	0	0	0	0	0	0	0	0
500	0	15.53	0	0	0	0	0	0	0	0	0	0	0
525	0	15.53	0	0	0	0	0	0	0	0	0	0	0
550	0	15.53	0	0	0	0	0	0	0	0	0	0	0
575	0	15.53	0	0	0	0	0	0	0	0	0	0	0
600	0	15.53	0	0	0	0	0	0	0	0	0	0	0

D1162 P (44 %wt PS)

The weight of specimen (wt) = 0.0172 g

The length of specimen (l_0) = 15.53 mm

The initial length of specimen (L) = 22.50 mm

The thickness of specimen (t) = 0.340mm

The width of specimen (w) = 2.23 mm

G′ = 386262.4 Pa at E = 0 kV/mm, T = 300 K, strain = 0.02%, f = 1 rad/s.

d = deflection distance in x axis (mm), l= deflection distance in y axis (mm)

τ_i = induction time (sec), τ_r = recovery time (sec)

I = Moment of inertia (m^4) = $t^3w/12$

E = Modulus of elasticity (Pa)

F_e = elastic force (N) = $3dEI/l^3$ for linear deflection

F_e = elastic force (N) = dEI/l^3 for non linear deflection

F_d = dielectrophoretic force = F_e (N) + mgsinθ

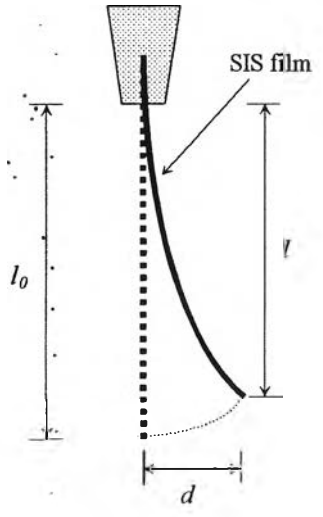

$$\text{Energy density} = \frac{1}{2}E\theta^2 \ (\text{J/m}^3)$$

$$\text{Force density} = \frac{F_d}{volume} \quad (\text{N/m}^3)$$

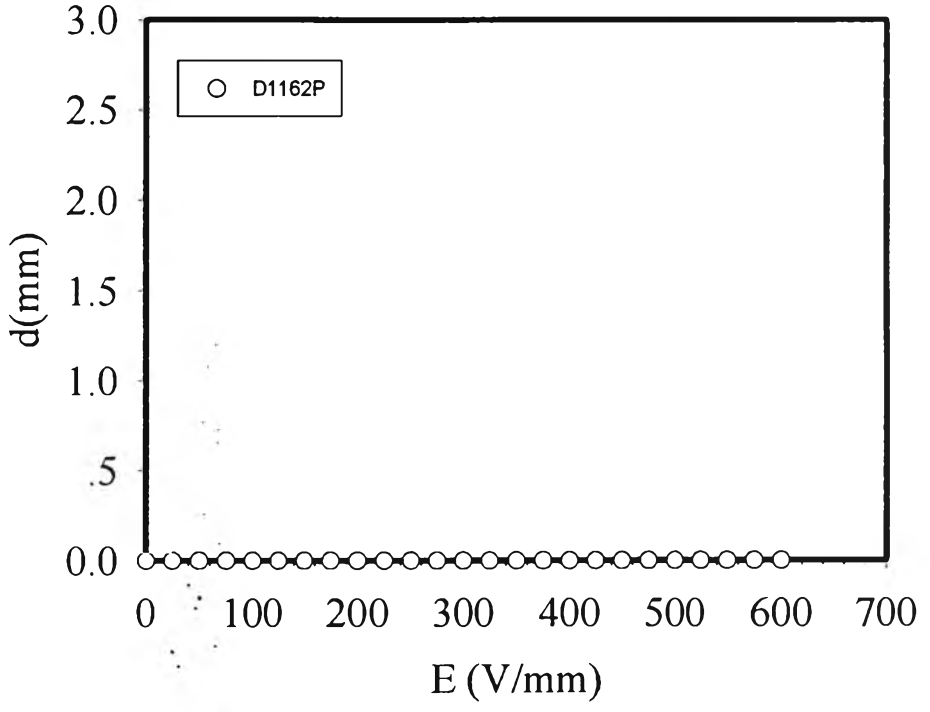
3.0
2.5
2.0
1.5
1.0
.5
0.0
d(mm)
D1162P
0
100
200
300
400
500
600
700
E (V/mm)

(a)

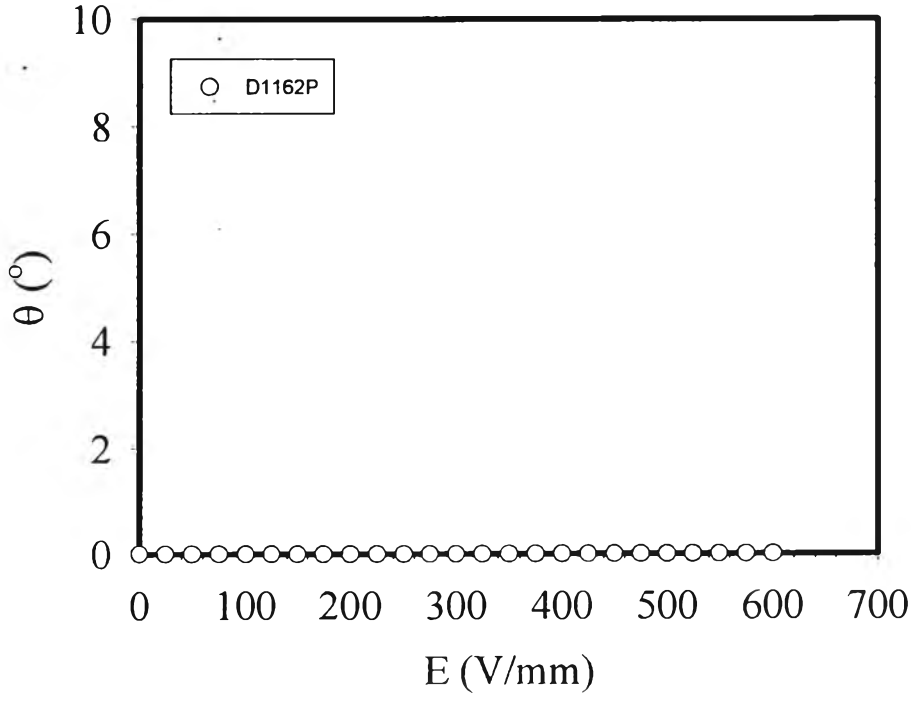
10
8
6
4
2
0
θ (°)
D1162P
0
100
200
300
400
500
600
700
E (V/mm)

(b)

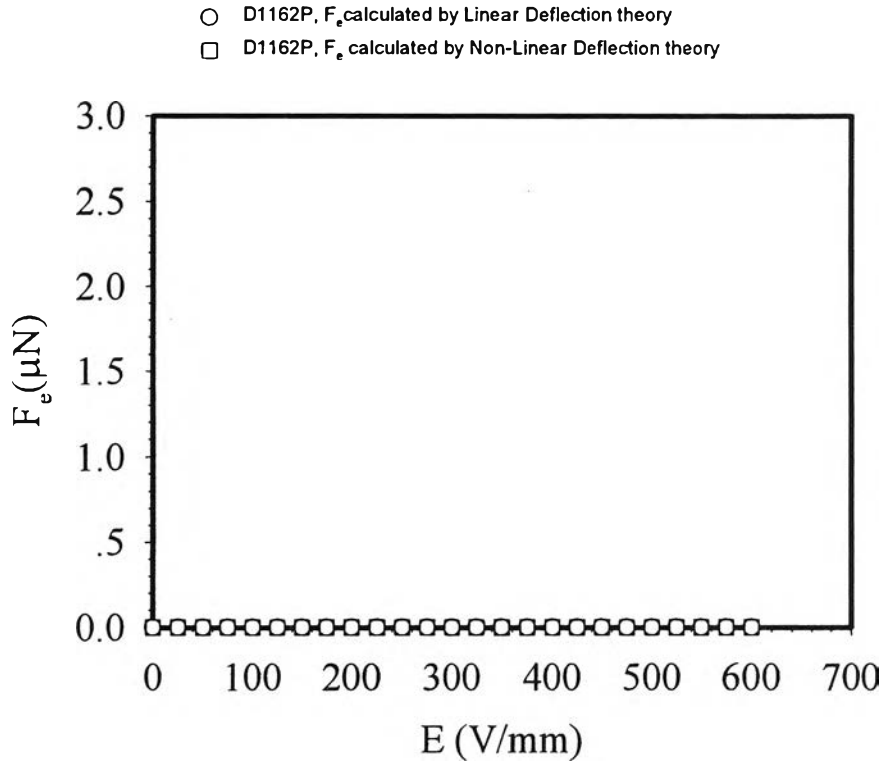
D1162P, $F_e$calculated by Linear Deflection theory
D1162P, F_e calculated by Non-Linear Deflection theory
3.0
2.5
2.0
1.5
1.0
.5
0.0
F_e(μN)
0
100
200
300
400
500
600
700
E (V/mm)

(c)

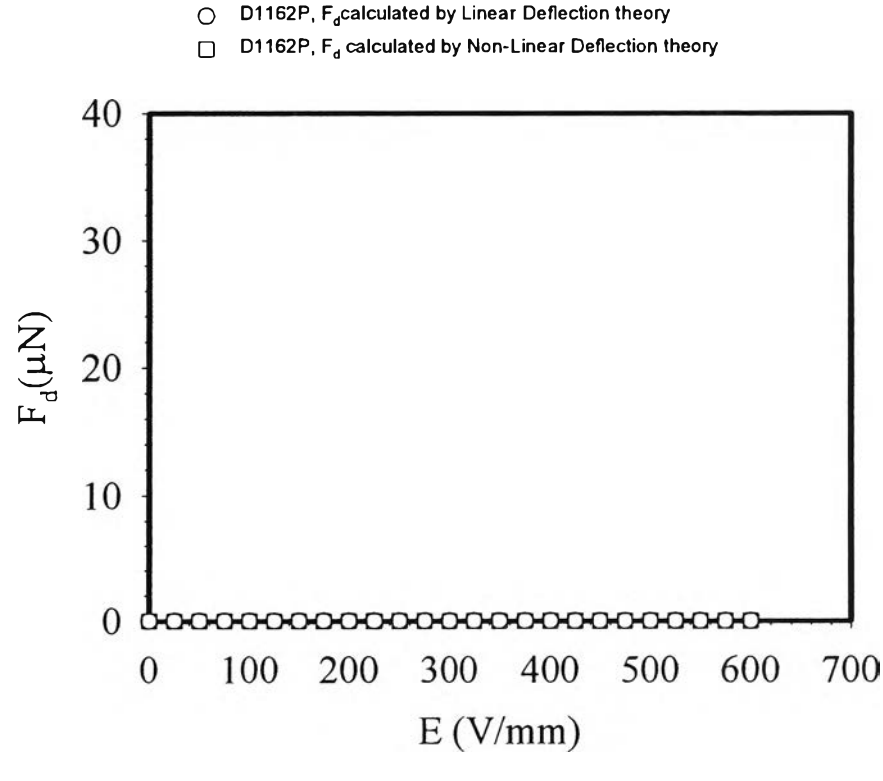
D1162P, $F_d$calculated by Linear Deflection theory
D1162P, F_d calculated by Non-Linear Deflection theory
40
30
20
10
0
F_d(μN)
0
100
200
300
400
500
600
700
E (V/mm)

(d)

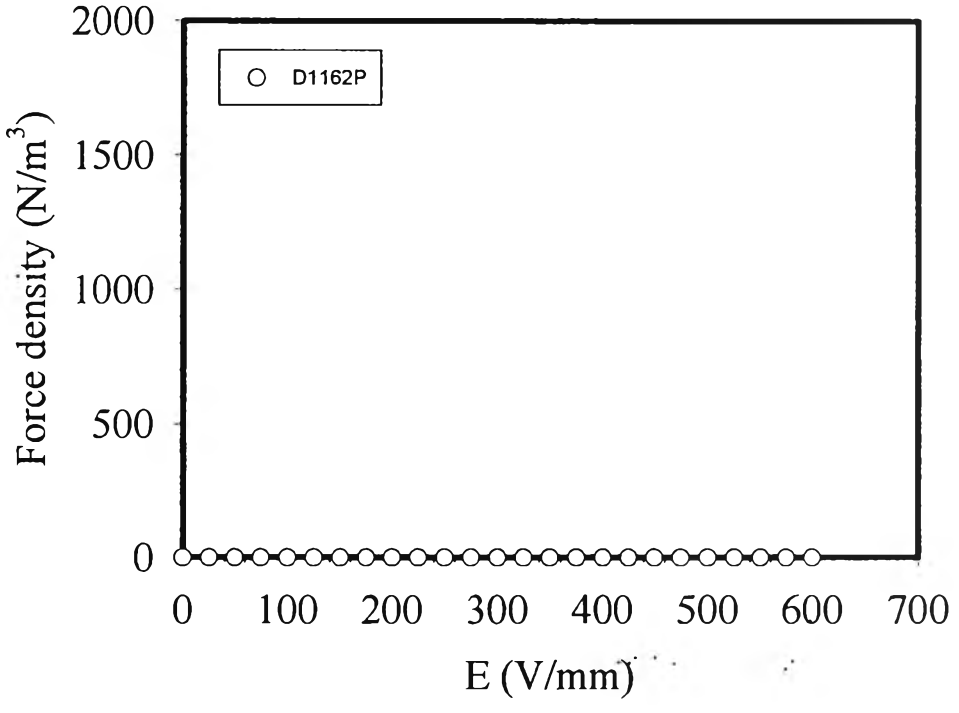
2000
1500
1000
500
0
Force density (N/m3)
D1162P
0
100
200
300
400
500
600
700
E (V/mm)

(e)

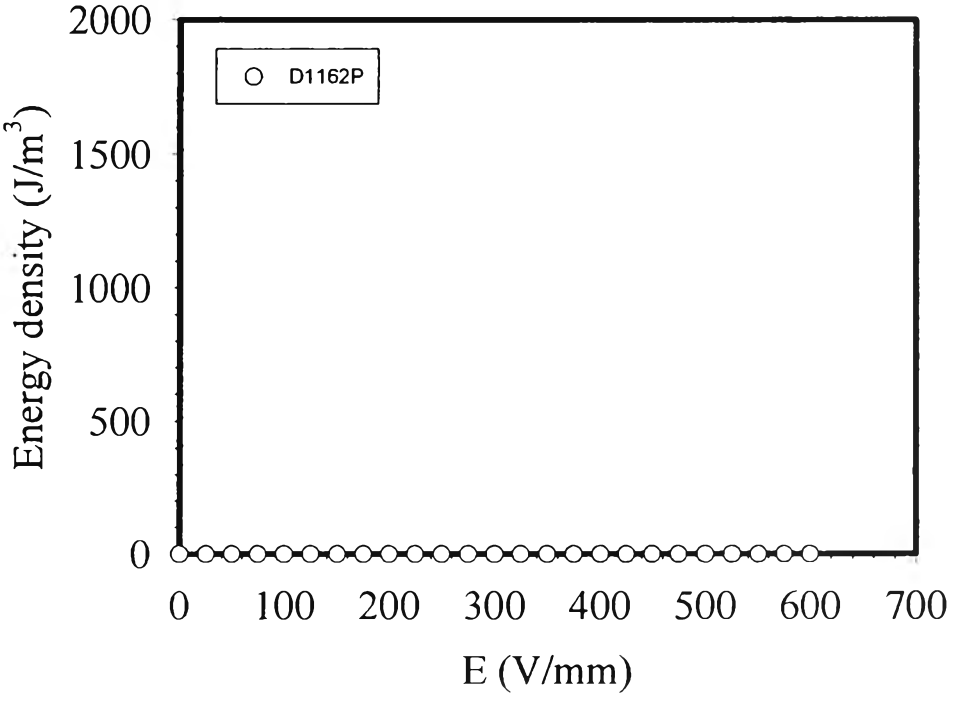
2000
1500
1000
500
0
Energy density (J/m3)
D1162P
0
100
200
300
400
500
600
700
E (V/mm)

(f)

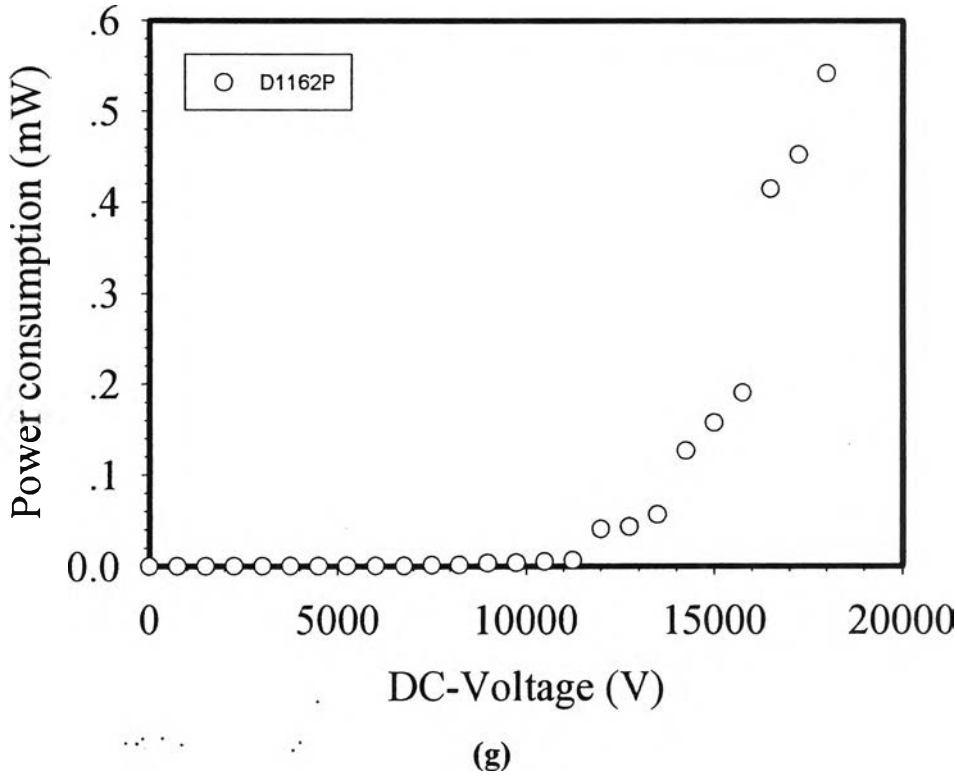

(g)

Figure K5 Electromechanical responses of pure SIS D1162P at various electric field strengths: (a) deflection lengths; (b) deflection angles; (c) elastic force (F_e); (d) dielectrophoretic forces (F_d); (e) force density; (f) energy density; (g) power consumption.

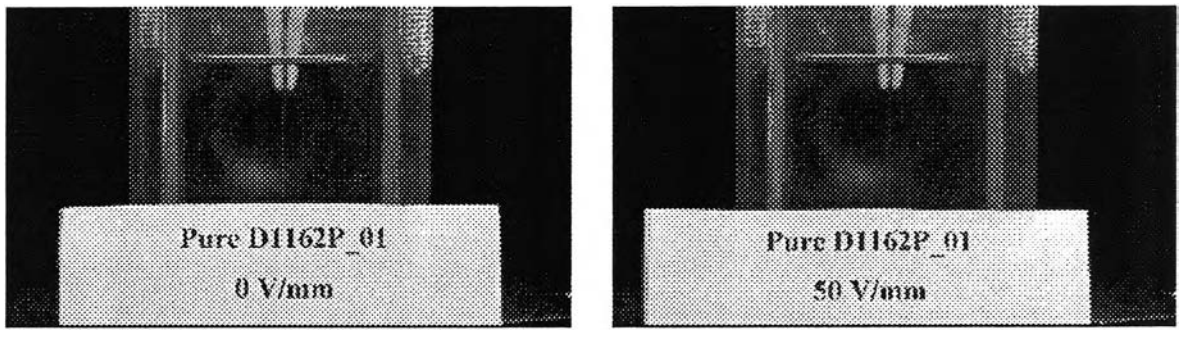

(a) **(b)**

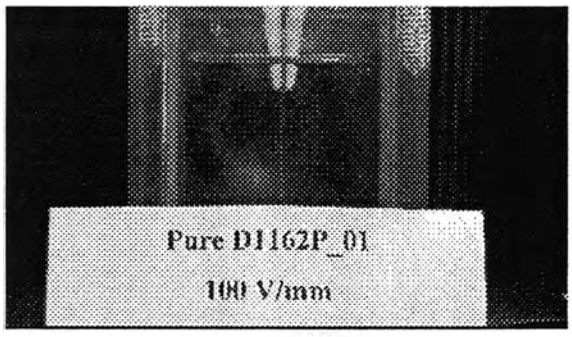
Pure D1162P_01
100 V/mm

(c)

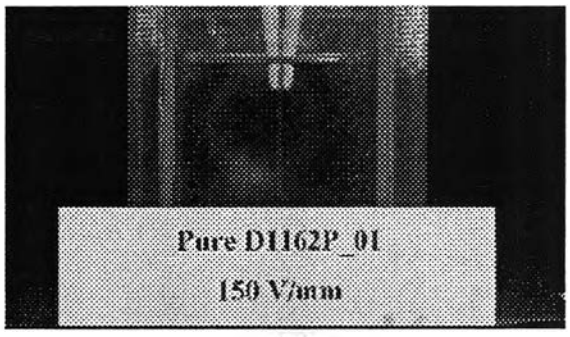
Pure D1162P_01
150 V/mm

(d)

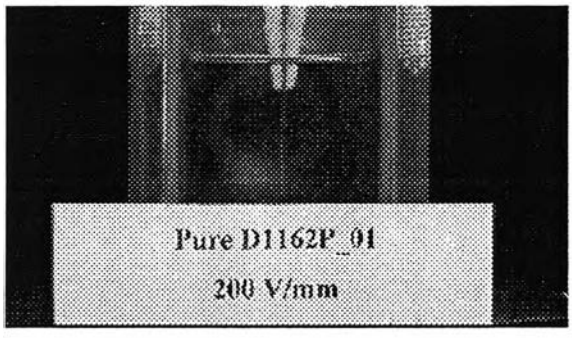
Pure D1162P_01
200 V/mm

(e)

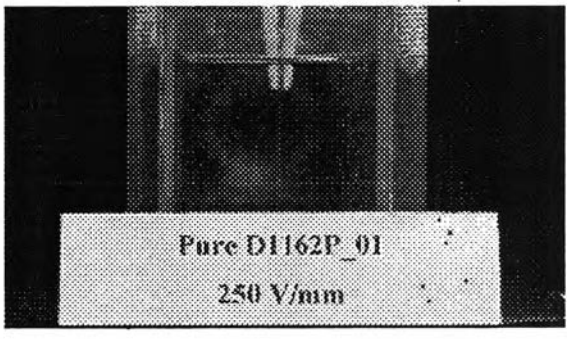
Pure D1162P_01
250 V/mm

(f)

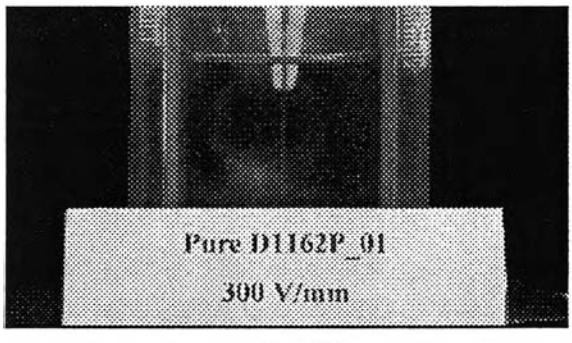
Pure D1162P_01
300 V/mm

(g)

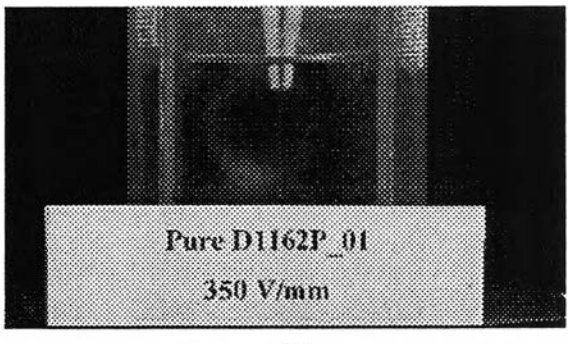
Pure D1162P_01
350 V/mm

(h)

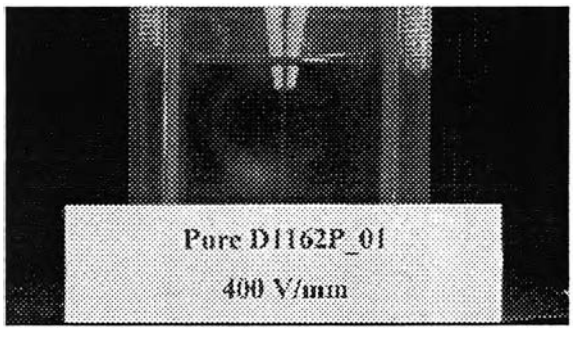
Pure D1162P_01
400 V/mm

(i)

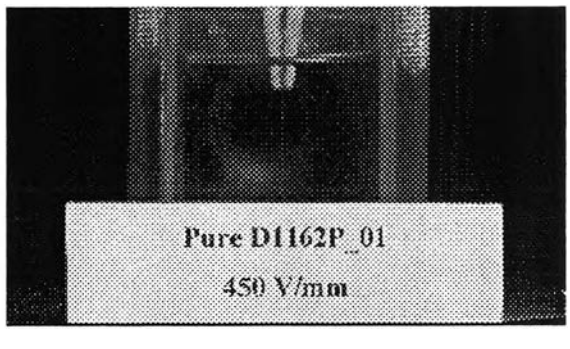
Pure D1162P_01
450 V/mm

(j)

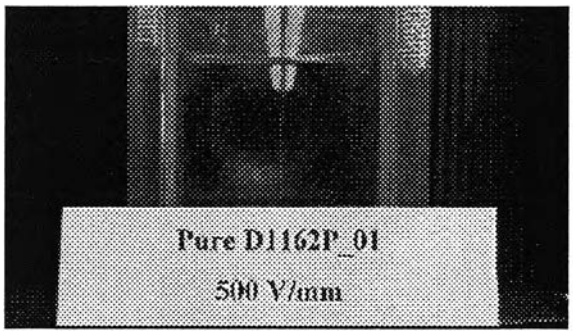

(k)

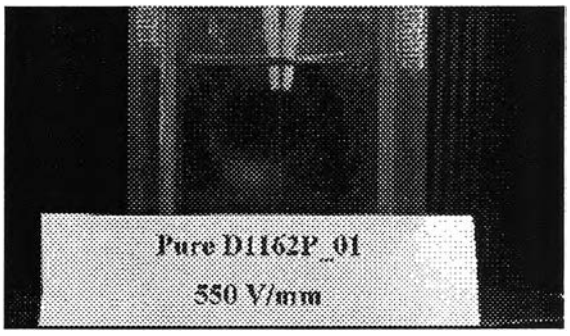

(l)

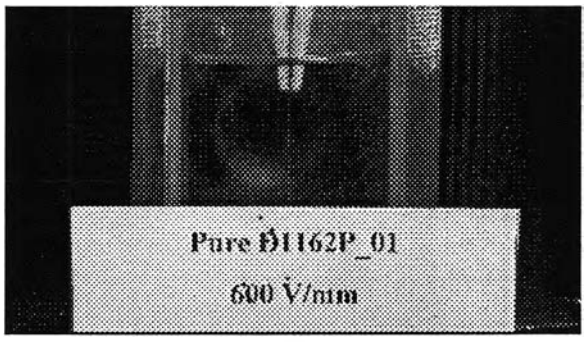

(m)

Figure K6 Electromechanical responses of pure SIS D1162P at various electric field strengths: (a) 0 V/mm; (b) V = 50 V/mm; (c) 100 V/mm; (d) 150 V/mm; (e) 200 V/mm; (f) 250 V/mm; (g) 300 V/mm; (h) 350 V/mm; (i) 400 V/mm; (j) 450 V/mm; (k) 500 V/mm; (l) 550 V/mm; (m) 600 V/mm.

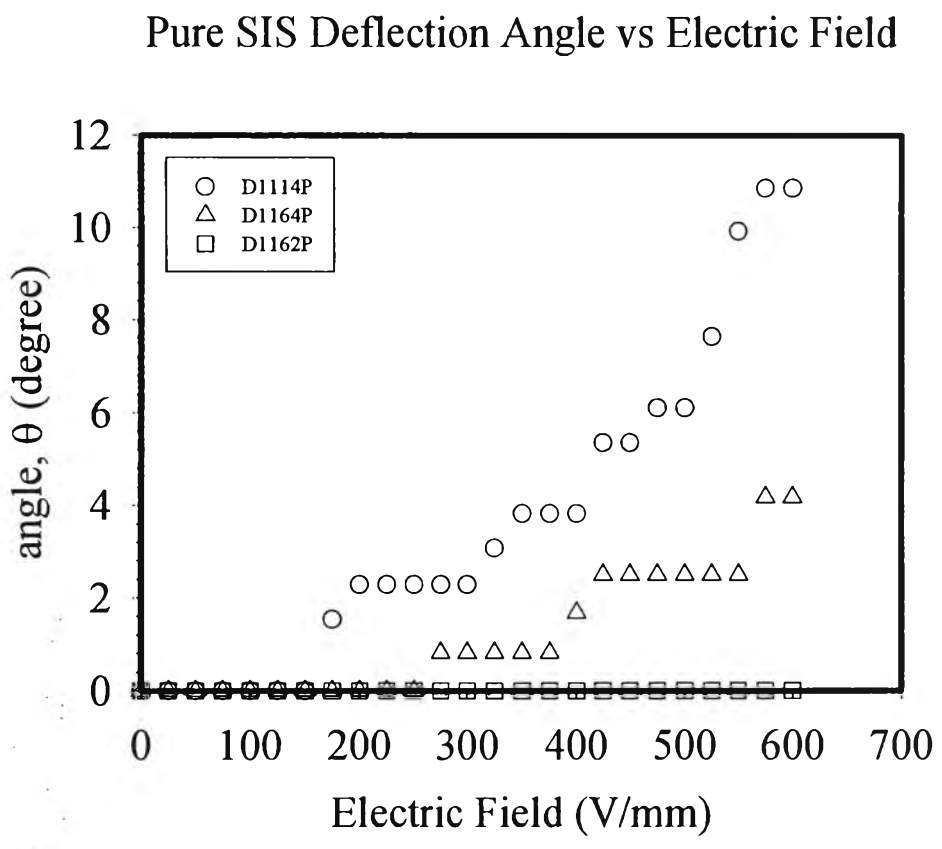

Figure K7 Deflection angle of pure SIS, D1114P, D1164, and D1162P at various electric field strengths calculated through Linear Deflection theory.

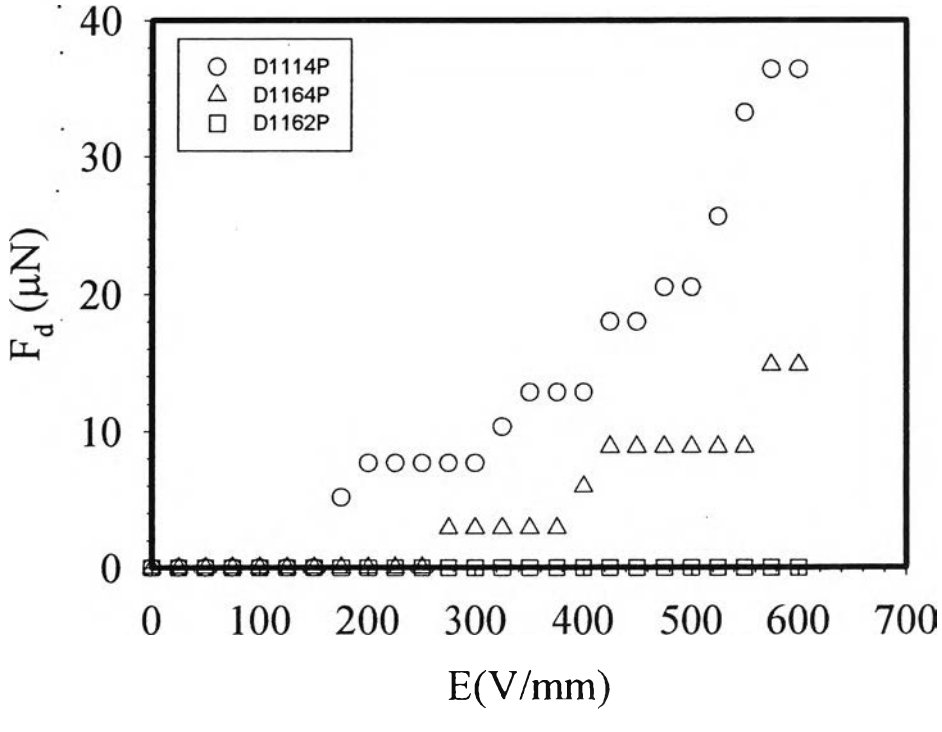

Figure K8 Dielectrophoretic force (F_d) of pure SIS, D1114P, D1164, and D1162P at various electric field strengths calculated through Linear Deflection theory.

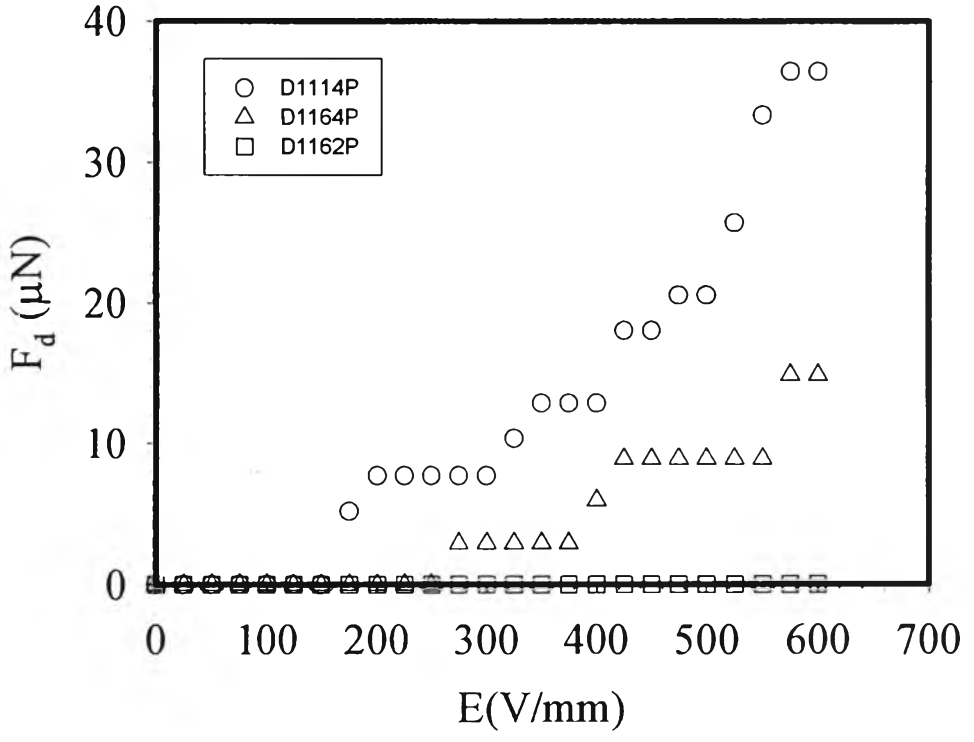

Figure K9 Dielectrophoretic force (F_d) of pure SIS, D1114P, D1164, and D1162P at various electric field strengths calculated through Non-Linear Deflection theory.

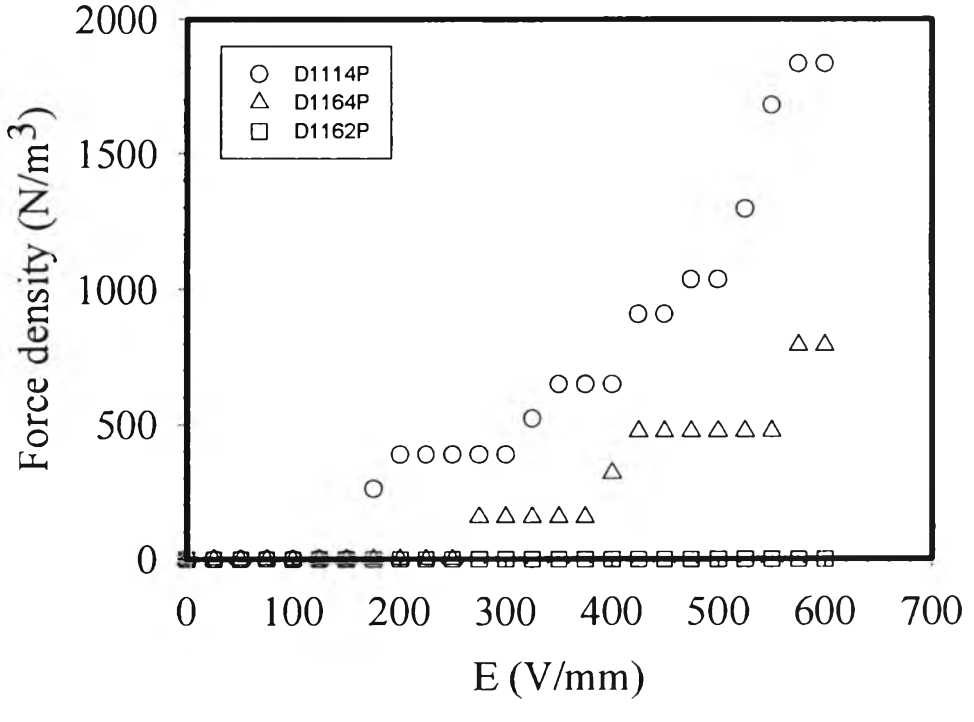

Figure K10 Force density of pure SIS, D1114P, D1164, and D1162P at various electric field strengths.

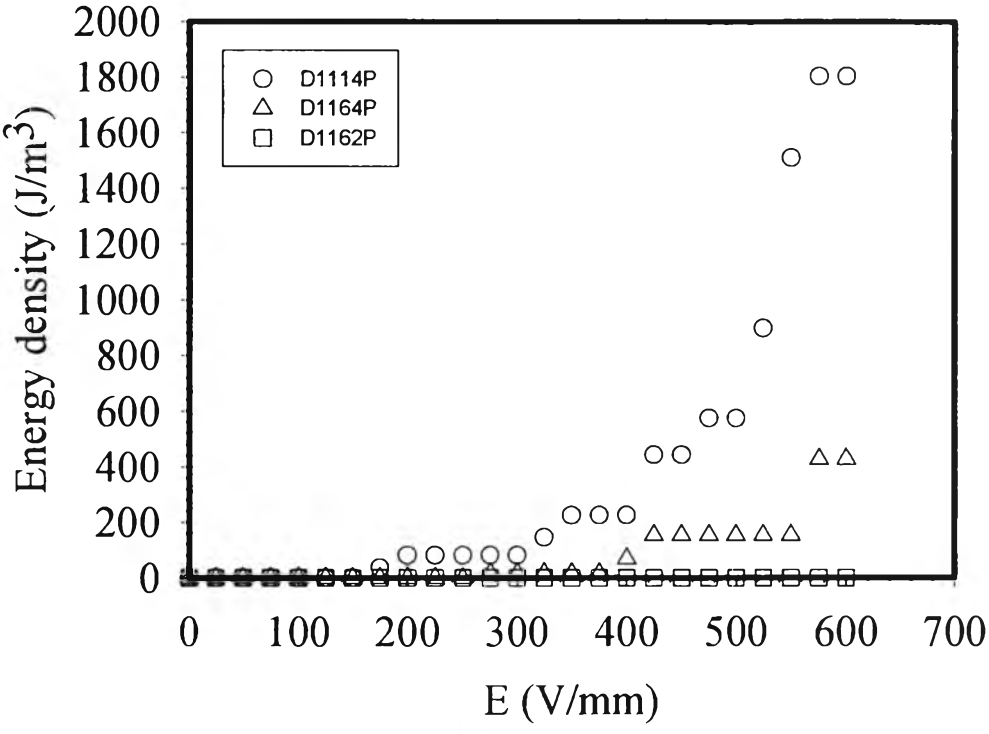

Figure K11 Energy density of pure SIS, D1114P, D1164, and D1162P at various electric field strengths.

Table K4 Electromechanical responses of 5 %DePDPA/D1114P at various electric field strengths

E (V/mm)	d (mm)	l (mm)	θ (°)	sin(θ)	mg sin(θ) (N)	F_e from linear deflection (N)	F_d from linear deflection (N)	F_e from non linear deflection (N)	F_d from non linear deflection (N)	τ_i (sec)	τ_r (sec)	Energy density (J/m3)	Force density (N/m3)
0	0	14.24	0	0	0	0	0	0	0	0	0	0	0
25	0	14.24	0	0	0	0	0	0	0	0	0	0	0
50	0	14.24	0	0	0	0	0	0	0	0	0	0	0
75	0	14.24	0	0	0	0	0	0	0	0	0	0	0
100	0	14.24	0	0	0	0	0	0	0	0	0	0	0
125	0	14.24	0	0	0	0	0	0	0	0	0	0	0
150	0.43	14.24	1.7	0.030	4.793E-06	3.880E-07	5.181E-06	3.919E-07	5.185E-06	40	20	46	329
175	0.43	14.24	1.7	0.030	4.793E-06	3.880E-07	5.181E-06	3.919E-07	5.185E-06	40	20	46	329
200	0.43	14.24	1.7	0.030	4.793E-06	3.880E-07	5.181E-06	3.919E-07	5.185E-06	40	20	46	329
225	0.43	14.24	1.7	0.030	4.793E-06	3.880E-07	5.181E-06	3.919E-07	5.185E-06	40	21	46	329
250	0.43	14.24	1.7	0.030	4.793E-06	3.880E-07	5.181E-06	3.919E-07	5.185E-06	40	22	46	329
275	0.65	14.24	2.6	0.046	7.244E-06	5.865E-07	7.831E-06	5.924E-07	7.837E-06	40	22	104.5	498
300	0.65	14.24	2.6	0.046	7.244E-06	5.865E-07	7.831E-06	5.924E-07	7.837E-06	40	22	104.5	498
325	0.65	14.24	2.6	0.046	7.244E-06	5.865E-07	7.831E-06	5.924E-07	7.837E-06	40	22	104.5	498
350	0.86	14.24	3.5	0.060	9.582E-06	7.759E-07	1.036E-05	7.838E-07	1.037E-05	40	22	182.9	659
375	0.86	14.24	3.5	0.060	9.582E-06	7.759E-07	1.036E-05	7.838E-07	1.037E-05	36	24	182.9	659
400	1.08	14.24	4.3	0.076	1.203E-05	9.744E-07	1.300E-05	9.862E-07	1.302E-05	52	30	288.2	827
425	1.51	14.24	6.1	0.106	1.680E-05	1.362E-06	1.817E-05	1.384E-06	1.819E-05	59	30	562.4	1155
450	1.94	14.24	7.8	0.136	2.156E-05	1.750E-06	2.331E-05	1.787E-06	2.335E-05	61	29	926.0	1483
475	1.94	14.24	7.8	0.136	2.156E-05	1.750E-06	2.331E-05	1.787E-06	2.335E-05	55	35	926.0	1483
500	2.16	14.24	8.7	0.151	2.399E-05	1.949E-06	2.594E-05	2.003E-06	2.599E-05	60	30	1146.2	1651
525	2.37	14.24	9.5	0.166	2.630E-05	2.138E-06	2.844E-05	2.211E-06	2.851E-05	60	30	1377.8	1811
550	2.87	14.24	11.5	0.202	3.178E-05	2.589E-06	3.437E-05	2.720E-06	3.450E-05	60	30	2011.8	2192
575	2.87	14.24	11.5	0.202	3.178E-05	2.589E-06	3.437E-05	2.720E-06	3.450E-05	70	30	2011.8	2192
600	2.87	14.24	11.5	0.202	3.178E-05	2.589E-06	3.437E-05	2.720E-06	3.450E-05	100	30	2011.8	2192

5 %DePDPA/D1114P

The weight of specimen (wt) = 0.0162 g

The length of specimen (l_0) = 14.24 mm

The initial length of specimen (L) = 21.10 mm

The thickness of specimen (t) = 0.373 mm

The width of specimen (w) = 2.00 mm

G′ = 33468.04 Pa at E = 0 kV/mm, T = 300 K, strain = 0.2 %, f = 1 rad/s.

d = deflection distance in x axis (mm), l = deflection distance in y axis (mm)

τ_i = induction time (sec), τ_r = recovery time (sec)

I = Moment of inertia (m^4) = $t^3w/12$

E = Modulus of elasticity (Pa)

F_e = elastic force (N) = $3dEI/l^3$ for linear deflection

F_e = elastic force (N) = dEI/l^3 for non linear deflection

F_d = dielectrophoretic force = F_e (N) + mgsinθ

Energy density = $\frac{1}{2}E\theta^2$ (J/m^3)

Force density = $\frac{F_d}{volume}$ (N/m^3)

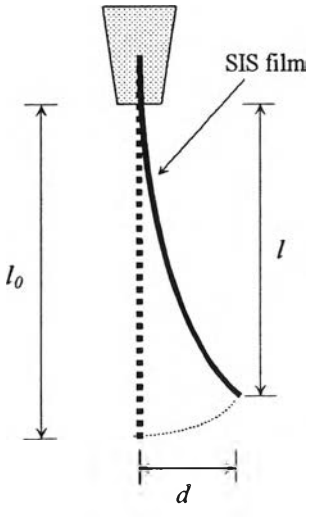

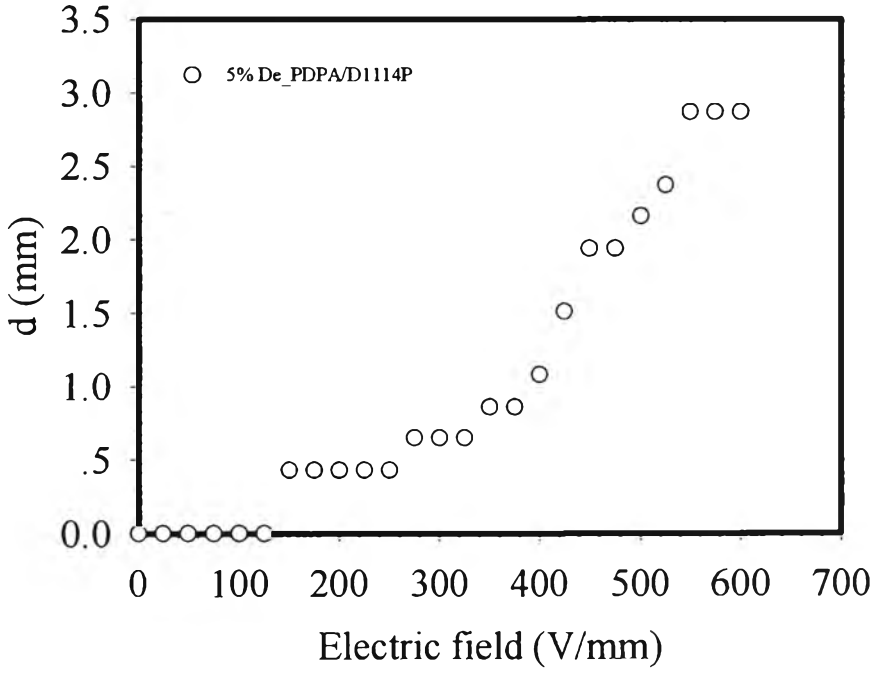
5% De_PDPA/D1114P
d (mm)
3.5
3.0
2.5
2.0
1.5
1.0
.5
0.0
0
100
200
300
400
500
600
700
Electric field (V/mm)

(a)

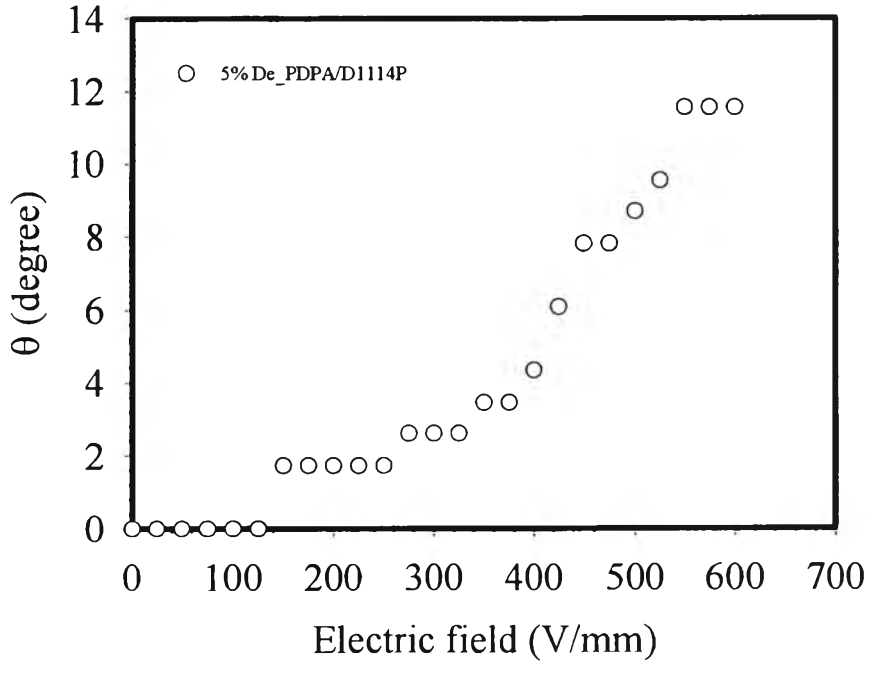
5% De_PDPA/D1114P
θ (degree)
14
12
10
8
6
4
2
0
0
100
200
300
400
500
600
700
Electric field (V/mm)

(b)

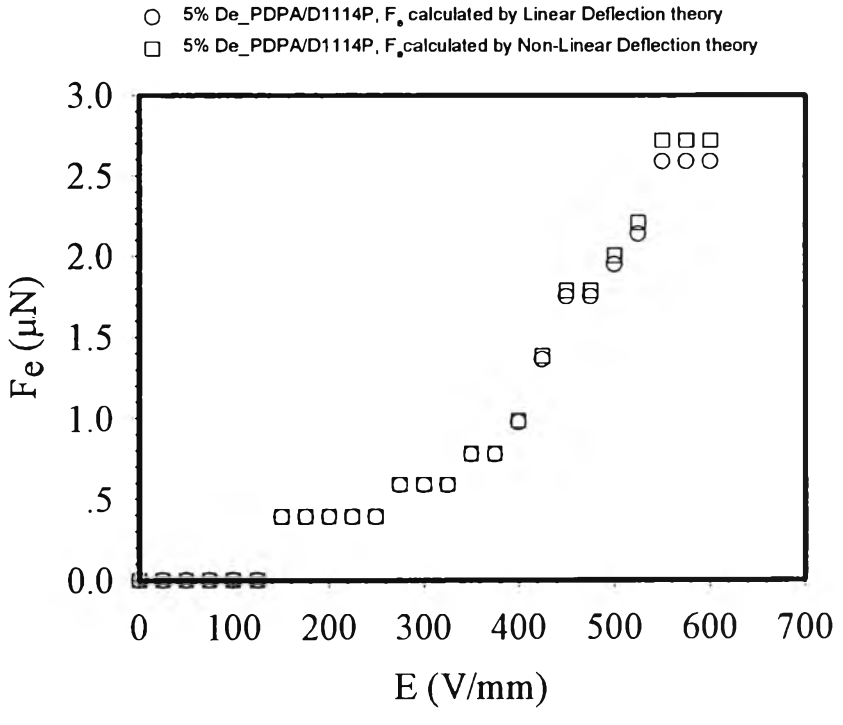
5% De_PDPA/D1114P, F_e calculated by Linear Deflection theory
5% De_PDPA/D1114P, $F_e$calculated by Non-Linear Deflection theory
F_e (μN)
3.0
2.5
2.0
1.5
1.0
.5
0.0
0
100
200
300
400
500
600
700
E (V/mm)

(c)

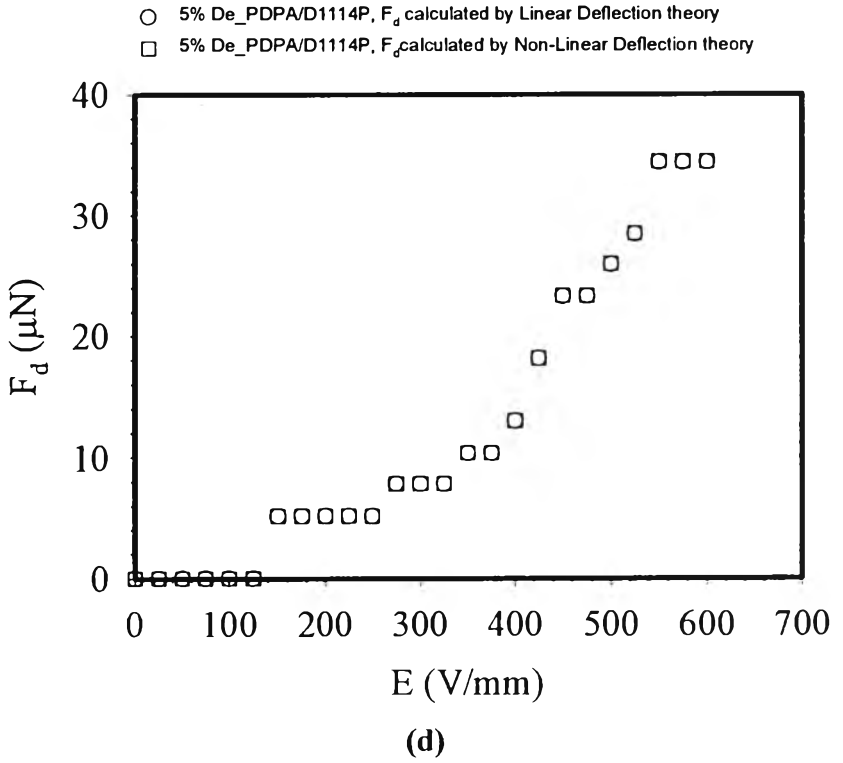
5% De_PDPA/D1114P, F_d calculated by Linear Deflection theory
5% De_PDPA/D1114P, $F_d$calculated by Non-Linear Deflection theory
F_d (μN)
40
30
20
10
0
0
100
200
300
400
500
600
700
E (V/mm)

(d)

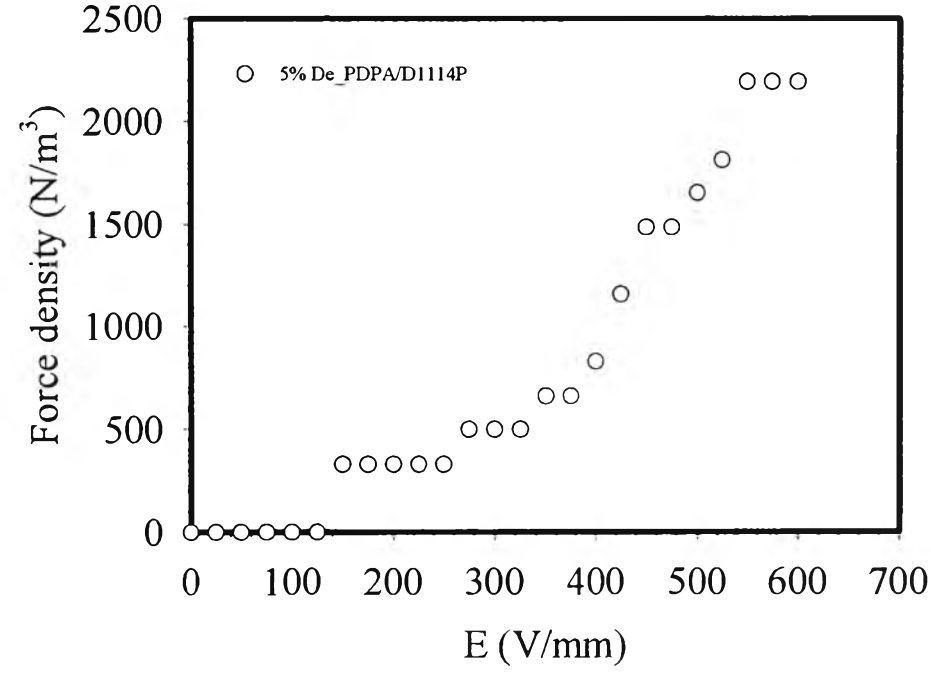

(e)

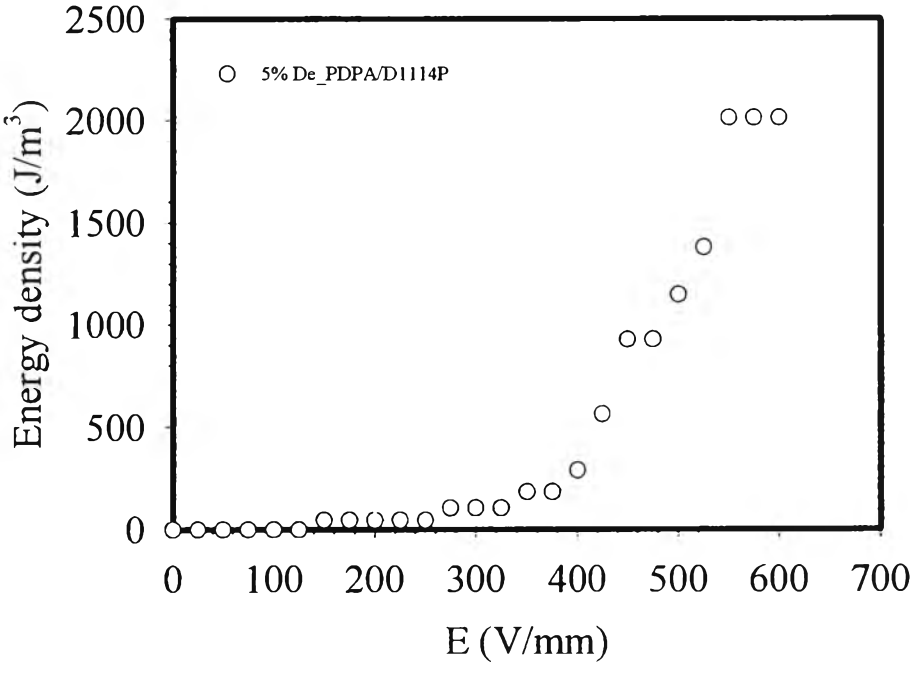

(f)

Figure K12 Electromechanical responses of 5% DePDPA/D1114P at various electric field strengths: (a) deflection lengths; (b) deflection angles; (c) elastic force (F_e); (d) dielectrophoretic forces (F_d); (e) force density; (f) energy density.

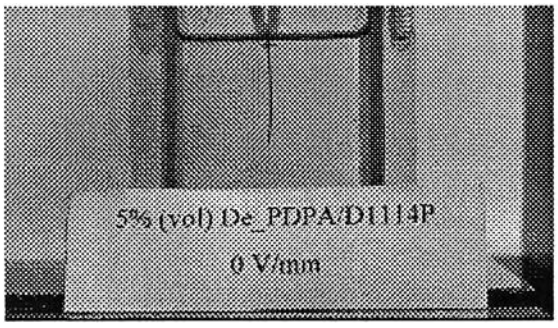
5% (vol) De_PDPA/D1114P
0 V/mm

(a)

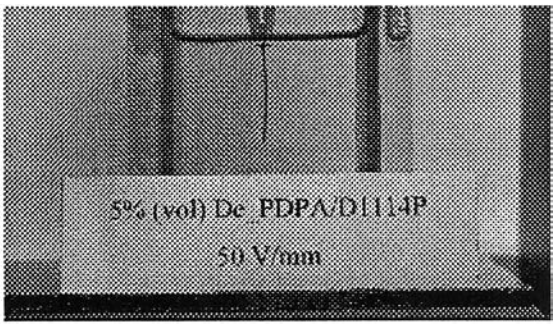
5% (vol) De_PDPA/D1114P
50 V/mm

(b)

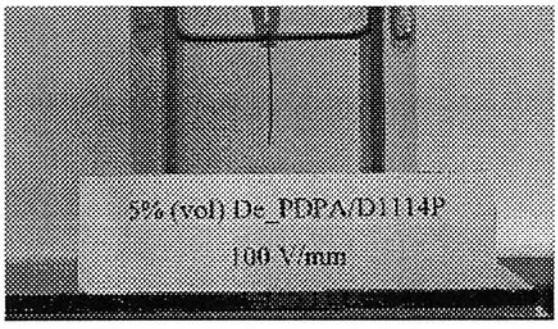
5% (vol) De_PDPA/D1114P
100 V/mm

(c)

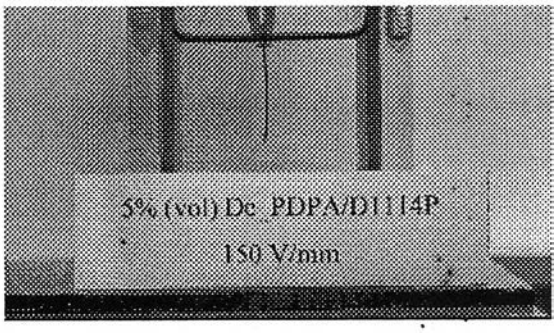
5% (vol) De_PDPA/D1114P
150 V/mm

(d)

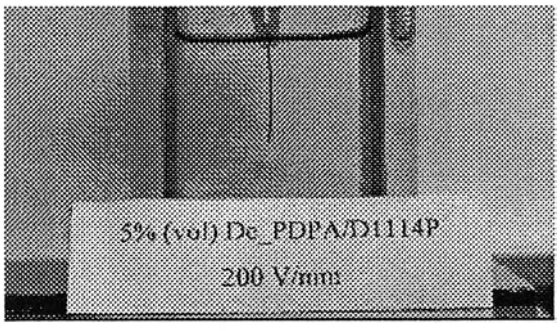
5% (vol) De_PDPA/D1114P
200 V/mm

(e)

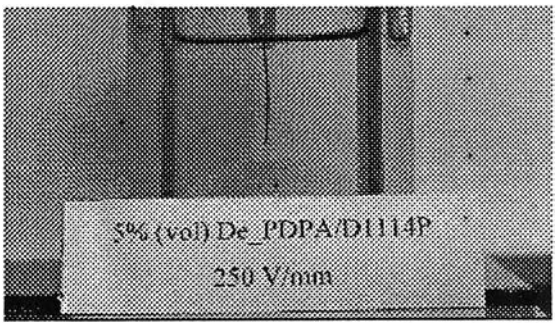
5% (vol) De_PDPA/D1114P
250 V/mm

(f)

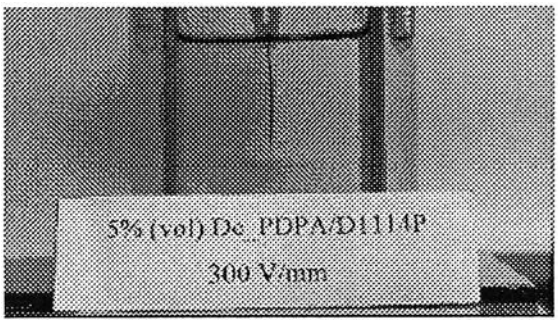
5% (vol) De_PDPA/D1114P
300 V/mm

(g)

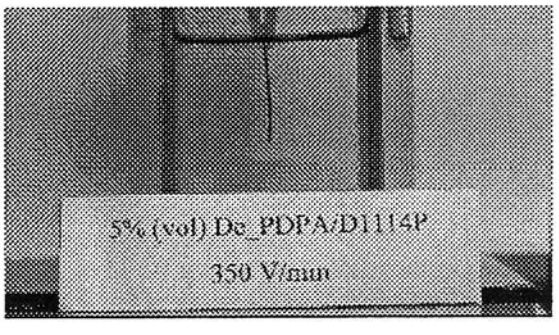
5% (vol) De_PDPA/D1114P
350 V/mm

(h)

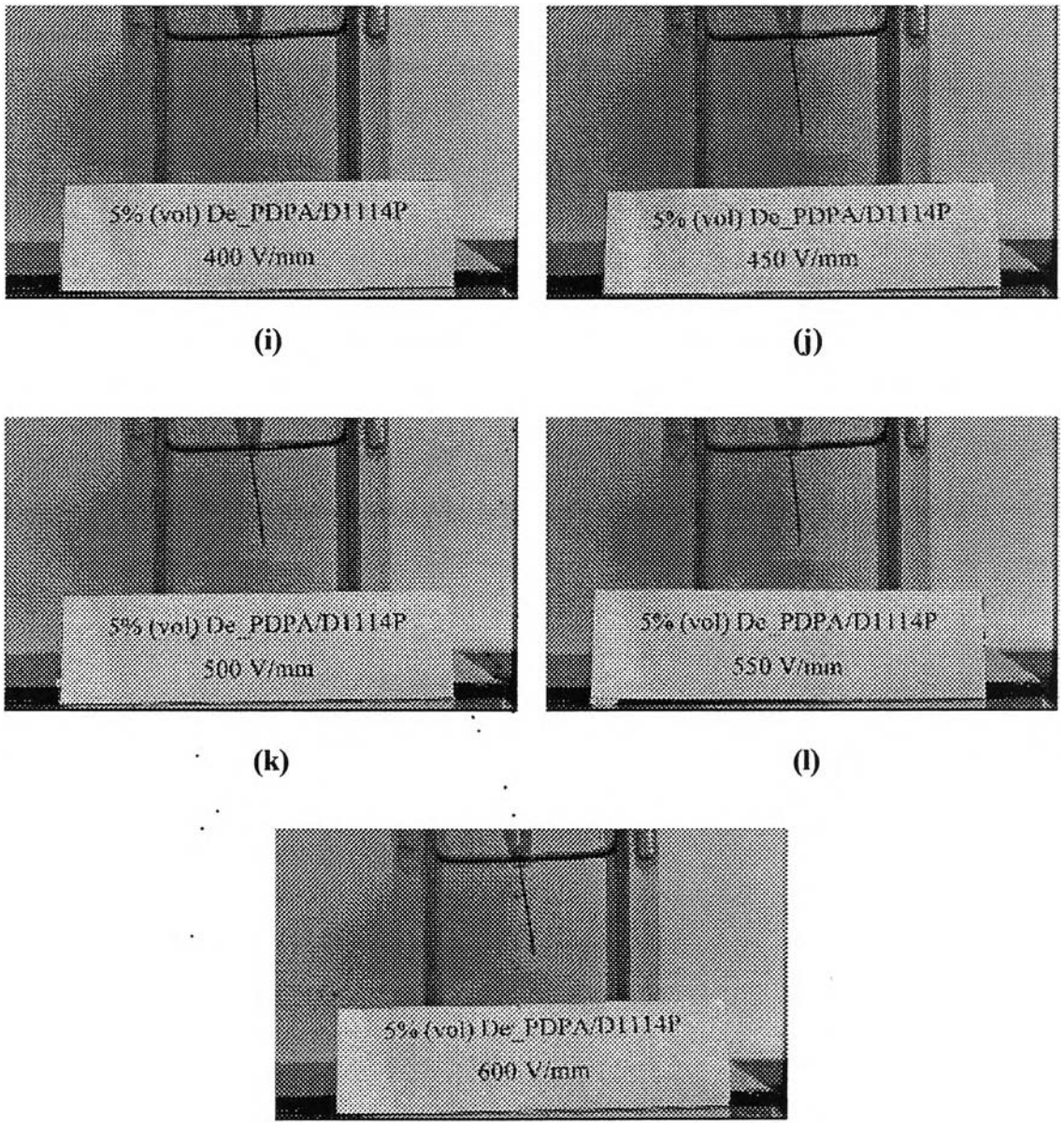

Figure K13 Electromechanical responses of 5 %DePDPA/D1114P at various electric field strengths: (a) 0 V/mm; (b) 50 V/mm; (c) V = 100 V/mm; (d) 150 V/mm; (e) 200 V/mm; (f) 250 V/mm; (g) 300 V/mm; (h) 350 V/mm; (i) 400 V/mm; (j) 450 V/mm; (k) 500 V/mm; (l) 550 V/mm; (m) 600 V/mm.

Table K5 Electromechanical responses of 10 % DePDPA/D1114P at various electric field strengths

E (V/mm)	d (mm)	l (mm)	θ (°)	sin(θ)	mg sin(θ) (N)	F_e from linear deflection (N)	F_d from linear deflection (N)	F_e from non linear deflection (N)	F_d from non linear deflection (N)	τ_i (sec)	τ_r (sec)	Energy density (J/m3)	Force density (N/m3)
0	0	13.81	0	0	0	0	0	0	0	0	0	0	0
25	0	13.81	0	0	0	0	0	0	0	0	0	0	0
50	0	13.81	0	0	0	0	0	0	0	0	0	0	0
75	0	13.81	0	0	0	0	0	0	0	0	0	0	0
100	0	13.81	0	0	0	0	0	0	0	0	0	0	0
125	0	13.81	0	0	0	0	0	0	0	0	0	0	0
150	0	13.81	0	0	0	0	0	0	0	0	0	0	0
175	0	13.81	0	0	0	0	0	0	0	0	0	0	0
200	0.43	13.81	1.8	0.0311	4.027E-06	2.568E-07	4.284E-06	2.594E-07	4.287E-06	30	12	52	308
225	0.43	13.81	1.8	0.0311	4.027E-06	2.568E-07	4.284E-06	2.594E-07	4.287E-06	30	12	52	308
250	0.43	13.81	1.8	0.0311	4.027E-06	2.568E-07	4.284E-06	2.594E-07	4.287E-06	30	14	52	308
275	0.65	13.81	2.7	0.0470	6.086E-06	3.881E-07	6.475E-06	3.921E-07	6.478E-06	30	15	117.9	466
300	0.86	13.81	3.6	0.0622	8.051E-06	5.135E-07	8.564E-06	5.187E-07	8.569E-06	29	18	206.3	616
325	1.51	13.81	6.3	0.1091	1.412E-05	9.017E-07	1.502E-05	9.163E-07	1.503E-05	43	19	634.3	1081
350	1.51	13.81	6.3	0.1091	1.412E-05	9.017E-07	1.502E-05	9.163E-07	1.503E-05	46	20	634.3	1081
375	1.51	13.81	6.3	0.1091	1.412E-05	9.017E-07	1.502E-05	9.163E-07	1.503E-05	48	20	634.3	1081
400	1.73	13.81	7.2	0.1249	1.616E-05	1.033E-06	1.720E-05	1.051E-06	1.721E-05	33	24	831.6	1238
425	2.16	13.81	9.0	0.1558	2.015E-05	1.290E-06	2.144E-05	1.328E-06	2.148E-05	32	25	1292.6	1544
450	2.59	13.6	10.9	0.1893	2.449E-05	1.619E-06	2.611E-05	1.609E-06	2.610E-05	50	25	1908.7	1876
475	2.59	13.6	10.9	0.1893	2.449E-05	1.619E-06	2.611E-05	1.609E-06	2.610E-05	70	26	1908.7	1876
500	3.24	13.6	13.6	0.2360	3.053E-05	2.026E-06	3.255E-05	2.060E-06	3.259E-05	80	30	2966.6	2343
525	4.53	13.17	19.7	0.3372	4.362E-05	3.119E-06	4.674E-05	3.077E-06	4.670E-05	80	30	6057.8	3357
550	4.53	13.17	19.7	0.3372	4.362E-05	3.119E-06	4.674E-05	3.077E-06	4.670E-05	90	30	6057.8	3357
575	4.53	13.17	19.7	0.3372	4.362E-05	3.119E-06	4.674E-05	3.077E-06	4.670E-05	100	30	6057.8	3357
600	4.53	13.17	19.7	0.3372	4.362E-05	3.119E-06	4.674E-05	3.077E-06	4.670E-05	100	30	6057.8	3357

10 %DePDPA/D1114P

The weight of specimen (wt) = 0.0132 g

The length of specimen (l_0) = 13.81 mm

The initial length of specimen (L) = 20.50 mm

The thickness of specimen (t) = 0.295 mm

The width of specimen (w) = 2.30 mm

G' = 35513.33 Pa at E = 0 kV/mm, T = 300 K, strain = 0.3 %, f = 1 rad/s.

d = deflection distance in x axis (mm), l= deflection distance in y axis (mm)

τ_i = induction time (sec), τ_r = recovery time (sec)

I = Moment of inertia (m^4) = $t^3w/12$

E = Modulus of elasticity (Pa)

F_e = elastic force (N) = $3dEI/l^3$ for linear deflection

F_e = elastic force (N) = dEI/l^3 for non linear deflection

F_d = dielectrophoretic force = F_e (N) + mgsinθ

Energy density = $\frac{1}{2}E\theta^2$ (J/m^3)

Force density = $\frac{F_d}{volume}$ (N/m^3)

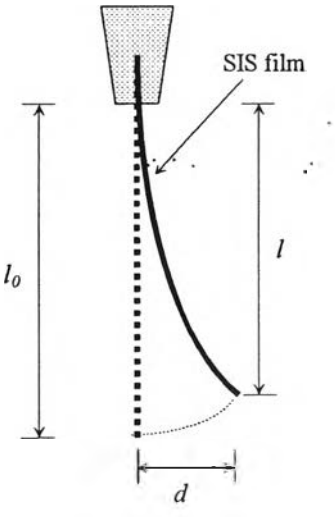

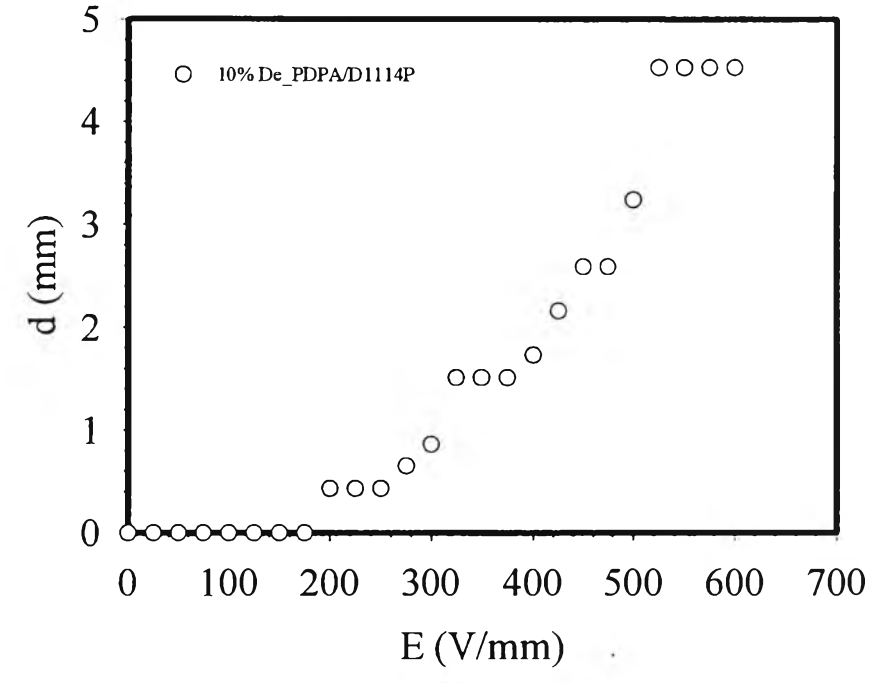
10% De_PDPA/D1114P
d (mm)
E (V/mm)
0
1
2
3
4
5
0
100
200
300
400
500
600
700

(a)

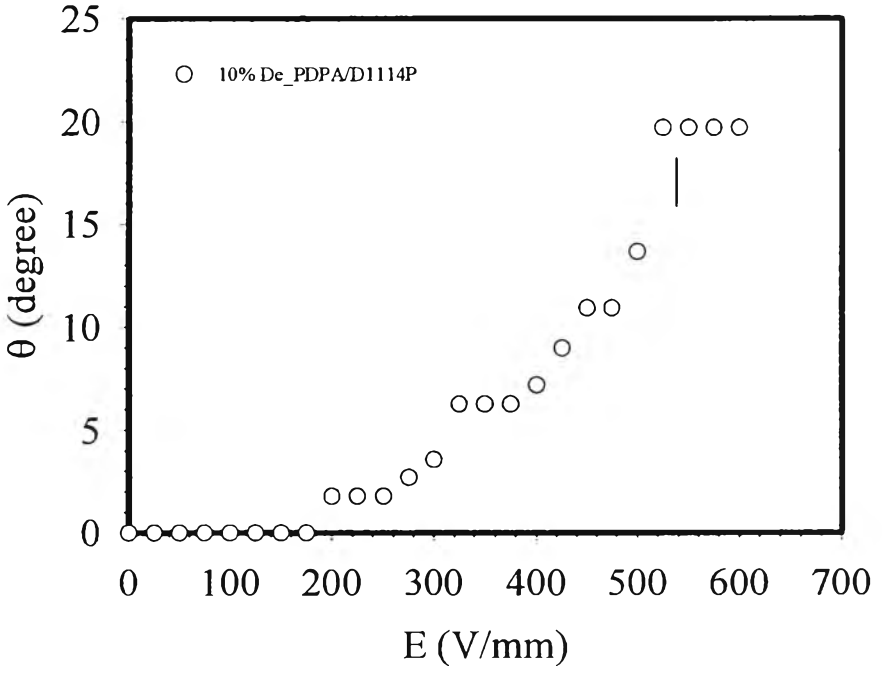
10% De_PDPA/D1114P
θ (degree)
E (V/mm)
0
5
10
15
20
25
0
100
200
300
400
500
600
700

(b)

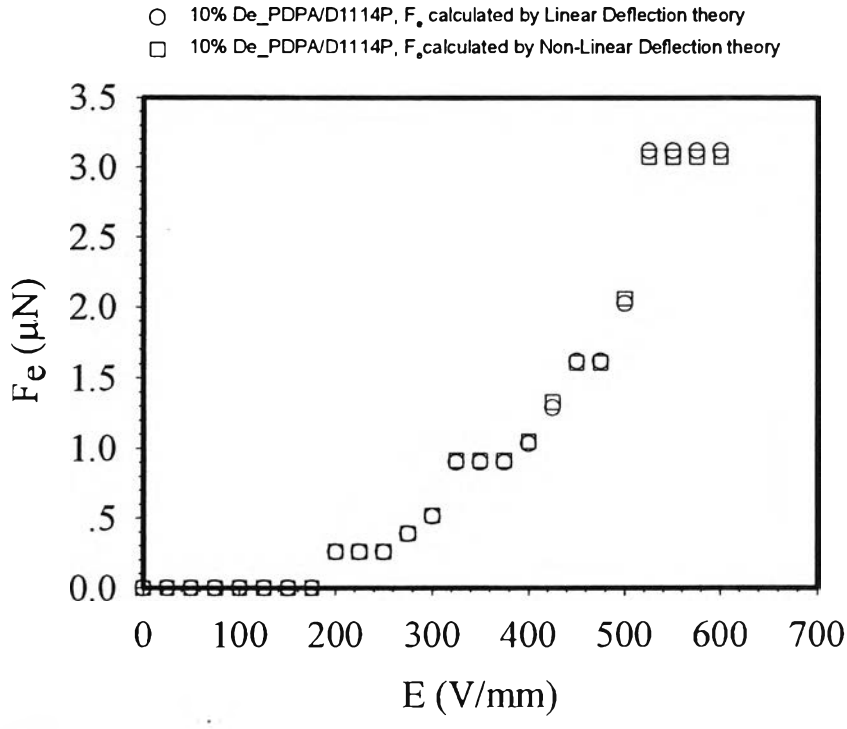
10% De_PDPA/D1114P, Fe calculated by Linear Deflection theory
10% De_PDPA/D1114P, Fecalculated by Non-Linear Deflection theory
Fe (μN)
3.5
3.0
2.5
2.0
1.5
1.0
.5
0.0
0
100
200
300
400
500
600
700
E (V/mm)

(c)

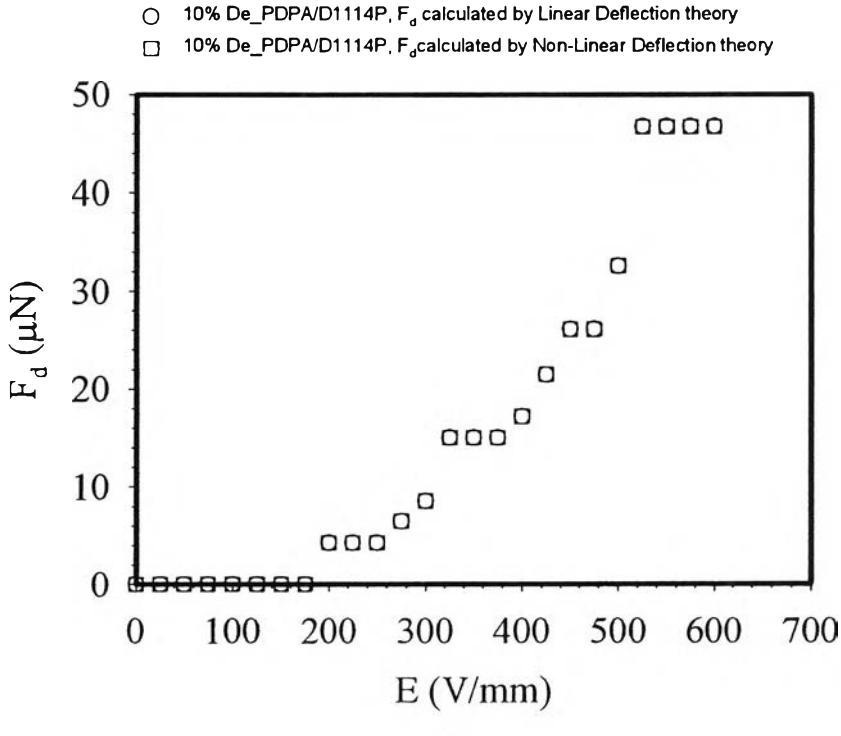
10% De_PDPA/D1114P, Fd calculated by Linear Deflection theory
10% De_PDPA/D1114P, Fdcalculated by Non-Linear Deflection theory
Fd (μN)
50
40
30
20
10
0
0
100
200
300
400
500
600
700
E (V/mm)

(d)

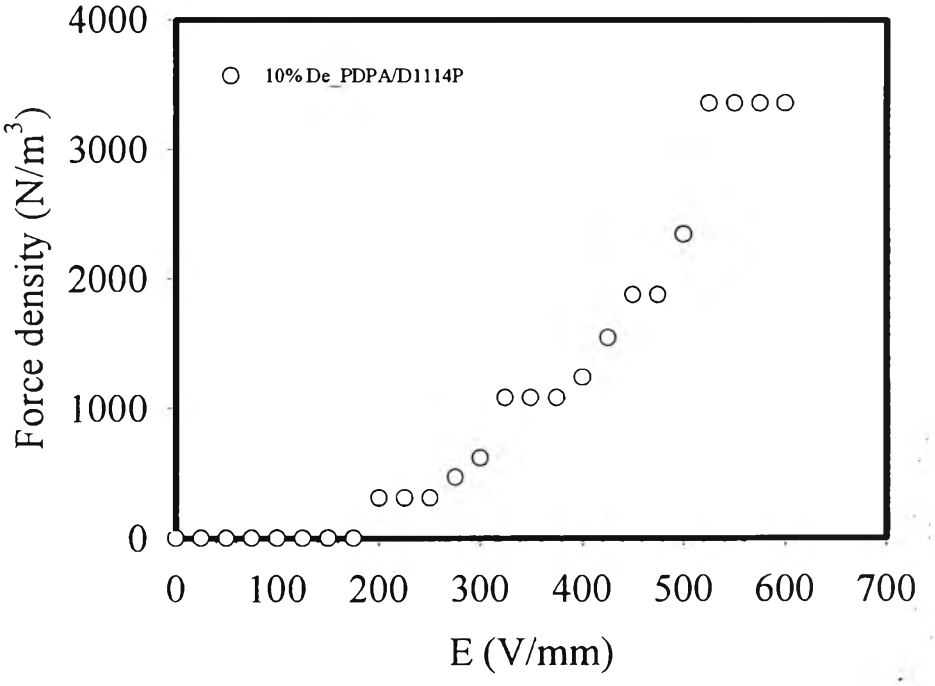

(e)

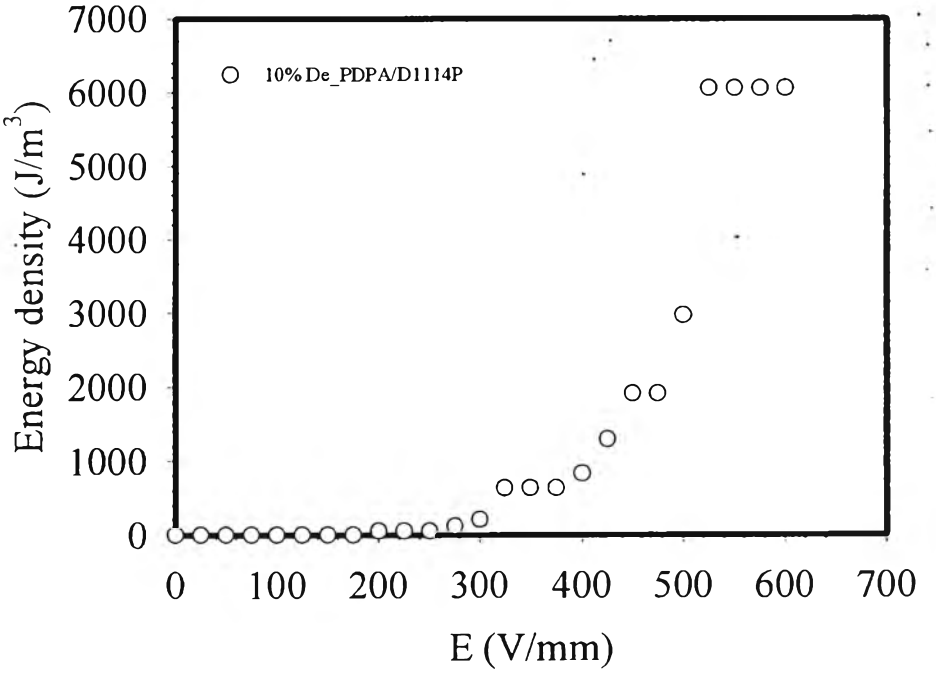

(f)

Figure K14 Electromechanical responses of 10 %DePDPA/D1114P at various electric field strengths: (a) deflection lengths; (b) deflection angles; (c) elastic force (F_e); (d) dielectrophoretic forces (F_d); (e) force density; (f) energy density.

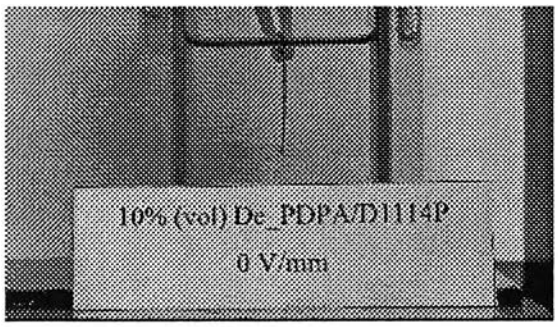
10% (vol) De_PDPA/D1114P
0 V/mm

(a)

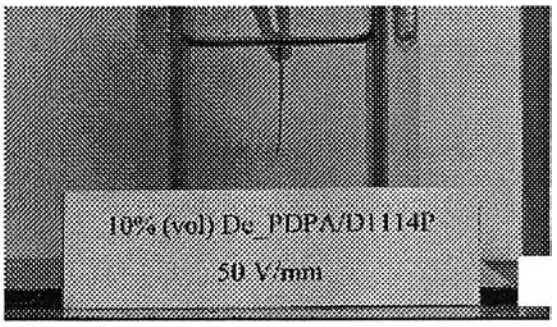
10% (vol) De_PDPA/D1114P
50 V/mm

(b)

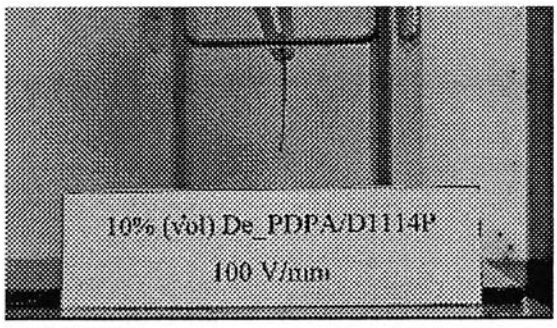
10% (vol) De_PDPA/D1114P
100 V/mm

(c)

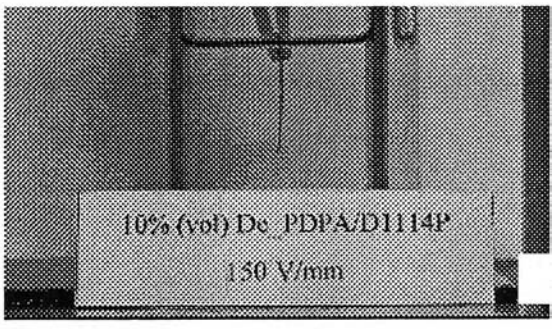
10% (vol) De_PDPA/D1114P
150 V/mm

(d)

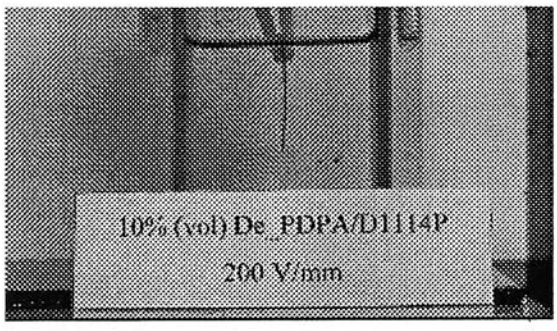
10% (vol) De_PDPA/D1114P
200 V/mm

(e)

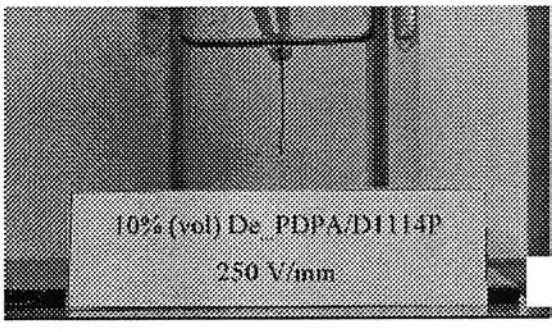
10% (vol) De_PDPA/D1114P
250 V/mm

(f)

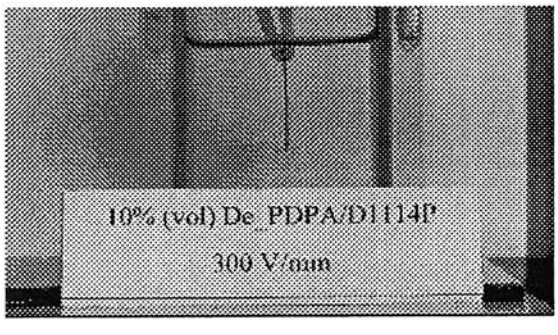
10% (vol) De_PDPA/D1114P
300 V/mm

(g)

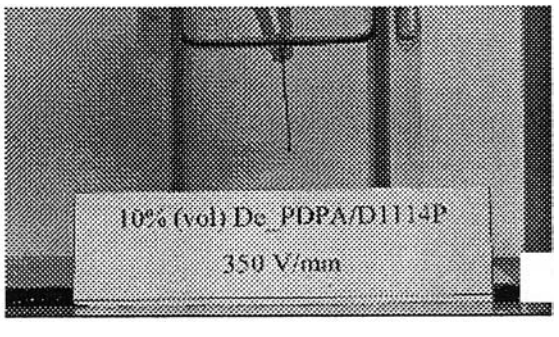
10% (vol) De_PDPA/D1114P
350 V/mm

(h)

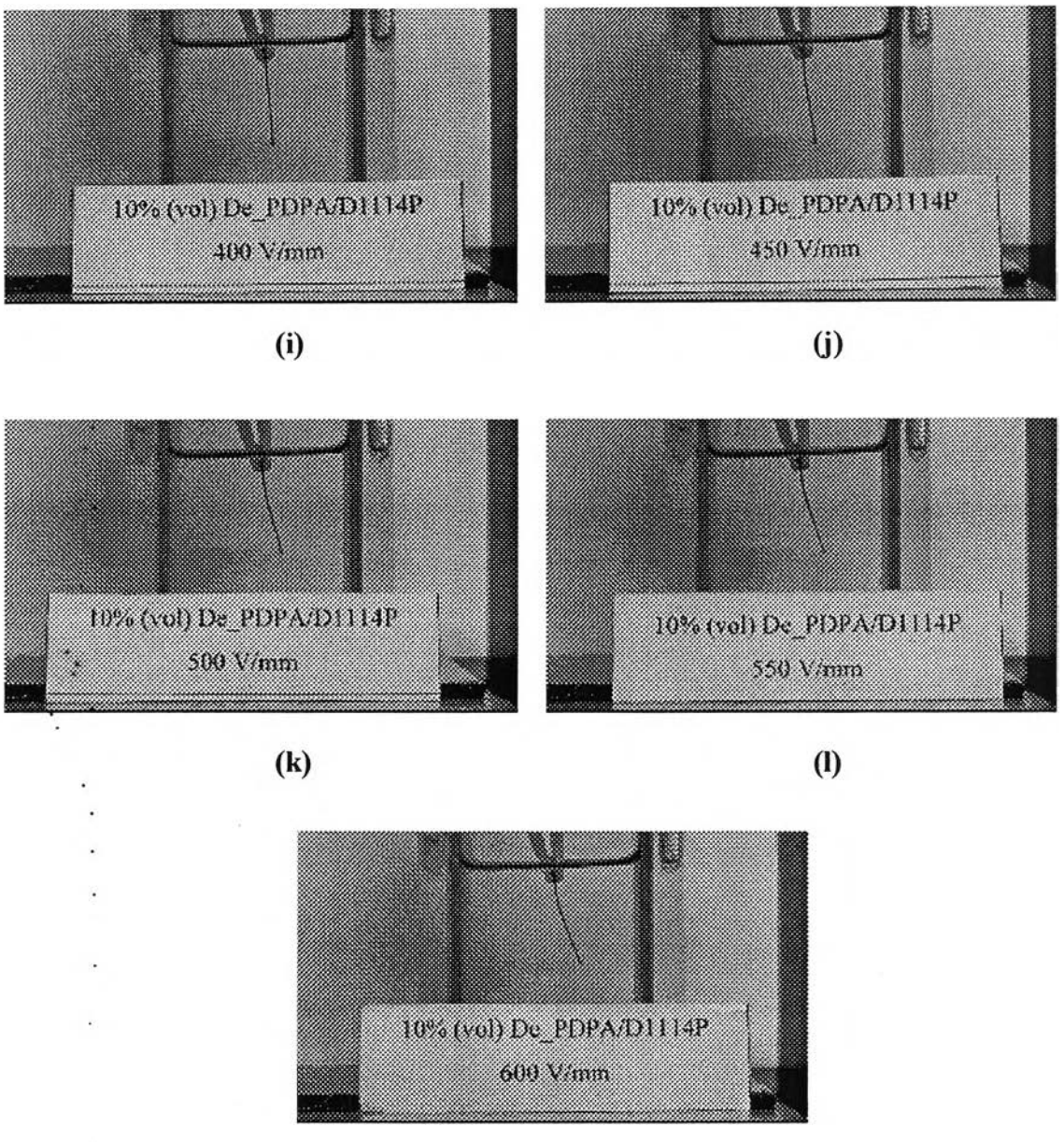

Figure K15 Electromechanical responses of 10 %DePDPA/D1114P at various electric field strengths: (a) 0 V/mm; (b) 50 V/mm; (c) V = 100 V/mm; (d) 150 V/mm; (e) 200 V/mm; (f) 250 V/mm; (g) 300 V/mm; (h) 350 V/mm; (i) 400 V/mm; (j) 450 V/mm; (k) 500 V/mm; (l) 550 V/mm; (m) 600 V/mm.

Table K6 Electromechanical responses of 20 %DePDPA/D1114P at various electric field strengths

E (V/mm)	d (mm)	l (mm)	θ (°)	sin(θ)	mg sin(θ) (N)	F_e from linear deflection (N)	F_d from linear deflection (N)	F_e from non linear deflection (N)	F_d from non linear deflection (N)	τ_l (sec)	τ_r (sec)	Energy density (J/m3)	Force density (N/m3)
0	0	13.83	0	0	0	0	0	0	0	0	0	0	0
25	0	13.83	0	0	0	0	0	0	0	0	0	0	0
50	0	13.83	0	0	0	0	0	0	0	0	0	0	0
75	0	13.83	0	0	0	0	0	0	0	0	0	0	0
100	0	13.83	0	0	0	0	0	0	0	0	0	0	0
125	0	13.83	0	0	0	0	0	0	0	0	0	0	0
150	0	13.83	0	0	0	0	0	0	0	0	0	0	0
175	0	13.83	0	0	0	0	0	0	0	0	0	0	0
200	0.23	13.83	1.0	0.017	3.064E-06	1.026E-06	4.090E-06	1.036E-06	4.100E-06	25	12	39	194
225	0.47	13.83	1.9	0.034	6.260E-06	2.096E-06	8.356E-06	2.117E-06	8.377E-06	28	12	162	397
250	0.47	13.83	1.9	0.034	6.260E-06	2.096E-06	8.356E-06	2.117E-06	8.377E-06	28	12	162	397
275	0.47	13.83	1.9	0.034	6.260E-06	2.096E-06	8.356E-06	2.117E-06	8.377E-06	29	15	161.6	397
300	0.47	13.83	1.9	0.034	6.260E-06	2.096E-06	8.356E-06	2.117E-06	8.377E-06	30	15	161.6	397
325	0.7	13.83	2.9	0.051	9.321E-06	3.122E-06	1.244E-05	3.153E-06	1.247E-05	30	15	358.3	591
350	0.7	13.83	2.9	0.051	9.321E-06	3.122E-06	1.244E-05	3.153E-06	1.247E-05	40	20	358.3	591
375	0.7	13.83	2.9	0.051	9.321E-06	3.122E-06	1.244E-05	3.153E-06	1.247E-05	48	21	358.3	591
400	0.7	13.83	2.9	0.051	9.321E-06	3.122E-06	1.244E-05	3.153E-06	1.247E-05	51	23	358.3	591
425	0.94	13.83	3.9	0.068	1.251E-05	4.192E-06	1.671E-05	4.236E-06	1.675E-05	53	24	645.7	793
450	0.94	13.83	3.9	0.068	1.251E-05	4.192E-06	1.671E-05	4.236E-06	1.675E-05	54	24	645.7	793
475	1.17	13.83	4.8	0.084	1.557E-05	5.218E-06	2.079E-05	5.289E-06	2.086E-05	44	26	999.5	988
500	1.17	13.83	4.8	0.084	1.557E-05	5.218E-06	2.079E-05	5.289E-06	2.086E-05	56	30	999.5	988
525	1.41	13.83	5.8	0.102	1.875E-05	6.288E-06	2.504E-05	6.386E-06	2.514E-05	48	30	1450.0	1191
550	1.41	13.83	5.8	0.102	1.875E-05	6.288E-06	2.504E-05	6.386E-06	2.514E-05	58	30	1450.0	1191
575	2.11	13.83	8.7	0.152	2.800E-05	9.410E-06	3.741E-05	9.678E-06	3.768E-05	46	30	3233.3	1785
600	2.11	13.83	8.7	0.152	2.800E-05	9.410E-06	3.741E-05	9.678E-06	3.768E-05	53	30	3233.3	1785

20 %DePDPA/D1114P

The weight of specimen (wt) = 0.0188 g

The length of specimen (l_0) = 13.83 mm

The initial length of specimen (L) = 20.75 mm

The thickness of specimen (t) = 0.407 mm

The width of specimen (w) = 2.5 mm

G' = 93325.56 Pa at E = 0 kV/mm, T = 300 K, strain = 0.1 %, f = 1 rad/s.

d = deflection distance in x axis (mm), l= deflection distance in y axis (mm)

τ_i = induction time (sec), τ_r = recovery time (sec)

I = Moment of inertia (m^4) = $t^3w/12$

E = Modulus of elasticity (Pa)

F_e = elastic force (N) = $3dEI/l^3$ for linear deflection

F_e = elastic force (N) = dEI/l^3 for non linear deflection

F_d = dielectrophoretic force = F_e (N) + mgsinθ

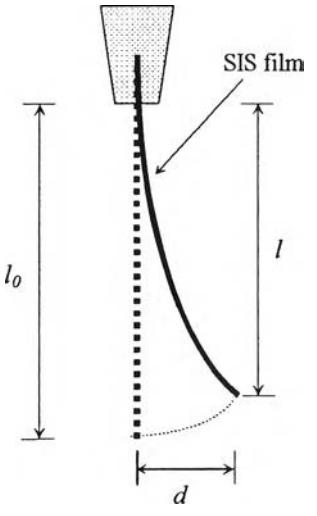

Energy density = $\frac{1}{2}E\theta^2$ (J/m^3)

Force density = $\frac{F_d}{volume}$ (N/m^3)

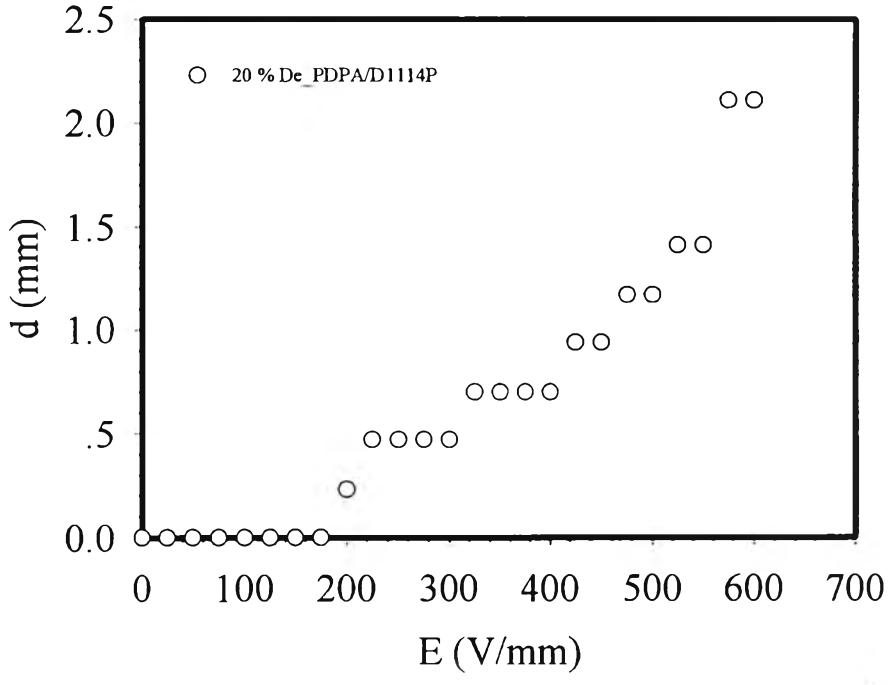
20 % De_PDPA/D1114P
d (mm)
2.5
2.0
1.5
1.0
.5
0.0
0
100
200
300
400
500
600
700
E (V/mm)

(a)

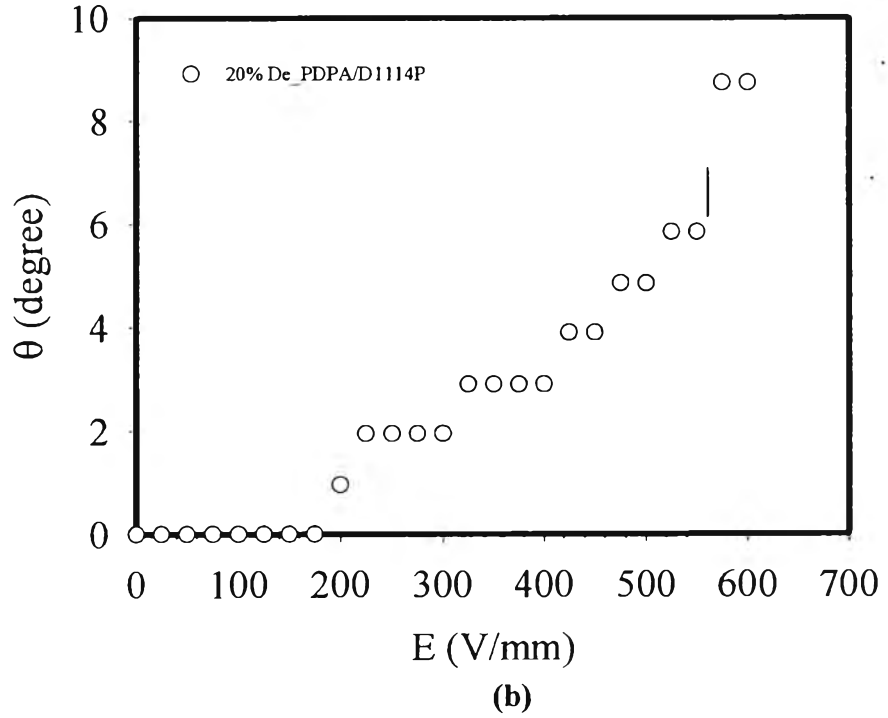
20% De_PDPA/D1114P
θ (degree)
10
8
6
4
2
0
0
100
200
300
400
500
600
700
E (V/mm)

(b)

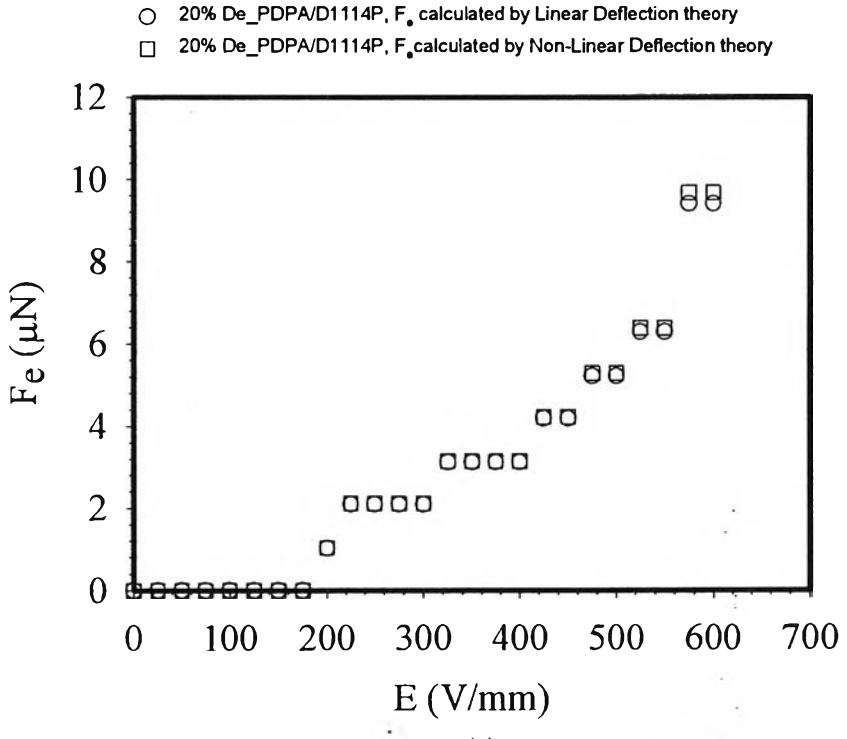
20% De_PDPA/D1114P, F_e calculated by Linear Deflection theory
20% De_PDPA/D1114P, F_e calculated by Non-Linear Deflection theory
F_e (μN)
E (V/mm)
0
2
4
6
8
10
12
0
100
200
300
400
500
600
700

(c)

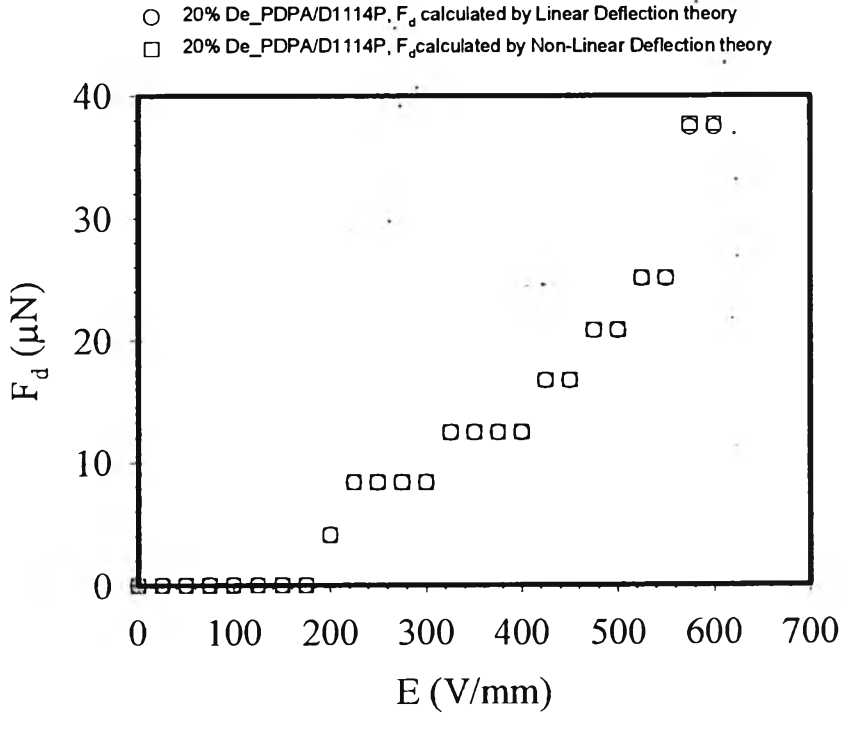
20% De_PDPA/D1114P, F_d calculated by Linear Deflection theory
20% De_PDPA/D1114P, F_d calculated by Non-Linear Deflection theory
F_d (μN)
E (V/mm)
0
10
20
30
40
0
100
200
300
400
500
600
700

(d)

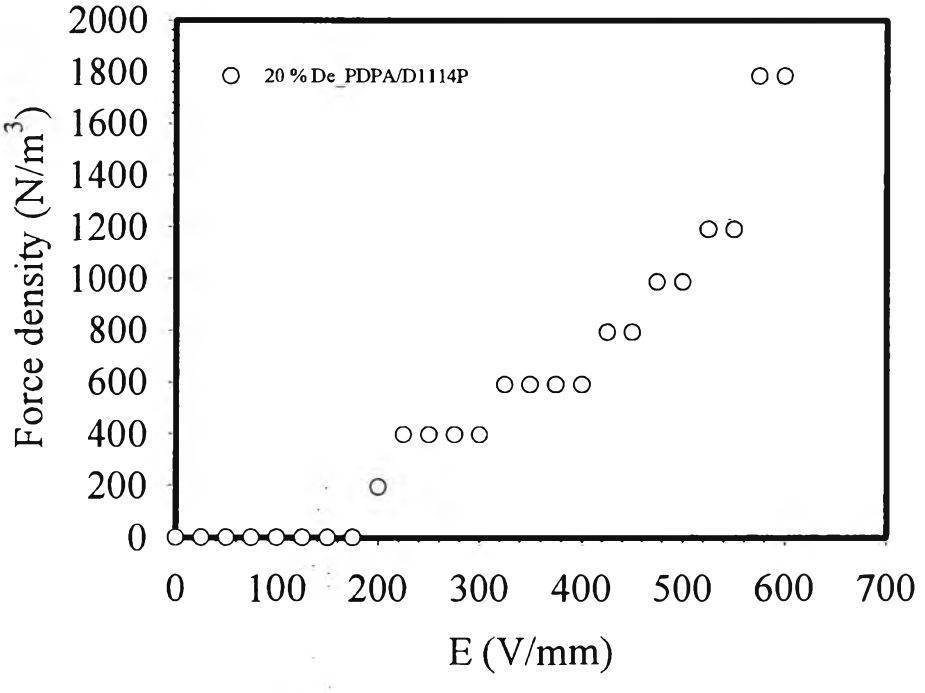

(e)

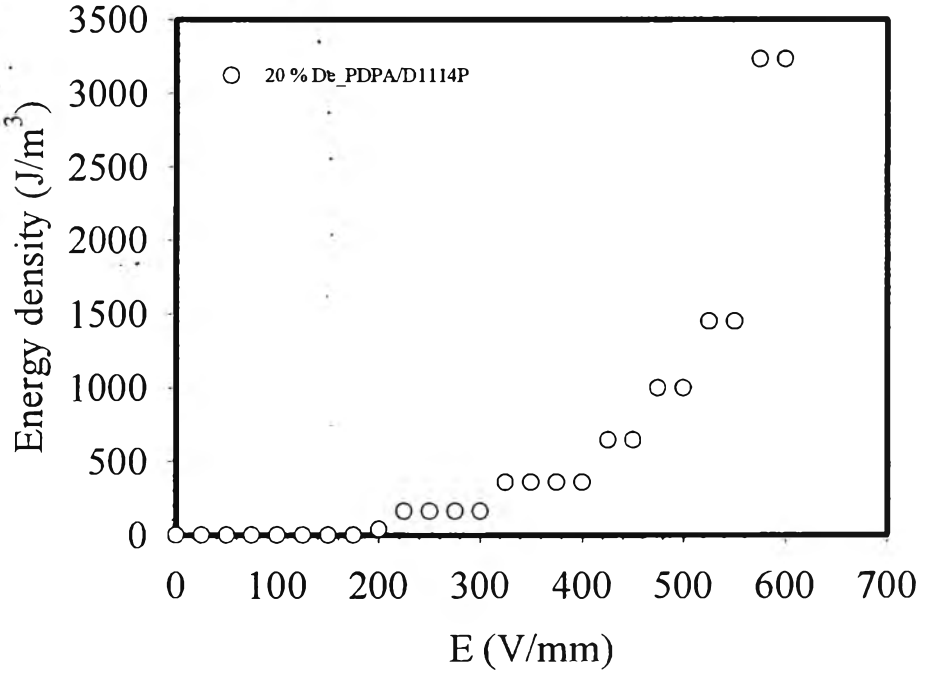

(f)

Figure K16 Electromechanical responses of 20 %DePDPA/D1114P at various electric field strengths: (a) deflection lengths; (b) deflection angles; (c) elastic force (F_e); (d) dielectrophoretic forces (F_d); (e) force density; (f) energy density.

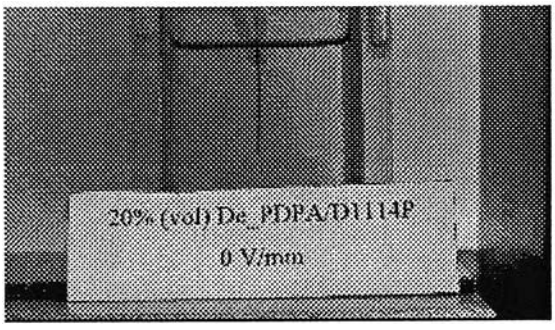
20% (vol) De_PDPA/D1114P
0 V/mm

(a)

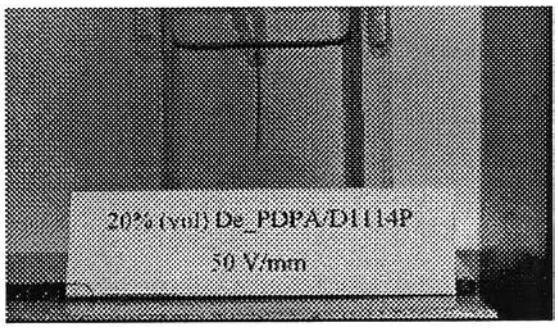
20% (vol) De_PDPA/D1114P
50 V/mm

(b)

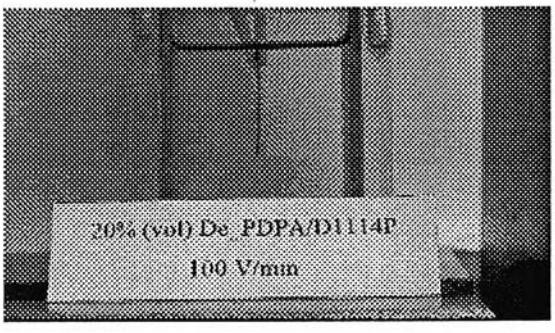
20% (vol) De_PDPA/D1114P
100 V/mm

(c)

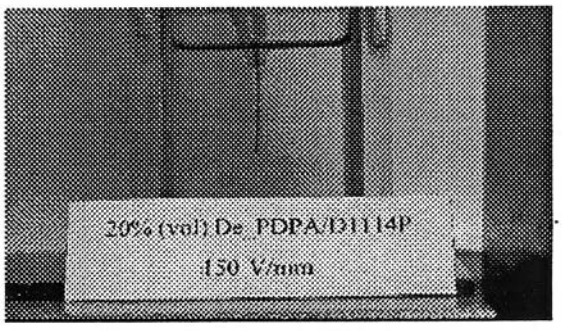
20% (vol) De_PDPA/D1114P
150 V/mm

(d)

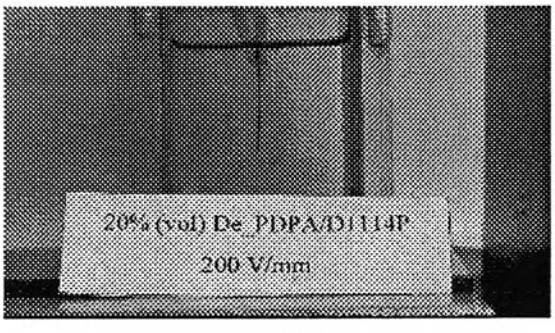
20% (vol) De_PDPA/D1114P
200 V/mm

(e)

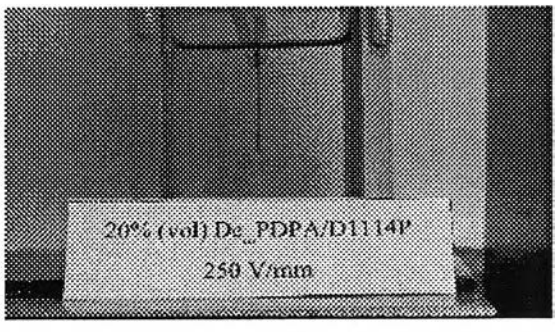
20% (vol) De_PDPA/D1114P
250 V/mm

(f)

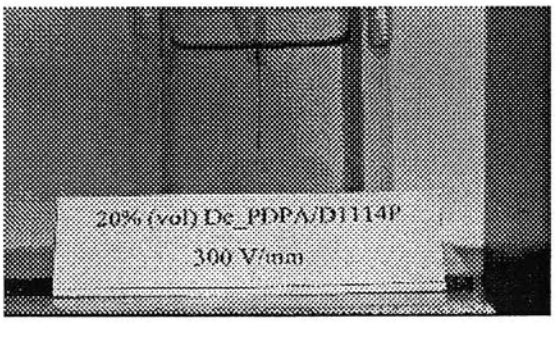
20% (vol) De_PDPA/D1114P
300 V/mm

(g)

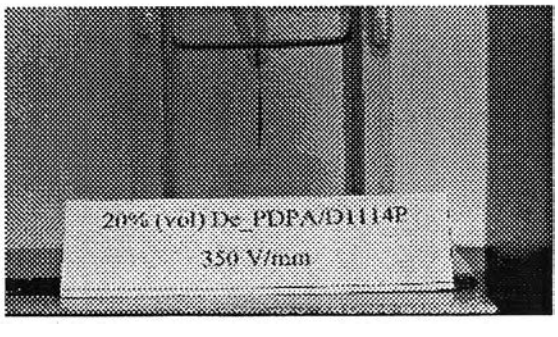
20% (vol) De_PDPA/D1114P
350 V/mm

(h)

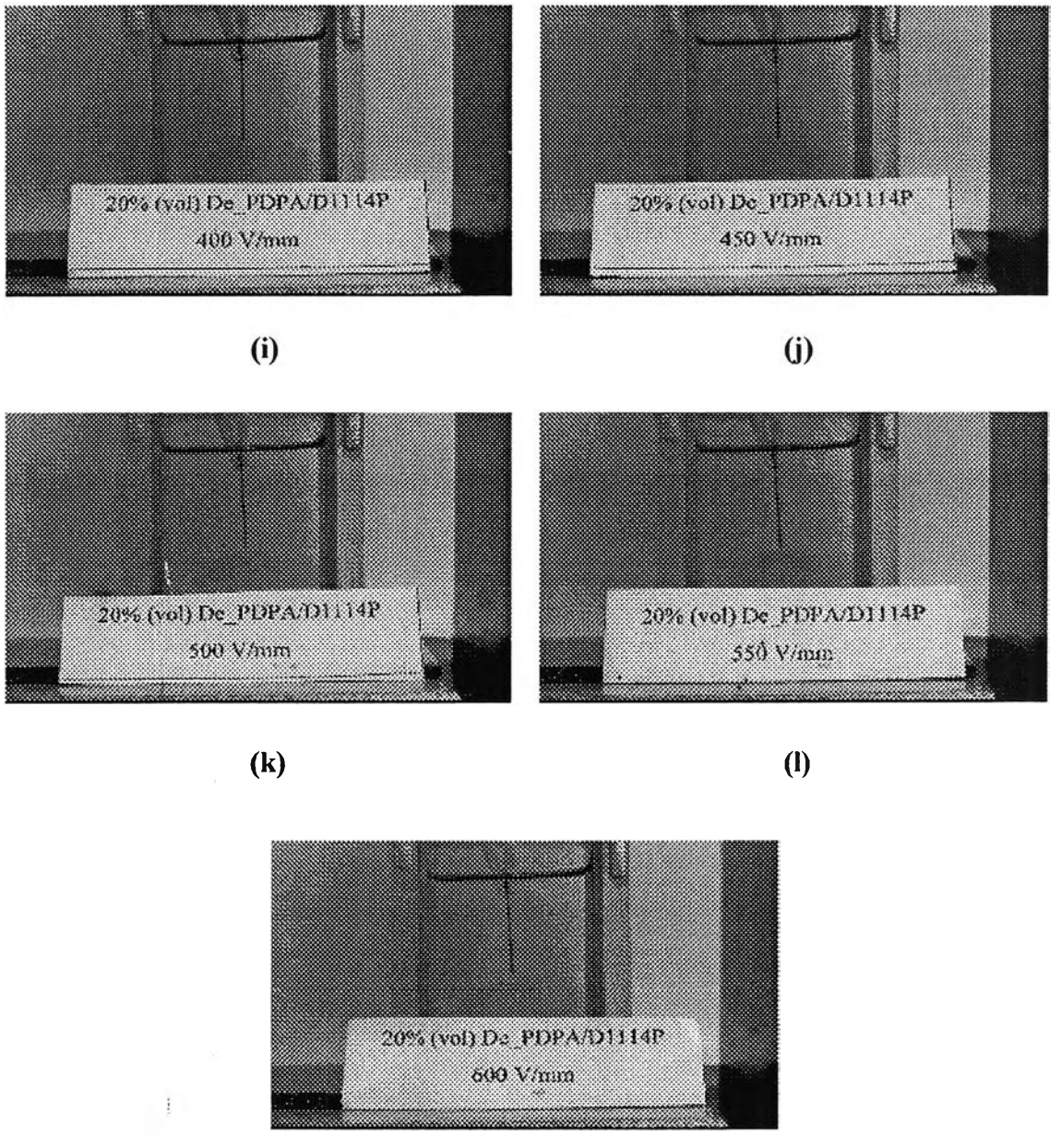

Figure K17 Electromechanical responses of 20 %DePDPA/D1114P at various electric field strengths: (a) 0 V/mm; (b) 50 V/mm; (c) V = 100 V/mm; (d) 150 V/mm; (e) 200 V/mm; (f) 250 V/mm; (g) 300 V/mm; (h) 350 V/mm; (i) 400 V/mm; (j) 450 V/mm; (k) 500 V/mm; (l) 550 V/mm; (m) 600 V/mm.

Table K7 Electromechanical responses of 30% DePDPA/D1114P at various electric field strengths

E (V/mm)	d (mm)	l (mm)	θ (°)	sin(θ)	mg sin(θ) (N)	F_e from linear deflection (N)	F_d from linear deflection (N)	F_e from non linear deflection (N)	F_d from non linear deflection (N)	τ_i (sec)	τ_r (sec)	Energy density (J/m3)	Force density (N/m3)
0	0	13.8	0	0	0	0	0	0	0	0	0	0	0
25	0	13.8	0	0	0	0	0	0	0	0	0	0	0
50	0.2	13.8	0.8	0.014	1.917E-06	6.222E-07	2.540E-06	5.554E-07	2.473E-06	11	3	70	196
75	0.4	13.8	1.7	0.029	3.834E-06	1.244E-06	5.079E-06	1.111E-06	4.945E-06	11	3	278	393
100	0.4	13.8	1.7	0.029	3.834E-06	1.244E-06	5.079E-06	1.111E-06	4.945E-06	11	3	278	393
125	0.4	13.8	1.7	0.029	3.834E-06	1.244E-06	5.079E-06	1.111E-06	4.945E-06	11	3	278	393
150	0.4	13.8	1.7	0.029	3.834E-06	1.244E-06	5.079E-06	1.111E-06	4.945E-06	12	4	278	393
175	0.4	13.8	1.7	0.029	3.834E-06	1.244E-06	5.079E-06	1.111E-06	4.945E-06	11	5	278	393
200	0.4	13.8	1.7	0.029	3.834E-06	1.244E-06	5.079E-06	1.111E-06	4.945E-06	13	5	278	393
225	0.6	13.8	2.5	0.043	5.750E-06	1.867E-06	7.617E-06	1.666E-06	7.417E-06	14	5	626	589
250	0.6	13.8	2.5	0.043	5.750E-06	1.867E-06	7.617E-06	1.666E-06	7.417E-06	20	10	626	589
275	0.6	13.8	2.5	0.043	5.750E-06	1.867E-06	7.617E-06	1.666E-06	7.417E-06	33	11	626.1	589
300	0.6	13.8	2.5	0.043	5.750E-06	1.867E-06	7.617E-06	1.666E-06	7.417E-06	35	12	626.1	589
325	0.6	13.8	2.5	0.043	5.750E-06	1.867E-06	7.617E-06	1.666E-06	7.417E-06	37	13	626.1	589
350	0.6	13.8	2.5	0.043	5.750E-06	1.867E-06	7.617E-06	1.666E-06	7.417E-06	37	15	626.1	589
375	0.8	13.8	3.3	0.058	7.665E-06	2.489E-06	1.015E-05	2.222E-06	9.887E-06	48	30	1112.6	785
400	1	13.6	4.2	0.073	9.719E-06	3.250E-06	1.297E-05	2.781E-06	1.250E-05	49	30	1788.7	993
425	1.2	13.6	5.1	0.088	1.166E-05	3.900E-06	1.556E-05	3.345E-06	1.500E-05	49	30	2573.6	1191
450	1.2	13.6	5.1	0.088	1.166E-05	3.900E-06	1.556E-05	3.345E-06	1.500E-05	49	30	2573.6	1191
475	1.2	13.6	5.1	0.088	1.166E-05	3.900E-06	1.556E-05	3.345E-06	1.500E-05	50	35	2573.6	1191
500	1.2	13.6	5.1	0.088	1.166E-05	3.900E-06	1.556E-05	3.345E-06	1.500E-05	54	36	2573.6	1191
525	1.2	13.6	5.1	0.088	1.166E-05	3.900E-06	1.556E-05	3.345E-06	1.500E-05	57	36	2573.6	1191
550	1.2	13.6	5.1	0.088	1.166E-05	3.900E-06	1.556E-05	3.345E-06	1.500E-05	58	40	2573.6	1191
575	1.6	13.6	6.7	0.117	1.553E-05	5.200E-06	2.073E-05	4.473E-06	2.000E-05	65	40	4566.1	1588
600	1.8	13.6	7.6	0.132	1.746E-05	5.850E-06	2.331E-05	5.036E-06	2.250E-05	66	40	5771.9	1786

30 %DePDPA/D1114P

The weight of specimen (wt) = 0.0135 g

The length of specimen (l_0) = 13.80 mm

The initial length of specimen (L) = 20.30 mm

The thickness of specimen (t) = 0.282 mm

The width of specimen (w) = 2.2 mm

G′ = 220952 Pa at E = 0 kV/mm, T = 300 K, strain = 0.3 %, f = 1 rad/s.

d = deflection distance in x axis (mm), l= deflection distance in y axis (mm)

τ_i = induction time (sec), τ_r = recovery time (sec)

I = Moment of inertia (m^4) = $t^3w/12$

E = Modulus of elasticity (Pa)

F_e = elastic force (N) = $3dEI/l^3$ for linear deflection

F_e = elastic force (N) = dEI/l^3 for non linear deflection

F_d = dielectrophoretic force = F_e (N) + $mg\sin\theta$

Energy density = $\frac{1}{2}E\theta^2$ (J/m^3)

Force density = $\frac{F_d}{volume}$ (N/m^3)

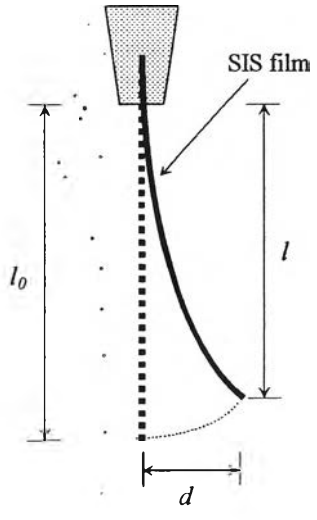

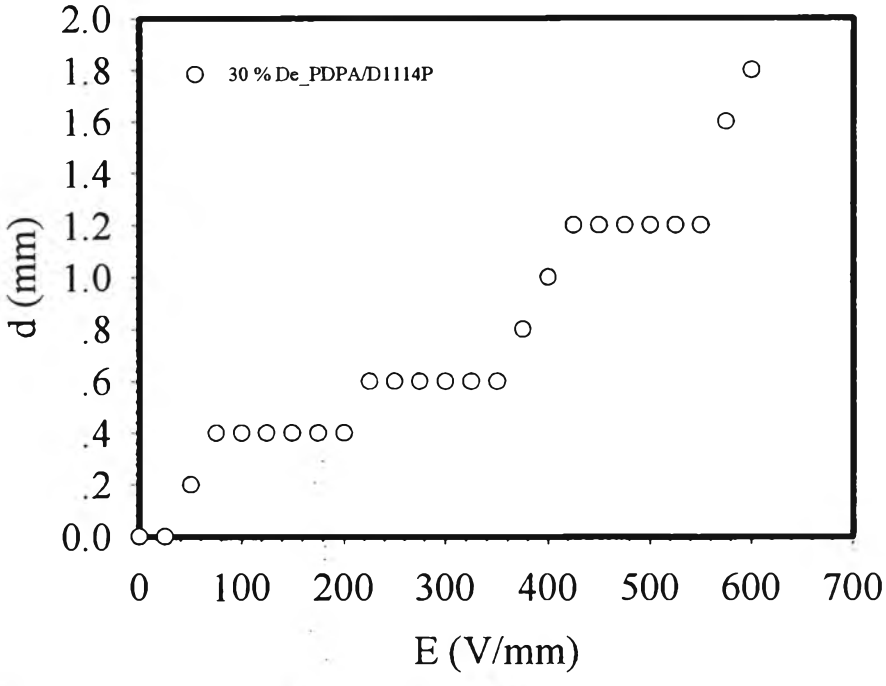
30 % De_PDPA/D1114P
d (mm)
2.0
1.8
1.6
1.4
1.2
1.0
.8
.6
.4
.2
0.0
0
100
200
300
400
500
600
700
E (V/mm)

(a)

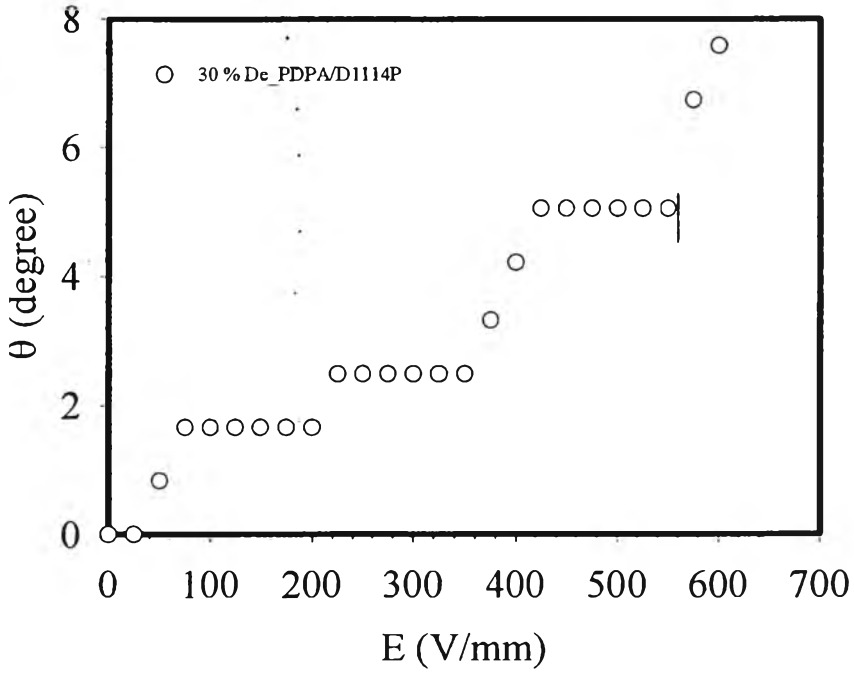
30 % De_PDPA/D1114P
θ (degree)
8
6
4
2
0
0
100
200
300
400
500
600
700
E (V/mm)

(b)

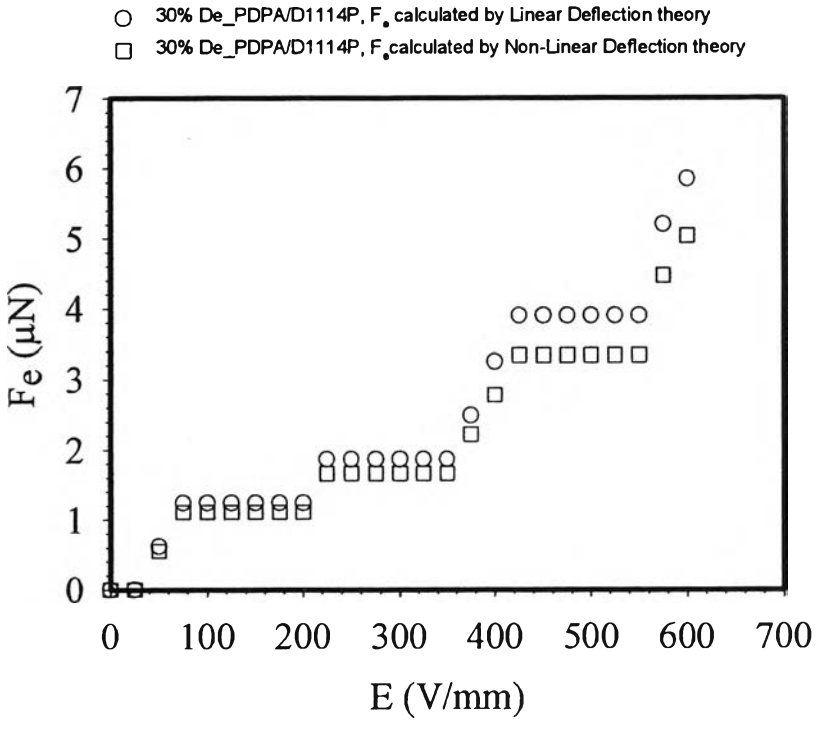
30% De_PDPA/D1114P, F_e calculated by Linear Deflection theory
30% De_PDPA/D1114P, F_e calculated by Non-Linear Deflection theory
F_e (μN)
0
1
2
3
4
5
6
7
0
100
200
300
400
500
600
700
E (V/mm)

(c)

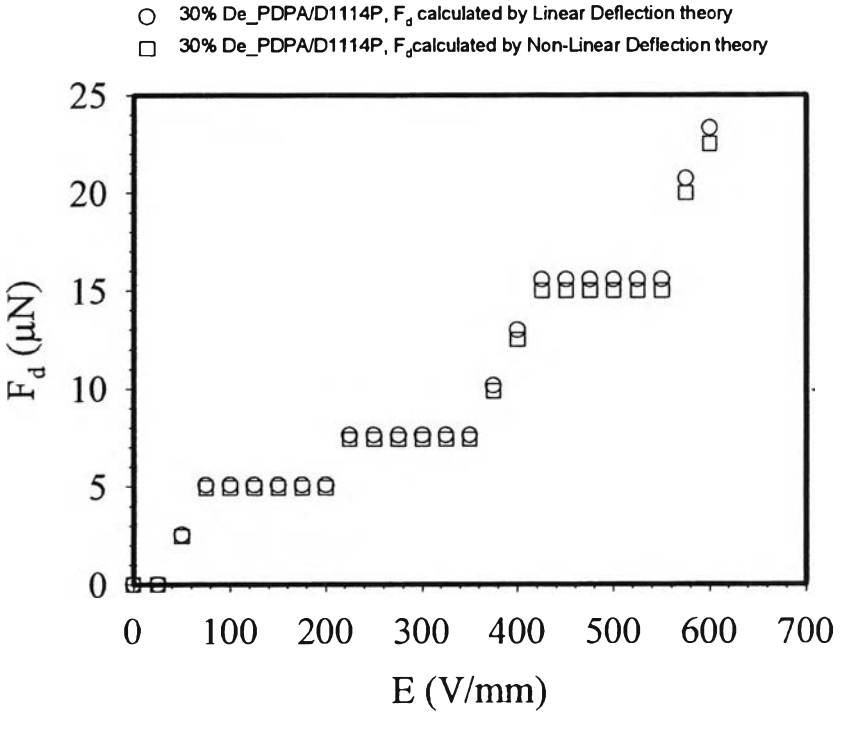
30% De_PDPA/D1114P, F_d calculated by Linear Deflection theory
30% De_PDPA/D1114P, F_d calculated by Non-Linear Deflection theory
F_d (μN)
0
5
10
15
20
25
0
100
200
300
400
500
600
700
E (V/mm)

(d)

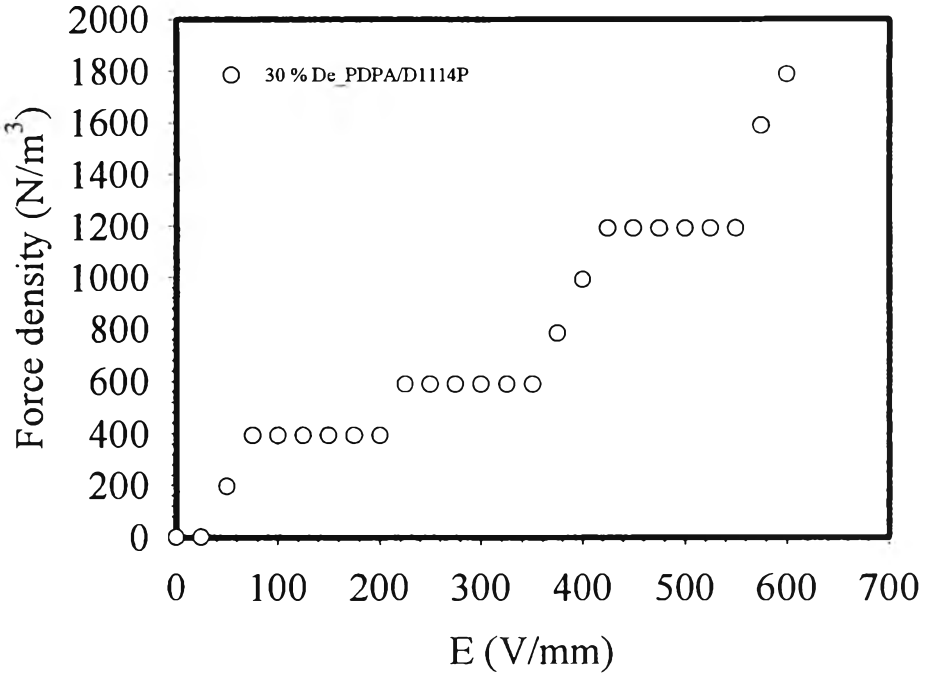

(e)

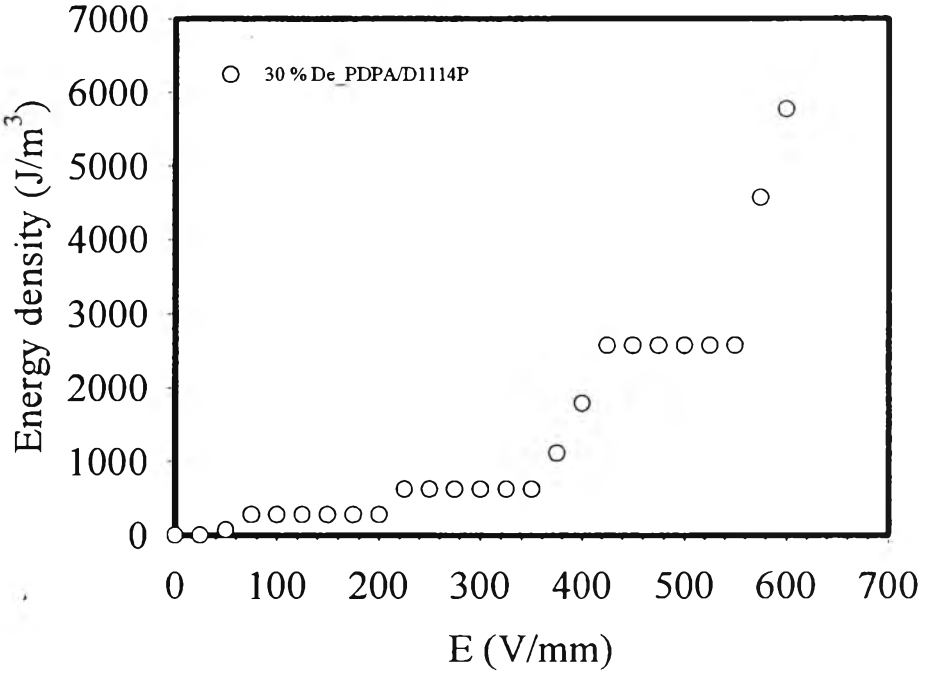

(f)

Figure K18 Electromechanical responses of 30 %DePDPA/D1114P at various electric field strengths: (a) deflection lengths; (b) deflection angles; (c) elastic force (F_e); (d) dielectrophoretic forces (F_d); (e) force density; (f) energy density.

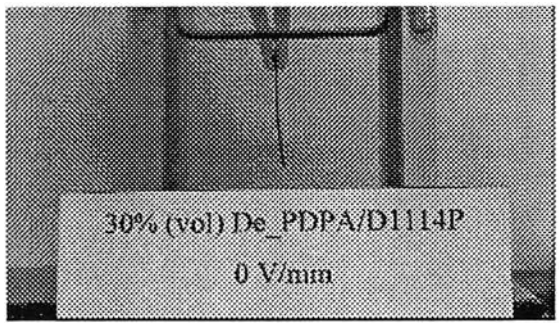
30% (vol) De_PDPA/D1114P
0 V/mm

(a)

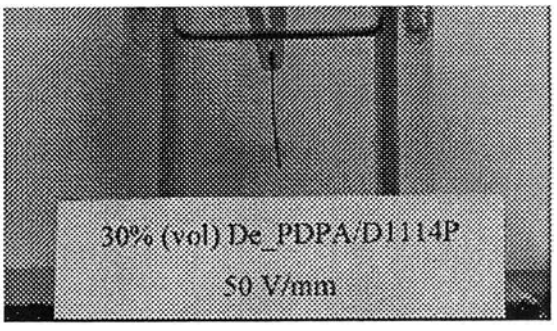
30% (vol) De_PDPA/D1114P
50 V/mm

(b)

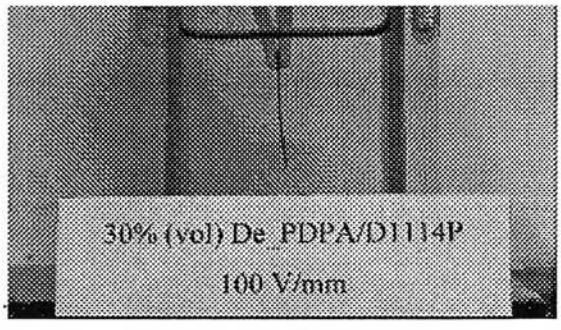
30% (vol) De_PDPA/D1114P
100 V/mm

(c)

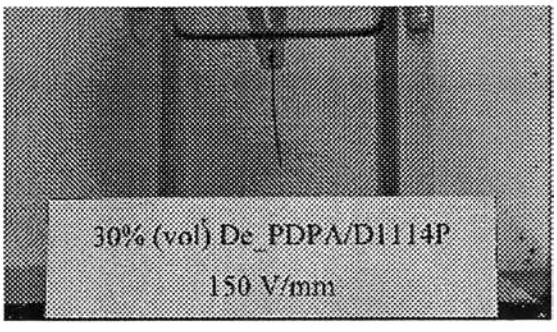
30% (vol) De_PDPA/D1114P
150 V/mm

(d)

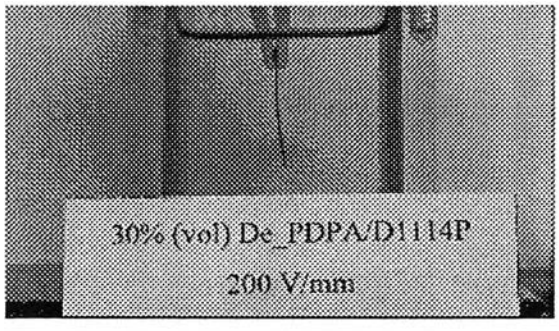
30% (vol) De_PDPA/D1114P
200 V/mm

(e)

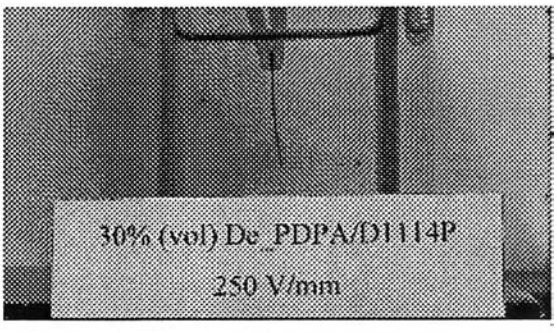
30% (vol) De_PDPA/D1114P
250 V/mm

(f)

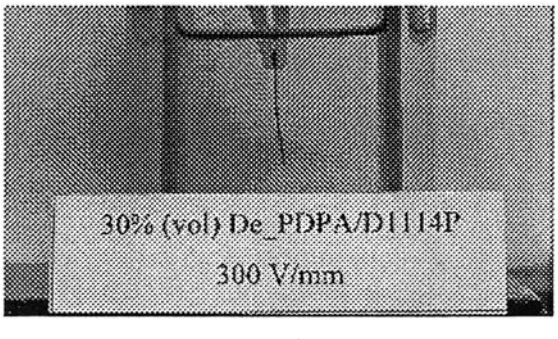
30% (vol) De_PDPA/D1114P
300 V/mm

(g)

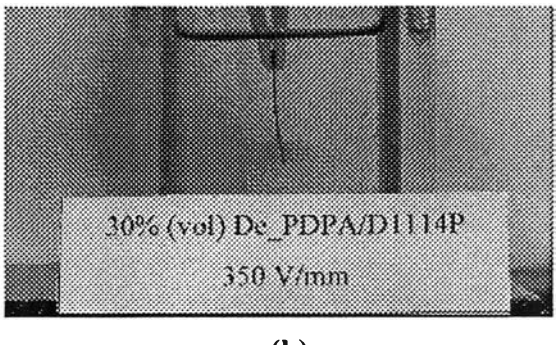
30% (vol) De_PDPA/D1114P
350 V/mm

(h)

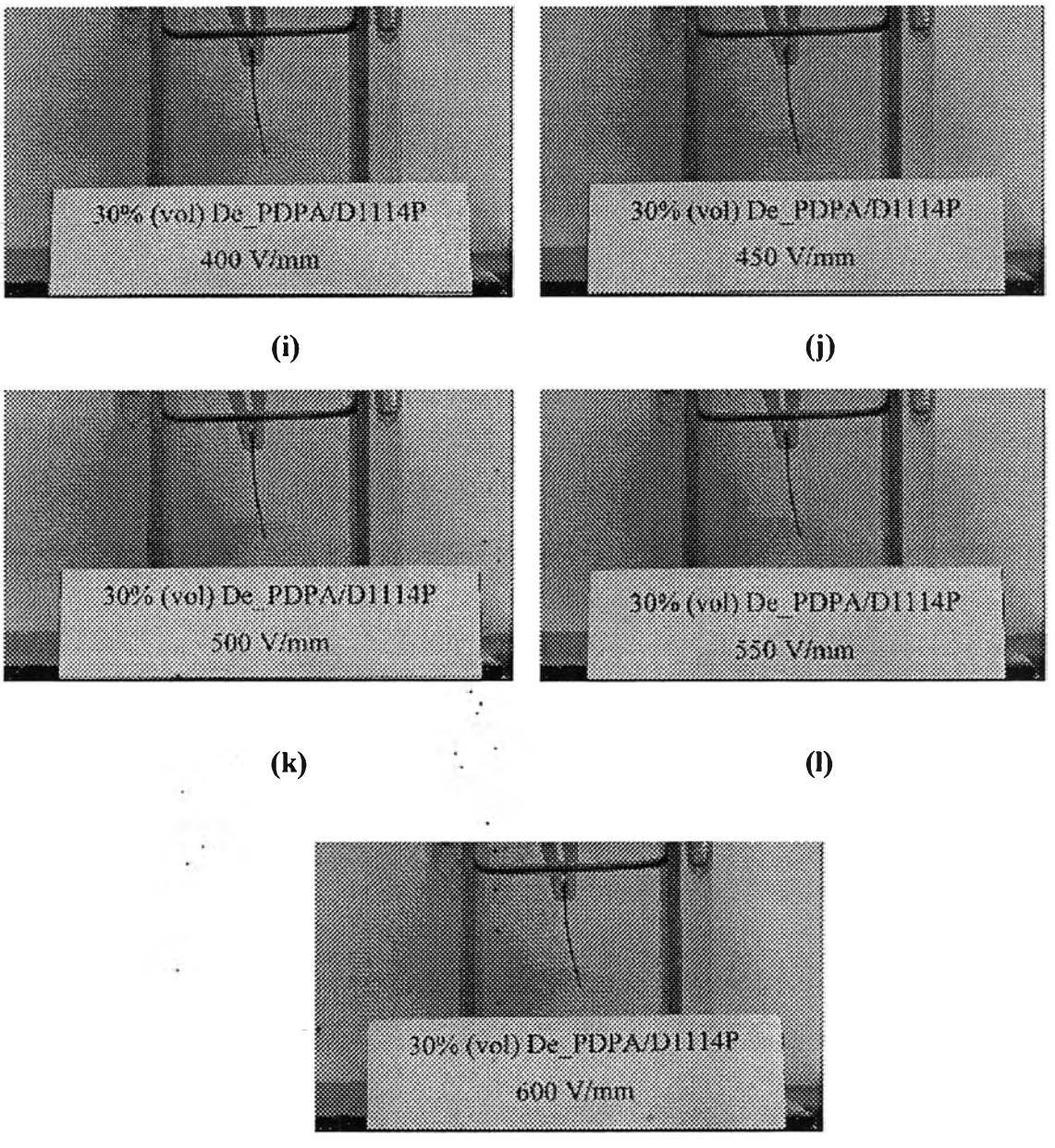

Figure K19 Electromechanical responses of 30 %DePDPA/D1114P at various electric field strengths: (a) 0 V/mm; (b) 50 V/mm; (c) V = 100 V/mm; (d) 150 V/mm; (e) 200 V/mm; (f) 250 V/mm; (g) 300 V/mm; (h) 350 V/mm; (i) 400 V/mm; (j) 450 V/mm; (k) 500 V/mm; (l) 550 V/mm; (m) 600 V/mm.

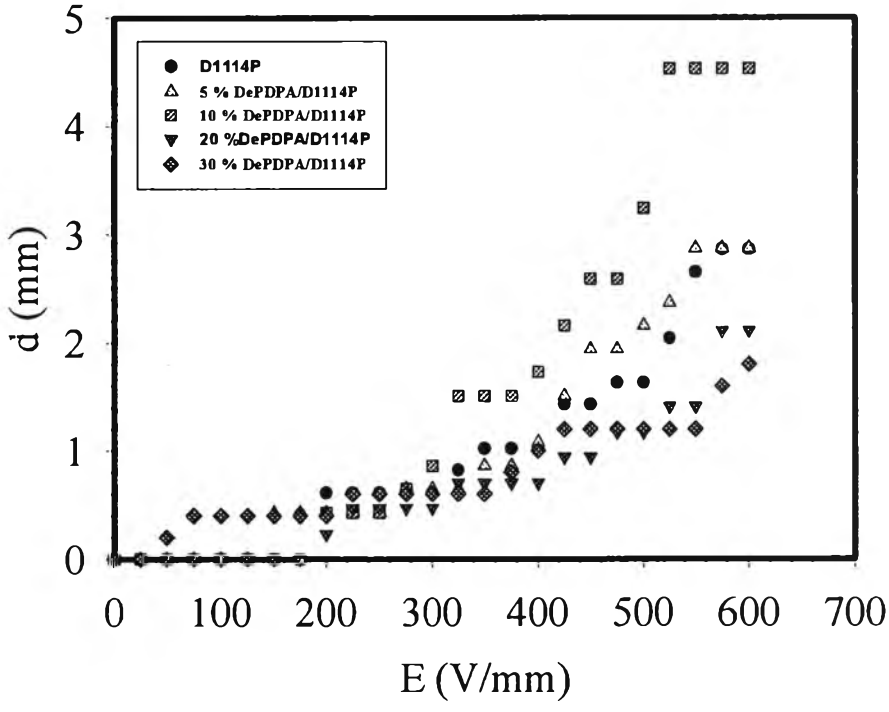

Figure K20 Deflection distances of D1114P and DePDPA/D1114P blends at various electric field strengths.

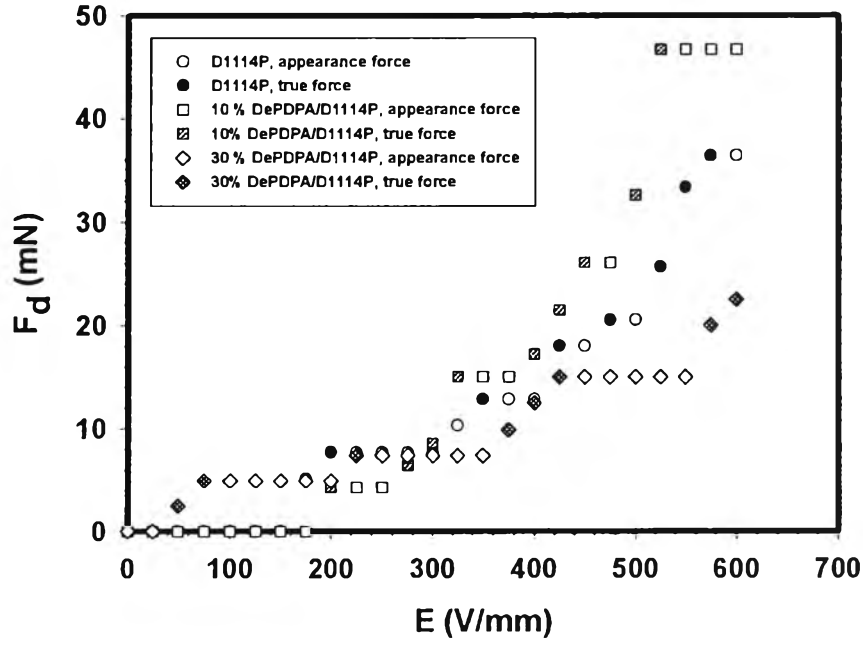

Figure K21 Dielectrophoretic force of D1114P, and De_PDPA/D1114P blends at various electric field strengths calculated through Non-Linear Deflection theory.

Appendix L Determination of Particle Sizes of Dedoped Polydiphenylamine (De_PDPA)

Table L1 Particle diameters of De_PDPA

Sample	Particle diameter (μm)			Average	STD (μm)
	1	2	3		
De_PDPA	8.27	8.34	8.21	8.27	0.065

Table L2 The raw data from particle size analysis of De_PDPA

Size		De_PDPA					
Low (μm)	High (μm)	1		2		3	
		In%	Under%	In%	Under%	In%	Under%
0.05	0.12	0.00	0.01	0.00	0.01	0.00	0.01
0.12	0.15	0.19	0.19	0.19	0.19	0.20	0.20
0.15	0.19	0.38	0.57	0.38	0.57	0.40	0.60
0.19	0.23	0.59	1.16	0.59	1.16	0.62	1.22
0.23	0.28	0.80	1.96	0.81	1.97	0.85	2.07
0.28	0.35	1.02	2.99	1.04	3.00	1.09	3.15
0.35	0.43	1.26	4.25	1.28	4.28	1.35	4.50
0.43	0.53	1.50	5.75	1.54	5.82	1.61	6.11
0.53	0.65	1.75	7.50	1.80	7.62	1.89	8.00
0.65	0.81	2.01	9.51	2.07	9.69	2.16	10.16
0.81	1.00	2.27	11.78	2.35	12.04	2.45	12.61
1.00	1.23	2.59	14.38	2.67	14.71	2.76	15.37
1.23	1.51	3.04	17.41	3.11	17.82	3.19	18.57
1.51	1.86	3.69	21.10	3.74	21.56	3.81	22.37
1.86	2.30	4.39	25.49	4.41	25.97	4.45	26.82
2.30	2.83	4.96	30.45	4.94	30.91	4.96	31.78
2.83	3.49	5.45	35.90	5.39	36.30	5.39	37.18
3.49	4.30	5.88	41.78	5.80	42.10	5.80	42.97
4.30	5.29	6.42	48.20	6.33	48.43	6.34	49.32
5.29	6.52	6.97	55.18	6.88	55.32	6.91	56.23
6.52	8.04	7.38	62.56	7.31	62.62	7.33	63.56
8.04	9.91	7.49	70.04	7.42	70.04	7.41	70.97
9.91	12.21	7.18	77.22	7.12	77.17	7.03	78.01
12.21	15.04	6.49	83.68	6.42	83.58	6.22	84.22
15.04	18.54	5.41	89.09	5.38	88.97	5.10	89.33
18.54	22.84	4.19	93.29	4.16	93.12	3.88	93.20
22.84	28.15	3.02	96.31	2.98	96.10	2.78	95.99
28.15	34.69	1.98	98.28	1.94	98.04	1.89	97.87
34.69	42.75	1.13	99.42	1.13	99.17	1.20	99.08
42.75	52.68	0.50	99.92	0.57	99.74	0.67	99.75
52.68	64.92	0.08	100	0.25	99.99	0.25	100
64.92	80.00	0.00	100	0.01	100	0.00	100

Appendix M Dielectric Constant Measurements

Pure SIS

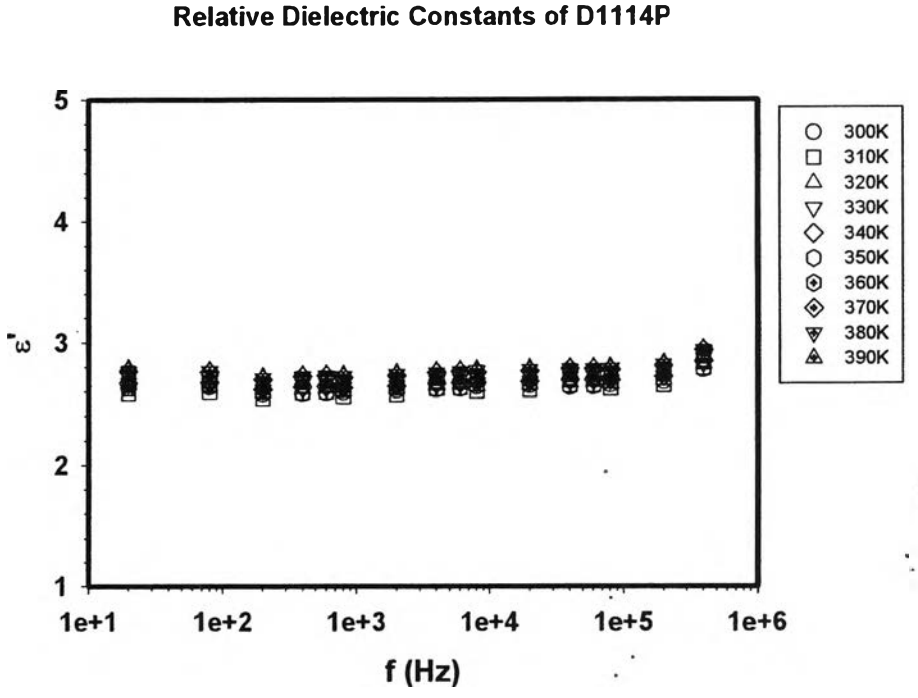

(a)

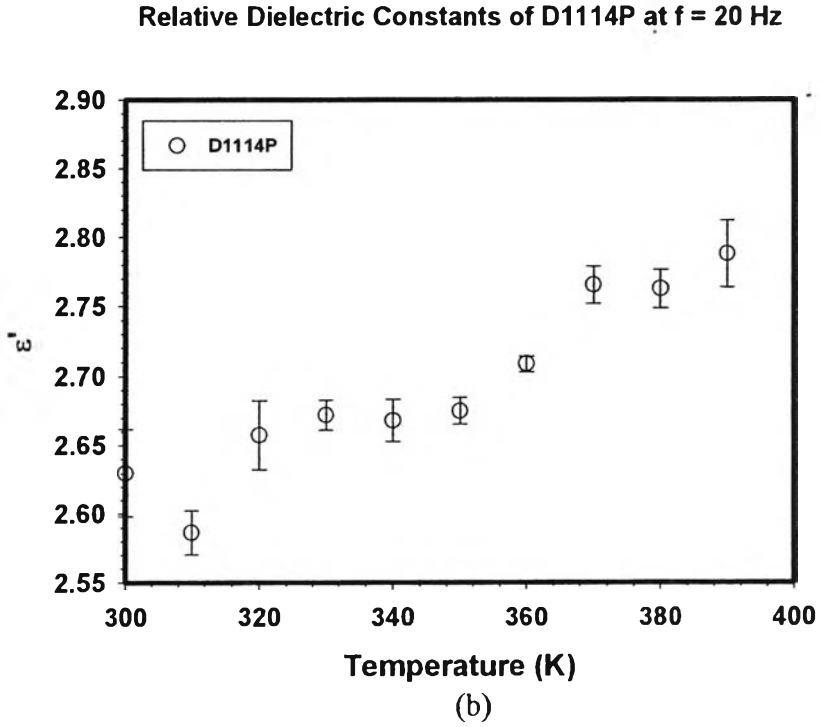

(b)

Figure M1 Dielectric constant of D1114P: (a) plot between relative dielectric constant (ε') versus frequency (f) at various temperature; (b) the plot between relative dielectric constant (ε') versus temperature at frequency of 20 Hz.

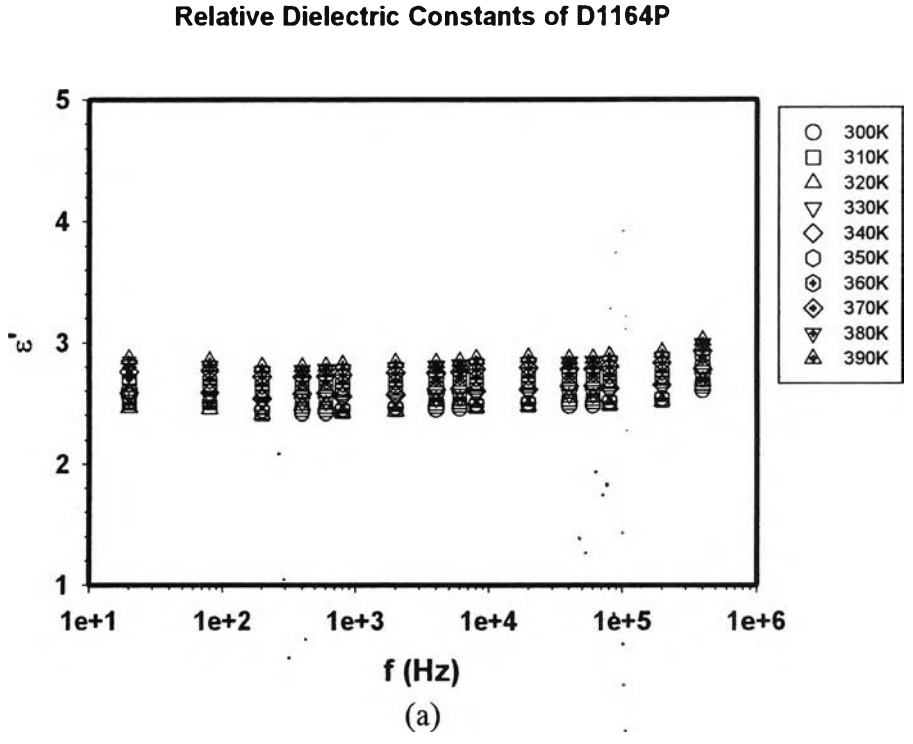

(a)

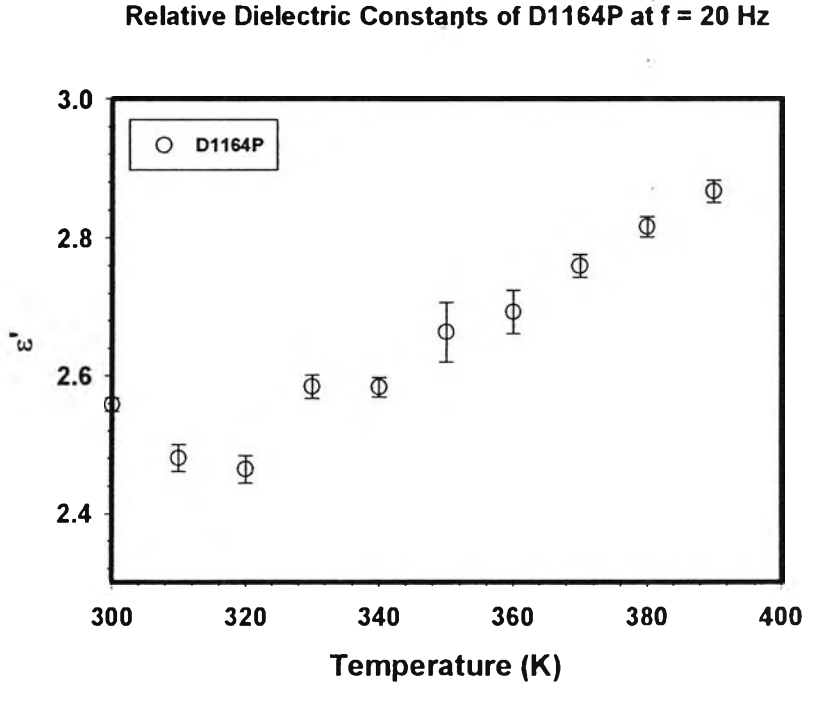

(b)

Figure M2 Dielectric constant of D1164P: (a) plot between relative dielectric constant (ε') versus frequency (f) at various temperature; (b) the plot between relative dielectric constant (ε') versus temperature at frequency of 20 Hz.

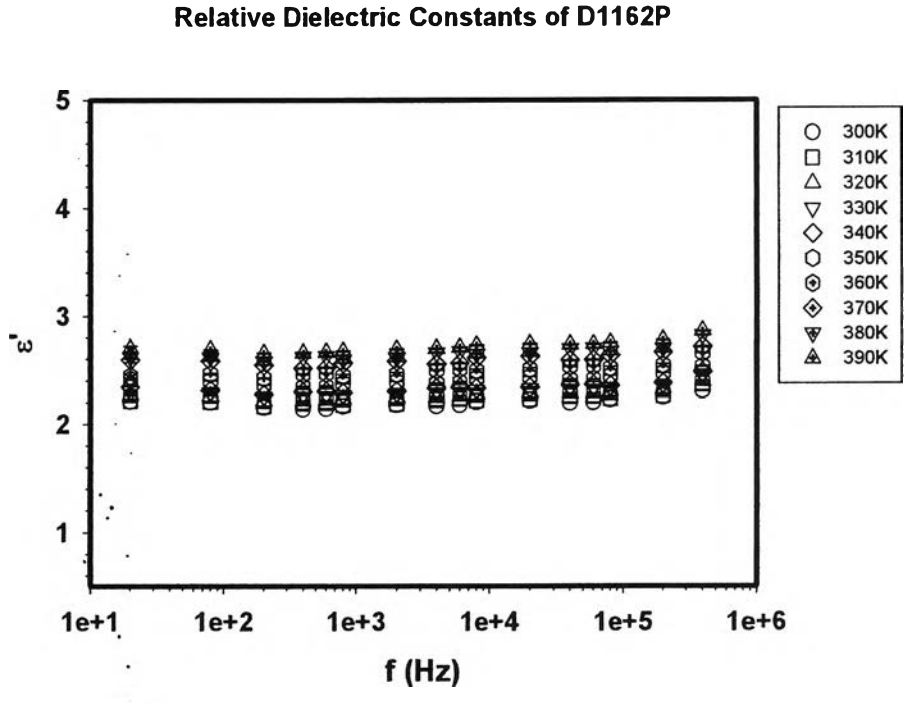

(a)

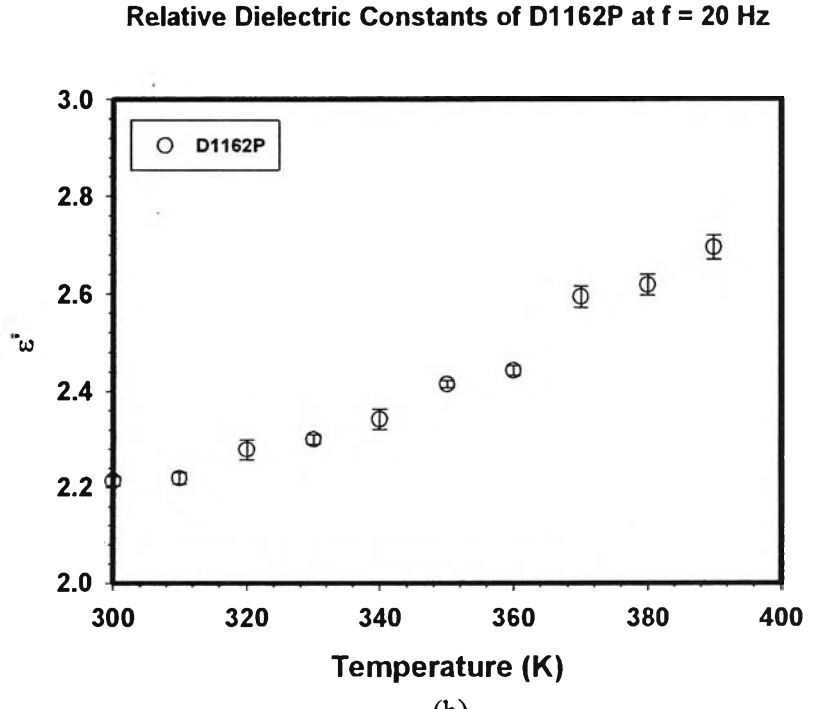

(b)

Figure M3 Dielectric constant of D1162P: (a) plot between relative dielectric constant (ε') versus frequency (f) at various temperature; (b) the plot between relative dielectric constant (ε') versus temperature at frequency of 20 Hz.

De_PDPA/D1114P blends

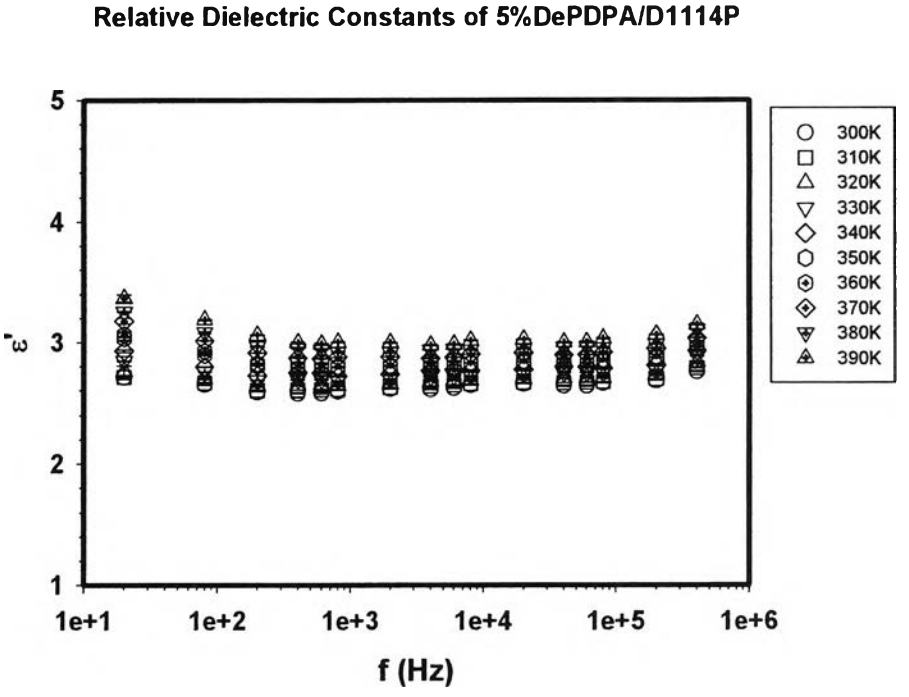

(a)

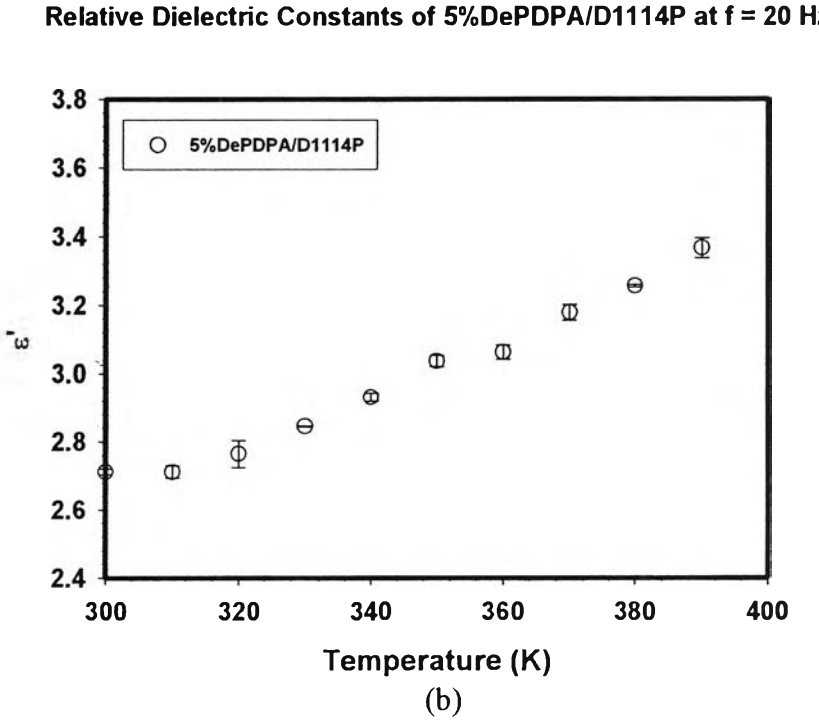

(b)

Figure M4 Dielectric constant of 5% De_PDPA/D1114P: (a) plot between relative dielectric constant (ε') versus frequency (f) at various temperature; (b) the plot between relative dielectric constant (ε') versus temperature at frequency of 20 Hz.

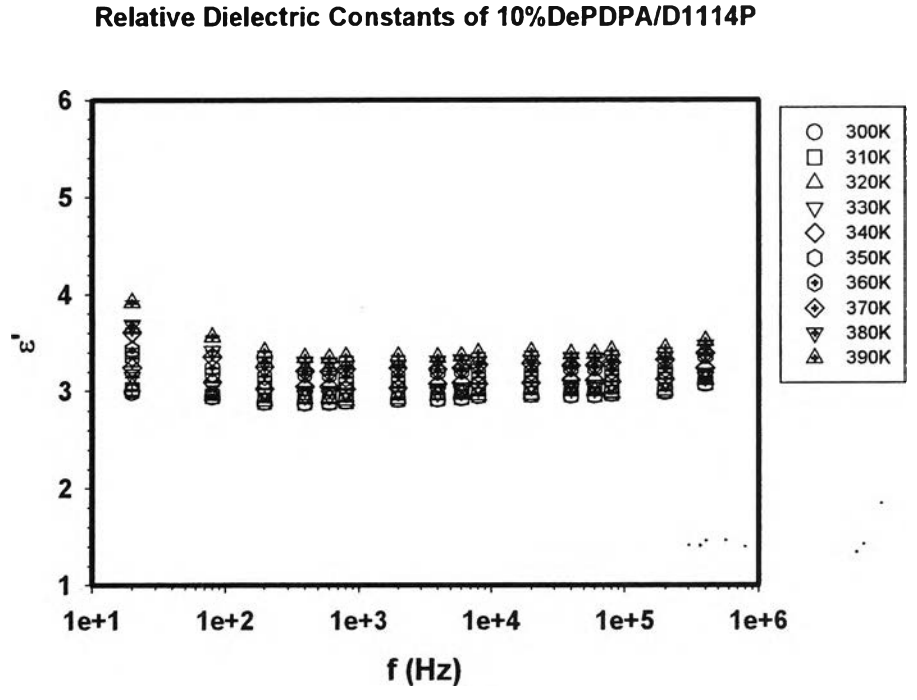

(a)

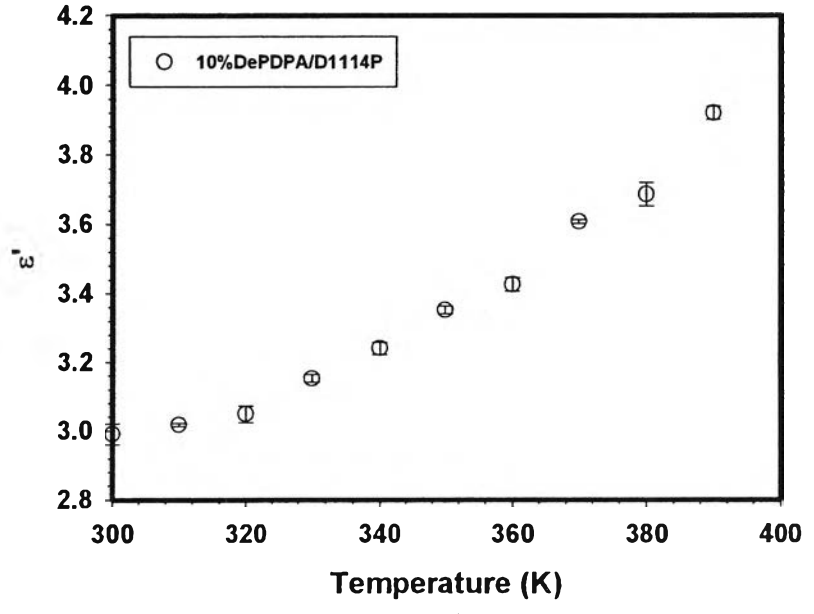

(b)

Figure M5 Dielectric constant of 10% De_PDPA/D1114P: (a) plot between relative dielectric constant (ε') versus frequency (f) at various temperature; (b) the plot between relative dielectric constant (ε') versus temperature at frequency of 20 Hz.

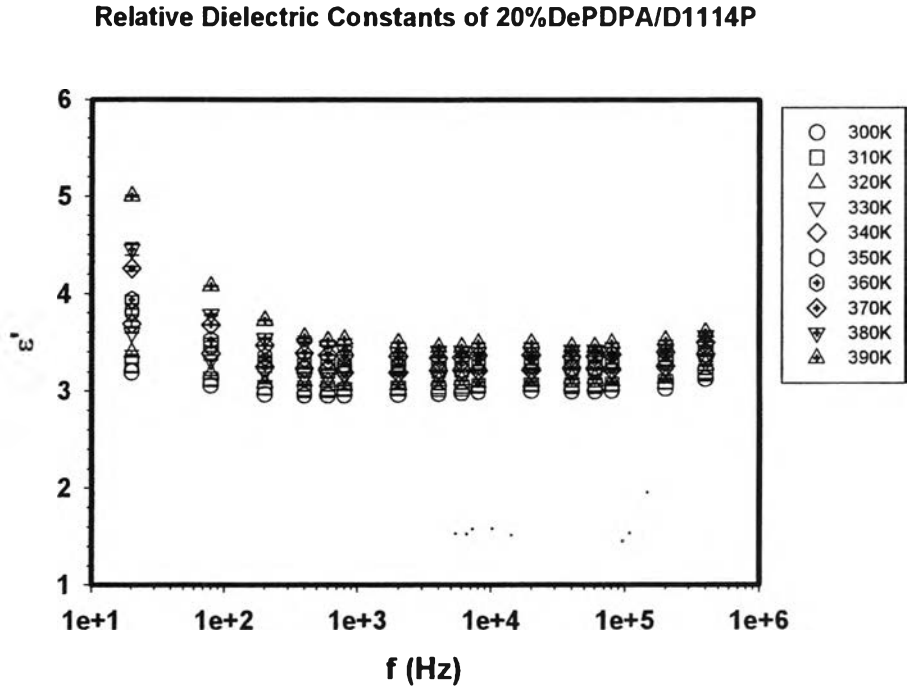

(a)

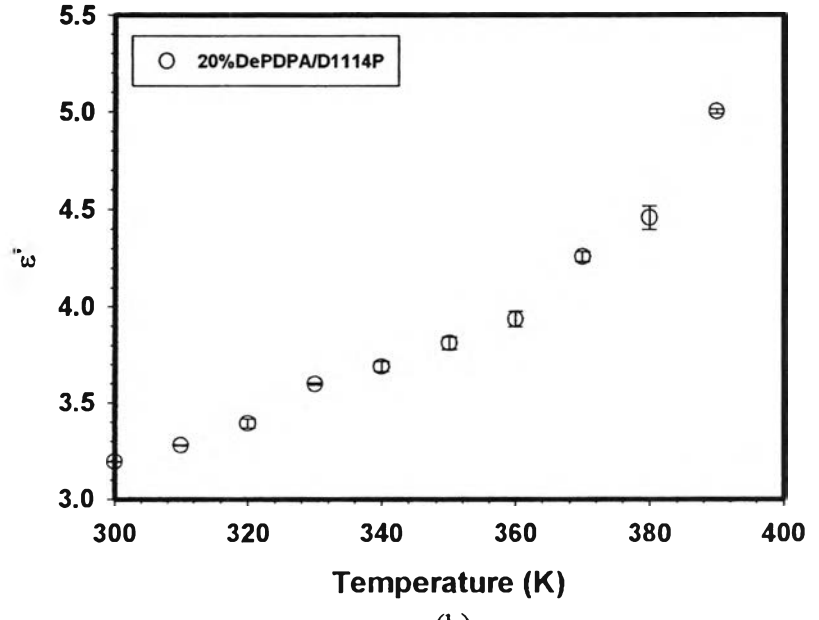

(b)

Figure M6 Dielectric constant of 20% De_PDPA/D1114P: (a) plot between relative dielectric constant (ε') versus frequency (f) at various temperature; (b) the plot between relative dielectric constant (ε') versus temperature at frequency of 20 Hz.

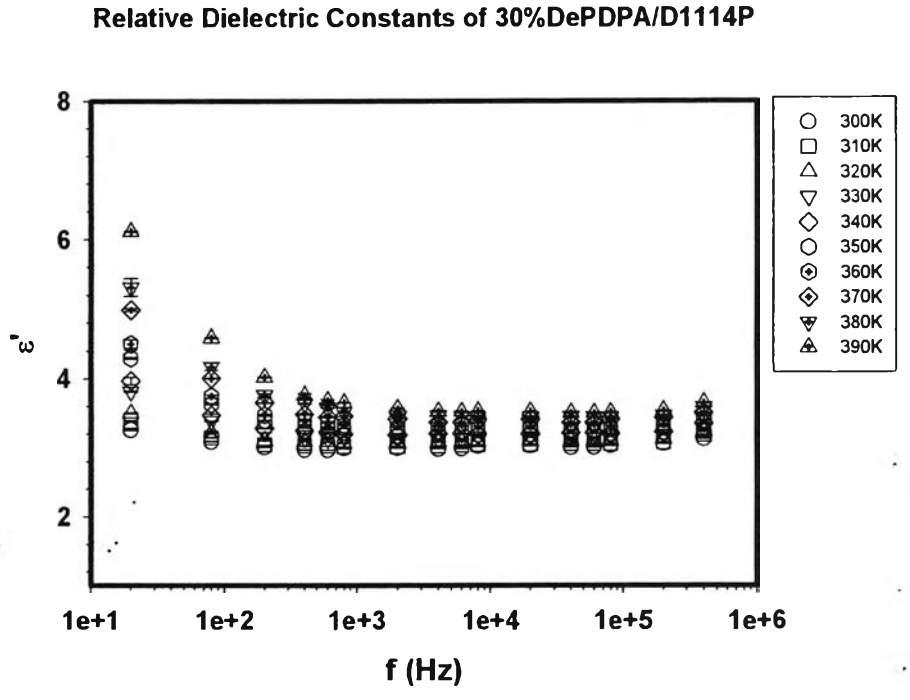

(a)

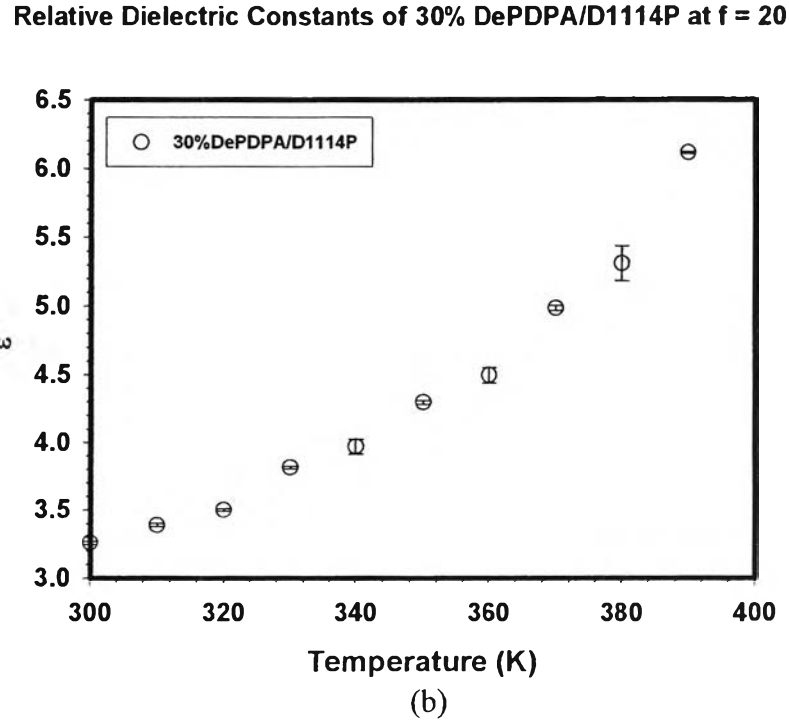

(b)

Figure M7 Dielectric constant of 30% De_PDPA/D1114P: (a) plot between relative dielectric constant (ε') versus frequency (f) at various temperature; (b) the plot between relative dielectric constant (ε') versus temperature at frequency of 20 Hz.

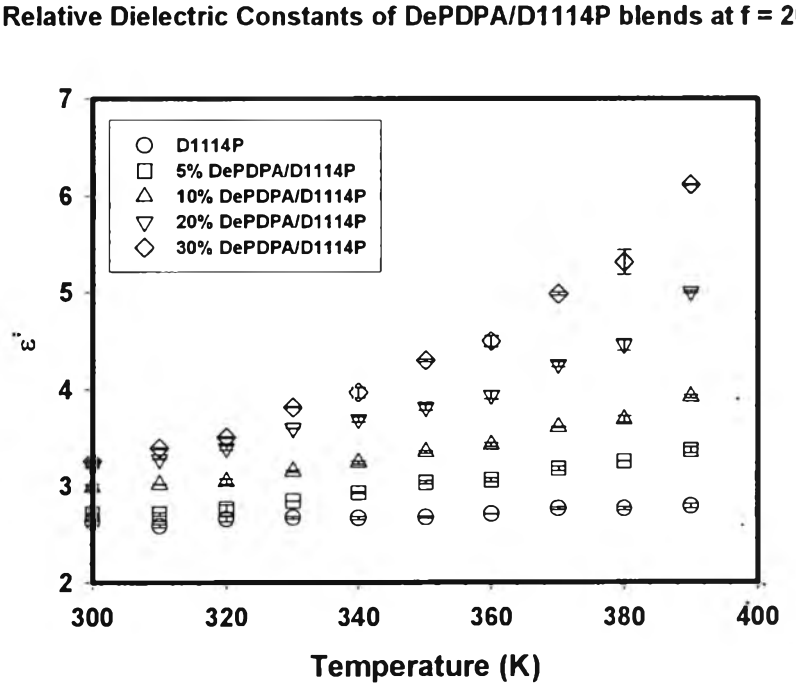

Figure M8 Comparison of dielectric constant of De_PDPA/D1114P blends at frequency of 20 Hz.

CURRICULUM VITAE

Name: Mr. Kraipop Thongsak

Date of Birth: September 29, 1984

Nationality: Thai

University Education:

2002-2006 Bachelor Degree of Engineering, Faculty of Engineering and Industrial technology, Silpakorn University, Nakornpathom, Thailand

Proceedings:

1. Thongsak, K., Sirivat, A., and Lerdwijitjarud, W. (2008, April 23). Electroactive Polydiphenylamine/Styrene-Isoprene-Styrene (SIS) blends in the effect of morphology and particle concentration Proceedings of the 14th PPC Symposium on Petroleum, Petrochemicals, and Polymers, Bangkok, Thailand.